Late Precambrian volcanic rocks of the Arabian shield, Saudi Arabia

Thesis

Late Precambrian volcanic rocks of the Arabian Shield, Saudi Arabia

A thesis presented for the degree of

Doctor of Philosophy

by

Hendrik Johan Duyverman

(B.Sc., M.Sc.; Utrecht, Netherlands)

The Open University

Department of Earth Sciences

Milton Keynes, U.K.

November 1981

Date of submission: 17.11.81

Date of award: 5.1.82

Abstract

Recent models for the evolution of the Pan-African (1200 - 500 Ma) Nubian-Arabian Shield either presume that these rocks are bounded by older cratonic areas, and so reflect an intracratonic environment, or they point to the existence of probable relict ophiolite assemblages and thick volcanic-sedimentary sequences as evidence for an accreting arc origin.

In this study, Late Precambrian volcanics of the Arabian Shield, locally named the Murdama and Shammar Groups (which are generally considered to belong to the youngest rock units of the Shield) have been studied in detail in three widespread areas across the Arabian Shield to test the intracratonic and island arc models. Field mapping, geochemical, sedimentological and isotope studies reveal these rocks to be a distinct group of volcanics and associated sediments in an island arc setting.

Geochemical analyses suggest that the Murdama and Shammar Groups belong to the calc-alkaline rock series with slight tholeiitic affinities for the older rock units. The volcanic rocks display a continuous trend of rock types, from basalts to andesites, rhyolites and ignimbrites, characteristic for an evolving island arc setting from mature arc to continental margin. The sedimentary environment varies from shallow marine for the older Murdama Group to clearly continental with a considerable relief for the Shammar Group. Data from older sequences of the Arabian Shield indicate that these trends fit in well with a multiple accreting island arc model, whereby three or more juvenile island arcs above easterly dipping subduction zones co-existed during the early stages of island arc evolution (ca. 1000 Ma) and that these arcs coalesced episodically in time with further subduction related volcanism and plutonism. Complete cratonization was reached during

deposition of the Shammar Group, the youngest of the studied volcanic groups. Three, more or less continuous ophiolite belts across the Arabian Shield probably represent the sutures between the island arc sequences.

Isotopic studies confirm the occurrence of the Murdama and Shammar volcanics in the Late Precambrian with an age range of 694 - 608 Ma, in the late stages of island arc evolution of the Arabian Shield. Initial strontium isotope ratios reveal a gradual increase in time from 1200 - 500 Ma, probably indicating a self-contained strontium evolution without necessarily implying an older craton below or east of the Shield. Petrogenetic studies, mainly on trace elements and REE suggest that basalts of the Late Precambrian sequences originate from partial melting of subducted oceanic crust and mixing with upper mantle; anomalous Zr and Ti abundances indicate the influence of processes during the late stages of subduction and cratonization, when subduction had ceased. Later extensive fractional crystallization is responsible for the characteristic andesite-rhyolite-ignimbrite sequences of the studied volcanics.

All available evidence in this study suggests that the multiple accreting island arc model is the most likely for the evolution of the Arabian Shield and, on a larger scale, for the evolution of the whole Nubian-Arabian Shield.

Acknowledgements

The following persons are thanked for helping in this study:

1. Ian Gass, for starting this project, enrolling me in the Pan-African research group and encouraging me throughout all stages of the thesis; without his help this study would have been impossible.

2. Nigel Harris, for help and friendship in Sudan, Saudi Arabia and around Cambridge.

3. John Roobol, for assisting me in the early stages in Saudi Arabia.

4. Chris Hawkesworth for luring me into the isotope research group.

5. Bill Fitches, for friendly advice and solving language problems.

6. Abdul Foum and Marc Coolen, for petrographic advice.

7. Ahmed Al-Shanti, for strong support in Saudi Arabia.

8. Martin Menzies, for aiding me in petrogenetic problems.

9. Hans Schellekens, for being a good Ph.D. rival and for help in metallogenetic problems.

10. At the Faculty of Earth Sciences in Jeddah, this group of people has been extremely co-operative: Ahmed Basahel, Gerald Cooray, Joop Moltzer, Pier and Sheila Binda, Colin Ramsay, Norman Jackson, Arthur Warden, Hashim Hakim and Abdulaziz Hussein.

11. Other geologists in Jeddah, who gave much advice, were: John Kemp (BRGM), Jacques Delfour (BRGM) and Malcolm Clark (DGMR).

12. At the Open University in England the following persons have been very helpful: Peter Webb, Phil Potts, Richard Thorpe, Olwen Thorpe, Ann Budd, John Watson, Peter van Calsteren, Ian Chaplin, Julian Pearce, Andy Tindle, Andy Gledhill, Jill Hewitt, Moira Staerk, Robert Shackleton and Alison Ries.

13. All research students at the Open University are thanked for their friendship and encouragement.

14. At the Institute of Geological Sciences in London, Norman Snelling and Chris Rundle advised me on problems concerning the fitting of isochrons.

15. John Taylor, for helping me with cartographic problems.

16. Janet Dryden, for painstakingly typing and correcting this thesis.

17. And - last but certainly not least - mother, Christel, Margriet, Han Pieter, Diederik and in-laws, many thanks for real and meaningful help and lots of patience; I hope to spend much more time with you from now on.

List of contents

List of Figures

List of Tables

List of Plates

1 Introduction

The Arabian-Nubian Shield is the name given to that part of NE Africa and Arabia, where mainly Precambrian crystalline basement is exposed. The aerial extent of these 1200 - 500 Ma ("Pan-African") old rocks in the Arabian Shield is shown in Figure 1.1. A growing body of evidence (especially from the Arabian Shield) suggests that during the Upper Precambrian the area evolved from intraoceanic island arc systems by repeated plutonism and volcanism and eventually arc accretion to have a truly continental character. This cratonization model, introduced by Greenwood et al. (1976), involved three cycles of magmatism and metamorphic activity, accompanied and interrupted by tectonism during arc collision. Alternative models, favouring an intracratonic origin for the evolution of the Arabian Shield, were put forward, amongst others, by Delfour (1981).

To understand the processes involved it is necessary to identify island arc structure and geology. Figure 1.2 indicates the major features of a modern island arc in a simple section. In the last five years the "accreting arc" model (as introduced by Bakor et al., 1976) has received wide acclaim (e.g. Neary et al., 1977; Hadley & Schmidt, 1980; Fleck et al., 1980) and is here accepted as the basic model, within which geochronology, geochemistry and field studies have to be explained. Other evolutionary models, like the intracratonic model, will also be tested extensively.

The studies, recorded in this thesis, concentrate on the last phase of this Late Precambrian island arc accretion and cratonization. The nature, age and origin of volcano-sedimentary rock units (and associated plutonic rocks) in three widespread areas (see Figure 1.1) is investigated in detail. Figure 1.3 shows a lithostratigraphic summary for the Arabian Shield (after DGMR, 1979). The Baish/Bahah Groups which

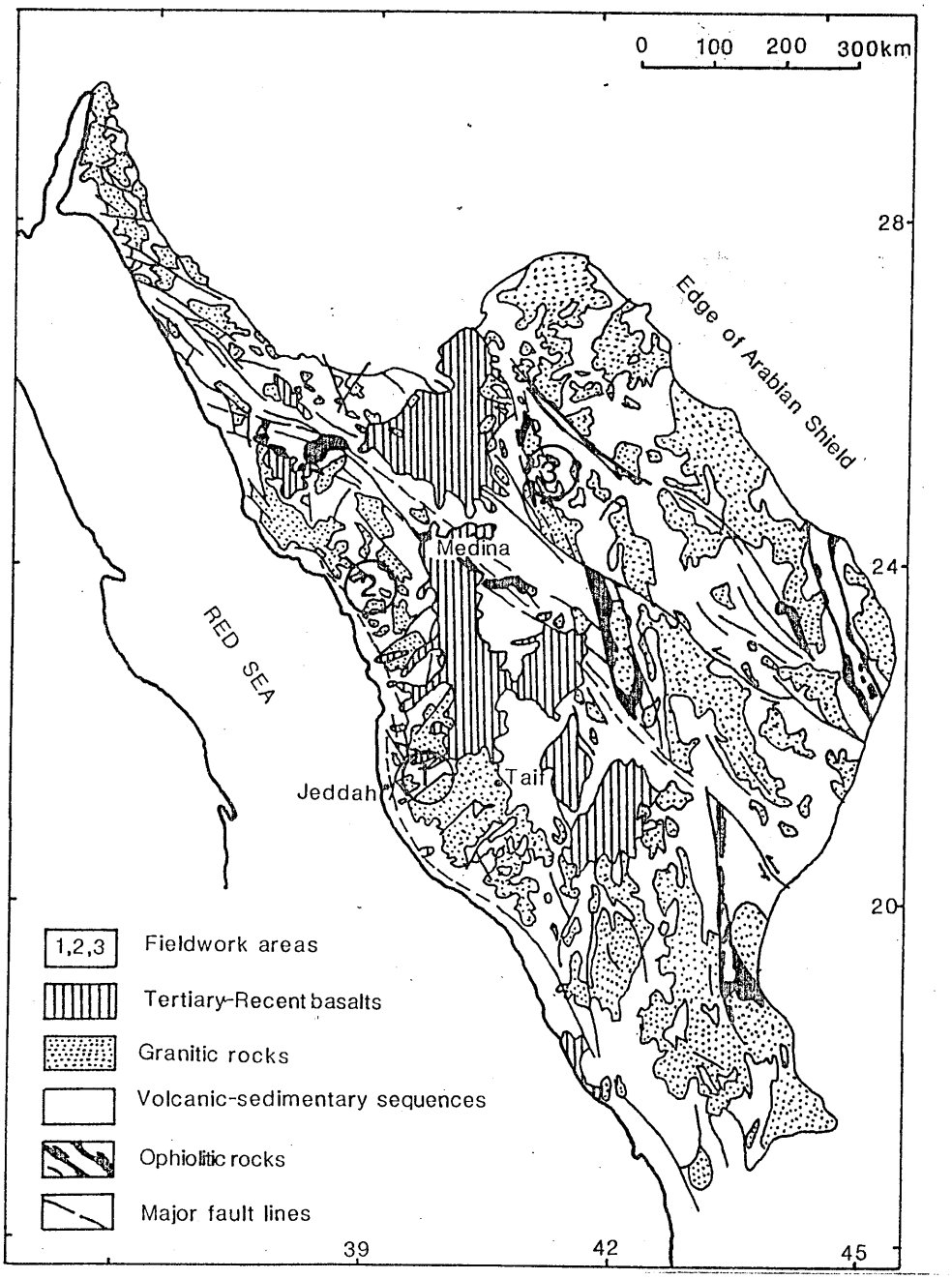

Figure 1.1 Major rock types and structure of the Arabian Shield and location of the fieldwork areas (1- Wadi Fatima area;2- Badr area; 3- Nuqrah area);after Nasseef and Gass, 1977.

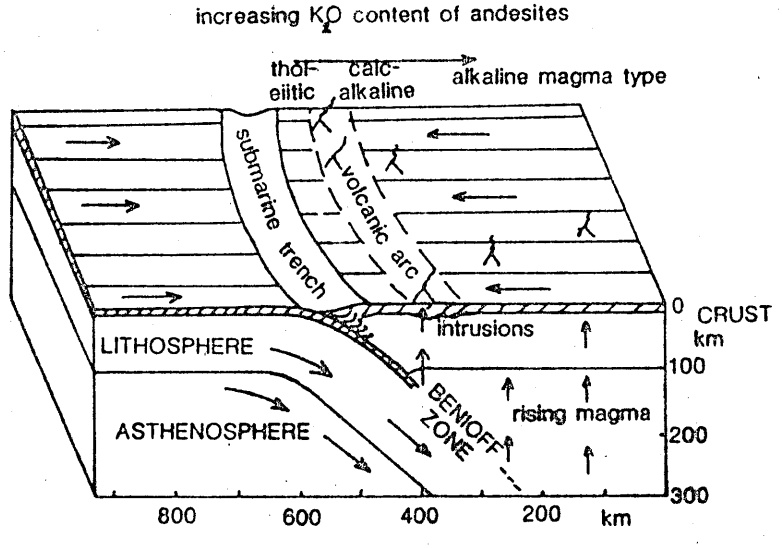

Figure 1.2 Block diagram showing the main features of modern island arcs, related to converging lithosperic plates (after Mitchell & Reading, 1971).

occur in the SW part of the shield consist of basalt, andesite, chert, quartzite and sandstone; the Halaban/Hulayfah Group (these names represent equivalent groups, but were used by the USGS - United States Geological Survey - and the BRGM - Bureau de Recherches Géologiques et Minières - respectively) consist of basalt, andesite, dacite, conglomerate and greywacke and can be found in the central part of the shield; the Ablah Group occurs in graben in the southern part of the shield and its stratigraphic position is not clear, it consists of andesite, dacite, marble and coarse clastic rocks; the Murdama Group occurs in the northern part of the shield and consists of andesite, rhyolite, marble, conglomerate and greywacke; the Shammar Group rocks occur in the northeastern part of the shield and consist of andesite, rhyolite and minor clastic rocks; the Jibalah Group occurs in graben in the northeastern part of the shield and consists of andesite, basalt, limestone and sandstone. The Murdama and Shammar Groups form the bulk of the younger rock units and these groups form the main topic of this thesis. The study of rock units in the three fieldwork areas, as discussed in the Chapters 2 (Wadi Fatima area), 3 (Badr area), 4 (Nuqrah area), combined with geochronological studies, presented in Chapter 5 and geochemical studies in Chapter 6, must assess the correlation of the studied rocks with the Murdama and Shammar Groups. The lack of previous geochronological, geochemical and lithostratigraphical studies in these areas necessitate this approach.

An evolutionary model for the Late Precambrian Murdama/Shammar volcanics (and associated other rock types) and their possible correlation with other rock units of the Nubian-Arabian Shield will be presented in Chapter 7. All analytical techniques, classifications and geochemical results are shown in the Appendix.

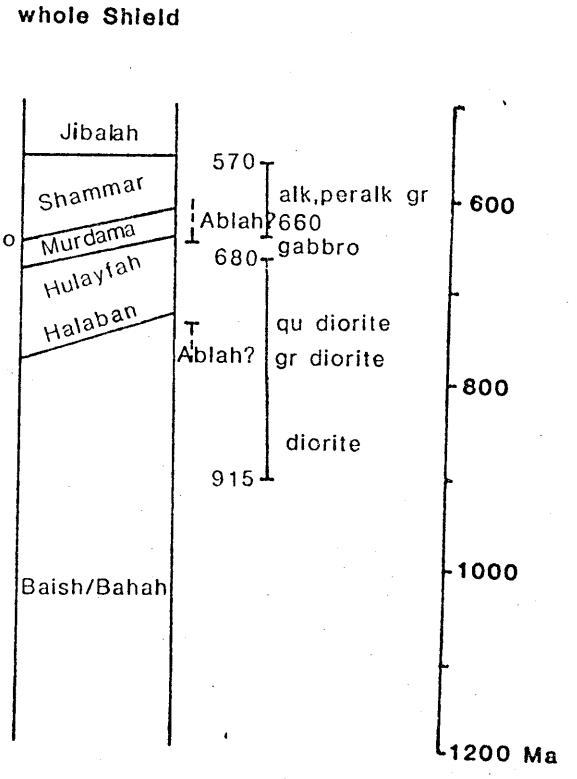

Figure 1.3 Lithostratigraphic summary for the Arabian Shield (after DGMR - Directorate General of Mineral Resources -, 1979; alk-alkaline, peralk-peralkaline, qu-quartz, gr-granite).

The fieldwork in the Wadi Fatima, Badr and Nuqrah areas was done during 1978 - 1980, while the author worked as a UNESCO expert at the King Abdul Aziz University (Faculty of Earth Sciences) in Jeddah. The IGCP (International Geological Correlation Programme) Project 164 - Evolution and mineralization of the Arabian-Nubian Shield, headed by A.M.S. Al-Shanti, former Dean of the Faculty of Earth Sciences, proved to be a good framework for the presented studies. The large geological community of Jeddah, the annual IGCP meetings, the IGCP Symposium in 1978 and the co-operation of the Saudi Arabian authorities were a major help in this project.

During the stay in Saudi Arabia, mapping, sampling and reference collection were done; detailed geochemical studies were performed at the Open University Laboratories in the U.K. During January 1981 a visit of a month was paid to the Red Sea Hills and the Sabaloka Ring Complex in Sudan to investigate correlations with the younger volcanic and plutonic complexes in NE Sudan and Saudi Arabia.

2 Wadi Fatima area

2.1 Introduction

The Wadi Fatima area is situated 50 kilometres E of Jeddah. The study area, comprising Late Precambrian volcanics and their granitic basement, is Jabal Daf (Figure 2.1) on the northwestern side of Wadi Fatima, a SW/NE trending fault-controlled graben. Accessibility is very good by the main Jeddah-Mecca road and smaller roads branching off near Haddah that follow Wadi Fatima. Aerial photographs on scale 1:60,000 and photomosaics on a larger scale make photogeological interpretation possible. Because of its proximity to Jeddah and accessibility this area has been well studied; outstanding problems are the geochemistry of the volcanics, their correlation with other volcano-sedimentary groups in the Arabian Shield and the exact age of this Group and the underlying granitic basement.

Field geology and petrography will be presented in this chapter. These data, combined with geochemistry and geochronology (Chapters 6 and 5) will be used to erect an evolutionary model for the Fatima Group (Chapter 7); the other two study areas, Badr and Nuqrah, will be discussed in a similar way.

2.2 Previous work

The first description of the Wadi Fatima area was by Karpoff (1955), who divided all rocks of the Arabian Shield into an older "série de Medina" and the younger "série du Wadi Fatima", noting a major unconformity between the two series. The "Medina series" comprises virtually all rocks of the Arabian Shield and as such is not a very useful term; the "Wadi Fatima series", however, has been generally accepted as a local unit. Karpoff (1957, 1960) subdivided it into a lower "detritic", a middle "schistose-calcareous" and an upper "volcanic" section. Stromatolitic limestones, very conspicuous in the Wadi Fatima area, were described by

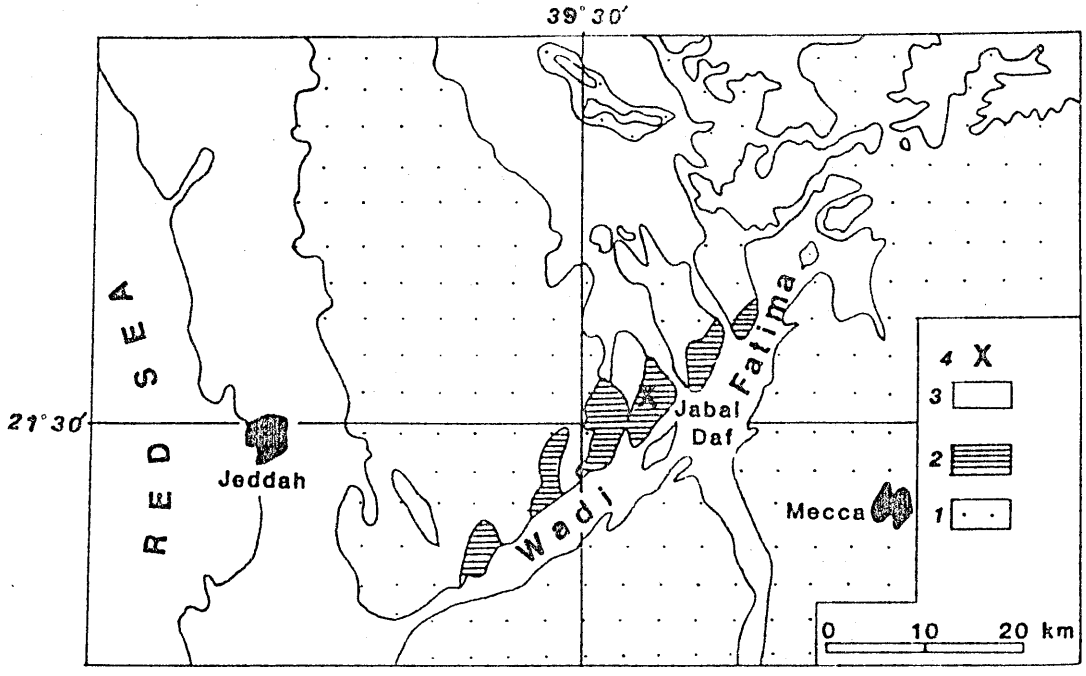

Figure 2.1 Simplified geological map of the Jeddah area.

(1 - Pre-Fatima rock units; 2 - Fatima Group; 3 - Tertiary and Quaternary; 4 - locality of section)

him (recognizing "Collenia" and "Conophyton" shapes) and used to correlate with other Precambrian-Cambrian sequences in Egypt, Morocco and the Sahara.

The "Wadi Fatima series" has become well established in the Arabian Shield literature (32 entries are given in Fitch's stratigraphic lexicons of 1978a, 1978b, 1979), first as the Fatima Formation (Brown & Jackson, 1960), and later as the Fatima Group by Eykelboom (1970) who regarded it as a rather informal rock unit. After 1975, the unit "Fatima Group" seems to be less used in describing the geology of previous unknown areas; the name appears only in general papers concerning correlation (Brown & Jackson, 1979; Jackson & Ramsay, 1980; Jackson, 1980 and Skiba, 1980). The only published maps, on which the Fatima Group appears are I-210A (Brown et al., 1962), I-270A (USGS, Aramco, 1963), Nebert et al. (1974) and Skiba (1980). It appears that the Fatima Group is of very limited extent and restricted to the coastal area from Jeddah to Rabigh. Many authors suggest that it correlates with the Ablah Formation (USGS, Aramco, 1963), with the Halaban Formation (Goldsmith & Kouther, 1965/66), with the Shammar/Murdama Groups (Eykelboom, 1970), or with the Murdama Group (Leca, 1970; Gilroy & Skiba, 1978a, b). The Fatima Group is a recognizable lithological unit E of Jeddah, where the type locality area is found NW of Wadi Fatima; other possible outcrops can be found E of Tuwwal (Skiba, 1980) and NE of Rabigh (Skiba, 1980; Brown & Jackson, 1960). As a unit for the whole Arabian Shield the Fatima Group is only marginally useful. In this study the Fatima Group will be assigned to the (Lower) Murdama Group, a major shield-wide unit with a good correlation to the Fatima Group.

2.3 The fieldwork area

Figure 2.1 snows the location of the fieldwork area, the geological map can be seen on Figure 2.2; Jabal Daf offers the most complete and continuous outcrop of the Fatima Group. A complete section, shown in

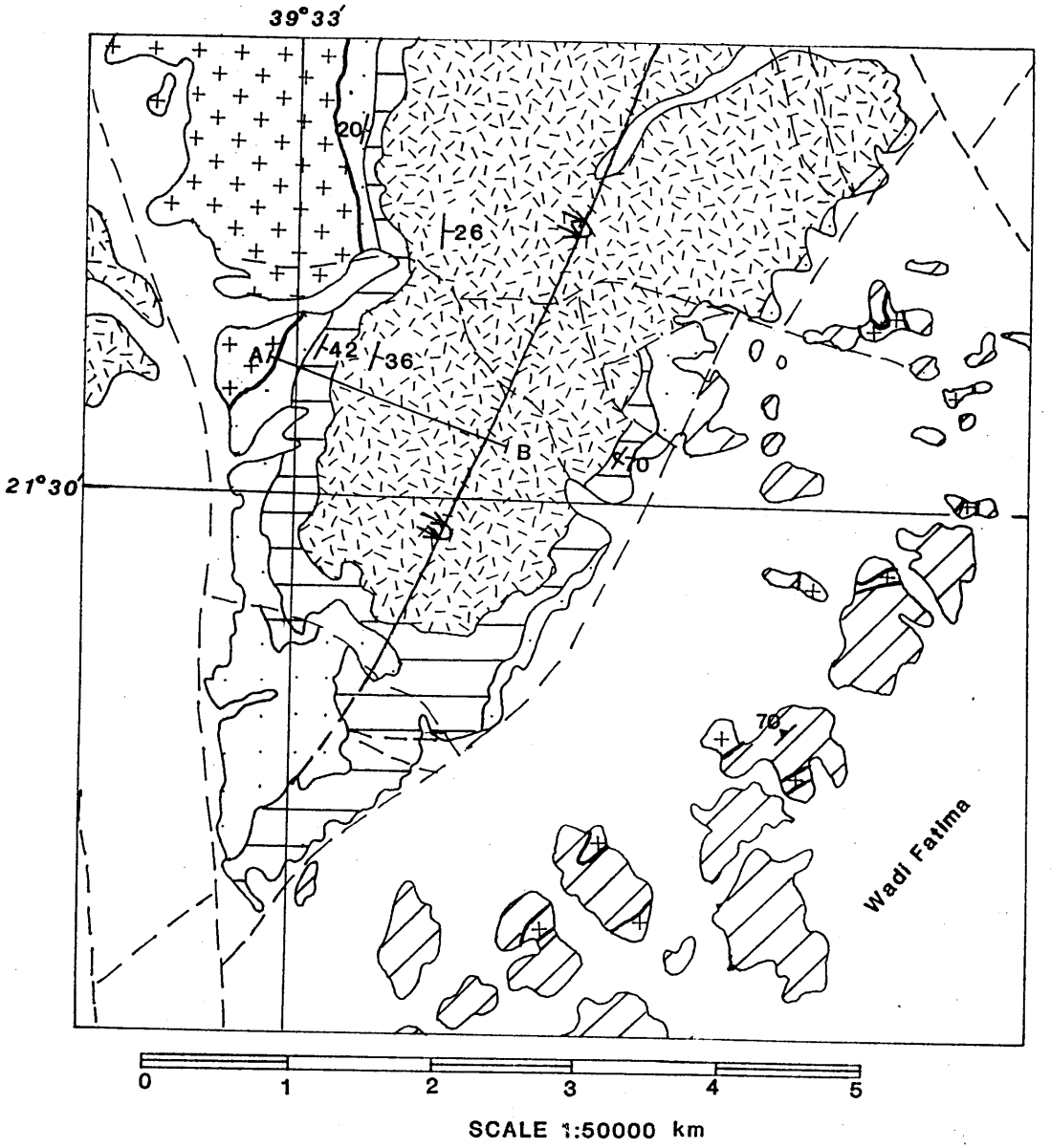

Figure 2.2 Geological map of the Jabal Daf area (After Nebert et al.,1974).

hornblende schist, granite, Lower Fatima Formation,

Middle Fatima Formation, Upper Fatima Formation,

Fan deposits and alluvium, fault, strike/dip,

foliation, indicates the stratigraphical section

(see Figure 2.3)

Figure 2.3 indicates the true thickness of this volcano-sedimentary group of 800 metres. The granitic basement is well-exposed in low-lying, undulating hills, separated from the Fatima Group by an angular unconformity.

The Fatima Group is developed on eight isolated hills, of which Jabal Daf (822 metres) is the highest of the seven north of the Jeddah-Mecca road (Jabal al Ujaysah, Jabal Shilwa, Jabal abu Bakr, Jabal Shobairim, Jabal Daf, Jabal Mukassar, and Jabal abu Gurrah); south of this road lies Jabal Kettana, an area never described in detail and overlooked on most geological maps.

The Fatima Group forms an elongated SW/NE trending belt on the NW side of the Wadi Fatima graben (Nebert et al., 1974; Skiba, 1980). In the centre of the graben are scattered outcrops of the oldest rocks of the area, namely hornblende and amphibolite schists. These may belong to the oldest Precambrian rocks of the Arabian Shield and were assigned by Skiba (1980) to the Arafat Group; Nebert et al. (1974) mention an age of 1000 Ma for these rocks, but this has never been supported by isotopic data. The schists are intruded by granites, which form the basement for the Fatima Group. North of Jabal Daf these granites and diorites are locally overlain by the Oligocene-Eocene Shumaysi Formation, well known for its rich iron oolites (Al-Shanti, 1966). In the Jabal Daf area, detailed sampling was made of the major rock units of the area, especially along a traverse (A-B on the geological map). The rock units will be discussed separately, including their petrography.

2.4 Structural geology

The dominating structure of the Jabal Daf area is the large, overturned plunging syncline with axis 10/030 (Nebert et al., 1974 indicates

15/045 as a maximum for all fold axes NW of Wadi Fatima). The Upper Fatima Group volcanics are found in the centre of the syncline (Figure 2.2). Within the Fatima Group, the dolomitic limestone often is internally folded and several examples of this disharmonic folding between limestone and intercalated sandstones can be seen on the western and southern flanks of Jabal Daf.

Jabel Daf is fault-bounded by SW/NE faults, bordering Wadi Fatima and NNE/SSW faults, separating the individual hills from each other, thus producing an en echelon pattern of the Fatima Group hills. No folding is observed in the granitic rocks underlying the Fatima Group, whereas the old amphibolites are steeply foliated (attitude 030/90 to 030/70 NW). The geological history of this area can be summarized as follows (after Nebert et al., 1974 with, where appropriate, isotopic and age control):

a. Folding (isoclinal?) and metamorphism (amphibolite facies) of the schists, now occupying Wadi Fatima - 1000 Ma?
b. Granitic intrusion into these rocks - 780 Ma (see Chapter 5)
c. Peneplainization, producing the pre-Fatima peneplain
d. Deposition of the Fatima Group - 680 Ma (see Chapter 5)
e. Folding of the Fatima Group
f. After a long period of denudation (to the Oligocene) - deposition of the Shumaysi Formation - Eocene-Oligocene (Al-Shanti, 1966)
g. NE/SW block faulting with tilting of the NE block and uplift of the SW block - post Oligocene-Pliocene
h. NNW/SSE block faulting, producing a series of Fatima Group hills in an en echelon pattern - Early Quaternary
i. Extensive erosion and deposition of alluvial fans during the present cycle of erosion

2.5 Lithological description of rock units

2.5.1 Introduction

The need was felt to establish a detailed stratigraphic section of the Fatima Group at Jabal Daf, being the most complete succession of this group in the type locality area (Karpoff, 1955). Nebert et al. (1974) and Hirayama (1977) show several stratigraphic columns of the Fatima Group, but these are not accurate enough, especially the higher, mainly volcanic parts of the sequence.

A detailed section was made across the western flank of Jabal Daf, where a complete and uninterrupted sequence of about 800 metres thick can be found. This complete section is shown in Figure 2.3. The detailed lithostratigraphic columns indicate rock type, structural data, sedimentological features and sample numbers. A three-fold subdivision of the Fatima Group, as described since 1957 (Karpoff) in most references on this Group (especially Nebert et al., 1974; Hirayama, 1977) was used with minor modifications. The basalt flows, occurring throughout the Fatima Group, will be dealt with separately.

The chemical composition of the samples can be found in the Appendix C.

2.5.2 Pre-Fatima Group rocks

2.5.2.1 Wadi Fatima Graben hornblende schists

These hornblende schists are considered to be the oldest rocks of the area with an approximate age of 1000 Ma (Nebert et al., 1974). They occupy the Wadi Fatima Graben as a scattered belt of outcrops (Figure 2.2) and incorporate minor amphibolite schists and marbles. The schists have been metamorphosed to the amphibolite grade with a characteristic assemblage of hornblende-plagioclase (plagioclase more calcic than albite). The primary rocks for the schists are uncertain, but interfingering of schists, marbles and rare quartz-eye rhyolites suggest a volcano-


rhyolite


andesite


basalt


sill


volcanic breccia


ignimbrite


tuff


fine tuff


(dolomitic) limestone


mudstone


siltstone


sandstone


conglomerate


granitic rocks

Sedimentological features

parallel lamination


small-scale and large-scale cross-bedding


erosional lower boundaries


gas pipe structures


columnar jointing

Fig 2.3 Legend for Jabal Daf section. True thickness in metres; measured strike and dip are indicated left of the column; sample numbers are also shown. The following abbreviations are used: d.-dark, l.-light, diam-diameter, fu-fining upwards, occ-occasional, ls-limestone, dol-dolomite, cr-crystal, pum-pumice, lith-lithic, porph-porphyritic, strom-stromatolithic, elong-elongated, sl-slightly, volc-volcanic, v-very, ves-vesicular, amygd-amygdaloidál, str-strongly.

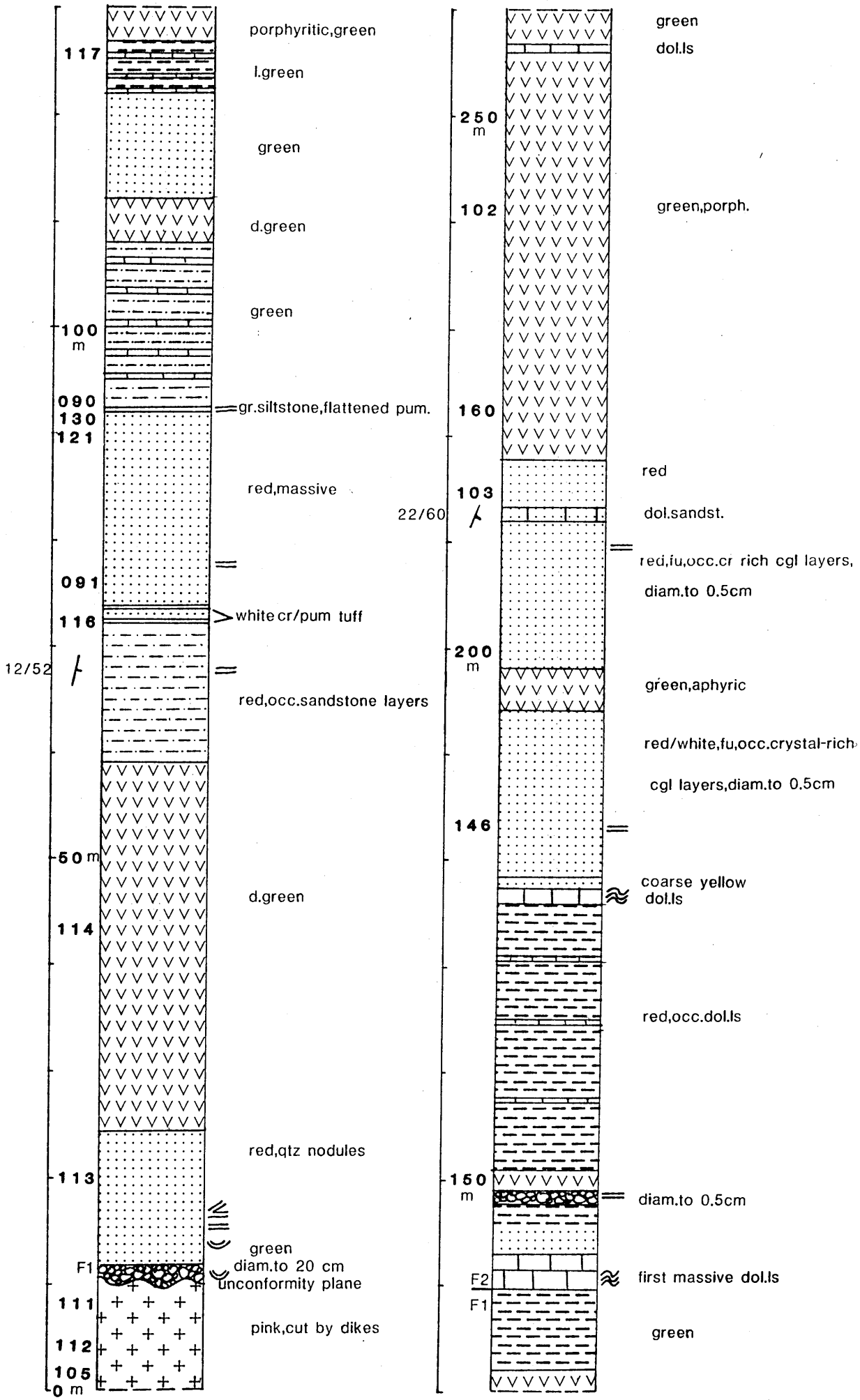
porphyritic,green
117
l.green
green
d.green
green
100
m
090
130
121
gr.siltstone,flattened pum.
red,massive
091
116
white cr/pum tuff
12/52
red,occ.sandstone layers
50 m
d.green
114
red,qtz nodules
113
green
F1
diam.to 20 cm
unconformity plane
111
112
105
0 m
pink,cut by dikes
green
dol.ls
250
m
102
green,porph.
160
red
103
22/60
dol.sandst.
red,fu,occ.cr rich cgl layers,
diam.to 0.5cm
200
m
green,aphyric
red/white,fu,occ.crystal-rich
cgl layers,diam.to 0.5cm
146
coarse yellow
dol.ls
red,occ.dol.ls
150
m
diam.to 0.5cm
F2
first massive dol.ls
F1
green

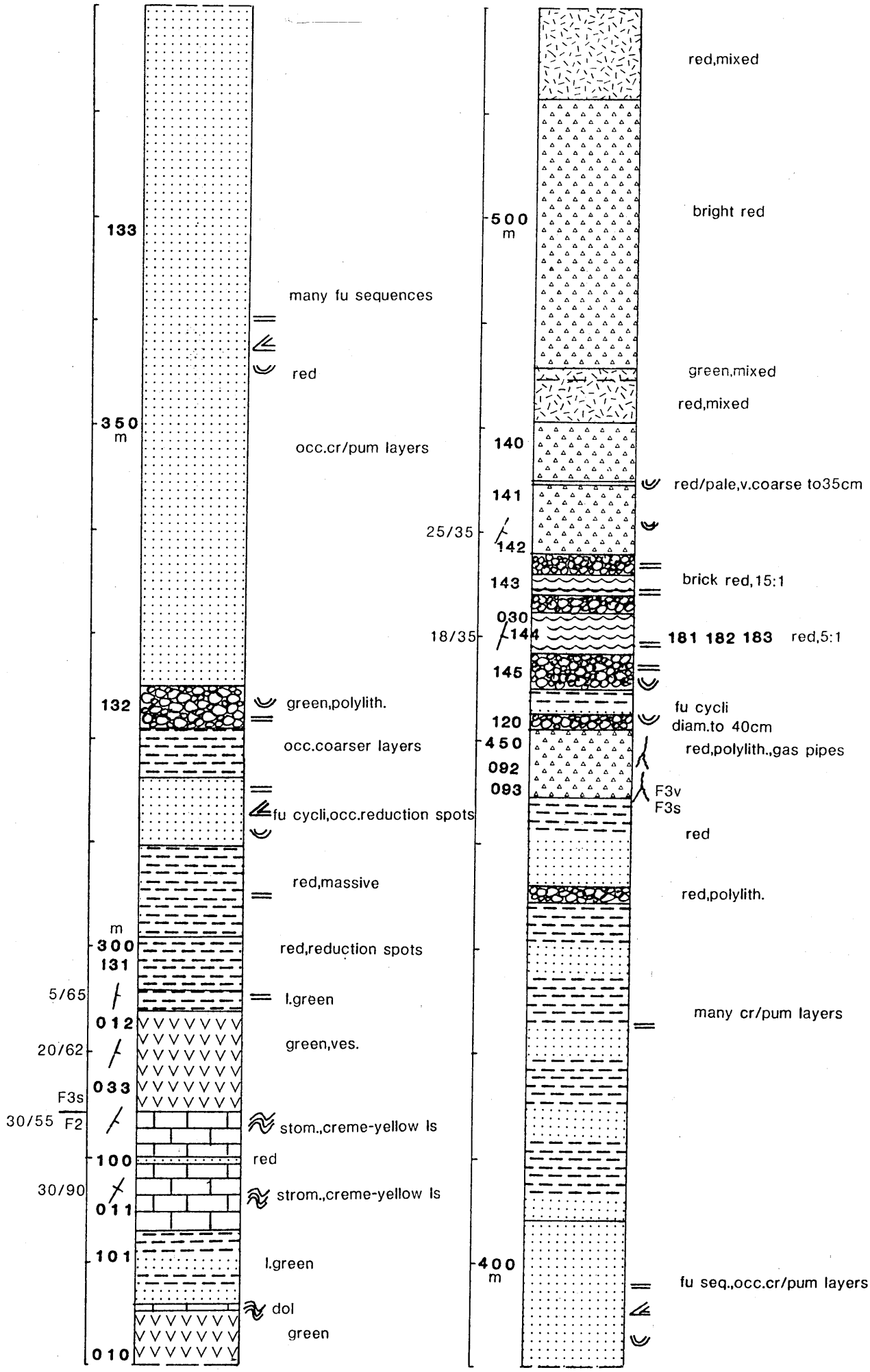
133
many fu sequences
red
350
m
occ.cr/pum layers
132
green,polylith.
occ.coarser layers
fu cycli,occ.reduction spots
red,massive
m
300
131
red,reduction spots
5/65
l.green
012
20/62
green,ves.
033
F3s
30/55 F2
stom.,creme-yellow ls
100
red
30/90
strom.,creme-yellow ls
011
101
l.green
dol
green
010
red,mixed
500
m
bright red
green,mixed
red,mixed
140
red/pale,v.coarse to35cm
141
25/35
142
143
brick red,15:1
030
18/35
144
181 182 183
red,5:1
145
fu cycli
diam.to 40cm
120
450
092
093
red,polylith.,gas pipes
F3v
F3s
red
red,polylith.
many cr/pum layers
400
m
fu seq.,occ.cr/pum layers

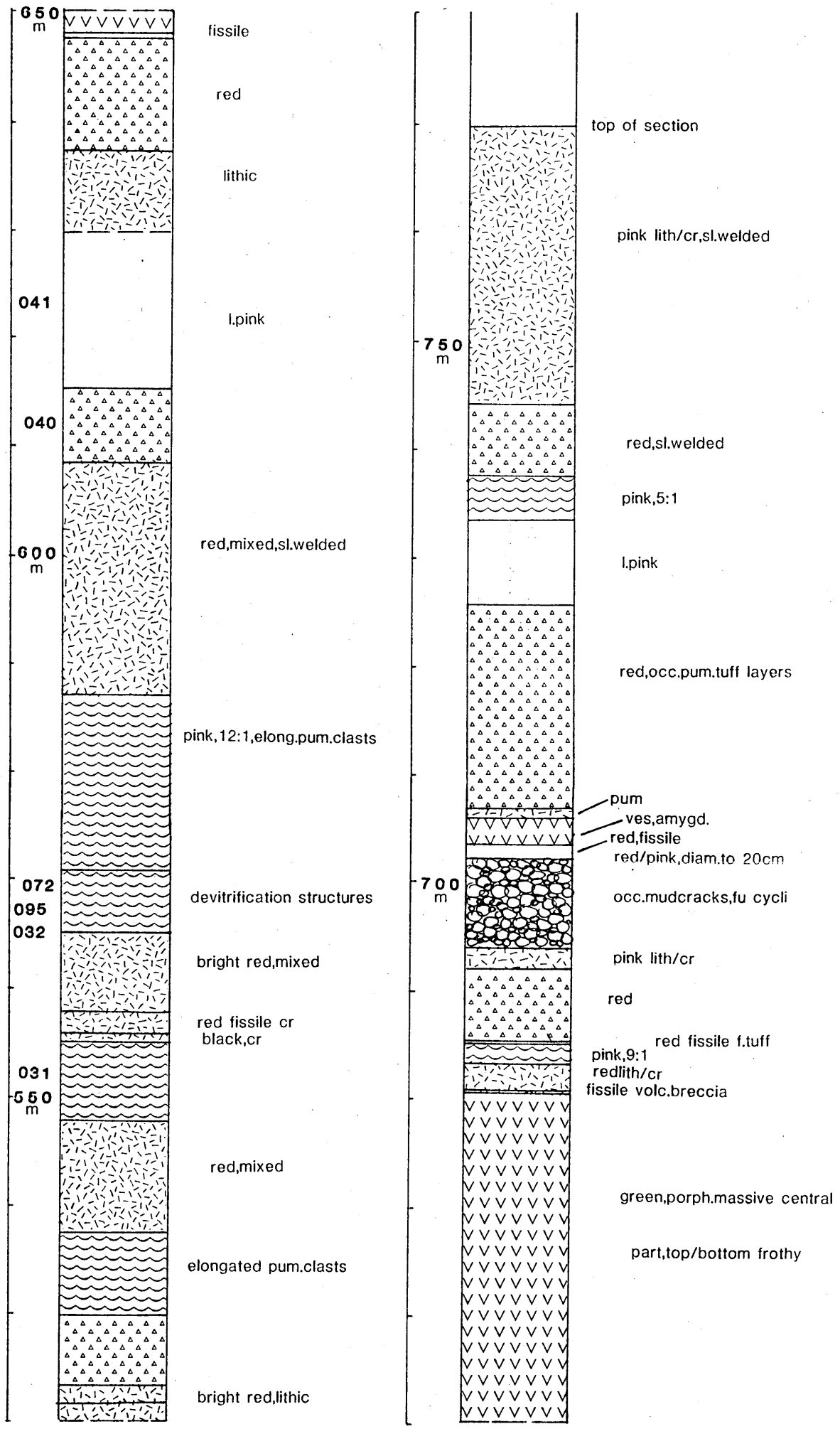
650 m
fissile
red
lithic
041
l.pink
040
red,mixed,sl.welded
600 m
pink,12:1,elong.pum.clasts
072
095
devitrification structures
032
bright red,mixed
red fissile cr
black,cr
031
550 m
red,mixed
elongated pum.clasts
bright red,lithic
top of section
pink lith/cr,sl.welded
750 m
red,sl.welded
pink,5:1
l.pink
red,occ.pum.tuff layers
pum
ves,amygd.
red,fissile
red/pink,diam.to 20cm
700 m
occ.mudcracks,fu cycli
pink lith/cr
red
red fissile f.tuff
pink,9:1
redlith/cr
fissile volc.breccia
green,porph.massive central
part,top/bottom frothy

sedimentary origin.

The hornblende schists are dark green to grey-green in colour, medium to fine grained and consist almost entirely of hornblende with minor plagioclase and quartz; epidote is common. A steeply inclined pervasive schistosity is pronounced, the attitude is roughly parallel to the SSW/NNE graben trend. Locally the schists are intruded by granitic rocks (see Section 2.5.2.2). The contact is normally sharp, but occasionally intermingling of the two rocks produces a migmatitic structure. The contacts between schists and granites define the age relation between these rocks; dating confirms that the granitic rocks are much younger (about 780 Ma). In thin section the schists consist of 80-90% amphibole (hornblende), 5-10% plagioclase (An_{15-10}), 3-6% quartz, approximately 5% epidote and accessory magnetite.

2.5.2.2 Granites

Plutonic rocks are widespread in the Wadi Fatima area; they occur as intrusive bodies in the hornblende schists and, NW of Wadi Fatima, as low-lying, undulating hills, directly underlying the Fatima Group. Because of the intense weathering, the relief of the plutonic rocks is generally moderate and smooth. The three main plutonic rocks (after Nebert et al., 1974) are granite, diorite and gabbro. In the Jabal Daf area only the granite occurs (see Figure 2.2) with occasional xenoliths of diorite and gabbros. The granite has intruded and partially assimilated the other rock types and is cut by several aplitic dykes.

The granites in the Jabal Daf area are leucocratic (colour index < 10), coarse grained, granular, pale pink to brown and often altered with epidote in veins and joints. This group of rocks has an average modal felsic composition of 24% quartz, 50% alkali-feldspar and 26% plagioclase

and they are granites sensu stricto according to Streckeisen (1976). In thin section they consist of orthoclase, (often normally zoned) plagioclase An_{42-33}, quartz, biotite, muscovite and accessory microcline, hornblende, chlorite, zircon, magmatite, sphene and epidote.

Chappell and White (1974) classify granites in I-types (magnetite series, derived from igneous material) and S-types (ilmenite series, derived from within continental crust). The discussed Fatima granites have many I-type characteristics (high sodium content - > 4.0% , low initial strontium isotope ratios, occurrence of magnetite, hornblende and sphene) and are probably derived from igneous material and not from reworked continental crust.

2.5.3 The Lower Fatima Formation (F1)

The three fold-subdivision of the Fatima Group, as suggested by Karpoff (1957, 1960) and further developed by Nebert et al. (1974), is accepted as a useful subdivision for this volcano-sedimentary sequence. The Lower, Middle and Upper Fatima Formations are named F1, F2 and F3, respectively. The Lower Fatima Formation consists mainly of clastic sediments, ranging from mudstone to conglomerate; higher in the F1 sequence the clastic sediments gradually give way to dolomitic limestones. Minor volcanic events are indicated by tuff beds and basalt flows.

F1 is about 130 metres thick and bounded at the base by a well defined angular unconformity on leucocratic granites. A poorly-bedded and -sorted conglomerate with boulders to 20 cm in diameter, consisting of granite, diorite, basalt, schists and dyke rocks mark the unconformity. Except for the basal conglomerate, the sediments in this Formation are fine grained. The main rock type (Figure 2.3) is green to red sandstone, often grading into mudstone. Several layers of pumice/crystal tuff, pumice lenses in mudstone (see Plate 6) and three thick basalt flows indicate the

extent of volcanic activity in the F1. Upwards, the clastic sediments start to alternate with dolomitic limestone beds; the relative amount of dolomitic limestone increases slowly and the boundary with the Middle Fatima Formation (F2) is chosen at the first massive dolomitic limestone bed. In thin section the grains of the clastic sediments are strongly aligned. Rounded, elongated grains of quartz, orthoclase, plagioclase and iron ore are embedded in a tuffaceous matrix, which is often altered to calcite. Quartz and feldspar crystals often have calcite rims; remnants of pumice shards (fiamme) consist of dark, glassy, fine grained matrix, completely altered to calcite; their ragged form remains visible. Normal grading of the sediments on a microscopic scale is commonly pronounced. The main sedimentary structures in F1 are parallel lamination in all clastic sediments; the basal conglomerates show channel-fill structures, small-scale and large-scale cross-bedding. In the upper part of F1, the parallel laminated clastics are interbedded with thin, well-bedded dolomitic limestone beds, which will be discussed at length in the next chapter.

The grain size distributions, sedimentary structures and rock types indicate a distal alluvial fan (as described by Bull, 1972) as the most probably sedimentary environment. The environment becomes shallow marine higher in the section. The widespread volcanic and tuffaceous material emphasizes the volcanic source for the clastic sediments.

2.5.4 The Middle Fatima Formation (F2)

This formation is very conspicuous in the field as light-toned competent limestone beds with interbedded sandstones; F2 has a total thickness of 144 metres. The main rock type is a fine- to medium-grained, locally semicrystalline, well-bedded, strongly jointed limestone with a colour varying from light grey to yellow. Red sandstones, normally grading into

siltstones of limited thickness are interstratified with the limestones. Four massive basalt flows are also found in F2; these will be discussed in Section 2.5.7.

The limestones, which have been metamorphosed to low-grade marbles, are all dolomitic (they all contain more than 2% MgO, which indicates the presence of dolomite according to Chave, 1952). They vary in composition from dolomitic limestone to pure limestone (see Table 2.1).

	% dolomite	approx. MgO equivalent
limestone	0 - 10	0 - 2.1
dolomitic ls.	10 - 50	2.1 - 10.8
calcitic dol.	50 - 90	10.8 - 19.5
dolomite	90 - 100	19.5 - 21.6

Table 2.1 Nomenclature of calcitic and dolomitic carbonates; after Pettijohn, 1975

Of particular interest to this study are the stromatolite beds, which are found at several horizons and can be traced along strike over several kilometres. They are thought to represent algal structures, formed by sediment trapping by algal mats (Pettijohn, 1975). Stromatolites in the Wadi Fatima area vary in character from flat-laminated non-columnar types to columnar and even branching types; forms with convex upward laminae "Collenia" and "Conophyton", described for the first time by Karpoff (1955), are recognizable. Characteristic for the Wadi Fatima stromatolites is that the apeces of the columns often are recrystallized into quartz columns (see Plate 1). The upwards convexity of the stromatolites can be used to establish top and bottom of the beds (Hofmann, 1973, see Plate 1).

Stromatolites occur from Precambrian to Recent. The oldest examples have been described in the Bulawayan Group (> 2,600 Ma after Schopf et al., 1971) of Zimbabwe, have their maximum development in the Proterozoic and continue till Recent times (Gebelein, 1971). Their decline after the Late Precambrian is probably caused by the fast evolution of other, especially grazing organisms (Garret, 1970). Many attempts have been made (especially by Russian authors) to establish a stromatolite stratigraphy and Korolyuk (1960) reports on a subdivision of the Cambrian and Precambrian of E. Siberia with Collenia and Conophyton as trace fossils. Conophyton is restricted to the Precambrian (> 570 ± 10 Ma, Hofmann, 1973), the occurrence of this type of stromatolite in the Fatima area confirms the Precambrian age of the Fatima Group (see also Chapter 5 - Geochronology - for further discussion). Correlations of stromatolites in time is still in an infant stage (Preiss, 1972) and the only well-described examples in the African continent are by Bertrand-Sarfati and Raaben (1971) for the Taoudenni Basin in the Sahara, where five distinct stromatolite horizons occur in the Late Precambrian.

Environmental studies for stromatolites indicate them to occur generally in a shallow water environment, especially intertidal (Gebelein, 1972; Preiss, 1972 and Hofmann, 1973). Deep water occurrences have been described, as well as freshwater forms, but these are volumetrically insignificant (Hofmann, 1973).

In thin section, the massive dolomite consists almost entirely of interlocking dolomite crystals with a rhombohedral cleavage (idiotopic fabric of Friedman, 1965). The original structures are often obliterated by the dolomitization; lamellar twinning is very common. In the less dolomitized limestones the stromatolitic mm-scale banding is well-preserved by alternating limestone and sediment bands. The dolomitic rhombohedra in a calcitic matrix show the incomplete dolomitization. The

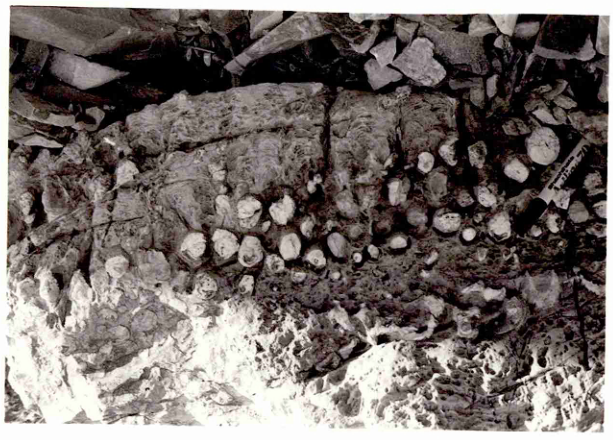

Plate 1 Stromatolite beds in F2, sample FA011

Plate 2 Tuffite layers in F3, sample FA133

Plate 3 Gas pipe structures, sample FA092

Plate 4 Accretionary lapilli, sample FA031

WADI FATIMA AREA

(western slope of Jabal Daf; $21^{o}33'$,$39^{o}55'$)

red sandstones are seen to be formed of rounded grains of quartz, orthoclase, and iron ore in a hematitized calcareous matrix, accessory minerals are muscovite and plagioclase.

Sedimentary structures in F2 are mainly the conspicuous growth banding of the stromatolites and the parallel lamination in the clastic sediments. The association of stromatolites and fine grained sediments supports the shallow marine (intertidal) environment, proposed for the stromatolites alone, with occasional clastic influxes. The upper boundary of F2 is sharp; the last thick dolomitic limestone bed indicates the upper boundary, above which no more limestones are found.

2.5.5 Upper Fatima Formation (sedimentary member) F3s

The Upper Fatima Formation (F3) consists of a thick sequence of sediments and volcanics, but is here subdivided in two members, a lower sedimentary and an upper volcanic member. The red coloured sedimentary member F3s is 161 metres thick and consists entirely of bright red, massive, medium to poorly bedded clastic sediments, varying in grain size from conglomerate to mudstone (see Figure 2.3). Only one basalt flow occurs in this member. The main rock type, a red, fining-upwards unit, displays many sedimentary features such as channel-fill, cross-bedding and parallel lamination. The bedding surfaces of the mudstones often show unimodal ripple marks and mud cracks. In the upper part of the member, many pumice and crystal layers (tuffites) are interbedded with the fining-upwards sediments (see Plate 2). The upper boundary of F3s is taken at the sharp contact with a red volcanic breccia with gas pipes, a clearly volcanic unit (Duyverman & Roobol, 1981). In thin section, the clastic sediments consist of subangular to rounded grains of feldspar and quartz with accessory muscovite in a fine grained hematitized tuffaceous matrix; the tuffites consist of subangular quartz

aggregates in a tuffaceous matrix with common muscovite.

The unimodal current direction (towards the WSW), fining-upwards sequences, composition and sheetlike geometry of the clastic units point at a proximal alluvial fan environment (Bull, 1972), the tuffites represent occasional volcanic events.

2.5.6 Upper Fatima Formation (volcanic member) F3v

The F3v member is a reddish, heterogeneous sequence of volcanics with minor sediments, occupying the upper slopes of Jabal Daf. The higher resistance to weathering and erosion of the often welded ash-flow tuffs (ignimbrites) and agglomerates gives rise to steep scarps on the north-western side of the mountain. The volcanic sequence consists of (for the use of terminology see Appendix B) fine tuffs, tuffs, volcanic breccias, ignimbrites and basalt flows. Although Jabal Daf shows the thickest succession (325 metres) of the F3v member in the whole Wadi Fatima area, this volcanic association was probably thicker, as the top has been removed by erosion.

Fine tuffs and tuffs occur throughout the F3v member; they form massive, poorly bedded sequences, consisting of crystal, pumice, lithic or mixed tuffs. In thin section these tuffs consist of fine grained quartz aggregates, as pumice fragments, or as angular grains, lithic fragments (basalt, andesite and rhyolite) and plagioclase (An_{25-8}) crystals in a fine tuffaceous matrix.

The volcanic breccias consist of very coarse, up to 35 cm in diameter, fragments of basalt, andesite and rhyolite in a fine grained hematitized matrix. Grading is totally absent and the pyroclastic character of tne breccias is indicated by gas pipes (Duyverman & Roobol, 1981) and occasionally by welding (otherwise the deposits might be confused with

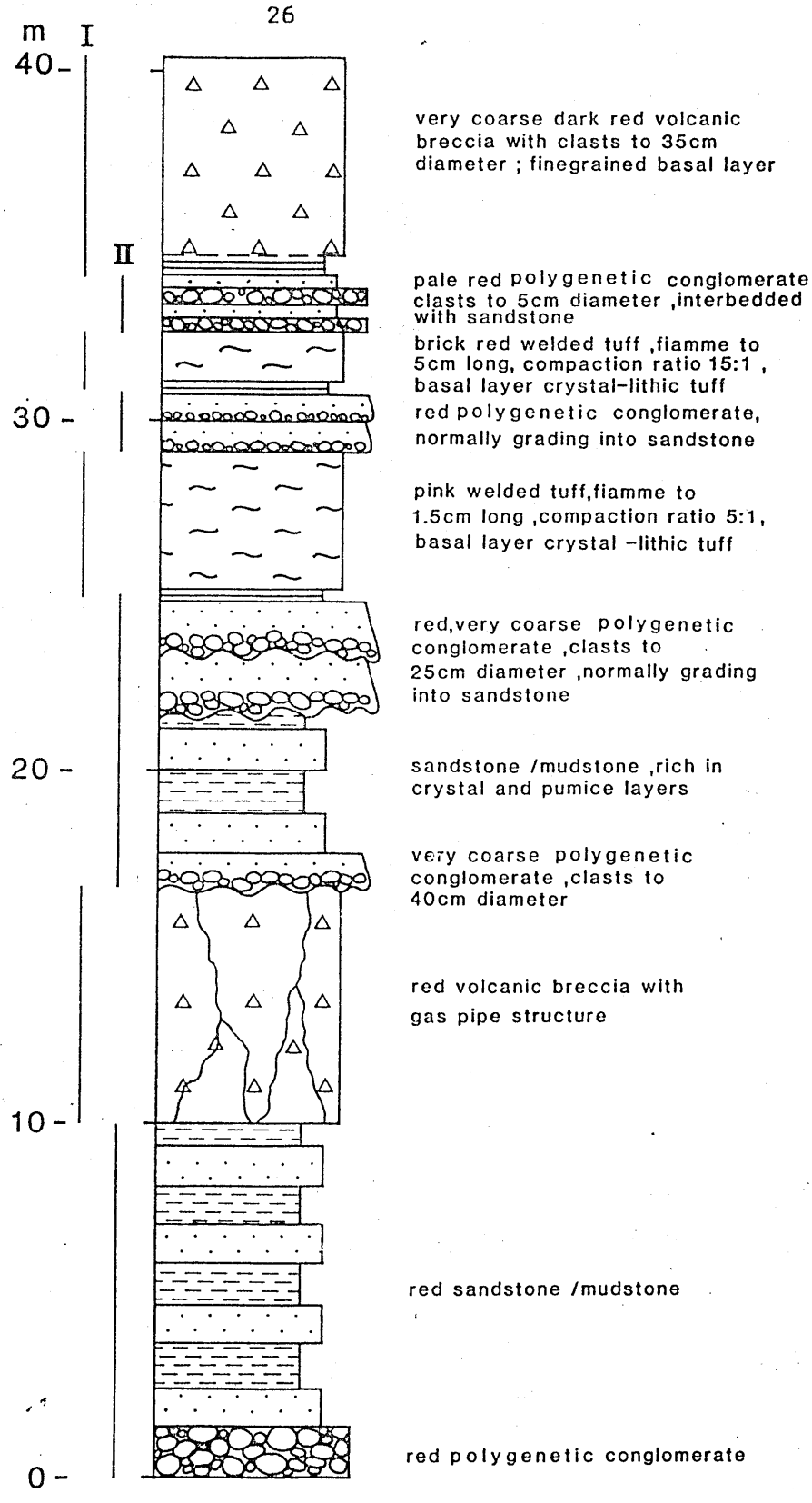

Figure 2.4 Section containing gas pipe structures; I - subaerial, II - subaquous (after Duyverman & Roobol, 1981).

epiclastic breccias such as lahars or mudflows). The gas pipes occur in the lower part of the F3v sequence (see Figures 2.3 and 2.4). These pipes are very striking in the field, since they were preserved by an infilling of calcite (see Plate 3); when this is removed by erosion the open gas pipes are identical to those of historical deposits (for example the flow breccias of Mt. Pelée, Martinique, as described by Perret, 1937 and Roobol & Smith, 1976). The pipes are several metres long, oriented normal to the stratification and occasionally bifurcate towards the base. They are not found in the welded ignimbrites on top of the breccias. The presence of numerous gas pipes indicates that these deposits have a subaerial, hot, pyroclastic origin, capable of heating underlying wet sediments (Duyverman & Roobol, 1981). In this section the breccia contains large angular clasts of aphyric or slightly porphyritic basalt, andesite and iron ore. The matrix is a fine grained complex of interlocking, hematitized quartz and feldspar (plagioclase An_9); accessory minerals and haematite, piedmontite (a Mn-epidote), titanite, chlorite and actinolite. The assemblage chlorite-actinolite-albite-epidote indicates greenschist metamorphism (after Winkler, 1974).

Ignimbrites are widespread in the F3v member. At least eight units have been distinguished (see Figure 2.3); ignimbrites (or ash-flow tuffs) are considered to be products of pyroclastic flows, irrespective of their volume or degree of welding (Sparks and Wright, 1979) and may consist of several flow units. No single characteristic is completely diagnostic for an ignimbrite, but they can be defined by a combination of mineralogy, colour, grain size, top-and-bottom features and style of welding (Sparks, 1977). None of the above-mentioned criteria, for example the occurrence and degree of welding, is a diagnostic criterion by itself, because some ignimbrites are completely unwelded.

Recognition of an ignimbrite flow unit will be discussed after Sparks et al. (1973): one flow unit always has a fine grained basal layer, an overlying layer which commonly shows layering by size grading of lithic and pumice fragments and on top a fine grained layer, often removed by erosion. A ground surge deposit, as defined by Sparks and Walker (1973), may underlie the flow unit. Figure 2.5 shows a complete flow unit after Sparks et al. (1973), compared with an ignimbrite flow in the Wadi Fatima area (F3v). Welding may occur in the central parts of flow units, whereby the degree of welding can be measured by the compaction ratio, i.e. the length/thickness ratio of flattened pumice clasts. Columnar jointing, often seen in the Wadi Fatima area, indicates cooling units, which may comprise several flows.

A typical Wadi Fatima ignimbrite flow (see Figure 2.5) is bright red coloured with darker, often pink, top-and-bottom layers. The fine grained basal layer is unwelded and overlain by a sometimes welded central part with poorly layered pumice, lithic and crystal clasts. On top a fine grained tuff layer is sometimes found. The degree of welding in the central part, as measured by the compaction ratios of the flattened pumice clasts, often is highest in the middle of this central unit and decreases towards the bottom and the top. Normal grading of lithics and reverse grading of pumice clasts, as indicated by Sparks et al. (1973), was not recognized, probably due to welding and metamorphism. In thin section, the welded parts of the ignimbrite clearly show the eutaxitic texture (caused by the linear arrangement of devitrified glass shards and collapsed pumice fragments). Crystals of sanidine, plagioclase (An_{20}), quartz, fragments of pumice and lithics (basalt and rhyolite) are embedded in a fine grained tuffaceous matrix (see Plate 5).

Accretionary lapilli are common in the ignimbrites and tuffs; they occur as round, often partially infilled bodies with a concentric structure

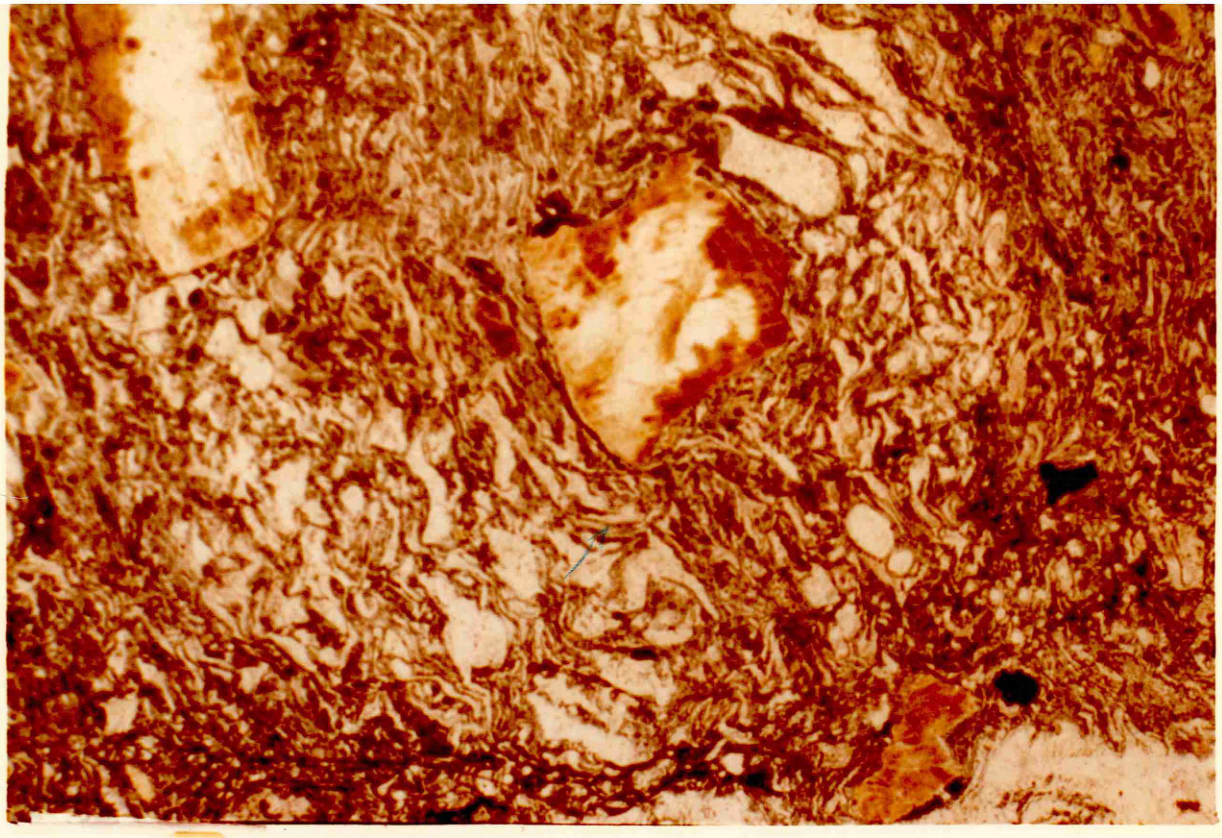

Plate 5 Plagioclase crystals in ignimbrites (note eutaxitic texture), sample FA 182

WADI FATIMA AREA (see Fig 2.3)

1 mm

Plate 6 Pumice lenses in F1 mudstone , sample FA090

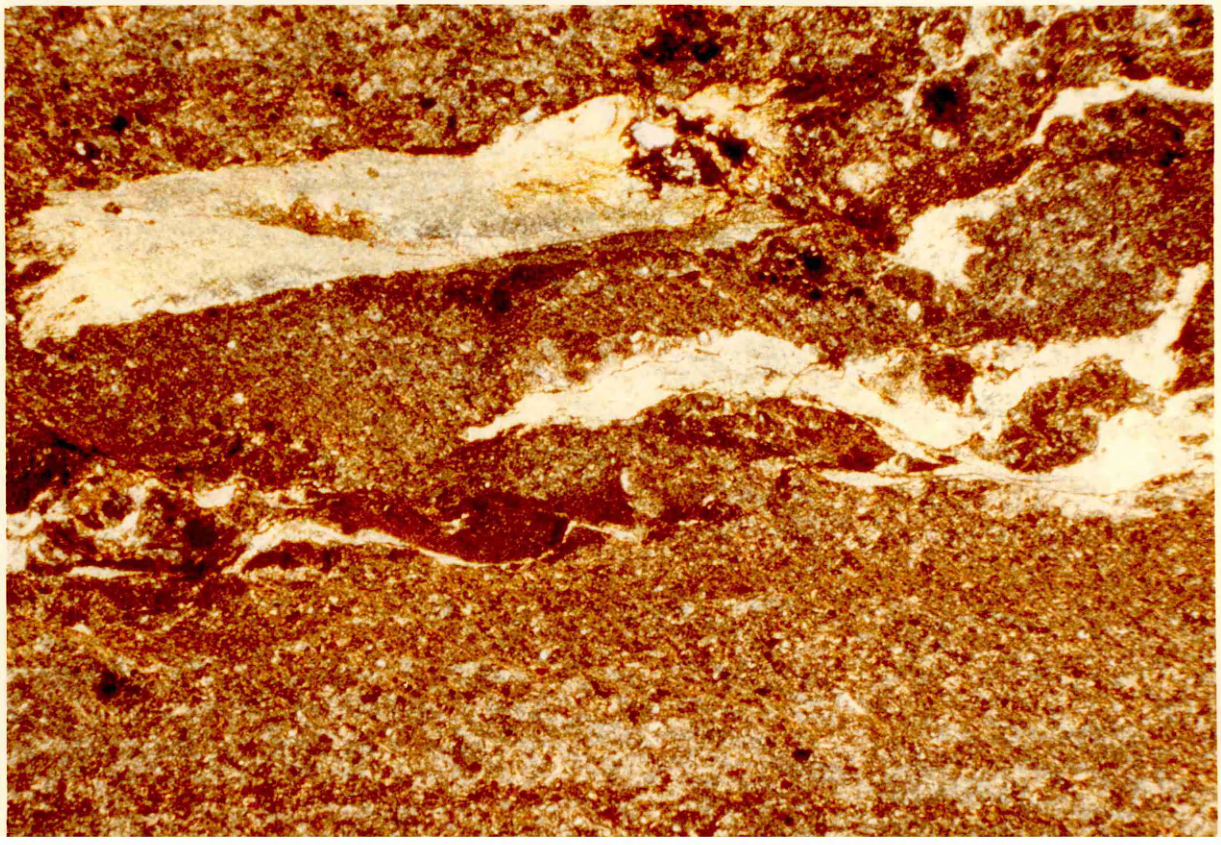

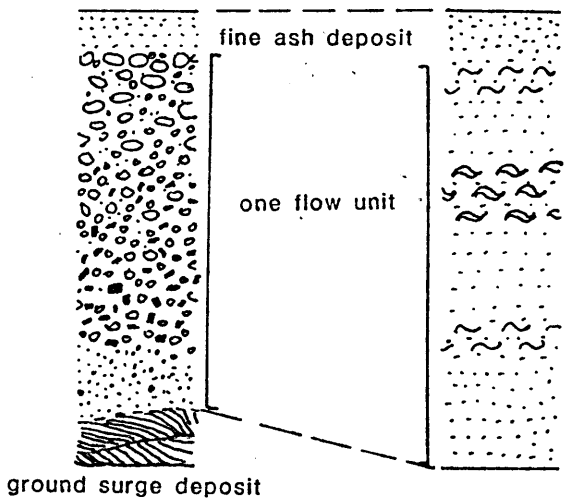

Figure 2.5 Comparison of flow units in ignimbrites between Recent ignimbrites (after Sparks et al.,1973) and Precambrian ignimbrites of Saudi Arabia; ○ -pumice crystals, ▪ -lithics, ∿∿ welded parts of ignimbrite. Finer grained layers often are seen in Precambrian ignimbrites, the ground surge deposit, however, was never visible. (see text for further discussion)

and are pea-shaped (see Plate 4). The lapilli show a distinct decrease in grain size from core to rim and consist entirely of clastic volcanic material and devitrified glass. They probably developed in an ash-charged volcanic cloud by the accretion of ash around a core due to the condensation of moisture on the core and fell to the ground much like hailstones (Moore & Peck, 1962). They indicate the extrusive character of the rocks enclosing the lapilli and also the subaerial environment of deposition. Recent examples all occur close to the eruption vent (Moore & Peck, 1962).

The sediments of the F3v member occur in the lowermost and uppermost parts of the sequence and are normally graded, red, cycles of conglomerate and sandstone/mudstone; occasional sheets of polygenetic conglomerates occur. These sediments show a prominent layering and imbrication, are subrounded to subangular and consist of boulders up to 40 cm in diameter. In thin section the sediments are indistinguishable from those in the F3s member.

The environment of deposition of the F3v member is clearly subaerial, as evidenced by the ignimbrites, accretionary lapilli and sediments. The presence of accretionary lapilli and coarse volcanic breccia indicate that the eruption vent for the volcanics must have been close.

2.5.7 Fatima Group basalt flows

Basalt flows (called andesite sills by other authors - Nebert *et al.*, 1974; Hirayama, 1977, but renamed because of geochemical and field evidence) occur throughout the Fatima Group and are not indicated separately on the geological map of the area. They are infolded in the Fatima Group. In the field the flows are light to dark green, aphyric to porphyritic (with feldspar phenocrysts up to 1 cm long) basalts with a very fine grained matrix. Vesicular and amygdaloidal textures are

common.

In thin section, the aphyric basalts consist of a very fine grained mass of aligned feldspars (microlites) in a micro- to cryptocrystalline, hematitized matrix (pilotaxitic texture); the more porphyritic types consist of plagioclase (An_{85-55}), augite, chlorite, epidote, quartz, olivine, magnetite and accessory hematite and actinolite. Vesicular and amygdaloidal types show rounded vesicles, partly to wholly infilled with quartz and calcite. The geochemical data of the basalts are indicated in Appendix C.

There has been a long-standing controversy as to whether this group of rocks represented volcanic flows or sills (the latter was supported by Nebert et al., 1974). Discordant contact and chilled margins were the main arguments for a sill origin, but these phenomena are very rare. The following arguments might indicate otherwise:

1. Flow structures are often displayed, both on microscopic and macroscopic scale; these structures occur mainly in the centre of the flow.
2. The deposits show generally a massive centre and a blocky, porous top and bottom.
3. Vesicular and amygdaloidal textures argue for a near-surface extrusion.

3 Badr area

3.1 Introduction

The Badr area lies halfway between Jeddah and Medina, in the northeastern corner of the Al Hamra quadrangle (see Figure 3.1). It consists mainly of NW/SE trending Late Precambrian volcanic rocks, occasionally intruded by diorites. Older, tonalitic and alkalic granitic rocks that have been sampled during the geochronological part of this study, lie to the south of the study area and are the basement on which the volcanics lie unconformably (see Figure 3.4 and Chapter 5). Access is good along the main Jeddah - Medina road along Wadi Safra; the area lies directly north of the town of Badr. The new liquified gas pipeline, running from Dhahran to Yanbu al Bahr crosses the area and has service dirt roads with it. In contrast to the Wadi Fatima area, no previous published geological work has been carried out in the Badr area; the BRGM (French geological mission), however, mapped areas to the north of 24^{o} latitude (see Figure 3.1). Similarities between the volcanics and associated sediments of the Wadi Fatima and Badr areas initiated the work in the latter area. Field studies, geochronology, geochemistry and correlation have been undertaken to clarify the geological history of these volcanics.

3.2 Previous work

Brown et al. (1962) in their 1:2,000,000 geological compilation map of Saudi Arabia show the whole area, here described, as belonging to one unit "gd" that comprises andesite, diabase, slate, greenstone, conglomerate, rhyolite and andesite porphyry. No more detailed geological map of the Badr area has ever since been produced; the Al Hamra quadrangle (see Figure 3.1) is currently being mapped by the DGMR. BRGM project reports for areas north of latitude 24^{o} are available. The picture emerging from these BRGM contributions, relating to the Badr area volcanics, is far from clear. A stratigraphic scheme for the large Yanbu al Bahr quadrangle (after Pellaton, 1979) is shown in Figure 3.2. The continuation

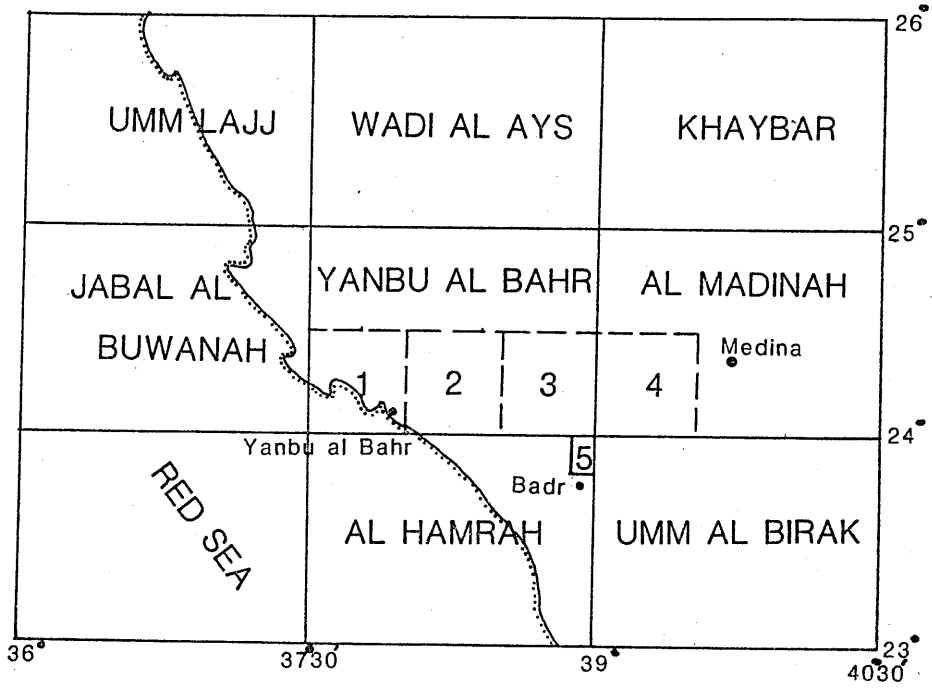

Figure 3.1 The northwestern part of the Arabian Shield, showing the location of the Badr fieldwork area (5) in the northeastern corner of the Al Hamra quadrangle. North of 24° latitude the following areas are of significance for this study : 1 - Wadi Kamal (Alabouvette et al., 1975), 2 - Yanbu al Bahr (Alabouvette et al., 1975), 3 - Jabal Sutayhat Sharq (Aguttes, 1973), 4 - Bi'r al Furaysh (Brosset, 1977).

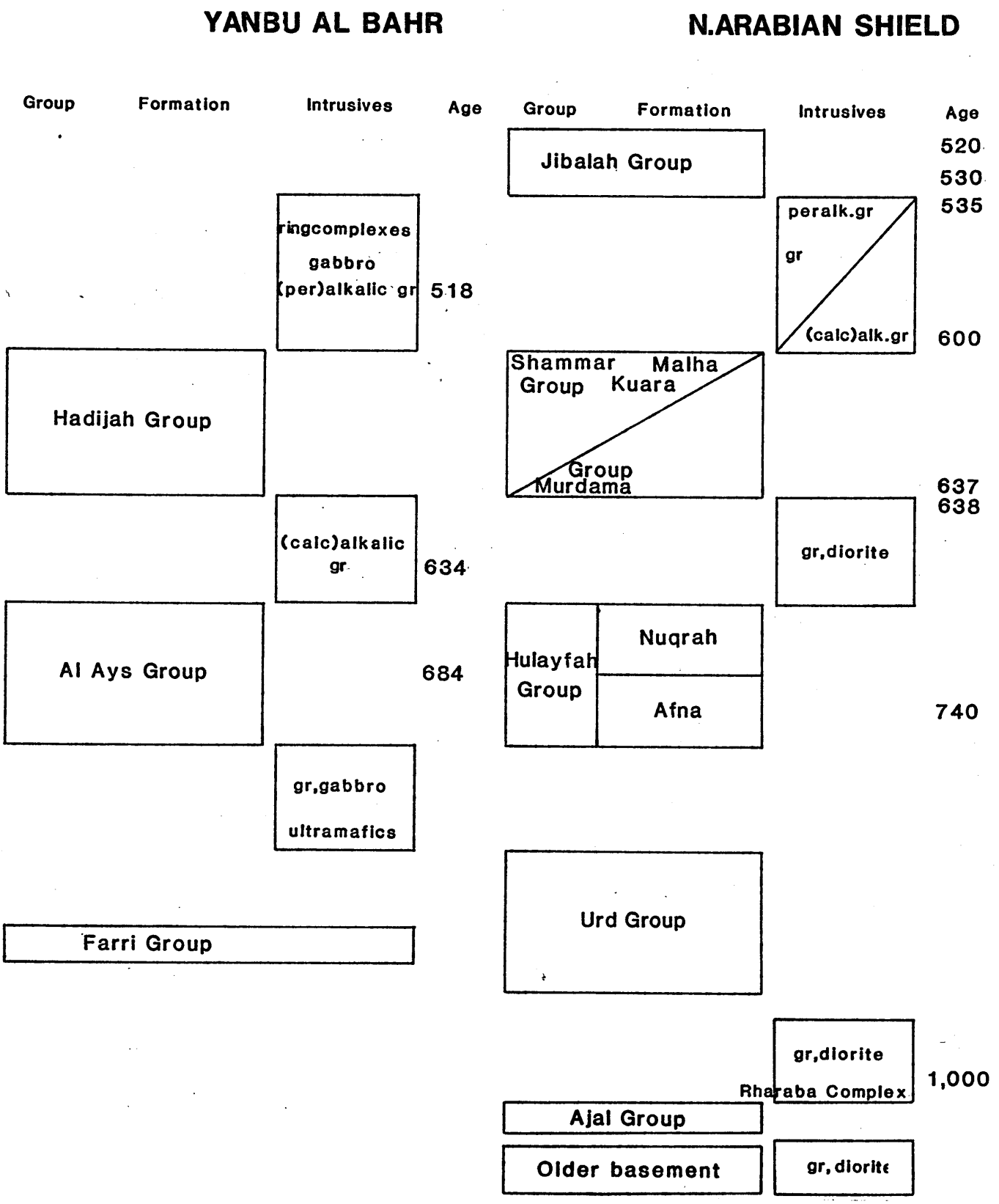

Figure 3.2 Lithostratigraphical columns for the Yanbu al Bahr quadrangle and the northern Arabian Shield (after Pellaton, 1979 and Delfour, 1977); gr - granite, alk - alkalic .

of the Badr area volcanics towards the northwest is considered to belong to the Halaban, Murdama and Shammar Groups in the Yanbu al Bahr area by Alabouvette et al. (1975, note that this area is a small part of the large Yanbu al Bahr quadrangle); to the Upper Hulayfah Group in the Jabal Sutayhat Sharq area by Aguttes (1973); to the Lower Hulayfah Group by Brosset (1977) and to the Middle Al Ays Group (probably equivalent to the Middle Hulayfah Group) by Pellaton (1979) and Kemp et al., (1980). Lack of geochronological work or highly variable results (Kemp et al., 1980) and little geochemical work to back up the correlation, seem to the author the main constraints.

According to the BRGM compilations, plutonic rocks occur throughout the stratigraphic column and have been used for geochronological studies. Intrusive relations enabled Kemp et al. (1980) to outline approximate age brackets for the Al Ays Group. Most authors agree that the plutonic rocks directly north of the Badr area are intrusive into the volcanics and of granitic to granodioritic composition. Granitic, gabbroic and ultramafic plutonic rocks probably underlie the Badr volcanics and its northerly extension.

3.3 The Badr area

The location of the Badr area is shown on Figure 3.1, whilst the geological map of the area is given on Figure 3.3. The Badr volcanics form steep, rugged mountains with altitudes in the fieldwork area up to 2000 metres. Wadi Safra, the main drainage channel in the area, is used by the main Jeddah - Medina road. Silicic and intermediate volcanic rocks with intercalated sediments form the bulk of the field-work area, but minor intrusive rocks crop out in the northern part. These plutonic rocks (an oval intrusion of quartzdiorite and a micro-granite sill) and probably older plutonic rocks to the south of the area will be discussed separately. By the author, together with M.G.

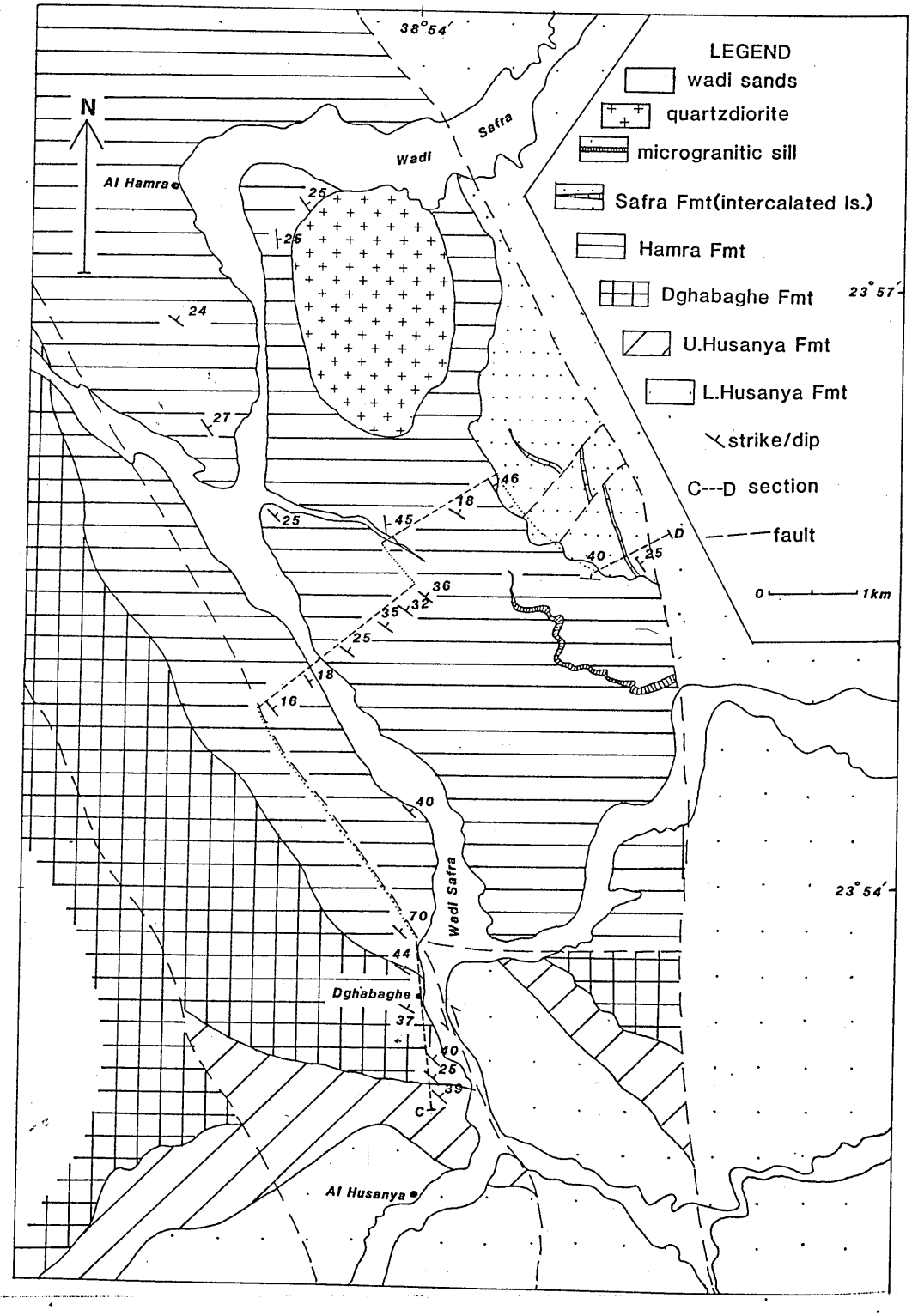

Figure 3.3 Geological map of the Badr area; the broken line C———D indicates the position of the detailed lithostratigraphical traverse, shown on Figure 3.5; ls-limestone, L.-Lower,U.-Upper.

Clark, the DGMR geologist responsible for mapping the Al Hamra area, plutonic rocks (tonalites and alkali granites) were sampled for geochronological studies (see Figure 3.4). The age dating results will be discussed in Chapter 5.6.3.

The main purpose of the fieldwork was to establish a detailed stratigraphic column of the volcanic rocks of 1800 metres thick by sampling along a SW/NE trending traverse (see Figures 3.3 and 3.5). The lithological description of the rock units will be discussed in chronological order under the sub-headings of pre-volcanic plutonic rocks, the volcanic Husanya (flowbanded rhyolites, basalts, andesites), Dghabaghe (silicic volcanics and intercalated sediments), Hamra (coarse silicic volcanics and sediments) and Safra (andesites and intercalated limestones) Formations and the post-volcanic intrusions.

The structural geology of the Badr area is simple. A NW/SE striking sequence with minor internal unconformities forms most of the area. A low-angle unconformity was reported (Warden, pers. comm.) between the Hysanya (andesitic) and Dghabaghe (rhyolitic) Formations, but in the field the two formations seem to be conformable. A clear unconformity can be seen between the Hamra and Safra Formations, where andesites and intercalated dolomitic limestones unconformably overlie rhyolitic tuffs and ignimbrites. The volcanic sequence as a whole is blockfaulted along NW/SE to N/S faults, whereby the blocks have been tilted towards the northeast. Minor E/W to SW/NE faults occur within the faulted blocks. No large-scale folding was observed in the Badr area. In the north of the area quartzdiorites clearly intrude the volcanic pile. All volcanic rocks have been metamorphosed to lower greenschist facies and show prominent NW/SE to N/S cleavage.

3.4 Lithological description of the rock units

3.4.1 Introduction

Because the detailed geology, geochronology and volcanic history of the Badr area were unknown, it was decided to construct a detailed stratigraphic column of the volcanic rocks that dominate the geology of the area. This column is shown in Figure 3.5. The 1800 metres thick succession consists of volcanics and minor volcaniclastics. The detailed lithostratigraphical column shows rock types, structural data, sample location and number and sedimentological data. Because of major differences in rock type, the volcanics and sediments were further subdivided into four formations, all named after local villages and wadis, namely the Husanya, Dghabaghe, Hamra and Safra Formations (see Figure 3.3 for the geological distribution of these formations). Older plutonic rocks outside the area and intrusive rocks within the area will be discussed separately. The Badr rock types were classified in the same way as those of Wadi Fatima in order to facilitate correlation; chemical compositions (majors, traces and rare earth elements) and classification are shown in the Appendix.

3.4.2 Pre-volcanic plutonic rocks

Two suites of alkali granites and tonalites crop out immediately south of the area and were collected for age dating. Contacts between plutonic and volcanic rocks suggest that the volcanic rocks unconformably overlie both plutonic rock types. Contacts between the tonalites and the alkali granites indicate that they are probably of the same age. Age dating supported these deductions (see Chapter 5).

Alkali granites crop out as large bodies directly south of the Badr area. They form large, low hills that are strongly N-S and E-W jointed. In hand-specimen they are leucocratic (colour index < 15), light grey to

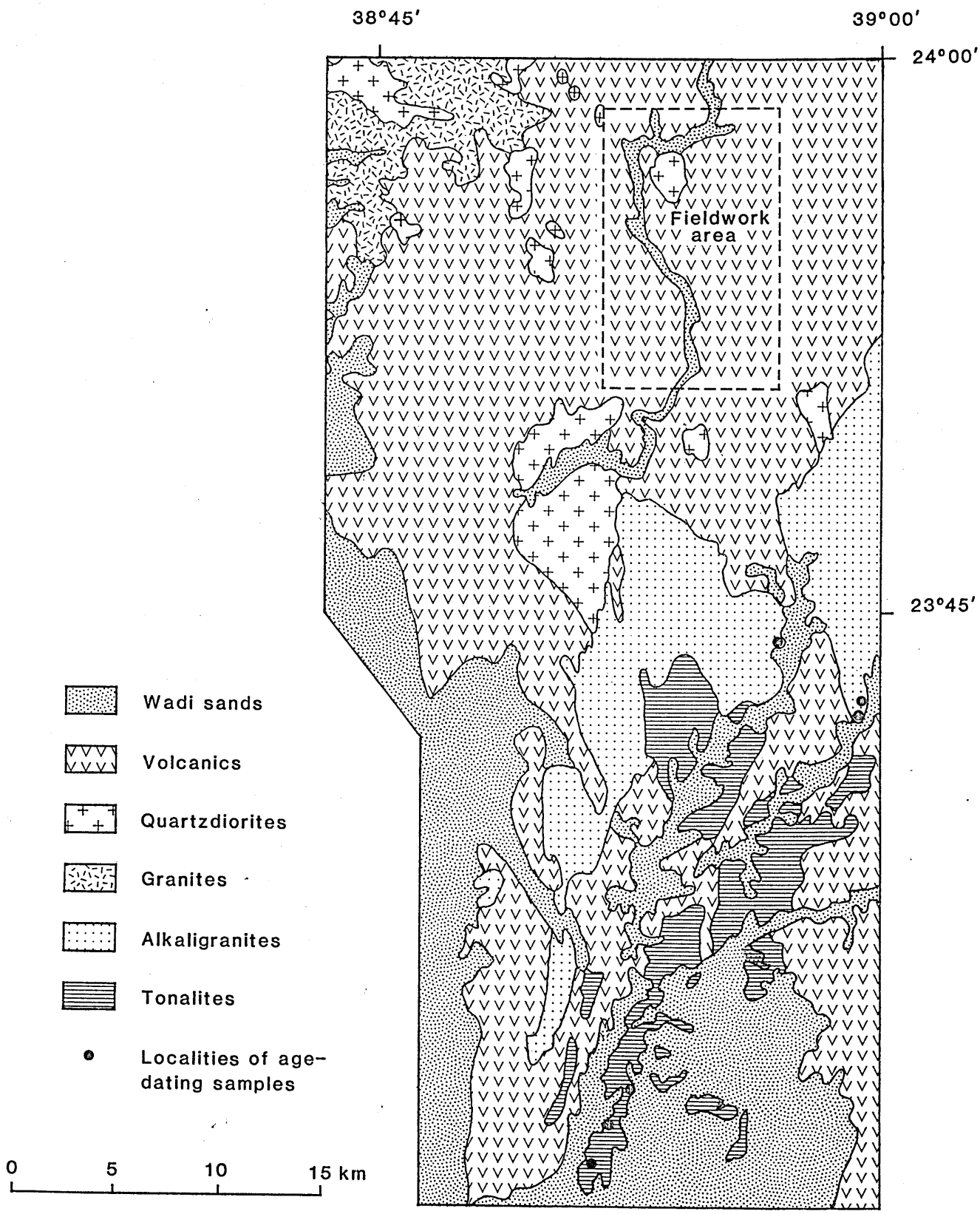

Figure 3.4 Granitic and volcanic terrain in the eastern part of the Al Hamra quadrangle (after an unpublished map of M.D.Clark,DGMR).

pink and medium to coarse grained; they have a massive fabric. This group of rocks has an average modal felsic analysis of 35% quartz, 60% alkali feldspar and 5% plagioclase and are alkali granites according to Streckeisen (1976). In thin section they can be seen to consist of microcline, orthoclase, plagioclase (An_{12-8}), hornblende (often replaced by biotite), chloritic aggregates (pennine ?), quartz and accessory sphene, muscovite and calcite. Perthitic and, more rarely, antiperthitic, textures occur in the feldspars (see Plate 8). Low initial strontium ratios, high Na_2O content (> 4.0%) and the occurrence of hornblende and sphene classify these granites as I-type granites (Chappell and White, 1974), being derived from igneous material.

The tonalites occur as elongated belts south of the alkali granites. They are also jointed along E-W and N-S trends and form low ridges. In the field they are grey-green to dark green, medium grained, often have a streaked appearance and are distinctly darker in colour than the alkali granites (colour index 40). Amphiboles show a weak lineation giving the rock a gneissose fabric. In thin section these plutonic rocks (with a modal felsic composition of 40% quartz, 5% alkali feldspar and 55% plagioclase they are tonalites according to Streckeisen, 1976) consist mainly of normally zoned plagioclase (An_{33-16}), muscovite, quartz, alkali feldspar, sphene, epidote, hornblende (often replaced by biotite) and accessory apatite, calcite and iron ore; the feldspars are often altered to sericite. Some sections show a mortar texture with rounded and fractured feldspar grains in a matrix of elongated and sutured quartz and schlieren of biotite; the sections with a well-developed mortar texture contain muscovite (see Plate 7).

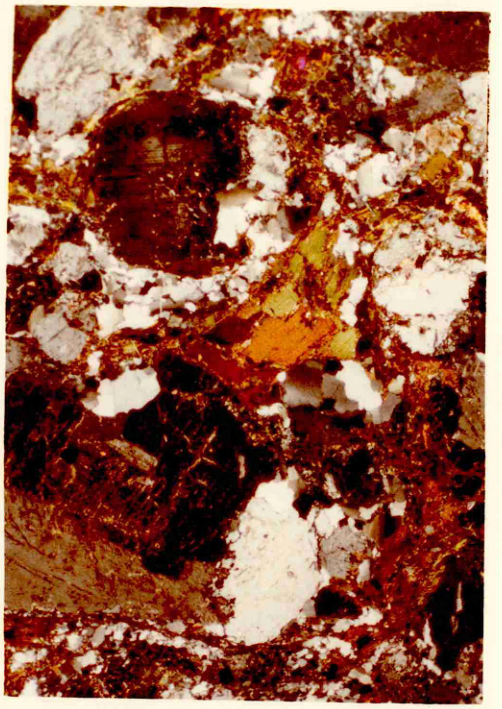

Plate 7 Tonalite with mortar texture (crossed nicols), sample HT1; locality 35 km south of Badr area, $23^{o}33'$,$38^{o}53'$

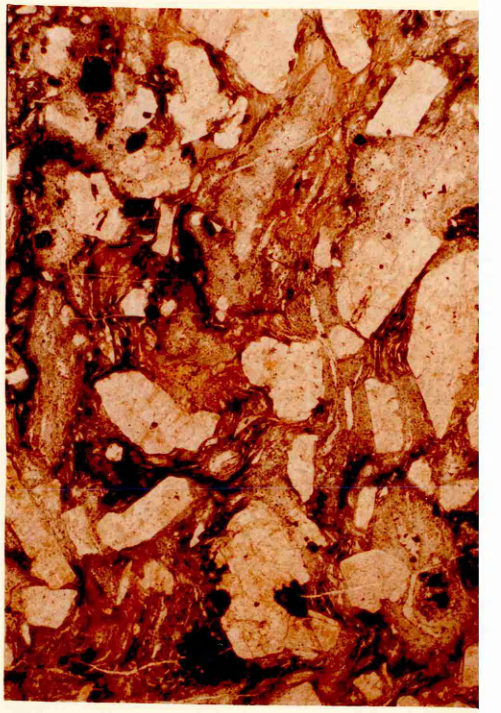

Plate 9 Strongly welded ignimbrite, sample BA205 near Dghabaghe village (see p. 37)

1mm

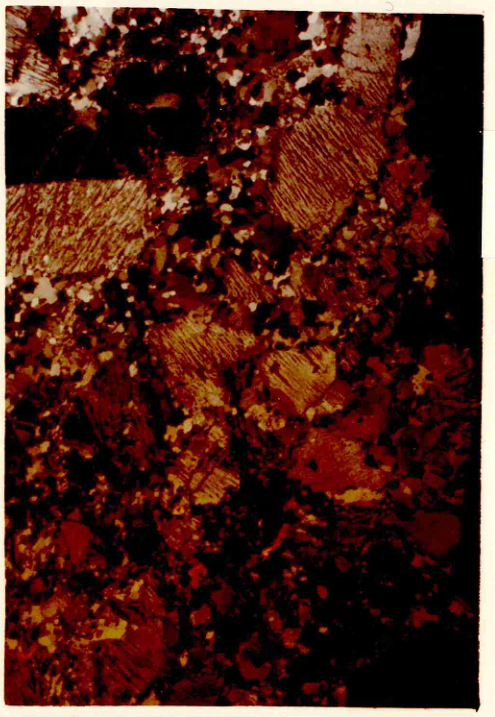

BADR AREA

Plate 8 Alkali granite with perthitic texture (crossed nicols), sample HA3; locality 15 km SSE of Badr area, $23^{o}45'$,$38^{o}56'$

3.4.3 The Badr volcanics

3.4.3.1 Subdivision

The Badr volcancis, largely occupying tne geological map of the area (see Figure 3.3) form a thick (more than 1800 metres) heterogeneous pile of different rock units, sometimes separated by angular unconformities. To enable a more accurate evaluation of the several rock types and their paleoenvironment, the Badr volcanics were subdivided into four, in the field distinguishable formations, namely the Husanya, Dghabaghe, Hamra and Safra Formations, named after local villages or wadis.

The Husanya Formation is a dark coloured, massive unit of flowbanded rhyolites and basic lavas with intercalated tuffs; the Dghabaghe Formation, possibly separated from the Husanya Formation by a low-angle unconformity, consists of a varicoloured, red, green and yellow succession of acidic volcanics and intercalated sediments and is conformably overlain by the Hamra Formation, formed of coarse volcanics and intercalated sediments; the youngest volcanic formation is the Safra Formation, which is separated from the Hamra Formation by a clear angular unconformity. It consists of dark basic lavas and rare intercalated limestones, comparable to the dolomitic limestones of the Wadi Fatima area.

3.4.3.2 The Husanya Formation

The Husanya Formation is the oldest volcanic formation in the area and consists of two divisions, a lower part formed of mainly flowbanded rhyolites and an upper part formed of basalts and andesites with intercalated tuffs. The Husanya Formation occurs in the southern part of the area, but because of blockfaulting and tilting the flowbanded rhyolites of the lower part of the formation crop out in the eastern part of the area.


rhyolite


andesite


basalt


sill


volcanic breccia


ignimbrite


tuff


fine tuff


(dolomitic) limestone


mudstone


siltstone


sandstone


conglomerate


granitic rocks

Sedimentological features

parallel lamination


small-scale and large-scale cross-bedding


erosional lower boundaries


gas pipe structures


columnar jointing

Figure 3.5 Legend for Badr section. True thickness in metres; measured strike and dip are indicated left of the column; sample numbers are also shown. The following abbreviations are used: d.-dark, l.-light, diam-diameter, fu-fining upwards, occ-occasional, ls-limestone, dol-dolomite, cr-crystal, pum-pumice, lith-lithic, porph-porphyritic, strom-stromatolithic, elong-elongated, sl-slightly, volc-volcanic, v-very, ves-vesicular, amygd-amygdaloidál, str-strongly.

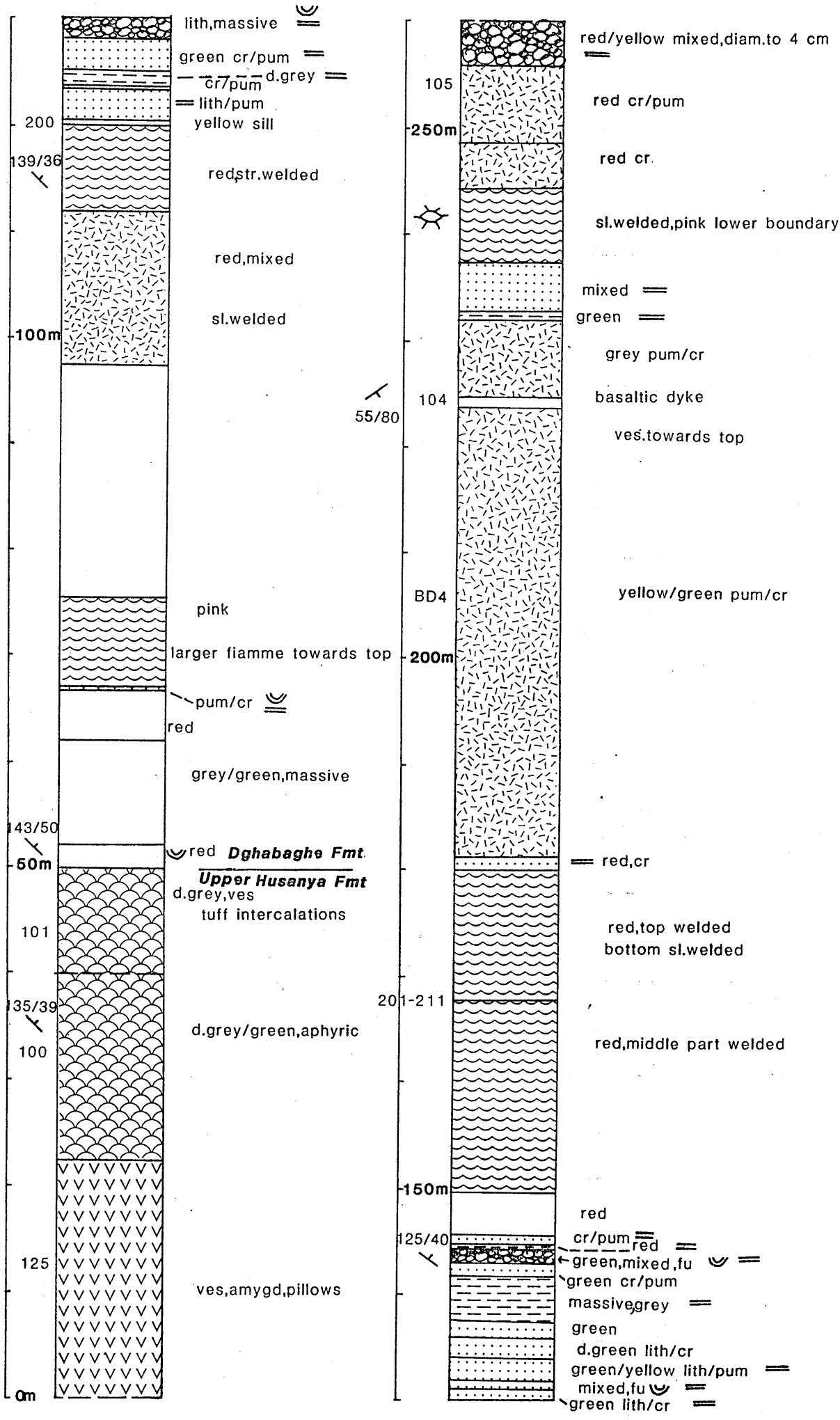
lith,massive
green cr/pum
d.grey
cr/pum
lith/pum
200
yellow sill
139/36
red,str.welded
red,mixed
sl.welded
100m
pink
larger fiamme towards top
pum/cr
red
grey/green,massive
143/50
red Dghabaghe Fmt
50m
Upper Husanya Fmt
d.grey,ves
tuff intercalations
101
135/39
d.grey/green,aphyric
100
125
ves,amygd,pillows
0m
red/yellow mixed,diam.to 4 cm
105
red cr/pum
250m
red cr
sl.welded,pink lower boundary
mixed
green
grey pum/cr
104
55/80
basaltic dyke
ves.towards top
BD4
yellow/green pum/cr
200m
red,cr
red,top welded
bottom sl.welded
201-211
red,middle part welded
150m
red
125/40
cr/pum
red
green,mixed,fu
green cr/pum
massive,grey
green
d.green lith/cr
green/yellow lith/pum
mixed,fu
green lith/cr

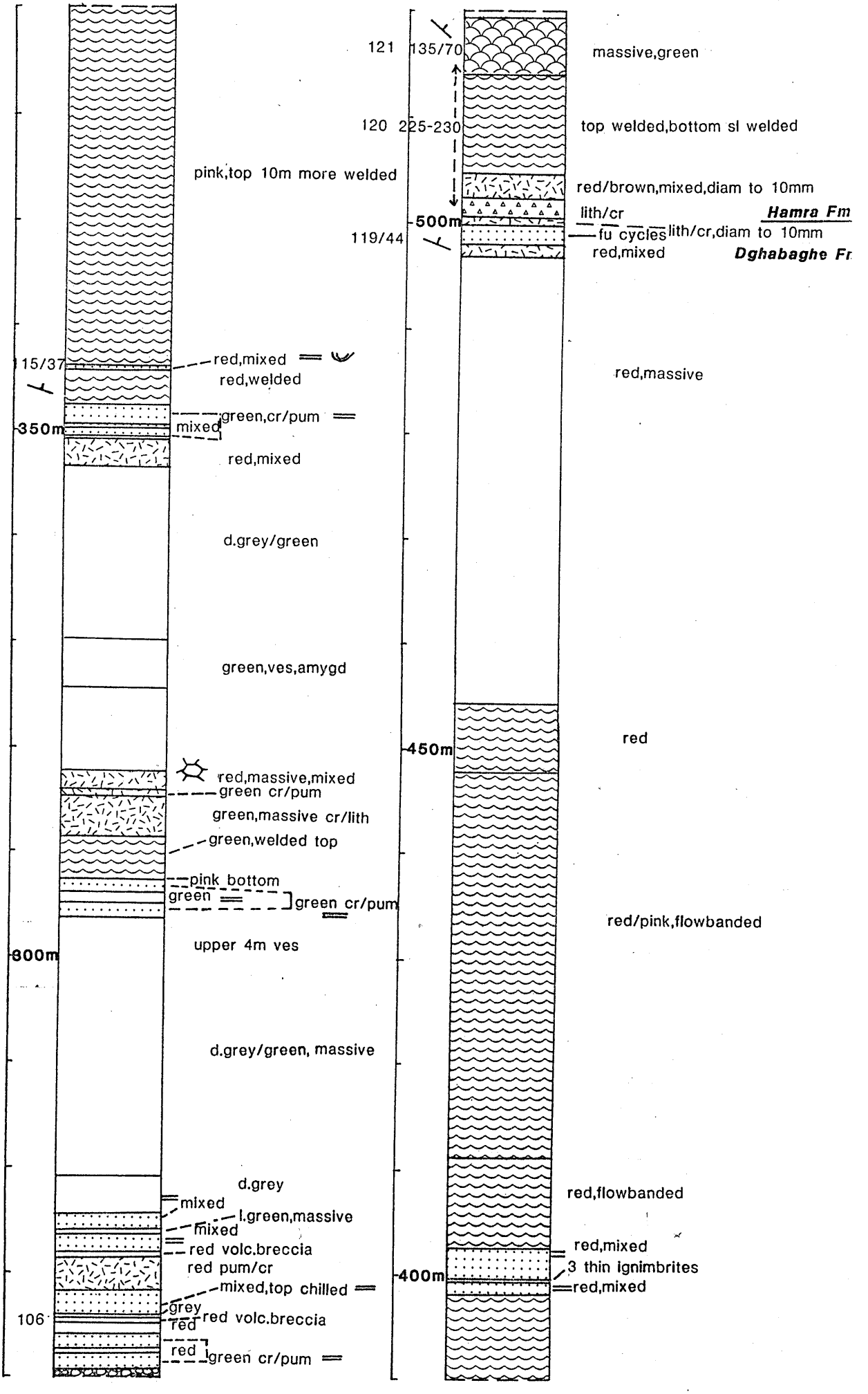
121
135/70
massive,green
120
225-230
top welded,bottom sl welded
pink,top 10m more welded
red/brown,mixed,diam to 10mm
lith/cr
Hamra Fm
500m
119/44
fu cycles
lith/cr,diam to 10mm
red,mixed
Dghabaghe Fr
115/37
red,mixed
red,welded
red,massive
green,cr/pum
350m
mixed
red,mixed
d.grey/green
green,ves,amygd
red,massive,mixed
450m
red
green cr/pum
green,massive cr/lith
green,welded top
pink bottom
green
green cr/pum
red/pink,flowbanded
upper 4m ves
800m
d.grey/green, massive
d.grey
red,flowbanded
mixed
l.green,massive
mixed
red volc.breccia
red,mixed
red pum/cr
3 thin ignimbrites
400m
mixed,top chilled
red,mixed
grey
106
red
red volc.breccia
red
green cr/pum

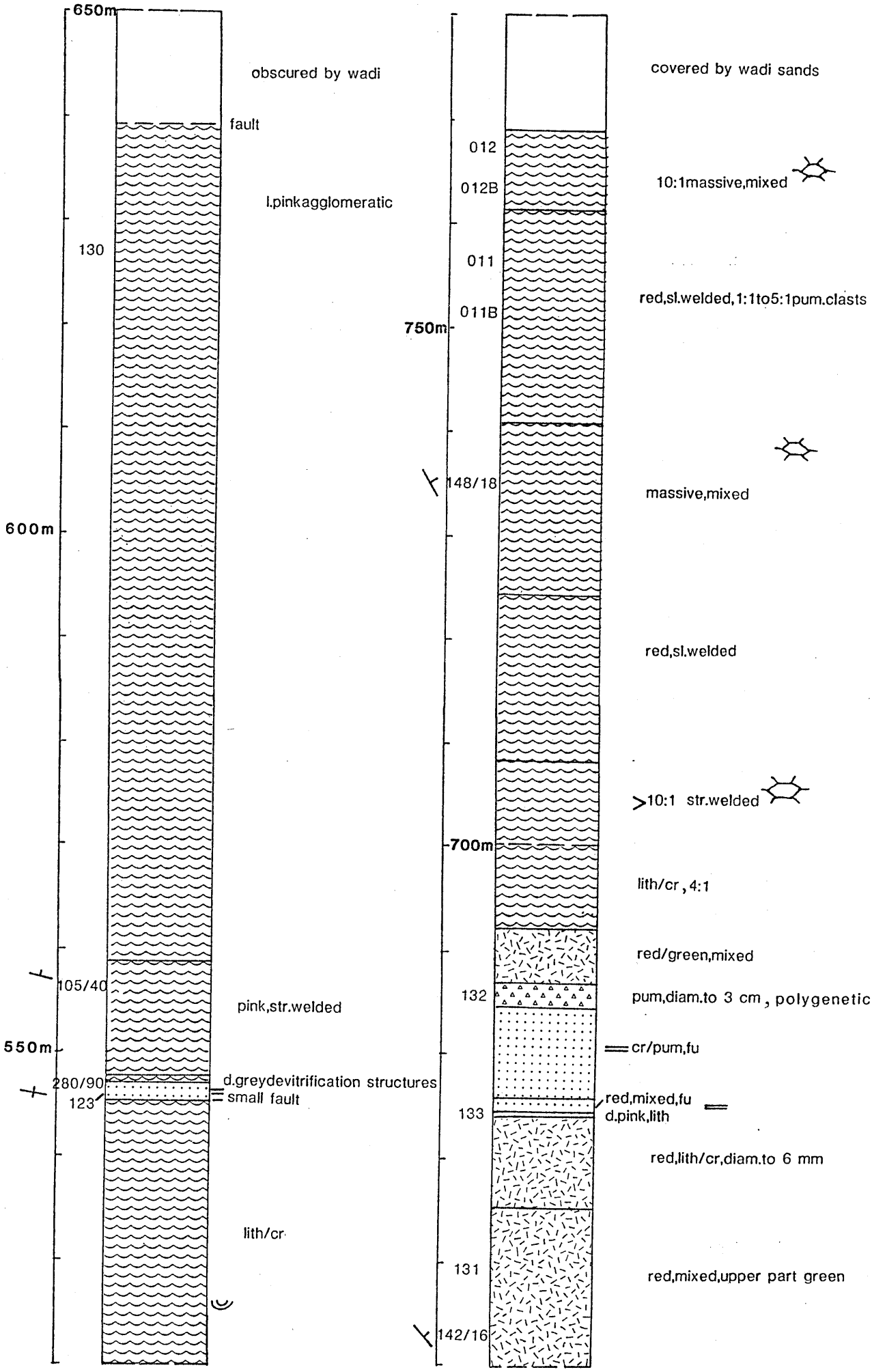
650m
obscured by wadi
fault
l.pinkagglomeratic
130
600m
105/40
pink,str.welded
550m
280/90
123
d.greydevitrification structures
small fault
lith/cr
covered by wadi sands
012
10:1massive,mixed
012B
011
red,sl.welded,1:1to5:1pum.clasts
011B
750m
148/18
massive,mixed
red,sl.welded
>10:1 str.welded
700m
lith/cr , 4:1
red/green,mixed
132
pum,diam.to 3 cm , polygenetic
cr/pum,fu
red,mixed,fu
d.pink,lith
133
red,lith/cr,diam.to 6 mm
131
red,mixed,upper part green
142/16

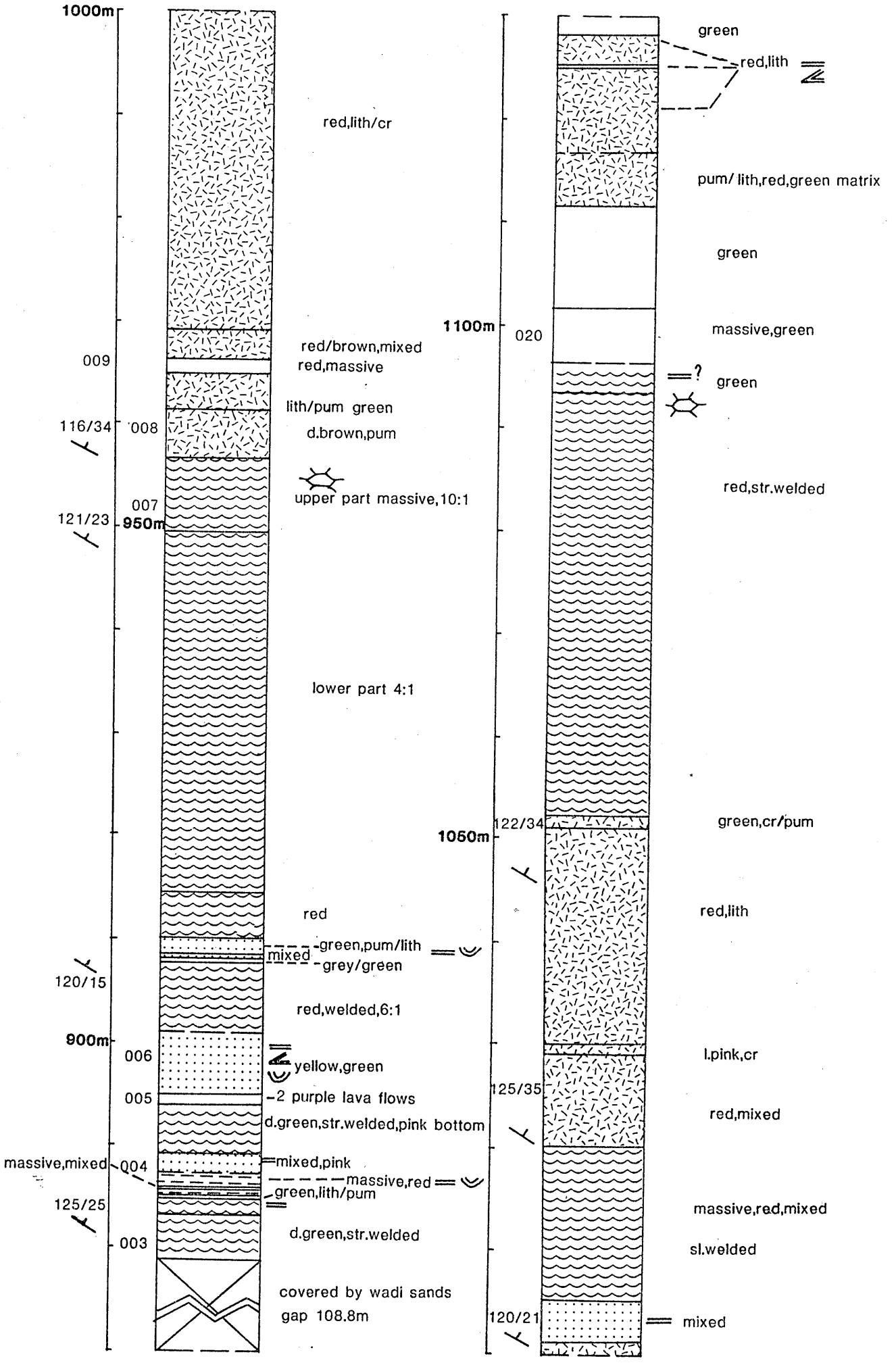
1000m
red,lith/cr
009
red/brown,mixed
red,massive
116/34
008
lith/pum green
d.brown,pum
007
upper part massive,10:1
121/23
950m
lower part 4:1
red
mixed
-green,pum/lith
-grey/green
120/15
red,welded,6:1
900m
006
yellow,green
005
-2 purple lava flows
d.green,str.welded,pink bottom
massive,mixed
004
mixed,pink
massive,red
green,lith/pum
125/25
003
d.green,str.welded
covered by wadi sands
gap 108.8m
1100m
020
green
red,lith
pum/ lith,red,green matrix
green
massive,green
green
red,str.welded
122/34
1050m
green,cr/pum
red,lith
l.pink,cr
125/35
red,mixed
massive,red,mixed
sl.welded
120/21
mixed

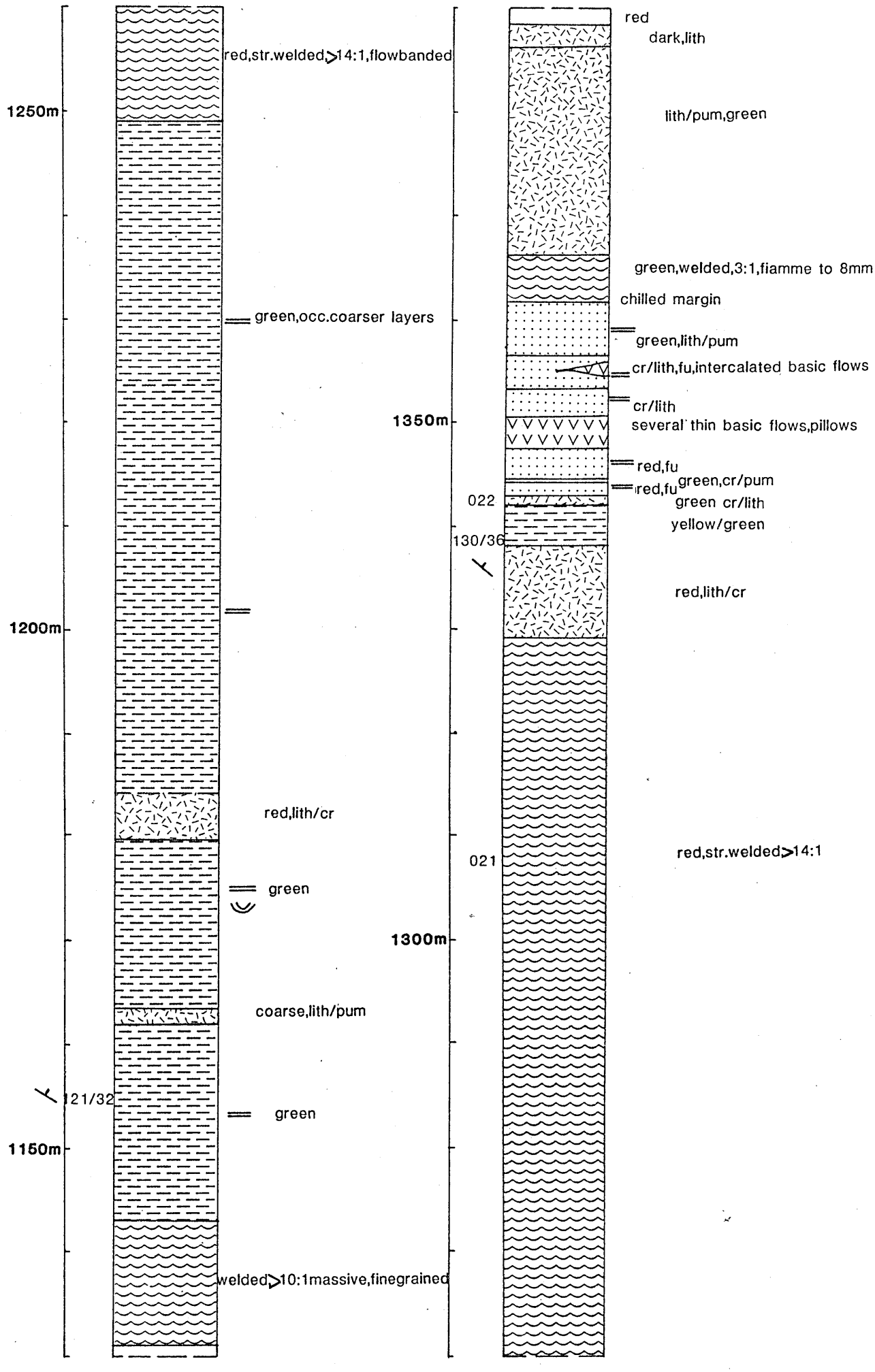
red,str.welded>14:1,flowbanded
1250m
green,occ.coarser layers
1200m
red,lith/cr
green
coarse,lith/pum
121/32
green
1150m
welded>10:1massive,finegrained
red
dark,lith
lith/pum,green
green,welded,3:1,fiamme to 8mm
chilled margin
green,lith/pum
cr/lith,fu,intercalated basic flows
cr/lith
1350m
several thin basic flows,pillows
red,fu
red,fu
green,cr/pum
022
green cr/lith
yellow/green
130/36
red,lith/cr
021
red,str.welded>14:1
1300m

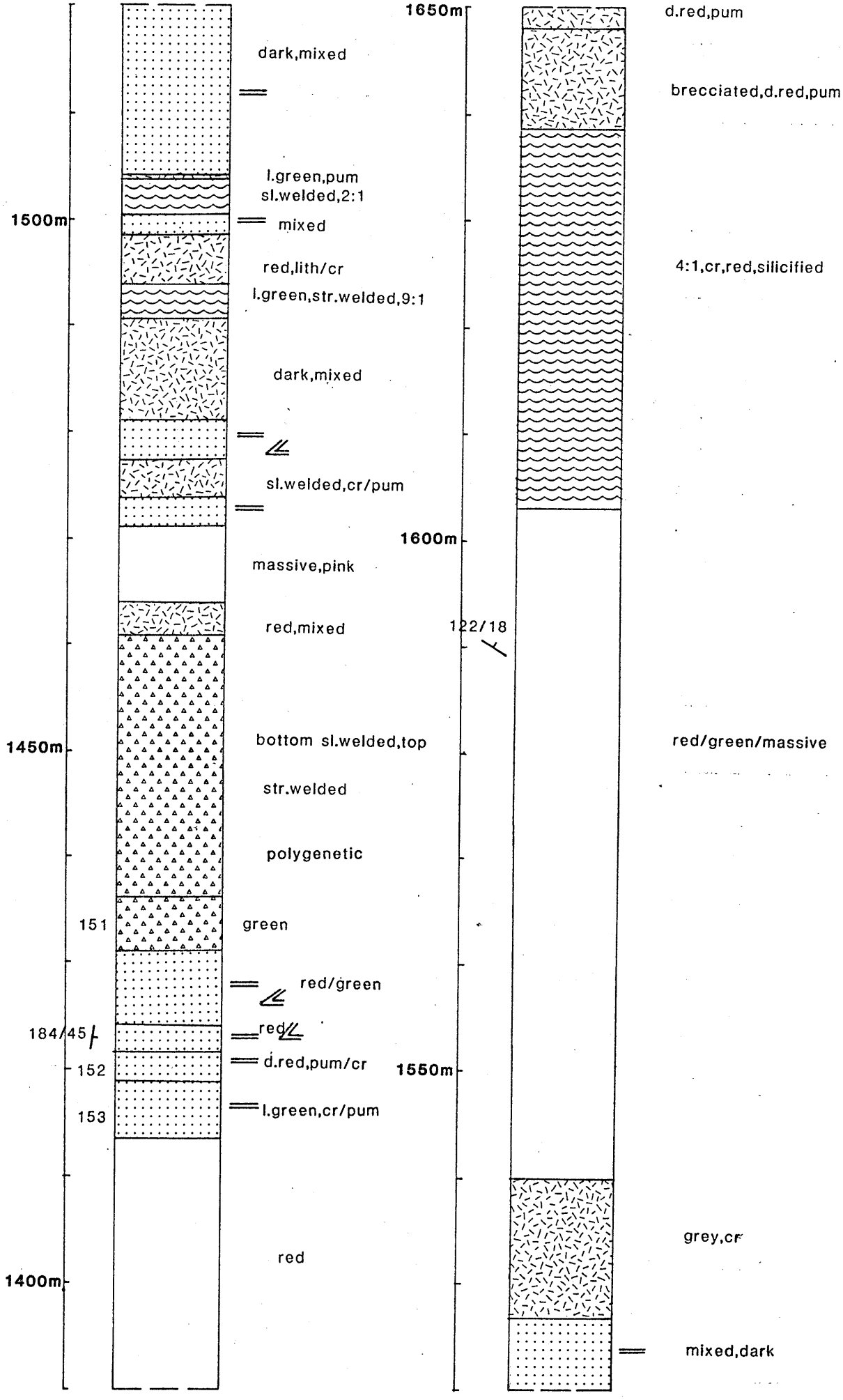
1650m
d.red,pum
brecciated,d.red,pum
4:1,cr,red,silicified
1600m
122/18
red/green/massive
1550m
grey,cr
mixed,dark
dark,mixed
l.green,pum
sl.welded,2:1
1500m
mixed
red,lith/cr
l.green,str.welded,9:1
dark,mixed
sl.welded,cr/pum
massive,pink
red,mixed
1450m
bottom sl.welded,top
str.welded
polygenetic
151
green
red/green
184/45
red
152
d.red,pum/cr
153
l.green,cr/pum
red
1400m

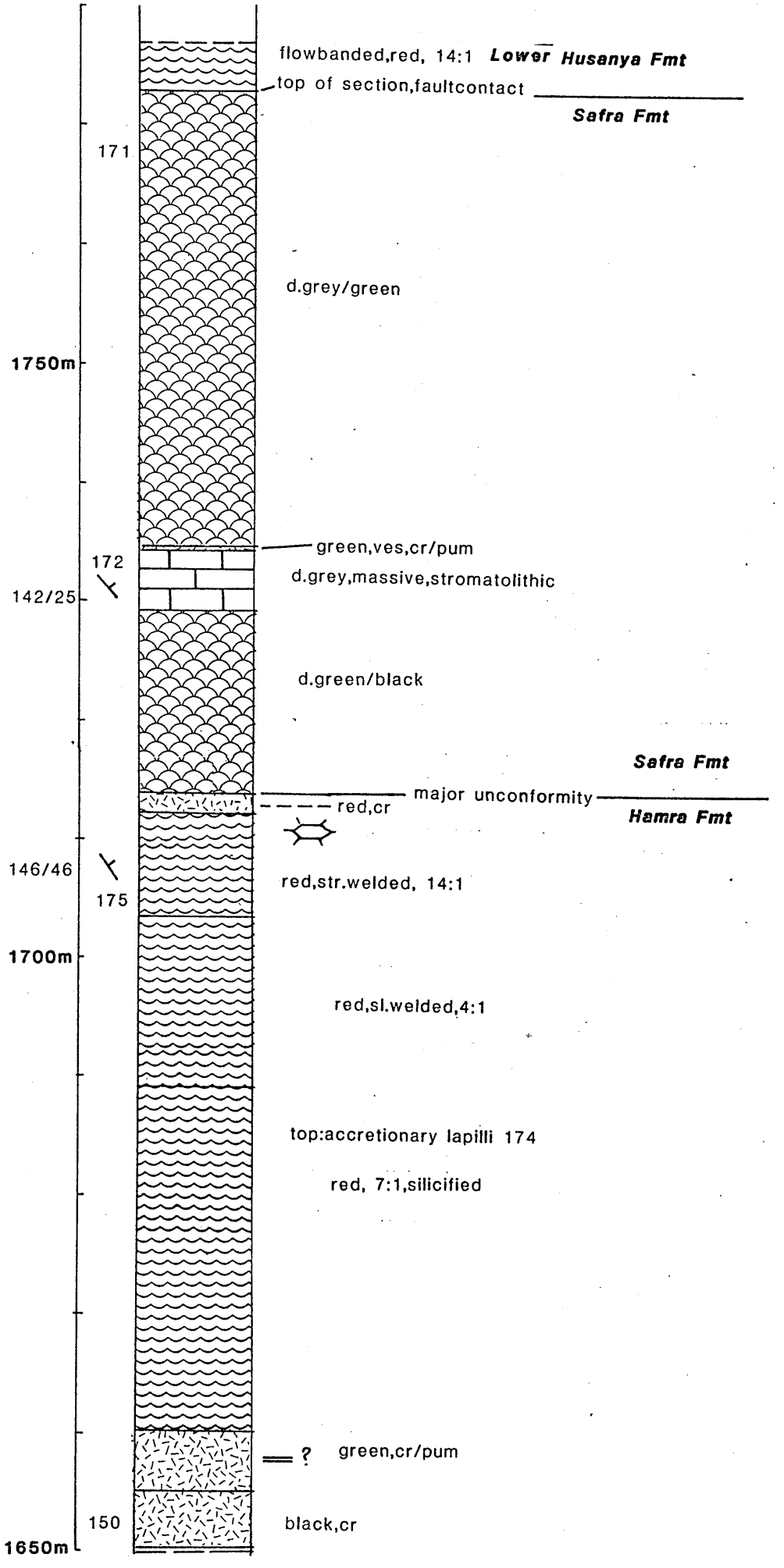
flowbanded,red, 14:1
Lower Husanya Fmt
top of section,faultcontact
Safra Fmt
171
d.grey/green
1750m
green,ves,cr/pum
172
d.grey,massive,stromatolithic
142/25
d.green/black
Safra Fmt
major unconformity
red,cr
Hamra Fmt
146/46
175
red,str.welded, 14:1
1700m
red,sl.welded,4:1
top:accretionary lapilli 174
red, 7:1,silicified
? green,cr/pum
150
black,cr
1650m

The lower part of the Husanya Formation is very conspicuous in the field for being very resistant to weathering and erosion, the welded ignimbritic rocks form massive, steep escarpments. The flowbanded rhyolites are dark red to brown in colour and the eutaxitic textures are very conspicuous in hand specimens and under the microscope. Compaction ratios are over 30:1, indicating extreme flattening of the pumice clasts. In thin section this rock type can be seen to consist of orthoclase, quartz, clinopyroxene and plagioclase (An_{10}) in a fine grained hematitized matrix of feldspar and quartz. The flattened pumice clasts (fiamme) are recognizable as darker bands of recrystallized cryptocrystalline material with occasional forked ends.

The upper part of the Hysanya Formation consists of green to dark grey basalts and andesites (the subdivision is done according to their SiO_2 content, whereby basalts, andesites and rhyolites have SiO_2 boundaries of 52 and 66%, respectively - see also Appendix B for classification). Pillowed basalt flows overlie conformably flowbanded rhyolites, whilst the upper boundary of the Hysanya Formation, sometimes (A. Warden, pers. comm.) interpreted as a major unconformity, is a sharp contact between dark grey vesicular andesites and red volcanic ash (consolidated to fine tuff) without an angular unconformity.

The grey-green basaltic rocks are clearly flows, showing remnants of pillow structures, vesicular top and bottom parts and a massive central part. The flows are normally porphyritic with feldspar crystals up to 2 cm and often amygdaloidal. Alteration to epidote is common. In thin section the basalts consist of augite, plagioclase (An_{9-5}) often altered to sericite, amphibole, epidote (piedmontite), chlorite and iron ore in a fine grained matrix of augite, epidote, chlorite, plagioclase, sericite and carbonate. Amygdales commonly consist of quartz, calcite and zeolites.

Dark grey to green andesite flows (with vesicular top and bottom parts and flow structures in the central part) occur in the higher division of the Husanya Formation. They are fine grained to slightly porphyritic with feldspar phenocrysts to 5 mm. In thin section they consist of zoned plagioclase (An_{33-9}), actinolite, biotite, chlorite (penninite), epidote (piedmontite) and iron ore in a matrix of fine grained amphibole and microlites of feldspar. The vesicles often are infilled with quartz and actinolite.

The metamorphic grade of these lavas can be assessed by their mineral content. The association of chlorite (penninite, actinolite,quartz, epidote (piedmontite), plagioclase with An < 10% indicates (partly after Winkler, 1974) a lower greenschist facies and as such is comparable with the metamorphic grade of the Wadi Fatima volcanics.

3.4.3.3 Dghabaghe Formation

The Dghabaghe Formation is a 450 metres thick succession of volcanics and intercalated sediments. It is very well developed near the village of Dghabaghe (see Figure 3.3) as a varicoloured sequence of pink, red to yellow ignimbrites and tuffs, intercalated with green, grey to yellow mudstones, sandstones and conglomerates of volcanic origin. The ignimbrites and tuffs are more resistant to weathering and erosion than the sediments and form steep escarpments. The lower boundary of this formation is described in Section 3.4.3.2, the upper boundary with the Hamra Formation is taken at the first polygenetic volcanic breccia.

The sediments occur mainly as fining upwards sequences, whereby conglomerates are overlain by sandstones and mudstones. They are in general green to yellow, poorly sorted and round and have lenticular to sheet-like overall shapes. The grain size, sorting, roundness and the occurrence of large lithic clasts of basalt and andesite, probably

derived from the Husanya Formation, indicate little transport and local provenance of the sediments. Sedimentary structures are large- and small-scale cross-bedding (indicating unimodal transport directions), parallel lamination and scour-and-fill structures (see Plate 10). The most likely sedimentary environment seems to be an alluvial fan bordering an active volcanic range, whereby coarse grained, poorly sorted channel and sheet deposits normally grade into overbank units (Reineck & Singh, 1973). Under the microscope the sediments can be seen to consist of subrounded to subangular grains of plagioclase (An_9), quartz, orthoclase and lithic clasts of andesite and basalt in a calcareous, hematitized matrix of quartz and feldspar.

The volcanics consist of (fine) tuffs and ignimbrites. The (fine) tuffs are in the field bright red to green and they can be seen to consist of pumice, crystal and lithic fragments in different proportions. These fragments are the basis for their classification, as discussed in Appendix B. In thin section they consist of pumice, crystal and lithic fragments in a fine grained matrix. The pumice clasts are rounded, fine grained quartz aggregates (with a small amount of flattening, as indicated by the rounded pumice clasts); the crystal fragments are plagioclase (An_{15}), anorthoclase, (often recrystallized) quartz, calcite, epidote and chlorite; lithic fragments are andesite and rhyolite. Accessory are sphene and iron ore. The matrix can be seen to consist of a fine grained mesh of quartz, feldspar and iron ore (hematite and magnetite). Flow structures often are visible due to the alignment of the quartz and feldspar crystals of the matrix.

Ignimbrites are widespread in this formation (see Plate 11); at least 11 flow units were identified, using the same criteria as in the Wadi Fatima area (see Chapter 2.5.6). Sometimes, however, it was difficult to assess, if the various (fine) tuffs bordering the ignimbrites belonged

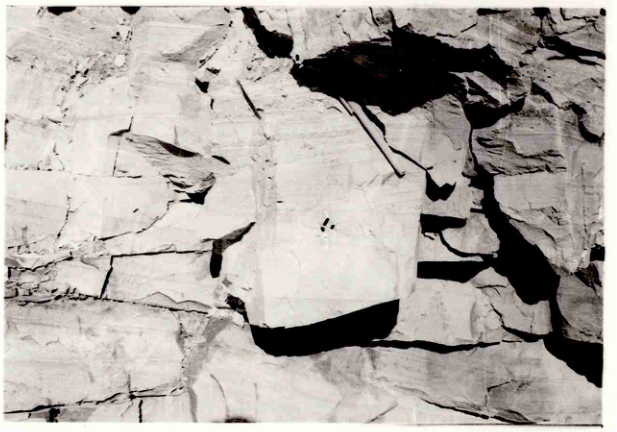

Plate 10 Scour-and-fill structures in Dgabaghe Formation, 500 metres south of Dghabaghe village

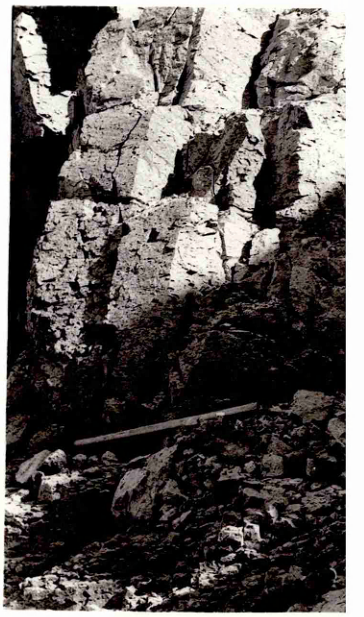

Plate 11 Columnar jointed ignimbrites, directly north of Dghabaghe village

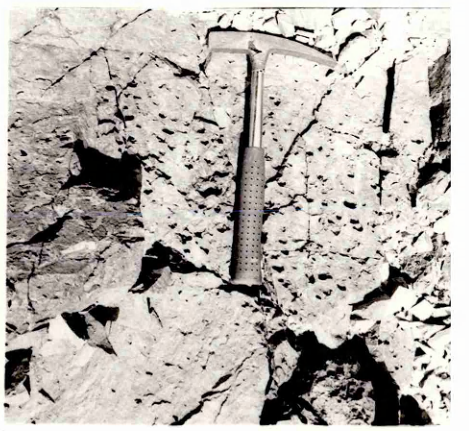

Plate 12 Accretionary lapilli in ignimbrites, upper part of Dghabaghe Formation, directly north of Dghabaghe village

BADR AREA (near Dghabaghe village; $23^{o}53'$,$38^{o}54'$)

to the same flow or not. As in the Wadi Fatima area, an ignimbrite flow unit is defined by finer top and bottom parts, a coarser, sometimes welded central part, by their petrology and sometimes by columnar jointing, indicating cooling units. Using these criteria, most (fine) tuffs could be separated from the ignimbrites. Two successive ignimbrite flows in the Dghabaghe Formation have been sampled in detail for petrological and geochemical studies (see Figure 3.5, samples BA 201-211). The thin sections of these rocks did not reveal any petrological variations within a flow unit (except differences in compaction ratios) and their major, trace and rare earth element distribution is also remarkably similar (see Chapter 6). In thin section the ignimbrites consist of microcline, orthoclase, plagioclase (An_{14-9}), quartz, sphene, clasts of andesite and basalt in a fine grained matrix of quartz, feldspar and ore minerals. The eutaxitic texture in the welded parts is very conspicuous, as forked and flattened pumice clasts (fiamme) form a linear fabric (see Plate 9). Accretionary lapilli, identical to those described in the Wadi Fatima area, occur frequently in the tuffs and ignimbrites (see Plate 12).

The combination of sediments and volcanics in the Dghabaghe Formation, their composition and sedimentary structures indicate clearly a subaerial environment. An alluvial fan environment is assumed, as proposed for the sediments alone, the subaerial tuffs and ignimbrites represent influxes of a nearby volcanic source, which also supplied the detritus for the sediments.

3.4.3.4 Hamra Formation

The Hamra Formation is a very thick (> 1200 metres) succession of coarse volcanics, mainly ignimbrites, volcanic breccias and tuffs, intercalated with fine grained sediments. In the field, this formation consists of red tuffs, varicoloured volcanic breccia and red ignimbrites; the

sediments are red to green and predominantly sand-sized. The welded ignimbrites are the most abundant rock type and tend to form steep scarps, especially east of Wadi Safra (see Figure 3.3). The lower boundary of the Hamra Formation was chosen at the appearance of the first polygenetic volcanic breccia; the upper boundary (with the Safra Formation) is a major angular unconformity, accompanied by a major change in rock type (see Figure 3.5).

The sediments are dominantly arenaceous; they occur as fining-upwards sequences, red to green in colour, and are well sorted and rounded. The overall shape of the sedimentary bodies is sheet-like. Sedimentary structures are parallel lamination, small- and large-scale cross-bedding and scour-and-fill structures. The structures indicate a unimodal transport direction towards the WNW. The grain size distribution, sorting, roundness and sedimentary structures favour a flood plain origin (after Reineck & Singh, 1973), whereby sandy channels and over-bank deposits (of predominant volcanic materials) are deposited in a plain, more distal to the volcanic source than the alluvial fan deposits of the Dghabaghe Formation (see Section 3.4.3.3). In thin section the sediments consist of rounded grains of quartz, iron ore, orthoclase, plagioclase (An_{20}), calcite and epidote in a fine grained recrystallized matrix, almost completely consisting of quartz. Lithic fragments of andesites and ignimbrites are common.

The volcanics are predominant in the Hamra Formation; they consist of (fine) tuffs, volcanic breccias and ignimbrites. The tuffs are equivalent to those of the Dghabaghe Formation; the volcanic breccias, however, only appear in the Hamra Formation (see Plate 13). They are reddish, sometimes welded rocks with polygenetic clasts up to 3 cm in diameter. In thin section they can be seen to consist of angular

clasts of andesite, basalt and rhyolite in a fine grained tuffaceous matrix, consisting of interlocking quartz and feldspar crystals; accessory minerals are piedmontite, chlorite and actinolite.

Ignimbrites are the most common rocks in the Hamra Formation; at least 28 separate ignimbrite flows were recognized in the field (see Figure 3.5). They are in colour, composition and degree of welding identical to those of the Dghabaghe Formation; the ignimbrites are, however, more widespread and thicker in the Hamra Formation, as evidenced by the massive, steep, often columnar jointed escarpments east of Wadi Safra. Accretionary lapilli are a common feature. Three isolated lavas of limited thickness and lateral continuity occur in the Hamra Formation.

Subaerial volcanism and sedimentation point to a continental sedimentary environment for this formation. For the sediments alone a flood plain environment is assumed; the volcanic activity during deposition of the Hamra Formation must have been more intense than during deposition of the Dghabaghe Formation, as evidenced by the amount and character of the ignimbrites.

3.4.3.5 Safra Formation

The Safra Formation (60 metres thick) crops out in the northeastern part of the area (see Figure 3.3) and is conspicuous because of its dark colour and subdued topography, due to its relatively small resistance (compared to the older, ignimbrite-dominated volcanics) to weathering and erosion. The lower boundary is an angular unconformity of at least 20^{o} with the Hamra Formation, whilst the upper boundary is a fault contact with the flowbanded rhyolites of the Husanya Formation, being the oldest volcanic formation in the area. Major rock types of the Safra Formation are dark green to black andesite flows and dark grey to brown, massive dolomitic limestones, which clearly show stromatolites, identical

to those described in the Wadi Fatima area (see Chapter 2.5.4).

The andesite flows are aphyric and have vesicular top and bottom parts; flow structures are common in the central part. In thin section they can be seen to consist of fine grained plagioclase (An_{51}), amphibole, epidote, zircon and iron ore. A fluidal texture is prominent by the alignment of the plagioclase and amphibole crystals.

The dolomitic limestone is developed as a grey to brown coloured, competent folded bed of 5 metres; it has been metamorphosed to a low-grade marble and is in thin section identical to the dolomitic limestones of the Wadi Fatima area. Stromatolites are common in this limestone bed, common forms are Conophyton and Collenia. As in the Wadi Fatima area, parts of the stromatolite structures have been recrystallized to produce quartz columns, approximately perpendicular to the lamination.

The sedimentary environment of the Safra Formation, as evidenced by the stromatolitic limestone beds, is probably shallow water (intertidal), analogous to the environment of the Wadi Fatima limestones. The Badr volcanics show a regular development of sedimentary environment from alluvial fan to flood plain and intertidal, i.e. a development from a clearly continental to a (shallow) marine environment.

3.4.4 Intrusive rocks within the Badr area

In the eastern part of the area (see Figure 3.3) a very weathered microgranite sill crops out. This yellow-greenish, very soft and almost decomposed rock type was intruded as a sill into the Hamra volcanics and is infolded between successive ignimbrite flows, indicating that it is probably contemporaneous with the volcanic rocks. This rock type is composed of quartz and feldspar crystals in a chloritic matrix. The weathered state of the rock prevented detailed thin section studies.

An oval intrusive body of quartzdiorite is found in the north of the area (see Figure 3.3), probably as a part of a belt of post-volcanic intrusive rocks, indicated on Figure 3.4. It is a massive, dark green, medium grained plutonic rock with a colour index of 25 and an average modal felsic composition of 15% quartz, 80% plagioclase and 5% alkali feldspar - a quartzdiorite according to Streckeisen (1976). Contacts of the plutonic body with the Hamra Formation volcanics and its shape indicate its intrusive character. In thin section this rock type has a subophitic texture and can be seen to consist of plagioclase (often zoned An_{42-20}), augite (altered to serpentine), iron ore, chlorite, quartz, epidote and orthoclase.

4 Nuqrah area

4.1 Introduction

The Nuqrah fieldwork area is located west of the village of Nuqrah (see Figure 4.1), famous for mineral exploration (polymetallic sulphides) since 800 A.D., mainly in the Hulayfah Group rocks. Since 1935 the Nuqrah quadrangle has been subject to extensive ground and aerial mapping, geophysical surveying and mineral exploration (Delfour, 1970, 1977, 1979). The relief in the Nuqrah quadrangle is moderate with maximum altitudes of 1200 metres in the west, sloping gently towards the east, where the mean elevation is 850 metres. The village Nuqrah lies along the main Ryadh - Medina road, 300 kilometres northeast of Medina. Smaller dirt roads, only suitable for four-wheel drive cars, branch off from this road and provide access to the fieldwork area.

Since the amount of time available for fieldwork was limited, the quadrangle map of Nuqrah (Delfour, 1977) was used as a base map, aided by stereoscopic photointerpretation, to produce a simplified geological map of the fieldwork area (Figure 4.2) and to select two traverses (Figure 4.3) in the Shammar Group volcanics, namely in the older Kuara and younger Malha Formations (see Figure 4.2 for the location of the traverses). Since the Nuqrah quadrangle is the type locality for the Shammar Group rocks, general mapping was done adequately (Delfour, 1975b, 1977) and most efforts were concentrated on collecting samples for geochronological studies and making two detailed traverses. Previous work will be discussed in Section 4.2, the development of the use of the name "Shammar" will be discussed in Section 4.3. Field studies, geochronology and geochemistry of the Shammar volcanics, described by various authors as one of the youngest Precambrian Arabian Shield rock types, are used to elucidate the geological history of these volcanic rocks and to correlate with the volcanic sequences occurring in the Wadi Fatima (Chapter 2) and Badr (Chapter 3) areas.

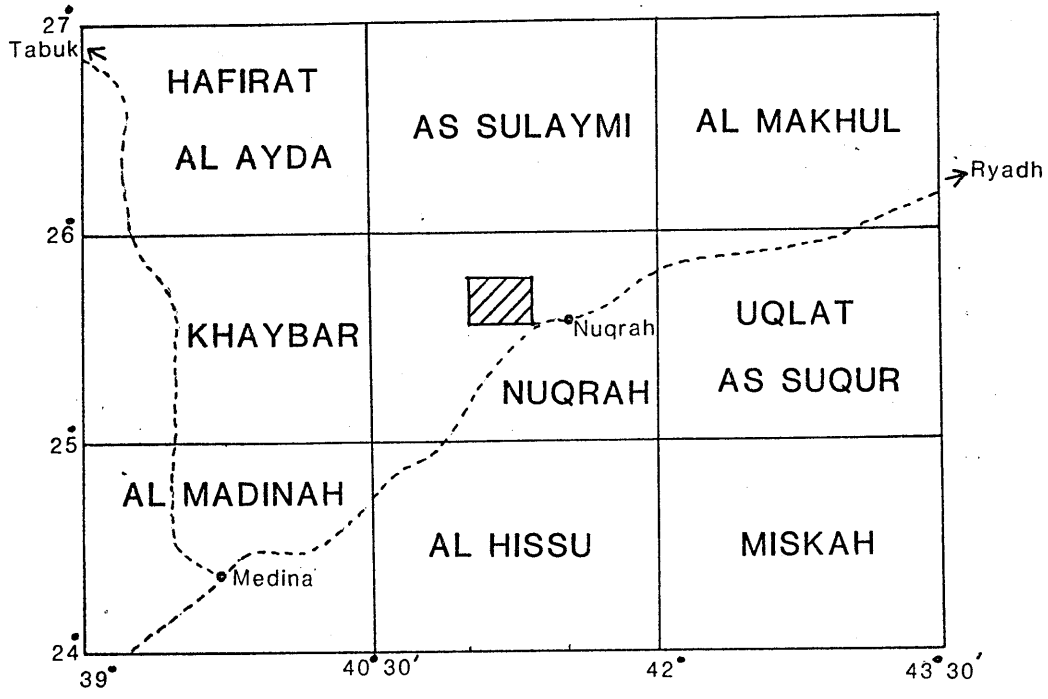

Figure 4.1 The northeastern part of the Precambrian Arabian Shield, showing the location of the fieldwork area. The Nuqrah and surrounding quadrangles are indicated and also the main roads crossing the area.

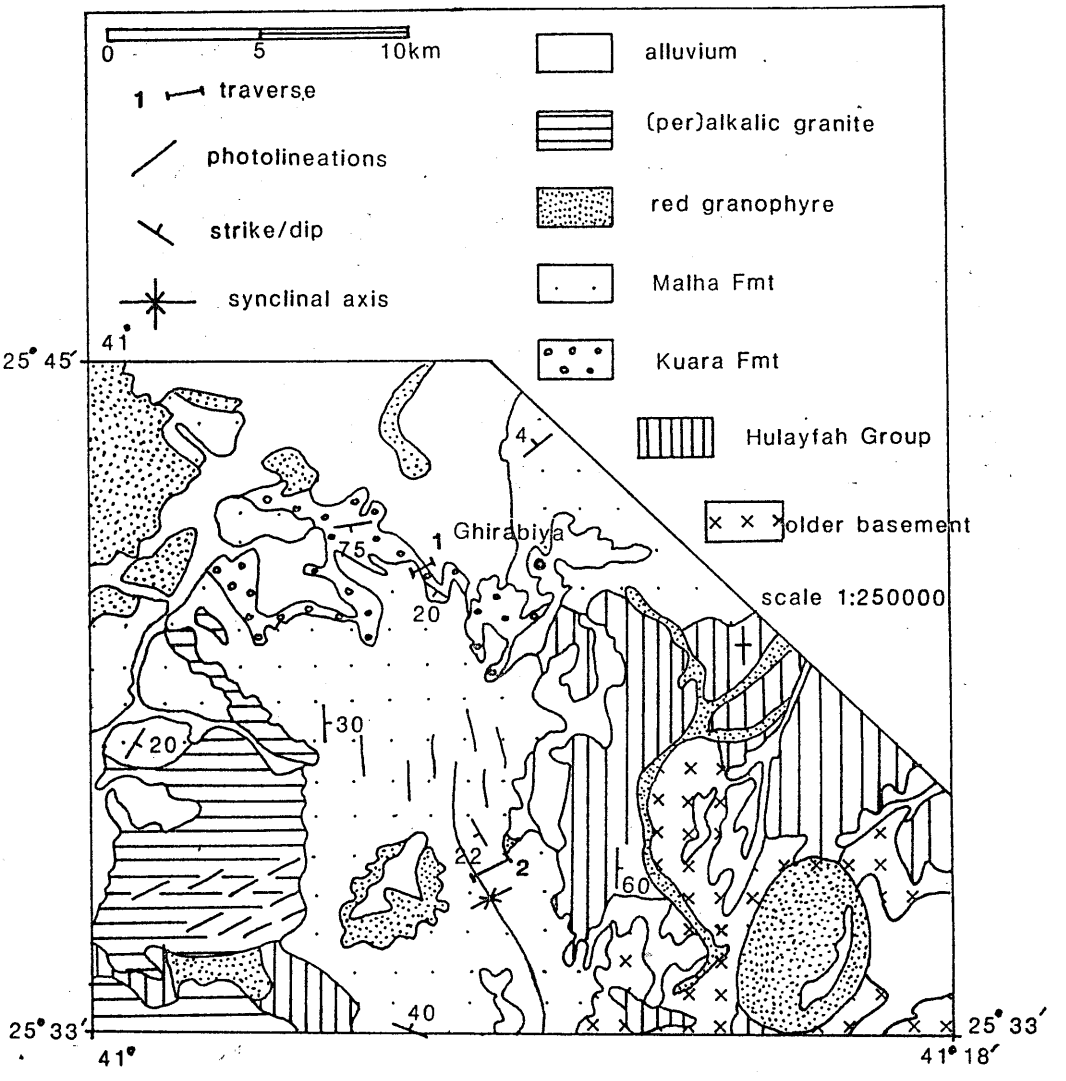

Figure 4.2 Geological map of the Nuqrah fieldwork area (after Delfour, 1977); the detailed lithostratigraphical traverses 1 and 2 are shown on Fig 4.3 .

4.2 Previous work

Brown et al. (1962) indicate the Nuqrah volcanics, studied by the author, as Shammar Rhyolite, surrounded by Halaban Group volcanics and sediments and various undefined plutonic rocks. Most later work was carried out by Delfour (1970, 1975a, 1975b, 1977, 1979). The geology of the fieldwork area was summarized by his map of 1977, which will be used as a framework for the current study. The stratigraphy of the Nuqrah quadrangle (Delfour, 1977) is shown on Figure 3.2. The oldest rocks in the area are the Ajal Group (biotite schists, quartzites, gneisses, amphibolites) and the "older basement" granites and orthogneisses. The ophiolitic Urd Group overlies these granites, separated by an unconformity from the younger Hulayfah Group, which is well represented in the Nuqrah quadrangle. The Hulayfah Group is characterized by subaerial to submarine volcanism and is host to most of the mineralization in the area. The overlying Murdama Group consists of a thick succession of clastic rocks in the eastern part of the area. Younger, but partly equivalent to the Murdama Group rocks, volcanics are the Shammar Group rocks which are widespread in the area. They are typical subaerial continental volcanics (Delfour, 1977). The Jibalah (also called J'balah) Group sediments and intermediate to basaltic volcanics form the youngest group involved in the NW/SE Najd fault system and are characteristically observed in NW/SE fault-bounded belts. The extensive Paleozoic cover is represented by outliers of near-horizontal red Cambro-Ordovician sandstones. Younger Cenozoic unconsolidated sediments and evaporites are partly covered by the extensive Miocene basalt flows; Recent clays, gravel and dune sands are extensively developed in the northern part of the quadrangle.

Intrusive rocks are layered gabbros and ultramafics from the Rharaba Complex, which, together with granites and diorites, are the oldest intrusive rocks in the area. Granites and diorites, slightly younger

than the Hulayfah Group also occur. The Shammar Group volcanics are surrounded by older calc-alkalic granites and granodiorites and younger per-alkalic granites and granophyres. The youngest group, the Jibalah sediments and volcanics are not intruded by plutonic rocks. Some radiometric data are shown on Figure 3.2 for the intrusive rocks of the northern Arabian Shield.

4.3 The development and use of the name "Shammar"

There are 75 entries under the name "Shammar" in Fitch's compilations (1978a, 1978b, 1979) and eight entries on the Kuara and Malha Formations, being parts of the Shammar Group; this alone indicates the importance of the Shammar Group in Arabian Shield geology. The name "Shammar" was used by Brown & Jackson (1960) as the "Shammar Rhyolite", comprising tuffs, rhyolites, dacites and andesites, disconformably overlying the Mahd al Dahab mineralized agglomerates of the Halaban Group. The Shammar Rhyolite is extensively exposed in the Jabal Shammar area, after which it is named. The term "Shammar Formation" was introduced by Kahr & Agocs (1962), incorporating andesites, rhyolites, tuffs, agglomerates and sediments. "Shammar Rhyolite" and "Shammar Formation" were then used indiscriminantly, until Schmidt et al. (1973) assigned these rocks a Group status as Shammar Group. After 1973 the term Shammar Group has been widely used and almost all authors agree that the Shammar Group comprises mainly acidic volcanic rocks, and minor andesites, agglomerates and sediments. The occurrence of ignimbrites was first described by Eykelboom (1970). Early correlations suggest that the Shammar Rhyolites were equivalent to the Mahd al Dahab Series (part of the Halaban/Hulayfah Group, Goldschmidt & Kouther, 1965), whereas others describe the Shammar Formation overlying the Halaban Group andesites (Johnson & Trent, 1967) and Murdama Group rocks (Johnson & Trent, 1966). Later work correlated the Shammar Formation with the upper part of the Fatima Group (Eykelboom, 1970); the Shammar Group as often overlying Murdama

Group rocks (le Chapelain, 1971; Brosset & Delfour, 1972; Delhemmes, 1976) and sometimes equivalent to the Murdama Group (Kemp, 1976). Age dating confirms this partial overlap (Greenwood et al., 1977). The Jibalah Group rocks unconformably overlie the Shammar Group (Brosset & Conraux, 1978).

The Shammar Group described by Delfour (1976, 1977) was subdivided by him into the Kuara and Malha Formations (the type locality of these formations lies in the author's fieldwork area). The Kuara Formation consists of coarse sediments, rhyolites, ignimbrites and volcanic breccias and the Malha Formation of rhyolites, ignimbrites, tuffs, andesites and sediments (Delfour, 1975b, 1976, 1977). The Shammar Group is essentially unmetamorphosed (Hadley, 1973; Brown & Jackson, 1979) and co-magmatic (because of field and geochemical relations) with granitic plutonic rocks (Delfour, 1977; Greenwood et al., 1974).

4.4 The Nuqrah field work area: Introduction and Structural geology

A simplified geological map (see Figure 4.2, mainly after Delfour, 1977) shows the Nuqrah fieldwork area and also the location of the two traverses, respectively in the Kuara Formation (1) and in the Malha Formation (2). A complete description of the two lithostratigraphical traverses is shown on Figure 4.3; the Kuara Formation occupies the first three columns and the Malha Formation the second three. Both traverses have true thicknesses of about 300 metres. The main hills in this area with moderate relief (in general the relief on the Arabian Shield becomes progressively more subdued eastwards) are Jabal al Malhah, where outcrops are extensive and the type locality of the Malha Formation (Delfour 1976) is situated, and Jabal al Abub, a granophyric ring complex in the southeastern corner of the area. Jabal Kuara, the type locality of the Kuara Formation (Delfour, 1975b), lies 15 kilometres northwest of Jabal al Malhah. The Kuara and Malha Formations form a N-S

to NNW-SSE trending belt, overlying the Hulayfah Group and the older granitic basement. Younger, partly intrusive red granophyres and peralkalic granites are common in the area and are considered by Delfour (1977) to be slightly younger than the Shammar Group rocks. The successive rock units will be discussed separately, and special attention will be given to the Shammar Group rocks and the younger granitic rocks.

The structural geology of the area is relatively simple. Older basement rocks, consisting of granites, gneisses and locally gabbros, are overlain by N/S trending, steeply inclined and isoclinally folded andesites, basalts and tuffs of the Hulayfah Group. The Hulayfah Group is unconformably overlain by the Shammar Group, which shows large open synclinal folds with NW/SE to N/S axes. Locally these axes exhibit secondary folding in a SW/NE direction. Younger granitic rocks intrude or interfinger with the Shammar Group volcanics.

4.5 Lithological description of the rock units

4.5.1 The older basement

The older basement, indicated on the stratigraphical column of the northern Arabian Shield (Figure 3.2), consists in the area of gneissose granites and gabbros which are reported to have an age of 1000 Ma (Delfour, 1977). The leucocratic (colour index < 15) granites and inliers of dark green gabbros form low-lying outcrops, possibly indicating an extensive old peneplain. The granites are pink to light brown in colour, have a distinct layered appearance because of the segregation in light- and dark-coloured bands and have an average modal felsic analysis of 29% quartz, 30% alkali feldspar and 41% plagioclase. In thin section the granites have a clear metamorphic fabric by segregation of quartz and feldspar in lighter, and biotite in darker bands. This


rhyolite


andesite


basalt


sill


volcanic breccia


ignimbrite


tuff


fine tuff


(dolomitic) limestone


mudstone


siltstone


sandstone


conglomerate


granitic rocks

Sedimentological features

parallel lamination


small-scale and large-scale cross-bedding


erosional lower boundaries


gas pipe structures


columnar jointing

Figure 4.3 Legend for Nuqrah section. True thickness in metres; measured strike and dip are indicated left of the column; sample numbers are also shown. The following abbreviations are used: d.-dark, l.-light, diam-diameter, fu-fining upwards, occ-occasional, ls-limestone, dol-dolomite, cr-crystal, pum-pumice, lith-lithic, porph-porphyritic, strom-stromatolithic, elong-elongated, sl-slightly, volc-volcanic, v-very, ves-vesicular, amygd-amygdaloidál, str-strongly.

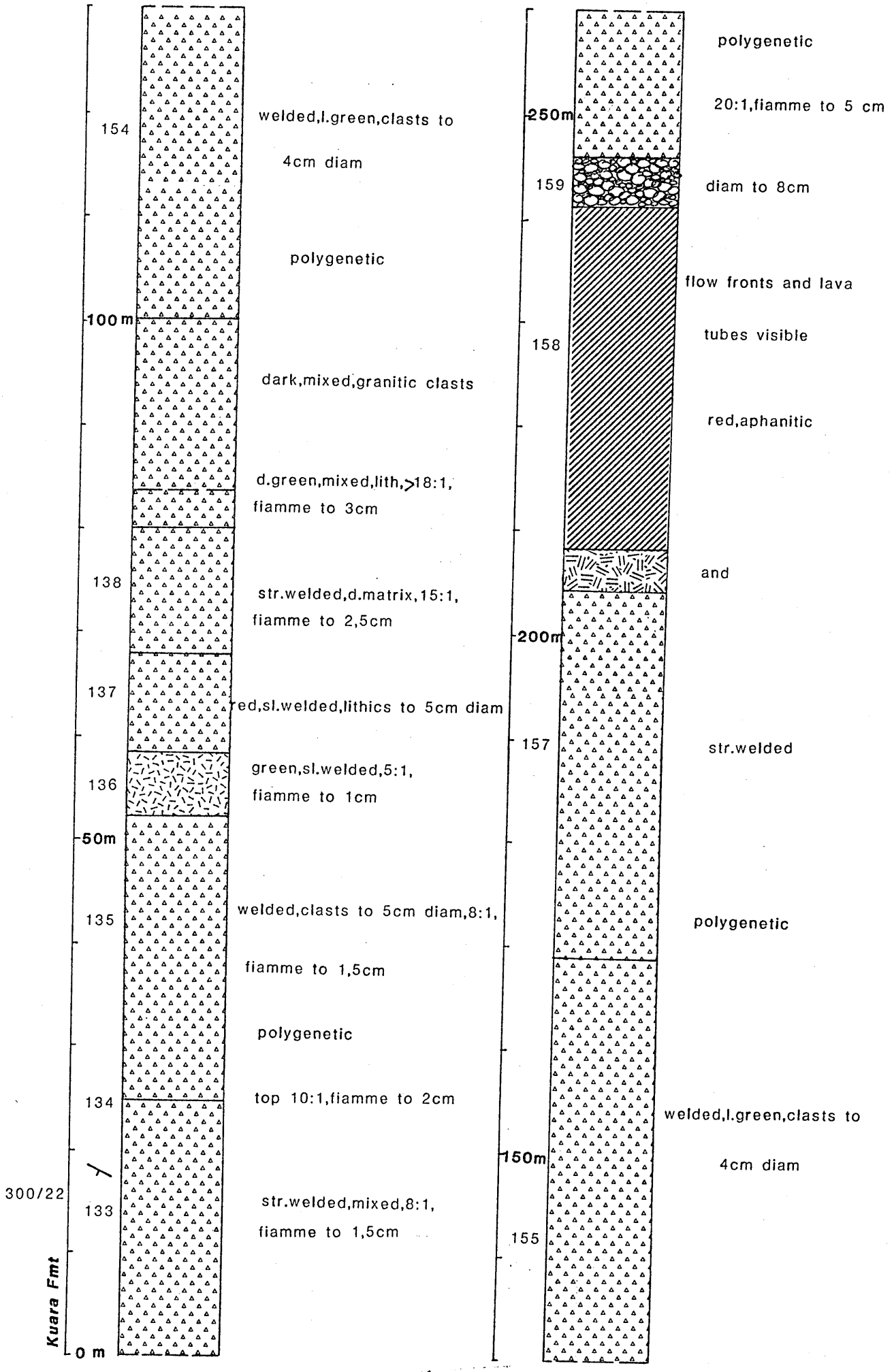
154
welded,l.green,clasts to
4cm diam
polygenetic
100 m
dark,mixed,granitic clasts
d.green,mixed,lith,>18:1,
fiamme to 3cm
138
str.welded,d.matrix,15:1,
fiamme to 2,5cm
137
red,sl.welded,lithics to 5cm diam
136
green,sl.welded,5:1,
fiamme to 1cm
50m
135
welded,clasts to 5cm diam,8:1,
fiamme to 1,5cm
polygenetic
134
top 10:1,fiamme to 2cm
300/22
133
str.welded,mixed,8:1,
fiamme to 1,5cm
Kuara Fmt
0 m
polygenetic
250m
20:1,fiamme to 5 cm
159
diam to 8cm
flow fronts and lava
158
tubes visible
red,aphanitic
and
200m
157
str.welded
polygenetic
welded,l.green,clasts to
150m
4cm diam
155

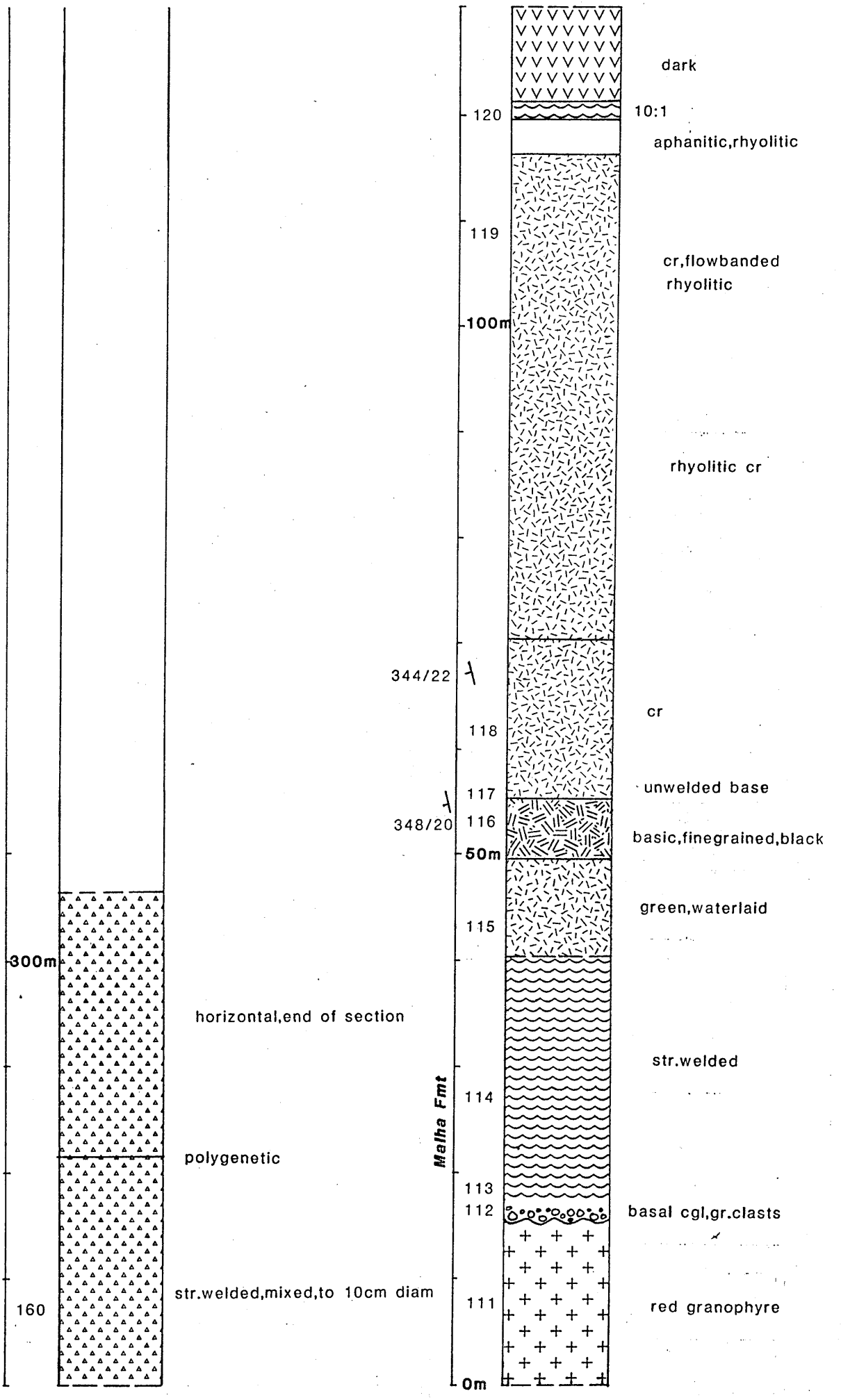
dark
10:1
aphanitic,rhyolitic
120
119
cr,flowbanded
rhyolitic
100m
rhyolitic cr
344/22
cr
118
unwelded base
117
348/20
116
basic,finegrained,black
50m
green,waterlaid
115
300m
horizontal,end of section
str.welded
Malha Fmt
114
polygenetic
113
112
basal cgl,gr.clasts
str.welded,mixed,to 10cm diam
160
111
red granophyre
0m

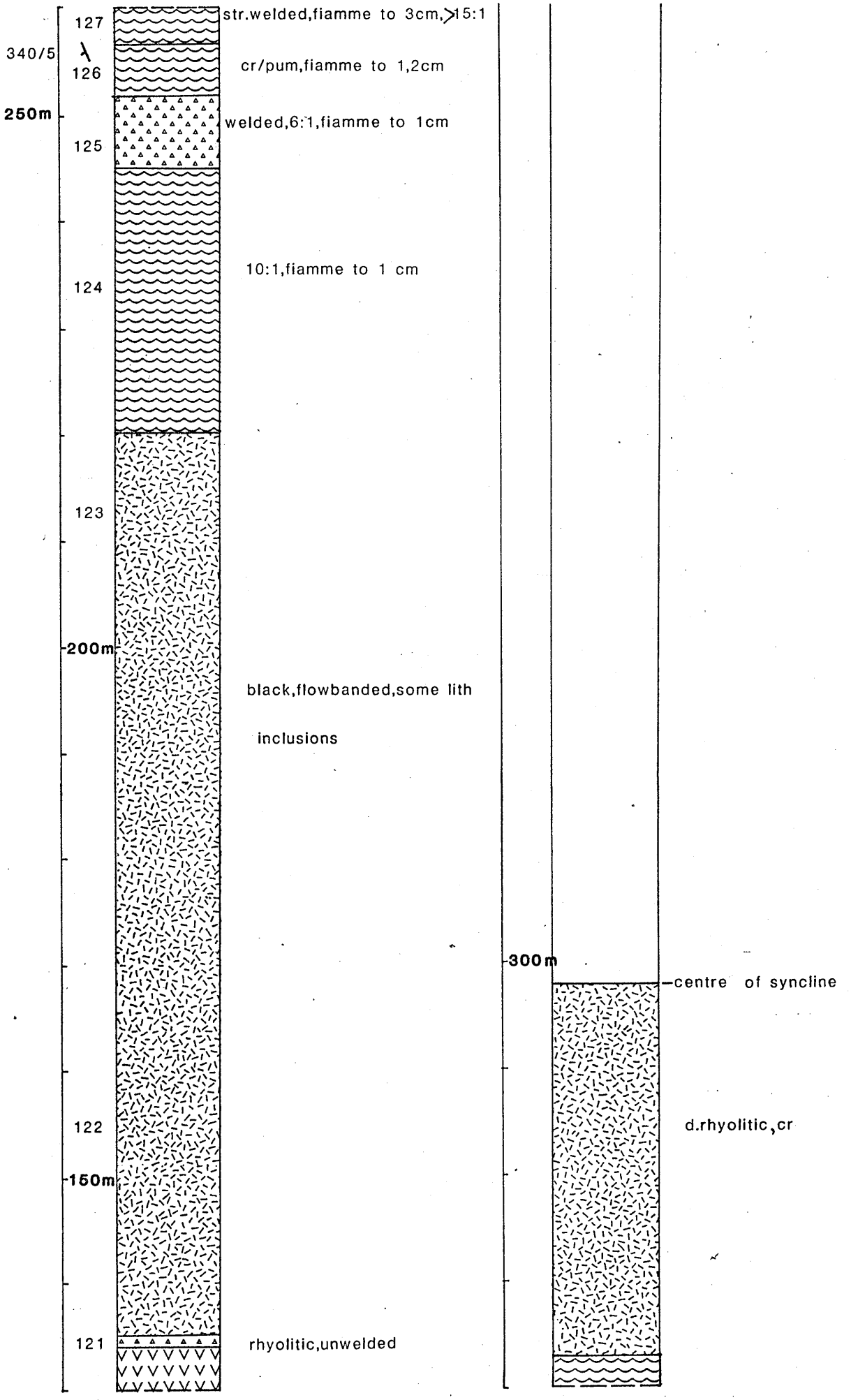
127
340/5
126
250m
125
124
123
200m
122
150m
121
str.welded,fiamme to 3cm,>15:1
cr/pum,fiamme to 1,2cm
welded,6:1,fiamme to 1cm
10:1,fiamme to 1 cm
black,flowbanded,some lith
inclusions
rhyolitic,unwelded
300m
centre of syncline
d.rhyolitic,cr

rock type can be seen to consist of quartz, plagioclase (An_{12}), orthoclase, biotite, iron ore, calcite and accessory apatite.

The gabbros form dark green, irregular shaped bodies, confined within the granites. They are massive and fine grained. In thin section they have an ophitic texture, whereby plagioclase crystals are euhedral and large augite crystals fill in the angular interstices. The components of this rock type are augite, plagioclase (An_{78}), olivine (forsterite, often altered to serpentine), chlorite, actinolite and tremolite (see Plate 13).

4.5.2 The Hulayfah Group

In this area, the Hulayfah Group consists mainly of metamorphosed, strongly foliated, green tuffs with traces of mineralization (most of the mineral exploration potential in the Nuqrah quadrangle lies in the Hulayfah Group and a major mining area, north of Nuqrah village, lies directly east of the field area). Metamorphism and mineralization make this rock type easy to distinguish from the Shammar Group volcanic rocks which are unmetamorphosed and barren. In thin section the fine grained tuffs have a strong linear fabric and can be seen to consist of angular clasts of quartz, orthoclase, plagioclase (An_{25}), iron ore (mainly magnetite) and chlorite in a chloritized, calcareous matrix.

4.5.3 The Kuara Formation

The Kuara Formation forms the lower, coarser grained formation of the Shammar Group volcanic rocks (see also Delfour, 1976, 1977). It is uniform in composition, minimal 300 metres thick and was not further subdivided in members by the author. The Kuara Formation crops out in the northern part of the area and is conformably overlain by the Malha Formation, being the upper formation of the Shammar Group volcanic rocks.

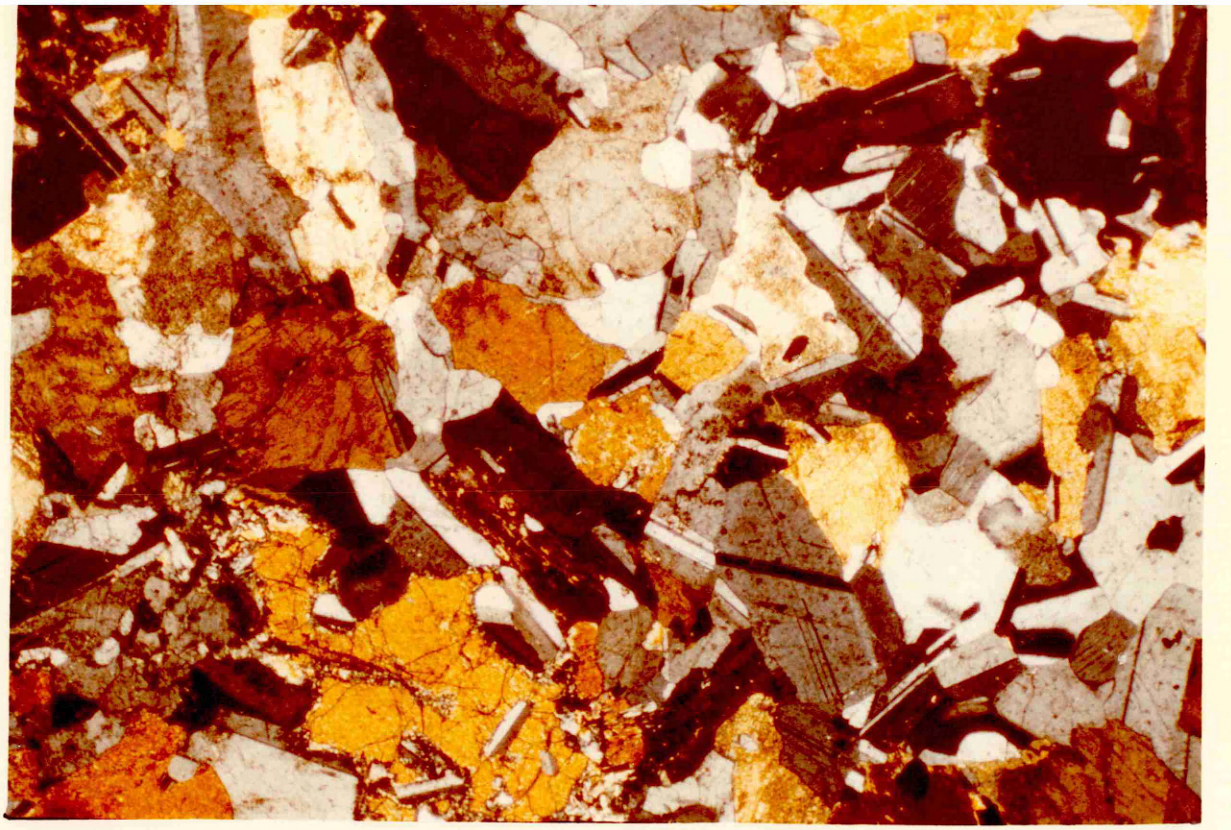

Plate 13 Ophitic textures in gabbro (crossed nicols), sample NU006; $25^{o}32'$,$41^{o}16'$

NUQRAH AREA

1mm

Plate 14 Red granophyre with biotite (crossed nicols), sample NU110, ringcomplex $25^{o}34'$,$41^{o}16'$

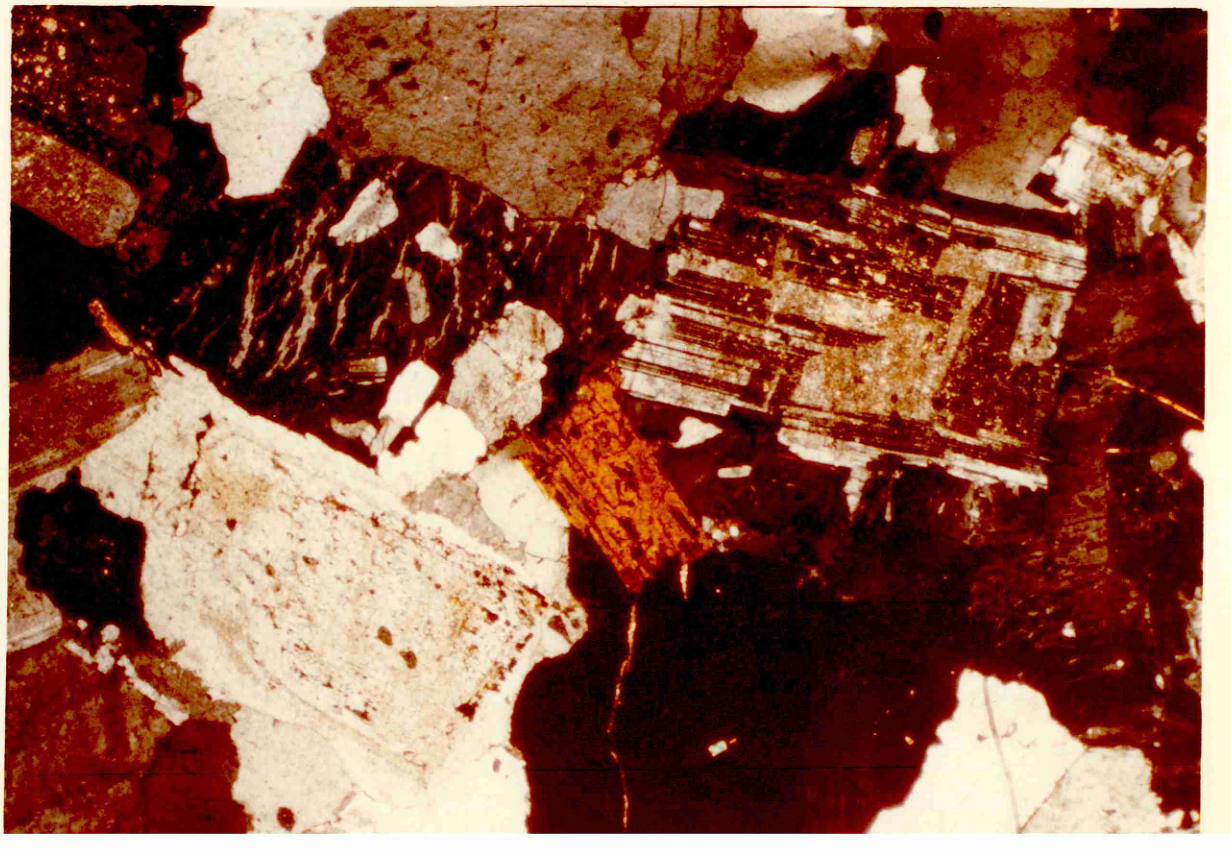

The Kuara Formation consists in the area (see Figures 4.2 and 4.3) almost entirely of polygenetic volcanic breccias and minor tuffs, flows and conglomerates. Because of its resistance to weathering and erosion, it tends to form steep escarpments, especially westwards of the village Ghirabiya (see Figure 4.2). A complete lithostratigraphical column has been measured and sampled (see Figure 4.3 for the complete column).

The volcanic breccia (see Plate 15) is red to green in colour, welded (with compaction ratios up to 20:1) and often columnar jointed. Large lithic, crystal and pumice clasts can be observed (lithic clasts of red granophyre are prominent) in a fine grained matrix. In thin section the welded volcanic breccias are composed of large lithic clasts of red granophyre (with a granophyric texture of quartz and alkali feldspar), tuff and aphyric andesite. Coarse grained crystals are quartz, microcline, plagioclase (An_{12}, often altered to sericite), biotite (often altered to chlorite), orthoclase, epidote and rare amphibole. The pumice clasts are lens-shaped to extremely elongated with ragged ends (fiamme), bending around lithic crystal fragments; they are composed of a dark fine grained matrix of recrystallized quartz. The matrix of the breccia consists of an extremely fine grained mesh of quartz and feldspars. Rare tuff beds, also slightly welded, occur within the volcanic breccia sequence.

One massive rhyolite flow occurs (with a thickness of more than 30 metres) in the Kuara Formation. This red, aphanitic rock type clearly shows flow fronts and lava tubes (see Plate 16) especially in the central parts of the flow. In thin section this rock type can be seen to consist of plagioclase (An_{15}), alkali feldspar (with perthitic textures), biotite and hornblende in a very fine grained, tuffaceous matrix.

A single conglomerate layer of 5 metres crops out on top of the rhyolite

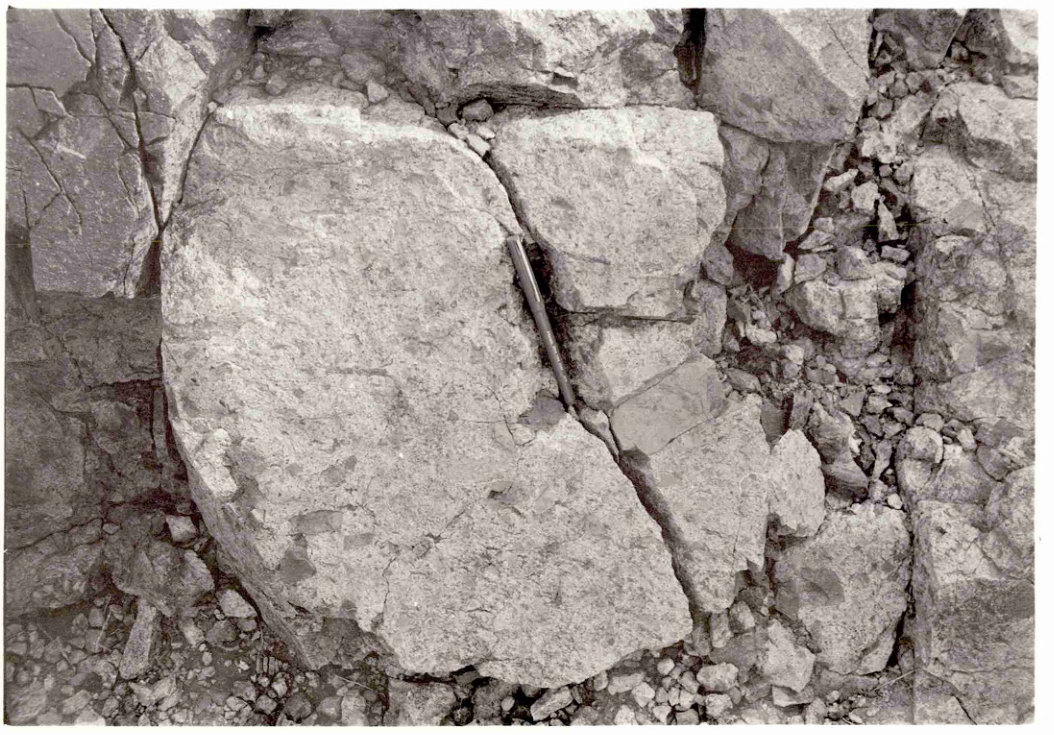

Plate 15 Volcanic breccia, Kuara Formation; west of Ghirabiyah (see p.63)

NUQRAH AREA, near Ghirabiyah ($25^{o}41'$,$41^{o}9'$)

Plate 16 Lava tubes in rhyolites, Kuara Formation, west of Ghirabiyah

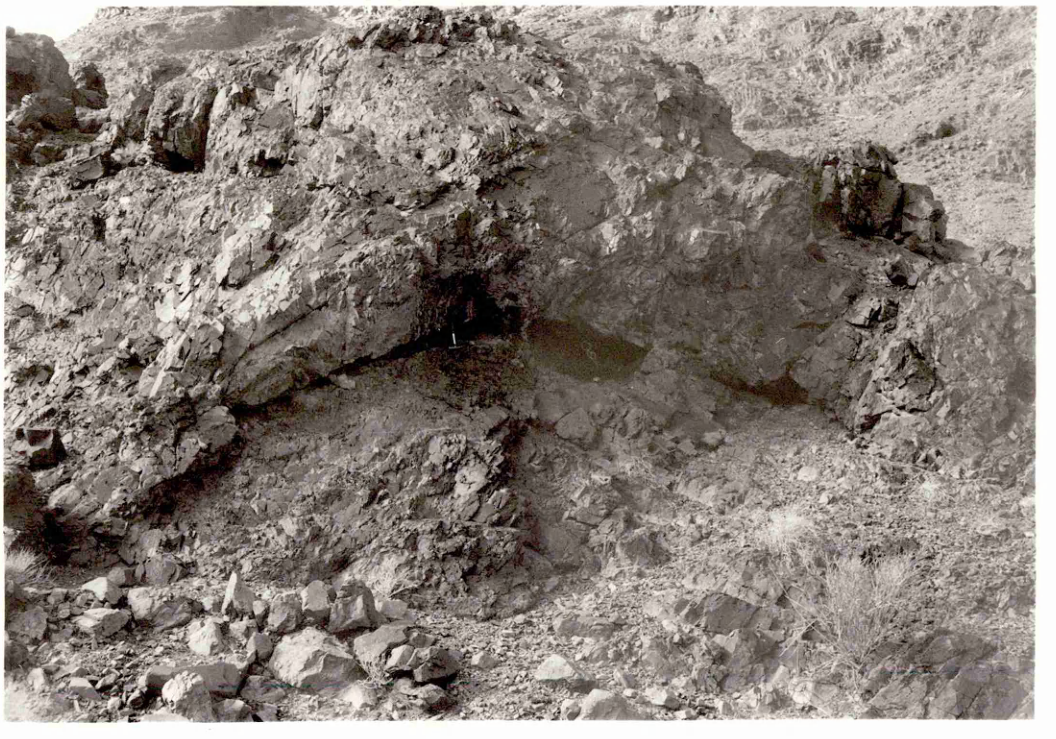

flow. This reddish and very coarse (clasts up to 8 cm in diameter) comglomerate consists of large, subrounded fragments of rhyolite, andesite, red granophyre, tuff and volcanic breccia in a fine grained, calcareous matrix. Sedimentary structures are rare except parallel lamination and a crude imbrication of the larger clasts.

4.5.4 The Malha Formation

The Malha Formation (see Figure 4.2) is the upper formation of the Shammar Group volcanic rocks and has been extensively described by Delfour (1976, 1977). In the Nuqrah area, this formation crops out in the central part, conformably covering the Kuara Formation in a synclinal structure. Locally the Malha Formation overlies unconformably red granophyres, as will be described in Section 4.5.5. The Malha Formation consists of red, green to black rock units, which are in order of abundance tuffs, ignimbrites, volcanic breccias and flow rocks. A basal conglomerate is the only sedimentary rock present. The volcanic rocks of this formation are generally finer grained than those of the Kuara Formation. The massive, often welded rocks of the Malha Formation form steep escarpments.

The tuffs are mainly crystal tuffs (for the classification see Appendix B), green to pink in colour and often flowbanded. In thin section this rock type can be seen to consist of quartz, epidote, plagioclase (An_{25}), calcite, pyroxene, alkali feldspar and biotite (often altered to chlorite). The calcareous matrix consists of fine grained quartz and feldspar. Some tuffs have subrounded clasts and macroscopical textures that suggest a water-laid origin.

The ignimbrites are red to pink in colour, strongly welded (with compaction ratios from 6:1 to 20:1) and were, as in the Wadi Fatima and

Badr areas, classified as ignimbrites by their grainsize distribution, colour, welding and composition. In thin section they consist of plagioclase (An_{20}), orthoclase, quartz, fragments of rhyolite flows and epidote. Elongated pumice lenses surround these clasts as dark, hematitized, microcrystalline fiamme.

The volcanic breccias are identical to those of the Kuara Formation. A dark, fine grained basalt flow of 14 metres thickness crops out in the Malha Formation. In thin section this rock type can be seen to consist of plagioclase (An_{70}), olivine and augite in a microcrystalline, hematitized groundmass of augite and feldspar laths. The basal conglomerate of Figure 4.3 consists mainly of red granophyre clasts; this unit is clearly fining upwards and has a fine grained tuffaceous matrix.

The environment of deposition of the Kuara and Malha Formation cannot easily be determined by looking at the scarce sediments alone. The combination of extensive subaerial volcanics (volcanic breccia, ignimbrites and tuffs) and, possibly, alluvial fan sediments (Reineck & Singh, 1973), makes a continental environment, as proposed by Delfour (1977), most likely.

4.5.5 Red granophyre

This rock type is represented in the area by ring structures, sills, stocks and other intrusive bodies of irregular shape (see Figure 4.2). Field, geochemical (see Chapter 6) and isotopic studies (see Chapter 5) indicate that they are equivalent to the Shammar Group volcanic rocks. In the field they occur at the base of the Malha Formation and as predominant clasts in the volcanic breccia of the Kuara Formation (see Figure 4.3) The granophyres are red to pink coloured, medium to fine

grained, intrusive rocks. Their average modal felsic composition is 35% quartz, 50% plagioclase and 15% alkali feldspar and they are classified as granodiorites. In thin section a granophyric texture is common for this rock type, whereby alkali feldspar and quartz show a regular intergrowth. Their composition is quartz, orthoclase, plagioclase (An_{25}), iron ore, amphibole (often replaced by epidote), biotite (often replaced by chlorite) and accessory zircon (see Plate 14).

4.5.6 (Per)alkalic granites

(Per)alkalic granites crop out in the western part of the area. Field observations, geochemical (see Chapter 6), and isotopic studies (see Chapter 5) suggest that the granites are closely related to the Shammar Group volcanic rocks and the red granophyres of the area. The (per)-alkalic granites are observed in a well-shaped batholith and also as irregular off-shoots with an almost horizontal contact with the surrounding Shammar Group volcanic rocks. Their contacts suggest tne (per)alkalic granite to be time-equivalent or slightly younger than the Shammar Group volcanic rocks. This is confirmed by new geochronological data, as shown in Chapter 5.6.4.2. Geochemical data indicate that the majority of these rocks are alkalic granites rather than peralkalic granites (this was done by calculating their agpaitic index after Carmichael et al., 1974). In thin section these rocks (with an average modal felsic composition of 45% quartz, 45% alkali feldspar and 10% plagioclase they were classified as alkali feldspar granites) can be seen to consist of quartz, plagioclase (An_{10}), orthoclase (often with a perthitic texture), microcline (with the typical cross-hatched texture), biotite (often replaced by chlorite), iron ore (goethite and magnetite), epidote, augite (often replaced by amphibole) and accessory zircon and apatite.

Low strontium initial ratios, high Na_2O content (> 4.5%) and the occurrence of magnetite probably classify these granites as I-type granites (Chappell & White, 1974), being derived from igneous material.

5 Lithostratigraphy and geochronology of the Nubian-Arabian Shield

5.1 Introduction

The fundamental problem in the investigation of the Nubian-Arabian Shield is the lack of a detailed time structure/framework within which detailed studies can be set. Indeed, the problem still exists and it is appropriate to evaluate here the basic problems and to indicate how the available geochronological data fit into the proposed petrogenetic model.

In Figure 1.2 the distribution of the main rock types in and adjacent to a simple arc system was depicted. So long as subduction continues, then the arc will remain active with the emplacement of plutonic masses, the eruption of volcanic products and the cannibalistic erosion of the arc superstructure to give a variety of flanking sediments. Obviously, in this kind of scenario virtually identical magmatic products will have been produced time and time again at the same time and in different arcs. Similarly, sedimentary products formed by the erosion of an arc at one period will be essentially similar to those produced by the erosion of similar rock types at another time. Within this type of setting, although it is easy to recognize and erect local formations, it is often impossible to indulge in regional correlations. For this reason attention has concentrated on the production and evaluation of existing radiometric age dating and their relation to, mainly radiometically controlled, lithostratigraphical schemes for the Nubian-Arabian Shield in the hope that these will provide the essential time control to the evolutionary processes. It is now proposed to discuss the stratigraphical framework of the Arabian Shield (with possible correlations with the adjacent parts of the Nubian-Arabian Shield) and to discuss and evaluate the new geochronological data in the Fatima, Badr and Nuqrah areas.

5.2 Lithostratigraphic models for the Arabian Shield

Four stratigraphic syntheses, indicating both volcanic, sedimentary and major plutonic events, are indicated in Figure 5.1. They are based on the field studies, geochemical analyses and, in later stages increasingly important, geochronological work of the DGMR (Directorate General of Mineral Resources) and the geological missions USGS (United States Geological Survey), BRGM (Bureau de Recherches Géologiques et Minières) and Riofinex (Riotinto Finance and Exploration) in Saudi Arabia. The columns 1 and 2, representing respectively the southern and northern part of the Arabian Shield, are remarkably different. In the south, the oldest Precambrian units are better defined, partly due to a much deeper level of erosion, whilst the younger units are better exposed in the north and a more detailed stratigraphy of younger groups can be erected there. The third column (Figure 5.1) shows the tentative correlation by Riofinex (1977) for the whole of the Arabian Shield, assuming large-scale interfingering and sometimes localized occurrences of groups. One of the most recent, and in the author's opinion, best compilation for the younger volcanics, is shown in column 4. This column indicates the continuous character of plutonism throughout most of the period 1000-500 Ma; most of the boundaries of the groups are diachronous and the lower boundaries of the Murdama, Shammar and Jibalah Groups are older than previously assumed, probably by depending more on recent Rb/Sr geochronology.

Two new attempts (as suggested in 1974 by Greenwood et al. who recognized for the first time the three-fold division of the Hijaz tectonic cycle) have been made lately to make a three-fold subdivision for the Arabian Shield. Figure 5.2 indicates the proposed subdivisions after Jackson and Ramsay (1980) and Gass (1981). Jackson and Ramsay divide the volcanic and sedimentary units of the Central Arabian Shield into three "sequences", informally named A, B and C; Gass proposes a threefold

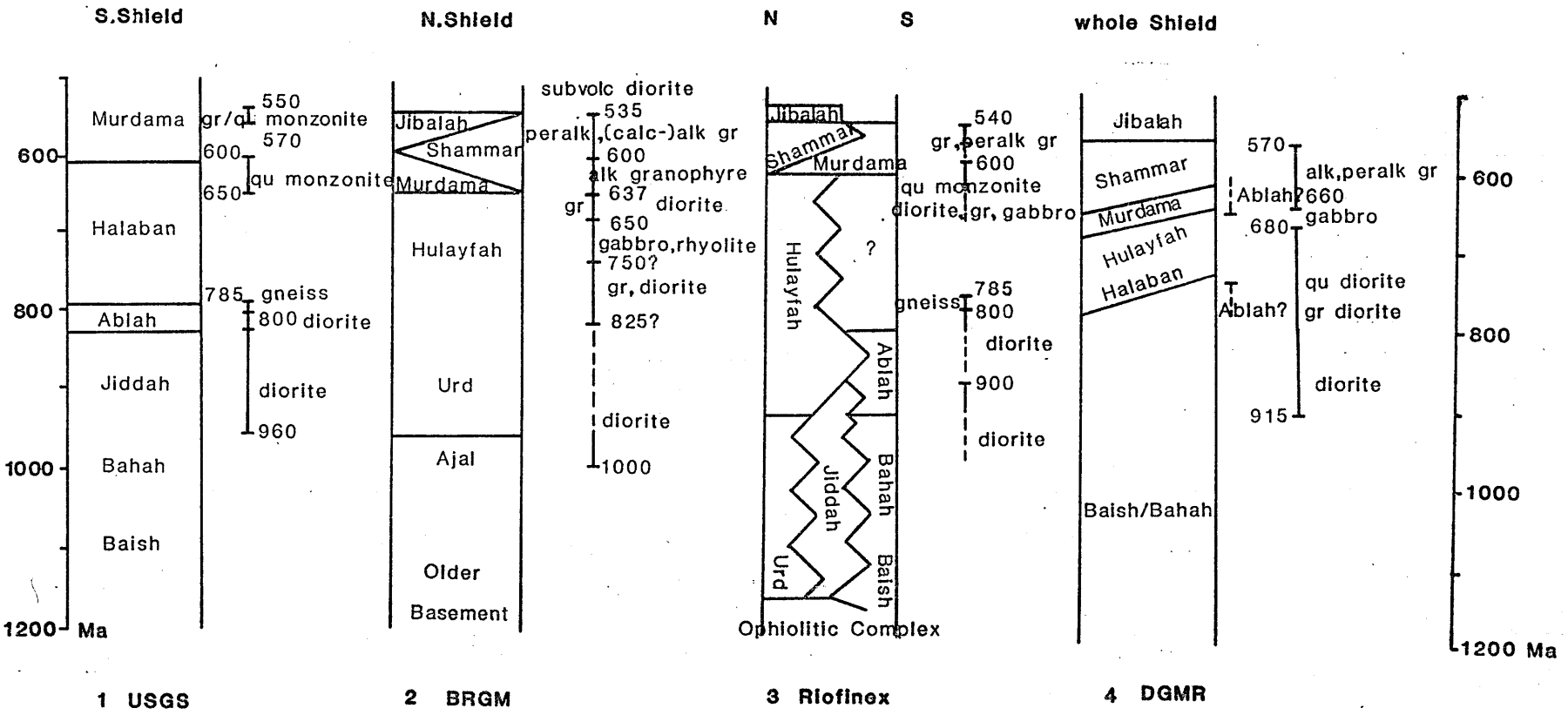

Figure 5.1 Stratigraphic summary of the Arabian Shield indicating major plutonic events (Column 1 after Greenwood et al., 1976; Column 2 after Baubron et al., 1976 and Delfour, 1979; Column 3 after Riofinex, 1977 and Column 4 after DGMR, 1979).

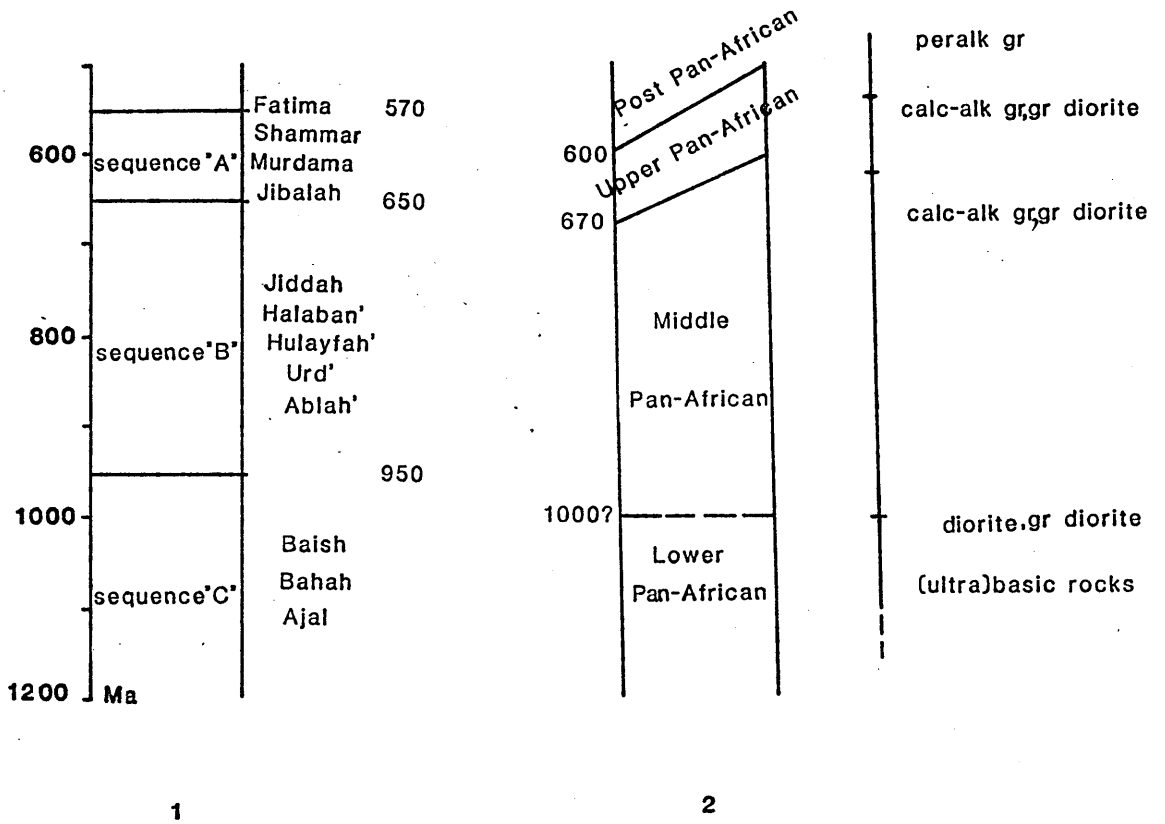

Figure 5.2 Two new three-fold subdivisions of the Pan-African (1200-500 Ma) time-span for the Arabian Shield (Column A after Jackson & Ramsay, 1980; Column B after Gass, 1981).

Ablah' means stratigraphic position uncertain

division for all Pan-African (1200 - 500 Ma) rock units of the Arabian-Nubian Shield. The stratigraphic models for Egypt and Sudan will be discussed together with their geochronology in the Chapters 5.4 and 5.5.

5.3 Geochronology of the Arabian Shield

5.3.1 Previous work

Age dating on Saudi Arabian basement rocks has been done mainly in the last twenty years by the DGMR, USGS and BRGM. Most results (103 Rb/Sr ages and 210 K/Ar ages) have been reported in Baubron et al. (1976), Fleck et al. (1976), Aldrich (1978), Brown et al. (1978) and Fleck et al. (1980). Additional age data can be found in Nasseef and Gass (1977), Kröner et al. (1979), Bokhari and Kramers (1981) and Kemp et al. (1980), whilst individual other data occur in numerous geological mission reports. Other radiometric methods for age dating, such as those using zircons (Cooper et al., 1979) and Sm/Nd isotopes (Bokhari and Kramers, 1981) are not yet widely used.

The geological missions and the DGMR worked in - aerially and geologically - completely different areas, thereby producing different stratigraphical columns (see Figure 5.1). Another factor might be the incautious use of two to three point "isochrons" or, even worse, a one point "isochron" with an assumed initial ratio. Resetting of geochronological ages by "thermal" events seems to be a major reason for clustering of K/Ar data in the age span 650 - 550 Ma. These data must be treated with extreme caution, since the rocks could represent much older formations (Aldrich, 1978).

5.4 Lithostratigraphy and geochronology of Eastern Egypt

5.4.1 General

In Egypt, probably more geochronological work has been done than in Saudi Arabia, albeit often of less accuracy. The stratigraphic sequence of the

Pan-African (1200 - 500 Ma) rock units is still largely unknown. Hashad (1980) in his paper "Present status of geochronological data on the Egyptian basement complex" gives us a compilation of 168 isotopic data (K/Ar, Rb/Sr, Pb/Pb) and more Rb/Sr data are given by Stern (1979) and Dixon (1979).

Early work (before 1970), using only K/Ar data indicated the oldest rocks to be Late Precambrian of maximal 600 Ma old; while these data undoubtedly indicate a major thermal event with isotopic resetting around 600 Ma, later, mainly Rb/Sr isotopic investigations indicated much older crust to 1200 Ma for the basement rocks (Hashad, 1980). Abdel-Monem and Hurley (1978) published an age of 1.77 Ga using U/Pb dating of detrital zircons in psammitic gneisses. This age probably reflects the age of the crustal block that supplied the zircon-carrying detritus.

Figure 5.3 shows in the first column a schematic correlation of Egyptian Pan-African units, mainly based on geochronological work (after Shackleton et al., 1980 and Hashad, 1980). We have, however, to bear in mind that the stratigraphic sequence is by no means accurate and that much more geochronological work has to be done, especially in the older units. The oldest rocks of E. Egypt are gneisses and migmatites (for example, the Meatiq and Hafafit gneisses), covering a long time-span of 1700 - 592 Ma (Shackleton et al., 1980). They are partly covered by the geosynclinal metasediments. Ultramafic and mafic rocks are abundant in E. Egypt and are always in tectonic contact with the other rock units. Shackleton et al. (1980) consider them to be tectonically transported fragments of oceanic crust (ophiolites). Younger calc-alkaline volcanics and sediments (for example, the Dokhan Group, as described by Basta et al., 1980) and the sedimentary Hammamat Group are the youngest Pan African units in E. Egypt.

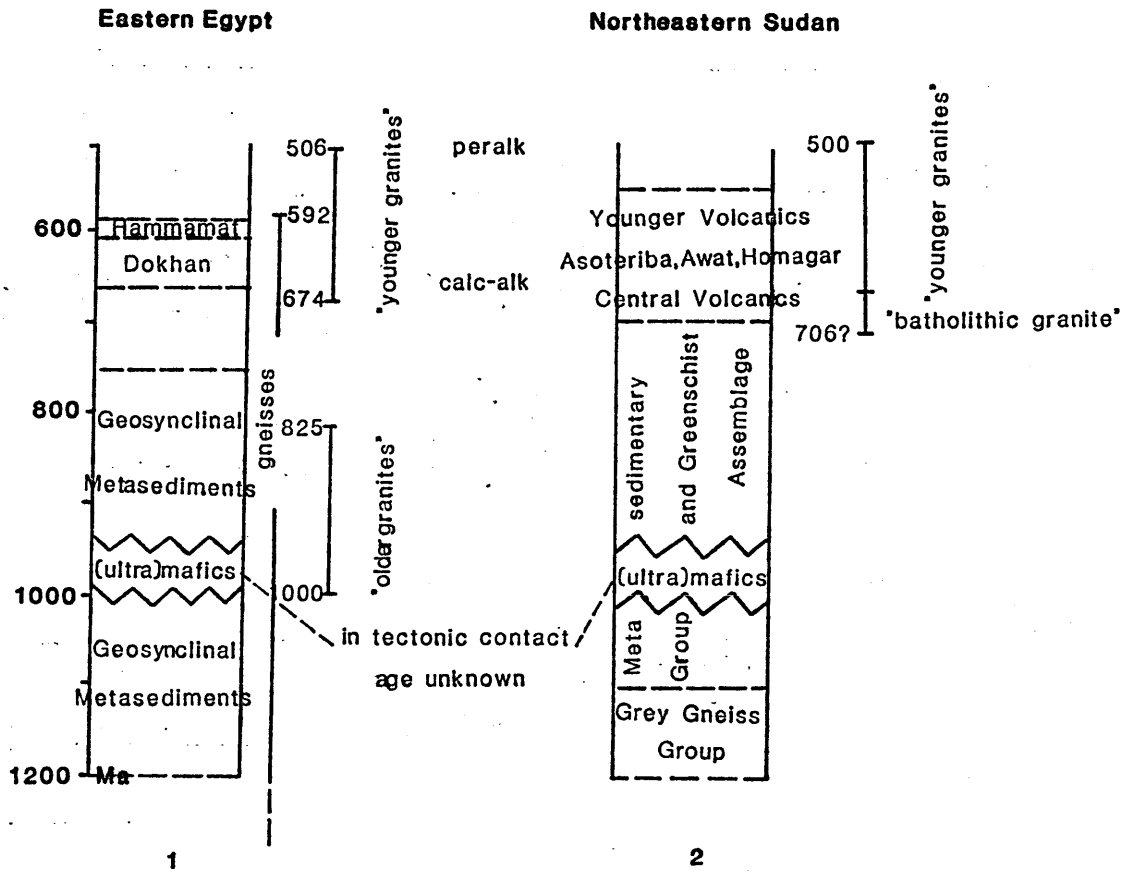

Figure 5.3 Simplified stratigraphic schemes for eastern Egypt and northeastern Sudan (E.Egypt after Hashad, 1980 and Shackleton et al., 1980; NE Sudan after Vail, 1976 and 1979).

Plutonic rocks have been described (Hashad, 1980 and Shackleton et al., 1980) in two main pulses in the Pan-African time-span, namely the older, often dioritic, granitoids (1000 - 825 Ma) and the younger granites (674 - 506 Ma), ranging in composition from calc-alkaline to peralkaline granites. Worthwhile mentioning, but outside the Pan-African range, is a group of alkaline rocks (volcanics and ring complexes) in the basement with an age range of 300 - 80 Ma. There is no equivalent of this alkaline period in the Arabian Shield; an extension into Sudan has been identified by Harris and Gass (1981). Initial $^{87}Sr/^{86}Sr$ ratios for the Pan-African Egyptian rocks cluster around 0.703 (see Figure 5.12); they are shown and discussed together with Arabian Shield initial ratios in Chapter 5.7.1.

5.4.2 The younger volcano-sedimentary units

The younger volcano-sedimentary units are of special interest for this study, because they might represent comparable rock units to the Murdama/Shammar Groups in Saudi Arabia. The Dokhan volcanics have been studied extensively by Basta et al. (1980), who conclude that the Dokhan Formation consists of a thick sequence of lava flows and minor pyroclastics. At Jabal Dokhan, the type locality area ($27^{o}15'N$, $33^{o}14'E$), the volcanics are 1200 metres thick and petrographically classified as andesites, dacites, latites, trachytes and pyroclastics. The volcanics are calc-alkaline with mildly tholeiitic affinities. Basta et al. (1980) suggest that the Dokhan volcanics represent a well developed island arc with a thick continental crust or active continental margin. The petrochemical data have been described to correlate well with the Afna Formation, being the lower part of the Hulayfah Group in the Arabian Shield (Delfour, 1976). The age range of the Hulayfah Group (780 - 658 Ma, compared to 678 - 633 Ma for the Murdama Group and 663 - 555 Ma for the Shammar Group - see Figure 5.1), the aerial extent of the Dokhan Formation and the Hulayfah, Murdama and Shammar Groups on both sides of the Red Sea and

the comparison of some geochemical data (see Table 5.1) make it more likely that the Dokhan Formation belongs to the Murdama Group.

	Hulayfah Group (24)	Fatima volcanics (33)	Badr volcanics (73)	Nuqrah volcanics (33)	Dokhan volcanics (48)
SiO_2	56	61	68	68	61
TiO_2	0.9	1.0	0.9	0.7	1.0
Al_2O_3	15	15	15	15	15
FeO*	8	7	5	4	7
K_2O	1.0	1.7	2.8	3.5	1.7
Na_2O/K_2O	8	2.4	2.3	1.5	1.6

Table 5.1 Comparison of major element data of the Hulayfah Group (Delfour, 1976), the Fatima and Badr volcanics, both belonging to the Murdama Group, the Nuqrah volcanics, belonging to the Shammar Group and the Dokhan volcanics (Basta et al., 1980). Average contents for major elements are given for each group; the amount of analyses, on which the averages are based, are given in brackets (see also Table 6.2).

The Hammamat sediments, dated 607 -596 Ma (Ries, pers. comm.) are described (Shackleton et al., 1980) as molasse-type conglomerates, greywackes and siltstones and could be an equivalent of the Shammar Group of Saudi Arabia. No detailed geochemical data of this sedimentary group, however, are available at present.

5.5 Lithostratigraphy and geochronology of Northeastern Sudan

5.5.1 General

Scarce geochronological data from the Precambrian Pan-African basement of Sudan cannot produce a clear outline for the geological history of this part of the Nubian-Arabian Shield. Vail (1976) and Bessoles and Trompette (1980) list most of the available radiometric data (K/Ar, Rb/Sr, Pb/Pb), more Rb/Sr dates are indicated by Neary et al. (1976), Cavanagh (1979) and Almond (1979). Figure 5.3 shows in the second column a tentative outline of the stratigraphy of NE Sudan, compared with time-equivalent rock units in E. Egypt. The oldest unit, according to Vail (1979) is the Grey Gneiss Group, consisting of biotite and muscovite granitic gneisses. The Metasedimentary Group locally (in the Bayuda Desert) covers the gneisses; this Group consists of psammites, schists and marbles. It is probably (Gass, pers. comm.) equivalent to the Greenschist Assemblage, cropping out in large areas in NE Sudan as intermediate to acidic volcanics and associated sediments (this Assemblage is locally called the Nafirdeib Group after Ruxton, 1956).

(Ultra)mafic bodies, as described by Fitches et al. (1981), have tectonic contacts with the Metasedimentary Group and the Greenschist Assemblage. A complete ophiolite sequence has been described at Sol Hamed, near the Sudanese/Egyptian border, by Fitches et al. (1981), as a possible source area for the ophiolitic mélange of the Eastern Desert in Egypt (Shackleton et al., 1980, Fitches et al., in prep.).

Extensive younger volcanics (less than 700 Ma in age) cover the earlier described rock units; they have been assigned local names as Awat Series (Ruxton, 1956), Asoteriba volcanics (Neary et al., 1976) and Homagar volcanics (Ali, unpubl. M. Phil. Thesis, 1979). The Central Volcanics (Almond, 1979) are probably also part of this unit.

The plutonic rocks (see Figure 5.3) comprise the Batholithic Granites, consisting of granodiorites, adamellites and diorites (Vail, 1979) and the younger granites, often characterized by ring complexes, consisting of granites, syenites and gabbros (Almond, 1979). Alkaline plutonism and related volcanism extends, like in Egypt (Harris and Gass, 1981) beyond the Pan-African time-span and Cavanagh (1979) describes a granite of 140 Ma in the extreme NE part of Sudan.

5.5.2 The younger volcanics

The younger volcanics with approximate age limits of 700 - 550 Ma are probably comparable to the younger volcano-sedimentary units of E. Egypt (Dokhan volcanics) and Saudi Arabia (Murdama/Shammar volcanics). Detailed geochemical analyses of the Sudanese volcanics to confirm this hypothesis are not available. The age brackets, the comparable metamorphic grade (lower greenschist facies) and the aerial extent on either side of the Red Sea, however, probably link the Sudanese younger volcanics with the Arabian Murdama/Shammar Groups.

5.6 New Rb/Sr geochronological data of the Arabian Shield

5.6.1 Introduction

Since the previous geochronological work in the study areas has been either insufficient or simply non-existent, it was thought to be of the greatest importance to complement extensive field and geochemical studies with radiometric age dating. Seven rock suites were sampled and analyzed according to the procedures described in the Appendix A. The localities of these seven suites is indicated in Figure 5.4. In each fieldwork area (Fatima, Badr and Nuqrah) both volcanics and related granitic rocks were sampled.

Isochron fitting, according to York (1967, 1969) and Williamson (1968) produces six isochrons (MSWD less than 2.5 after Brooks et al.,

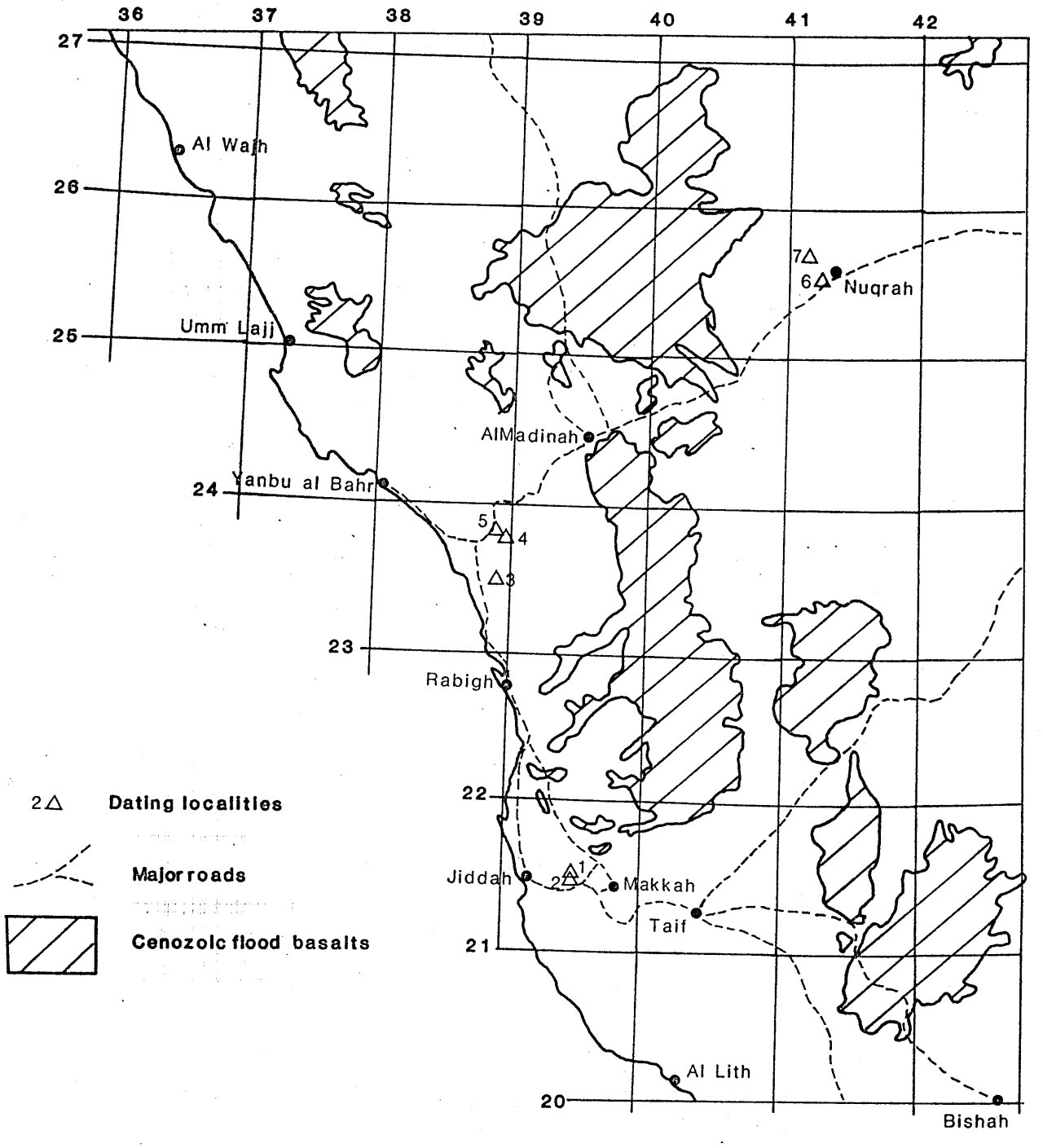

Figure 5.4 Locality map of new Rb/Sr geochronological investigations, Arabian Shield; 1 - Fatima granites, 2 - Fatima volcanics, 3 - Hamra tonalite, 4 - Hamra alkali granite, 5 - Badr volcanics, 6 - Nuqrah granites, 6 - Nuqrah volcanics.

Table 5.2

Summary of Rb/Sr geochronological investigations, Central Saudi Arabian Shield

($\lambda = 1.42 \times 10^{-11}\ yr^{-1}$)

Locality	Rock Type	Age	Initial Ratio	N	MSWD	Location on Figure 5.4 (with co-ordinates)
Wadi Fatima area						
W. Fatima, Jabal Daf	granite	772 ± 16	0.7023 ± 0.0002	4	1.76	1 - 21°33' ;39°33'
W. Fatima, Jabal Daf	volcanics	681 ± 13	0.7036 ± 0.0001	5	1.32	2 - 21°31' ;39°35'
Badr area						
SE of Badr	tonalite	654 ±173	0.7028 ± 0.0003	5	3.11	3 - 23°33' ;38°53'
SE of Badr	alkali-granite	686 ± 18	0.7023 ± 0.0010	5	2.49	4 - 23°45' ;38°56'
N of Badr	volcanics	634 ± 26	0.7031 ± 0.0004	9	1.11	5 - 23°53' ;38°55'
Nuqrah area						
NW of Nuqrah	granite	635 ± 14	0.7027 ± 0.0003	4	1.75	6 - 25°35' ;41°15'
W of Nuqrah	volcanics	626 ± 9	0.7025 ± 0.0002	8	1.25	7 - 25°38' ;41°10'

1972) and one errorchron (MSWD more than 2.5); a complete list of the data is shown in Table 5.2. The errors in Rb/Sr and $^{87}Sr/^{86}Sr$ ratios are 1.5 and 0.01%, respectively, unless otherwise stated (see Appendix A). All ages and initial ratios are quoted with 2σ errors. As decay constant was used the value $\lambda\ ^{87}Rb = 1.42 \times 10^{-11}\ a^{-1}$, as proposed by Steiger and Jäger, (1977).

5.6.2 Wadi Fatima area

5.6.2.1 Fatima granite (see Figures 5.4 and 5.5)

This granite is a part of a large igneous body, described by Skiba (1980) as the Wadi Al-Hefna batholith. This body underlies with a clear angular unconformity the Fatima Group (Nebert et al., 1974). Four granite samples with a good spread in Rb/Sr ratios produce an isochron with an age of 772 ± 16 Ma. The intercept is 0.7023 ± 0.0002 and the MSWD (mean square of weighted deviates) 1.76.

Brown et al. (1978) indicate an age of 763 ± 159 Ma with an initial ratio of 0.7026 ± 0.0019 for a granitic gneiss in the same Wadi Al-Hefna batholith near Jeddah Airport.

5.6.2.2 Fatima volcanics (see Figures 5.4 and 5.6)

Five samples of Fatima volcanics, varying in composition from andesite to rhyolite, give a good spread in Rb/Sr ratio. The rocks have been metamorphosed to lower greenschist facies (see Chapter 2). The age is 681 ± 13 Ma with an initial ratio of 0.7036 ± 0.0001 and MSWD 1.32; Brown et al. (1978) give K/Ar ages of 592 ± 23 Ma (altered basalt) and 576 ± 28 Ma (dacite) for the Fatima Group. These ages are probably reset and do not reflect the time of deposition. Derbyshire (pers. comm.) calculated a Rb/Sr radiometric age of 681 ± 25 Ma (with an initial ratio of 0.7033 ± 0.0002 and MSWD 2.15) for the Fatima Group volcanics at Jabal abu Gurrah, 15 kilometres NE of Jabal Daf.

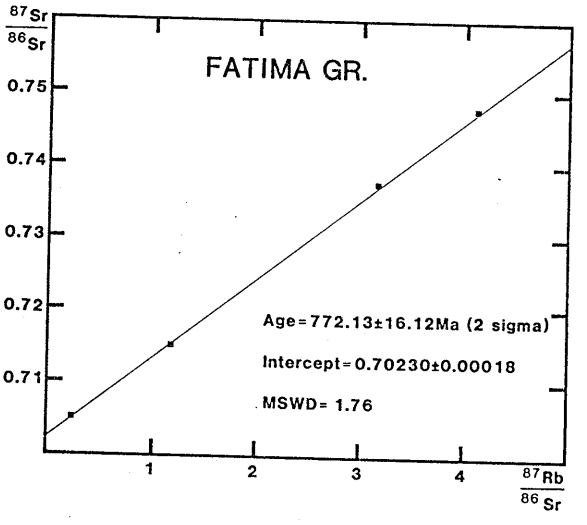

Figure 5.5 Rb/Sr isochron for Fatima granites

Line	$^{87}Rb/^{86}Sr$	S.D.	$^{87}Sr/^{86}Sr$	S.D.	Xres	Yres	Sample
1	4.111	.062	.74802	.00007	.03523	-.00000	FA 053
2	3.156	.047	.73745	.00007	.03127	-.00001	FA 073
3	.243	.004	.70502	.00007	.00081	-.00003	FD 12
4	1.190	.018	.71509	.00007	-.02676	.00004	FA 080

Number of cycles 4; slope = 0.011025 $\pm$ 0.000116

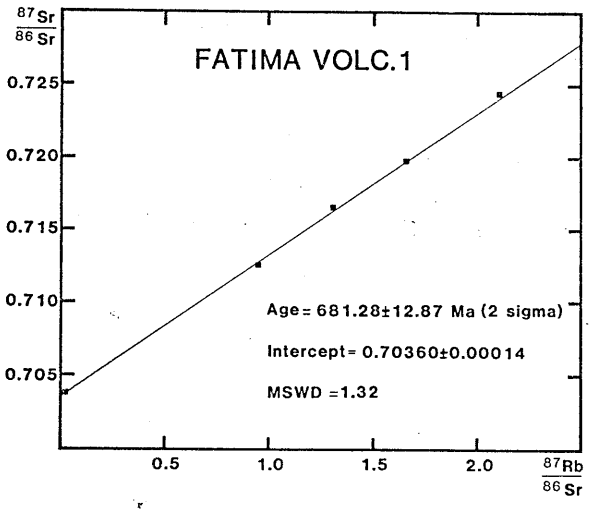

Figure 5.6 Rb/Sr isochron for Fatima volcanics

Line	$^{87}Rb/^{86}Sr$	S.D.	$^{87}Sr/^{86}Sr$	S.D.	Xres	Yres	Sample
1	1.310	.020	.71652	.00007	.01642	-.00002	FD 2
2	.953	.014	.71261	.00007	-.02097	.00005	FA 032
3	.017	.000	.70379	.00007	.00000	-.00002	FD 5
4	1.661	.025	.71975	.00007	.00000	-.00000	FD 4
5	2.114	.032	.72434	.00007	.01817	-.00001	FD 10

Number of cycles 4; slope = 0.009721 $\pm$ 0.000092

The age of 681 ± 13 Ma, the low metamorphic grade and the geochemical and field characteristics most likely put the Fatima volcanics in the Murdama Group. It is proposed that the use of the term "Fatima Group" after these and other geochronological studies, is terminated and the Fatima Group assigned to the lower parts of the Murdama Group, which is accepted as an extensive Shield-covering unit (see also Chapter 2 for further discussion).

5.6.3 Badr area

5.6.3.1 Introduction (see Figure 5.4)

The Badr volcanics are underlain, albeit not in such a clear way as in the Fatima area, by an older granitic basement. Two suites of this "basement", respectively tonalites and alkali-granites, were collected by tne author and M.D. Clark, the DGMR geologist responsible for mapping the Hamra sheet (see Figure 3.1). The localities of these suites are shown on Figure 3.4.

5.6.3.2 Hamra tonalites (see Figures 5.4 and 5.7)

Five samples of a large tonalite body indicate an unfavourable spread in Rb/Sr ratios. The errors are large and the MSWD indicates the result to be an "errorchron" rather than isochron (Brooks et al., 1972). The age indicated is 654 ± 173 Ma, the intercept 0.7028 ± 0.0006 and the MSWD 3.11 (the errors have been increased because of the large MSWD). There are no other ages known for tonalites in the Hamra sheet, but Kemp et al. (1980) indicate for the adjacent Yanbu al Badr sheet two ages for tonalites, namely Jabal Salajah tonalite of 725 ± 12 Ma and Jar tonalite of 796 ± 23 Ma. Both tonalites are probably equivalent to the Hamra tonalite.

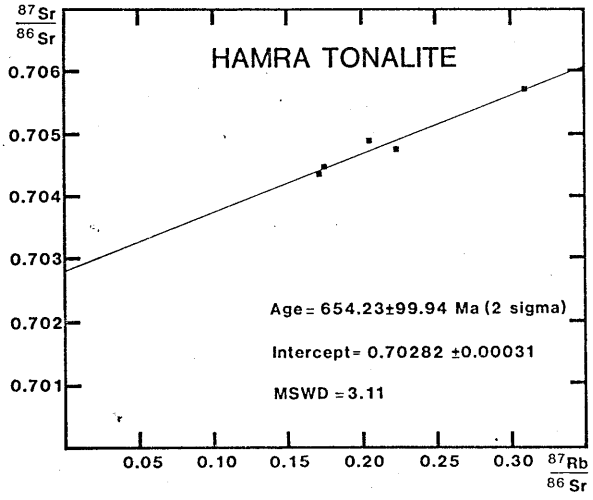

Figure 5.7 Rb/Sr errorchron for the Hamra tonalite, Badr area

Line	$^{87}Rb/^{86}Sr$	S.D.	$^{87}Sr/^{86}Sr$	S.D.	Xres	Yres	Sample
1	.174	.003	.70447	.00007	.00031	-.00002	HT 1
2	.205	.003	.70490	.00007	.00256	-.00014	HT 2
3	.223	.003	.70475	.00007	-.00264	.00013	HT 3
4	.310	.005	.70572	.00007	.00024	-.00001	HT 4
5	.171	.003	.70436	.00007	-.00061	.00005	HT 5

Number of cycles 4; slope = 0.009333 $\pm$ 0.000716

5.6.3.3 Hamra alkali-granite (see Figures 5.4 and 5.8)

Five of the samples indicate a good range of Rb/Sr ratios (sample HA 1 had to be discarded because of extremely low Sr content and, therefore, large errors in Rb/Sr ratio) and give an age of 687 ± 18 Ma with an intercept of 0.7023 ± 0.0010 and MSWD 2.49 (an error of 0.02% in $^{87}Sr/^{86}Sr_i$ was used because of drift in the NBS standard). The age is unusually old for alkaline plutonic rocks (see Figure 5.1), the DGMR reports the oldest alkaline granites at 660 Ma. No other ages are described from this area, but Kemp et al. (1980) mention in the Yanbu al Bahr sheet an alkali-granite of 634 ± 9 Ma (Rb/Sr isochron).

5.6.3.4 Badr volcanic association (see Figures 5.4 and 5.9)

This volcanic group, an association of basaltic and rhyolitic volcanics, was analyzed for the first time for age dating in the Hamra sheet. The nine samples range in composition from basalt to andesite and rhyolite and produce an isochron with a very good spread in Rb/Sr ratios. The calculated age is 634 ± 26 Ma, the intercept 0.7031 ± 0.0004 and MSWD 1.11 (rather low Sr contents and drift in NBS standards forced the respective errors up to 2.0% and 0.02% in Rb/Sr and $^{87}Sr/^{86}Sr$, respectively). The age indicates the Badr volcanics to belong to the Murdama Group (see also Chapter 3 for further discussion). Kemp et al. (1980) assign the northerly continuation of the Badr volcanics to the Al Ays Group with an age range of 476 - 923 Ma. They report big disturbances in Sr systems as the reason for age differences in acidic rocks. The Al Ays-Abathir Formation, which is probably equivalent to the Badr volcanics (Pellaton, 1979) was dated at 684 Ma.

5.6.4 Nuqrah area

5.6.4.1 Introduction

The Nuqrah area is relatively well studied and documented, especially by Delfour (1976, 1977, 1979). Since this area contains the type locality

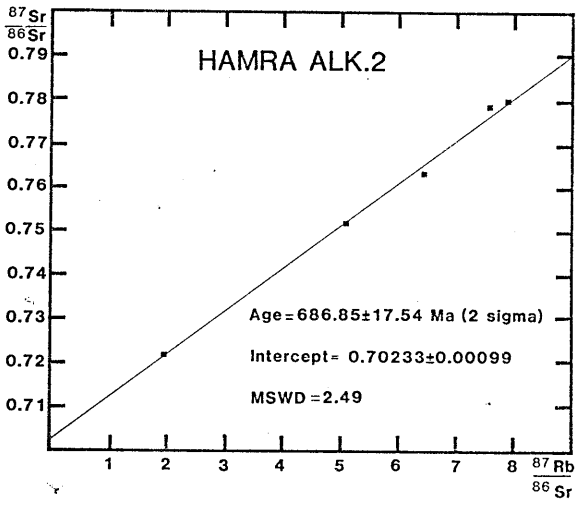

Figure 5.8 Rb/Sr isochron for the Hamra alkali granite,Badr area

Line	$^{87}Rb/^{86}Sr$	S.D.	$^{87}Sr/^{86}Sr$	S.D.	Xres	Yres	Sample
1	7.874	.118	.78008	.00016	.05801	-.00001	HA 2
2	7.587	.114	.77857	.00016	.18833	-.00004	HA 3
3	5.093	.076	.75184	.00015	-.03968	.00002	HA 4
4	6.441	.097	.76352	.00015	-.19257	.00005	HA 5
5	1.965	.029	.72168	.00014	.00758	-.00002	HA 6

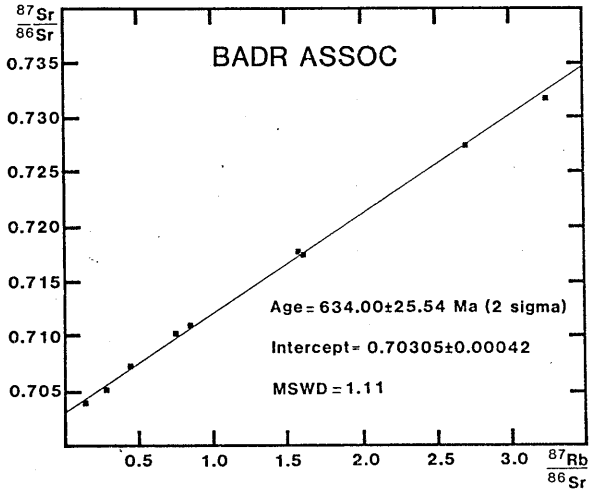

Figure 5.9 Rb/Sr isochron of the Badr Association volcanics, Badr area

Line	$^{87}Rb/^{86}Sr$	S.D.	$^{87}Sr/^{86}Sr$	S.D.	Xres	Yres	Sample
1	1.585	.032	.71770	.00036	.01300	-.00018	BD 2
2	.284	.006	.70518	.00035	-.00101	.00043	BA 104
3	.845	.017	.71097	.00036	.00470	-.00023	BA 120
4	.145	.003	.70391	.00035	-.00027	.00045	BA 216
5	.738	.015	.71023	.00036	.00687	-.00044	BA 227
6	.443	.009	.70735	.00035	.00158	-.00028	BA 006
7	1.614	.032	.71745	.01435	-.00001	.00021	BA 209
8	2.706	.054	.72745	.00036	-.00703	.00004	BA 175
9	3.252	.065	.73171	.00036	-.06237	.00022	BA 108

Number of cycles 4; slope = 0.009055 $\pm$ 0.000183

of the Shammar Group, one of the last volcanic events in the Precambrian Arabian Shield and as such of special interest to the author, the volcanics and related plutonic rocks were collected for age dating.

5.6.4.2 Nuqrah granites (see Figures 5.4 and 5.10)

According to Delfour (1977) plutonic and volcanic rocks are closely related for the Shammar Group rocks. Studies of field relations, geochemistry and isotope age dating could clarify these relations. Four samples define an isochron for the Nuqrah granites, indicating an age of 635 ± 14 Ma, an intercept of 0.7027 ± 0.0003 and MSWD 1.75. Delfour describes a peralkalic granite W of Nuqrah with an age of 600 Ma as an early example in a range of calc-alkalic to peralkalic plutonism from 600 - 535 Ma; slightly older granites and diorites were dated around 640 Ma (Delfour, 1977).

5.6.4.3 Nuqrah volcanics (see Figures 5.4 and 5.11)

The Nuqrah volcanics were extensively sampled in the type locality area (Delfour, 1976, 1977, 1979) of the Shammar Group. An eight-point isochron with a good Rb/Sr spread indicate an age of 626 ± 9 Ma, an intercept of 0.7025 ± 0.0002 and MSWD 1.25. Comparison with tne age of the Nuqrah granites shows that volcanics and plutonic rocks are (with analytical errors of about the same age. The same applies for the initial ratios and it can be safely assumed that plutonic and volcanic rocks had the same magma source.

Delfour (1976) indicates a range in age for the Shammar volcanics of 638 - 600 Ma; directly W of the study area Delfour (1977) describes an age of 600 ± 25 Ma and an initial ratio of 0.7067 ± 0.0033 for the volcanics of the Malha Formation - the younger of the Shammar Formations - near Jabal Awja; Baubron et al. (1976) give an age of 555 Ma (K/Ar) for the same locality.

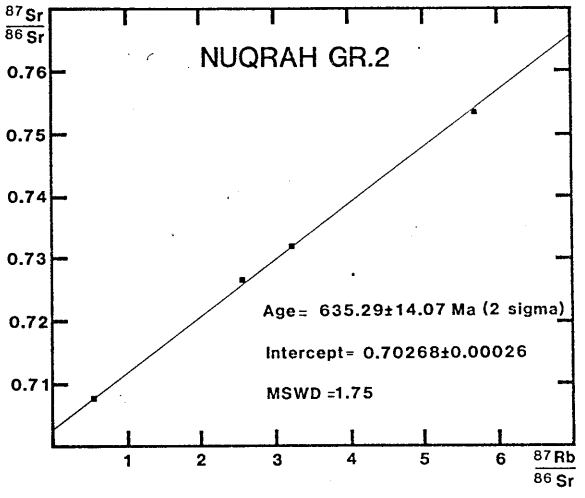

Figure 5.10 Rb/Sr isochron of the Nuqrah granites

Line	$^{87}Rb/^{86}Sr$	S.D.	$^{87}Sr/^{86}Sr$	S.D.	Xres	Yres	Sample
1	.550	.008	.70764	.00007	-.00140	.00001	NU 111
2	3.229	.048	.73192	.00007	-.00225	.00000	NU 007
3	5.690	.085	.75330	.00007	-.10303	.00001	NU 130
4	2.569	.039	.72646	.00007	.05288	-.00002	NU 110

Number of cycles 4; slope = 0.009062 $\pm$ 0.000101

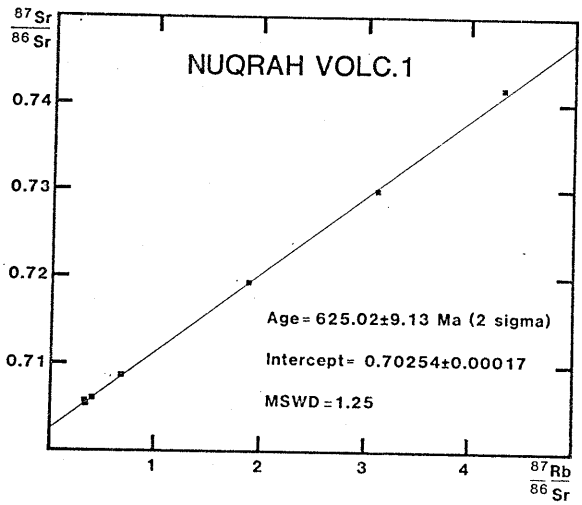

Figure 5.11 Rb/Sr isochron of the Nuqrah volcanics

Line	$^{87}Rb/^{86}Sr$	S.D.	$^{87}Sr/^{86}Sr$	S.D.	Xres	Yres	Sample
1	4.316	.043	.74174	0.00015	.06439	-.00009	NU 120
2	.391	.004	.70595	0.00014	-.00054	.00008	NU 116
3	.321	.003	.70561	0.00014	.00090	-.00019	NU 113
4	1.881	.019	.71937	0.00014	.00209	-.00001	NU 121
5	3.101	.031	.72993	0.00015	-.02638	.00007	NU 134
6	.336	.003	.70542	0.00014	-.00059	.00012	NU 122
7	.675	.007	.70861	0.00014	.00070	-.00003	NU 124
8	3.107	.031	.72998	0.00015	-.02672	-.02672	NU 118

Number of cycles 4; slope = 0.008929 $\pm$ 0.000065

Age dating and geochemical characteristics (see Chapter 4) of the Nuqrah volcanics clearly shows them to belong to the Shammar Group.

5.7.1 Initial ratios : age/intercept diagrams

The initial ratios of all isochrons of samples from the Fatima, Badr and Nuqrah areas are relatively low (less than 0.704), as shown in Table 5.2. This might indicate an upper mantle origin for the sampled plutonic and volcanic rocks, as postulated by Fleck et al. (1980) for the southern Arabian Shield, where initial ratios, averaging 0.703 ± 0.001 are thought to be indicative for an upper mantle origin. Hashad (1980) reports on initial ratios from Egypt (Precambrian basement) of around 0.706 as a result of contamination of mantle-derived magma. To test these hypotheses and evaluate the evolution of initial ratios in time, the new initial ratios, as mentioned in Table 5.2, and 44 other initial ratios from the Nubian-Arabian Shield (see Figure 5.14 for the source of the data) were plotted against their age (see Figure 5.12 for Egypt/Sudan and 5.13 for the Arabian Shield). In co-operation with Dr. N.B.W. Harris these data were compiled from isochrons, based on at least three points with errors in age of less than 10% and an initial ratio of less than 2%. Data with unknown errors were omitted and all data, where necessary, standardized to IUGS recommended constants (Steiger and Jäger, 1977).

Both the Egypt/Sudan data (whereby Sudan is seriously under-represented) and Arabian Shield data (see Figures 5.12, 5.13) show low (less than 0.703) initial ratios for the older rock units. Since the data on the Arabian Shield are more complete than the similar Egypt/Sudan data, this initial ratio/age diagram will be discussed in detail. The majority of the initial ratios of Figure 5.13 are low, but there is a sharp and progressive increase in the maximum initial ratios (0.705 - 0.711) for samples younger than 700 Ma. The oldest reported isochron of the Arabian

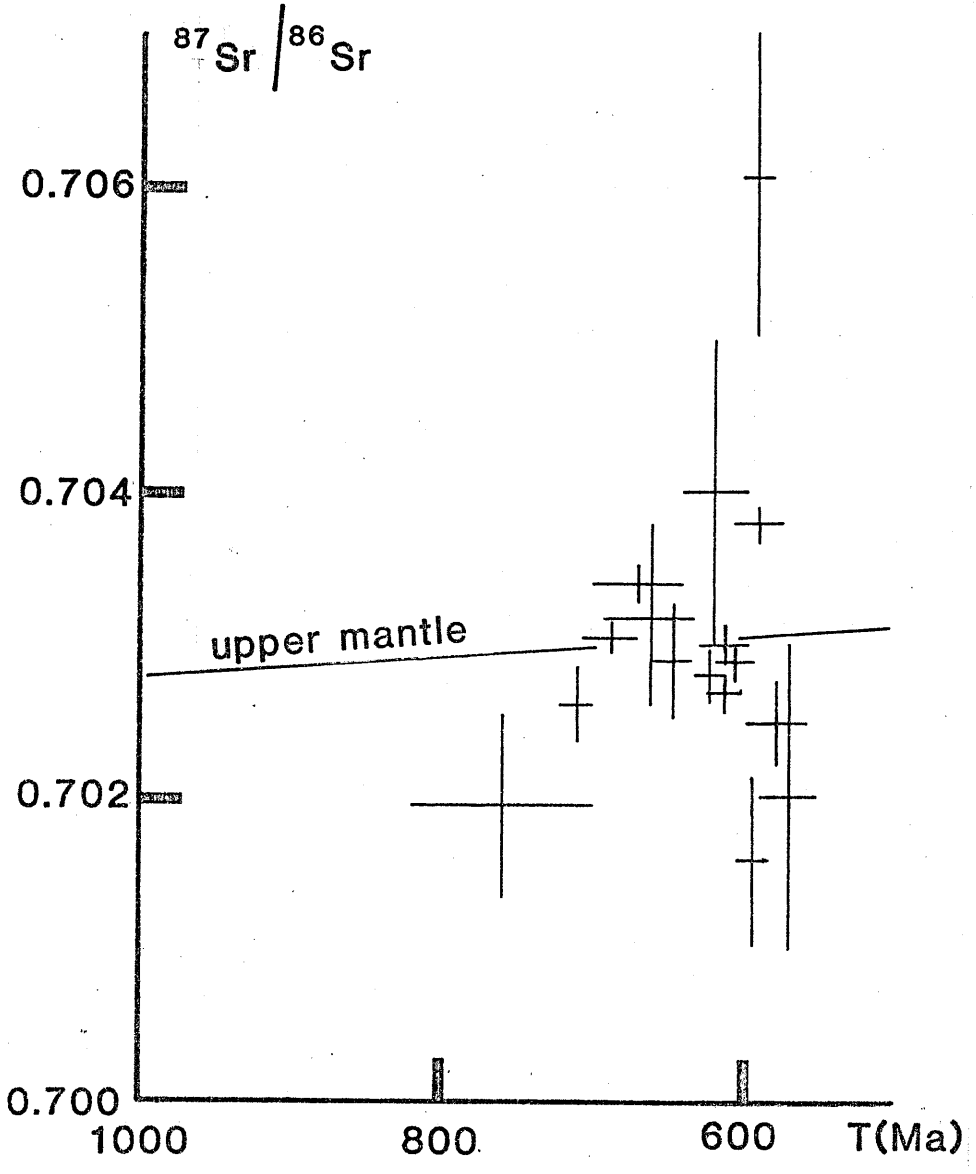

Figure 5.12 Strontium evolution diagram for samples from Egypt and Sudan, after Duyverman & Harris (1981, in press) - for explanation see text.

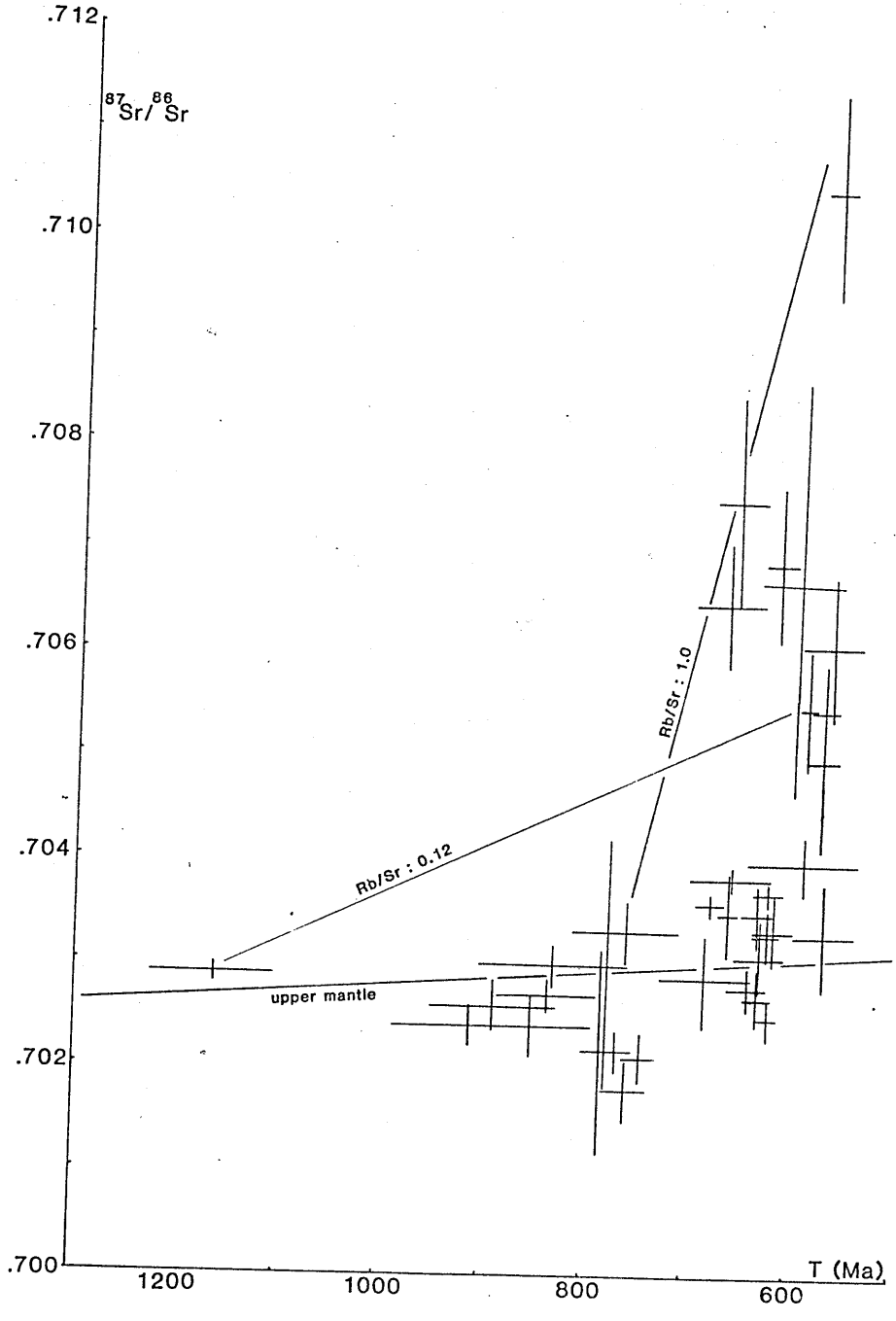

Figure 5.13 Strontium evolution diagram for samples from the Arabian Shield, after Duyverman & Harris (1981, in press) - for explanation see text.

Shield is a basalt of 1165 Ma (Fleck et al., 1980) from the Al Lith area. The reliability of this three-point isochron remains to be determined; the oldest reliable age is 912 Ma (Fleck et al., 1980) for meta-volcanics.

A single-stage strontium evolution of the older Arabian Shield rocks, assuming a Rb/Sr ratio of 0.12, typical for average andesitic crust (Weaver and Tarney, 1980) would only yield initial ratios of 0.7055 by 600 Ma (see Figure 5.13). A two-stage (as illustrated on Figure 5.13) or multi-stage model for the evolution of initial ratios through time is more likely. By 800 Ma granodioritic magmas of increased Rb/Sr ratios were being formed (up to 1.0) and the strontium growth line for such rocks indicates that they could be a suitable source for the late high initial ratios.

5.7.2 Initial ratios : spatial trends

Figure 5.14 indicates the aerial distribution of the data discussed in the previous chapter. Clearly, higher initial ratios are found in the central and northeastern part of the Arabian Shield. It has been suggested, that this trend is evidence for older sialic crust lying towards the east of the Arabian Shield (Delfour, 1977, Engel et al., 1980) and Pb/Pb isotopic data from massive sulphide deposits in the Arabian Shield have been invoked in support of the existence of a 2100 Ma continental crust in the eastern Shield (Stacey et al., 1980). Although this hypothesis cannot be discounted, model Rb/Sr ages from suites of high initial $^{87}Sr/^{86}Sr$ ratios suggest that their source region had separated from the upper mantle less than 100 Ma before their emplacement; also, no conventional Rb/Sr isotopic ages older than about 900 Ma have been reported from the eastern Arabian Shield. It is quite possible, as shown in Figure 5.13, that the strontium evolution was completely self-contained, without necessarily implying older sialic crust to account for the higher initial ratios. An eastward subduction

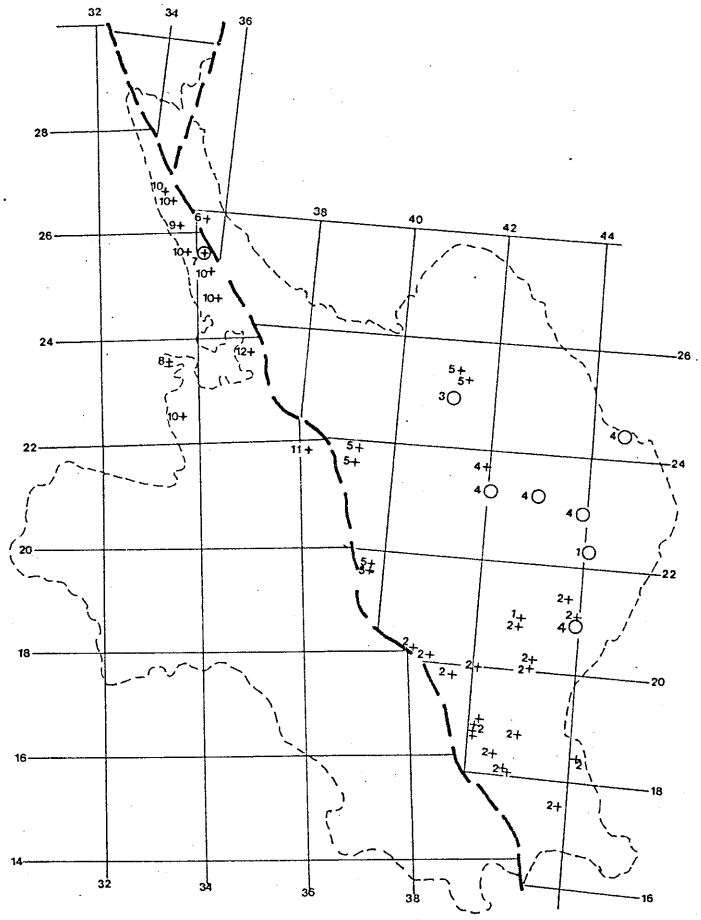

Figure 5.14 Aerial distribution of data points plotted in Figs. 5.12 and 5.13; the Nubian-Arabian Shield is shown in Pre-Red Sea position.

+ – $^{87}Sr/^{86}Sr_i$ less than 0.705

0 – $^{87}Sr/^{86}Sr_i$ greater than 0.705

(Data after 1-Kröner *et al.*,1979;2 -Fleck *et al.*,1980;3-Dodge *et al.*, 1979; 4-Baubron *et al.*,1976; 5-Duyverman,this thesis; 6-Harris,unpubl. data; 7-Rogers *et al.*,1978; 8-Leggo,1968; 9-Ries,unpubl.data; 10-Stern, 1979; 11-Cavanagh,1979; 12-Dixon,1979)

zone (as proposed by Greenwood et al., 1977) with newly formed and thickened crust towards the northeast, providing suitable conditions for crustal anatexis, could account for the temporal and spatial distribution of the initial ratios.

6 Geochemistry

6.1 Introduction

Two hundred and forty whole rock samples were analysed at the Open University Laboratories. After cleaning and crushing (see Appendix A for the preparation of the samples) the powders were used for analysis in the energy dispersive XRF system (EDXRF) for major and trace elements, the mass spectrometer (MS) for isotope studies and the instrumental neutron activation analysis (INAA) for rare earth elements (REE). The microprobe was used for additional mineral analyses. All standard techniques are discussed in Appendix A; tables with geochemical results can be found in Appendix C. The purpose of the geochemical analyses was to establish the detailed geochemical characteristics of the rock types in the three fieldwork areas and to identify rock associations which could be compared with existing information in order to define the environment of eruption of the volcanic rocks and their relation to the plutonic rocks of the area. In this Chapter, major and trace elements, rare earth elements and petrogenesis will be discussed successively.

6.2 Major element studies

6.2.1 General

Major elements, routinely run in the EDXRF system as oxides were Na, Mg, Al, Si, P, S*, K, Ca, Ti, V*, Mn, Fe, Ba* (S* means semi-quantitative data). Major elements are very susceptible to modification during low-grade metamorphism and submarine alteration and are therefore of limited use for determining magma trends in volcanic rocks (Jakeš & Gill, 1970; Pearce et al., 1977; Garcia, 1978).

Harker diagrams, plotting oxides versus silica content, have been used to establish overall trends in major oxides. In using these diagrams we have to bear in mind that they serve a qualitative purpose only; Harker

diagrams cannot be effectively used for comparing rock series because the SiO_2 content shows little to no increase during the main part of fractional crystallization in typical tholeiitic series (Miyashiro, 1974). Na_2O and K_2O show a positive correlation with SiO_2; the other major oxides show a negative correlation[1]. Relevant diagrams, like the alkali-silica diagram, are shown in the next Chapters.

6.2.2 Alkali-silica diagram

Granitic and volcanic rocks, in which lava flows were separately identified, were plotted in an alkali-silica diagram (see Figure 6.1). The dividing curve between subalkalic and alkalic of Irvine & Baragar (1971) was used, and is considered by Basta et al. (1980) to give a better separation between the two fields than a straight line, as proposed by Macdonald & Katsura (1964). The majority of the analysed samples have higher Na_2O than K_2O contents; Figure 6.1 shows that the majority of the specimens from all three areas plot in the subalkaline field. The Fatima and Badr areas, however, contain about 10% alkalic specimens, whereas all but two of the Nuqrah samples fall within tne subalkalic field. The flows in the Fatima area are all basic, whereas in the Badr and Nuqrah areas they range from basic to acid.

Since the majority of the volcanic rocks is subalkalic, we can subdivide them further using AFM diagrams (after Irvine & Baragar, 1971; see Section 6.2.4). Also, the samples of Figure 6.1 were plotted on an alkali-lime index diagram (after Peacock, 1931) to check whether the rocks belong to an alkalic, alkali-calcic, calc-alkalic or calcic differentiation series (see Section 6.2.3).

1 - Generally, the correlation for the Nuqrah samples is better than for the Fatima and Badr samples.

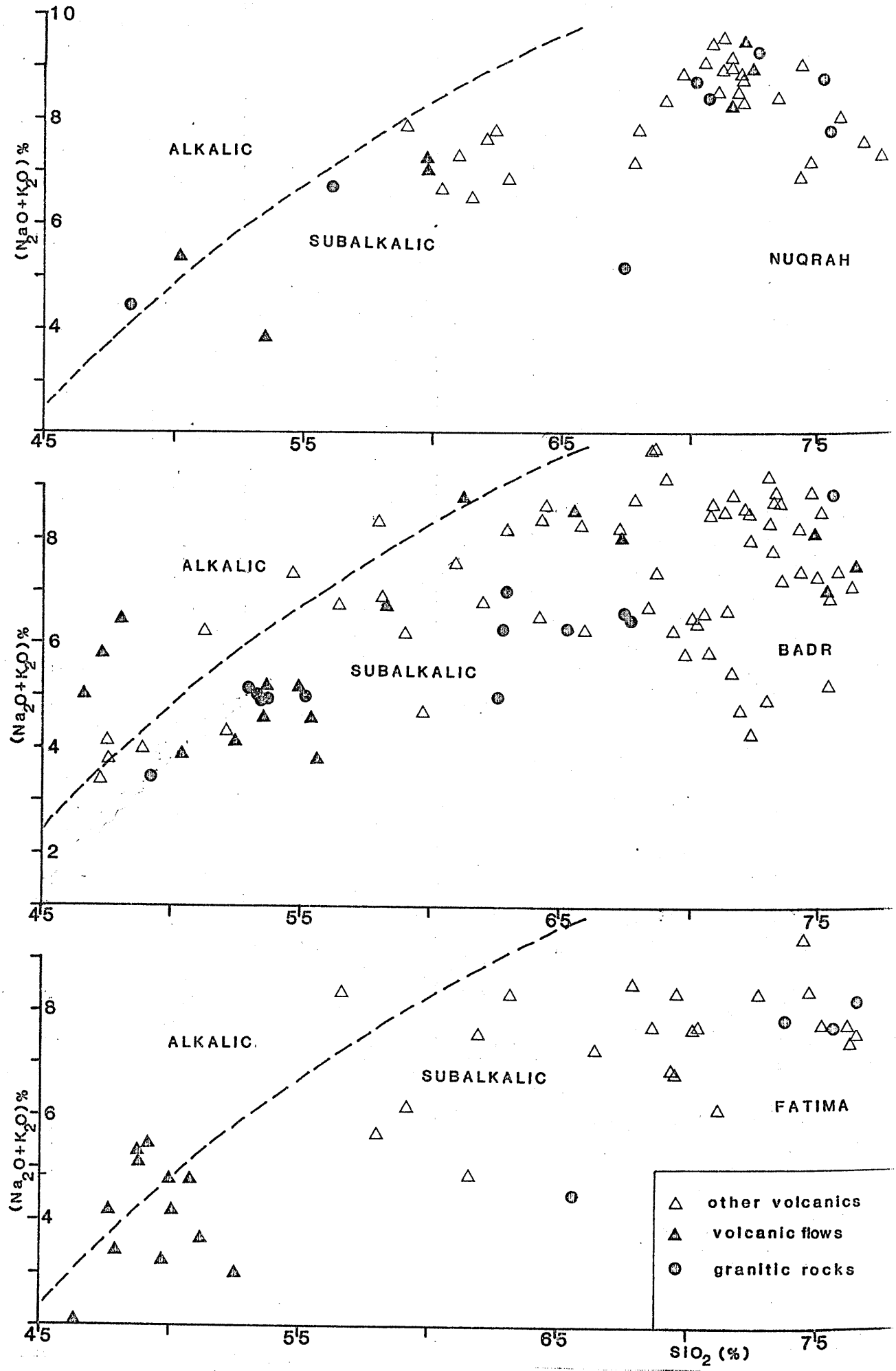

Figure 6.1 Alkali-silica diagram for the three fieldwork areas; the dividing curve between the subalkalic and alkalic fields is after Irvine&Baragar (1971

6.2.3 Alkali-lime index diagram

The granitic and volcanic rocks of the three areas were plotted on an alkali-lime diagram, as proposed by Peacock (1931). The alkali-lime index is the weight percentage of SiO_2 of a rock series at which the abundances of CaO and the alkali oxides (Na_2O and K_2O) are equal. Rock series with an index smaller than 51 are alkalic, with an index between 51 and 56 alkali-calcic, with an index between 56 and 61 calc-alkalic and with an index larger than 61 calcic.

Although the CaO and alkali contents of the Fatima and Badr sequences are variable, probably due to low-grade metamorphism and alteration (see Section 6.2.1), they indicate alkali-lime indices of c. 55 (Figure 6.2) for the Fatima area and of c. 57 for the Badr area. Although the position of the trend lines is poorly defined, they indicate alkali-calcic to calc-alkalic indices. The correlation of CaO and alkalis with SiO_2 is much better for the Nuqrah sequence; the alkali-lime index is 56, on the boundary between the alkali-calcic and calc-alkalic fields. The geochemical data of Delfour (1976) indicate a calcic alkali-lime index for the Hulayfah Group volcanic rocks.

6.2.4 AFM diagrams

AFM diagrams (A-Na_2O + K_2O, F-total iron as FeO, M-MgO) were originally constructed by Wager & Deer (1939) and they are commonly used to define iron depletion and iron enrichment trends characteristic of calc-alkalic and tholeiitic series respectively (Kuno, 1966). They are thought to provide a good pictorial definition of arc maturity (Brown, 1981). Iron depletion trends for lava series plot along a smooth band from the mafic side towards the alkali apex; iron enrichment trends display a strong deflection towards the iron apex. AFM diagrams do not discriminate well between acid residual liquids of different series (which cluster towards

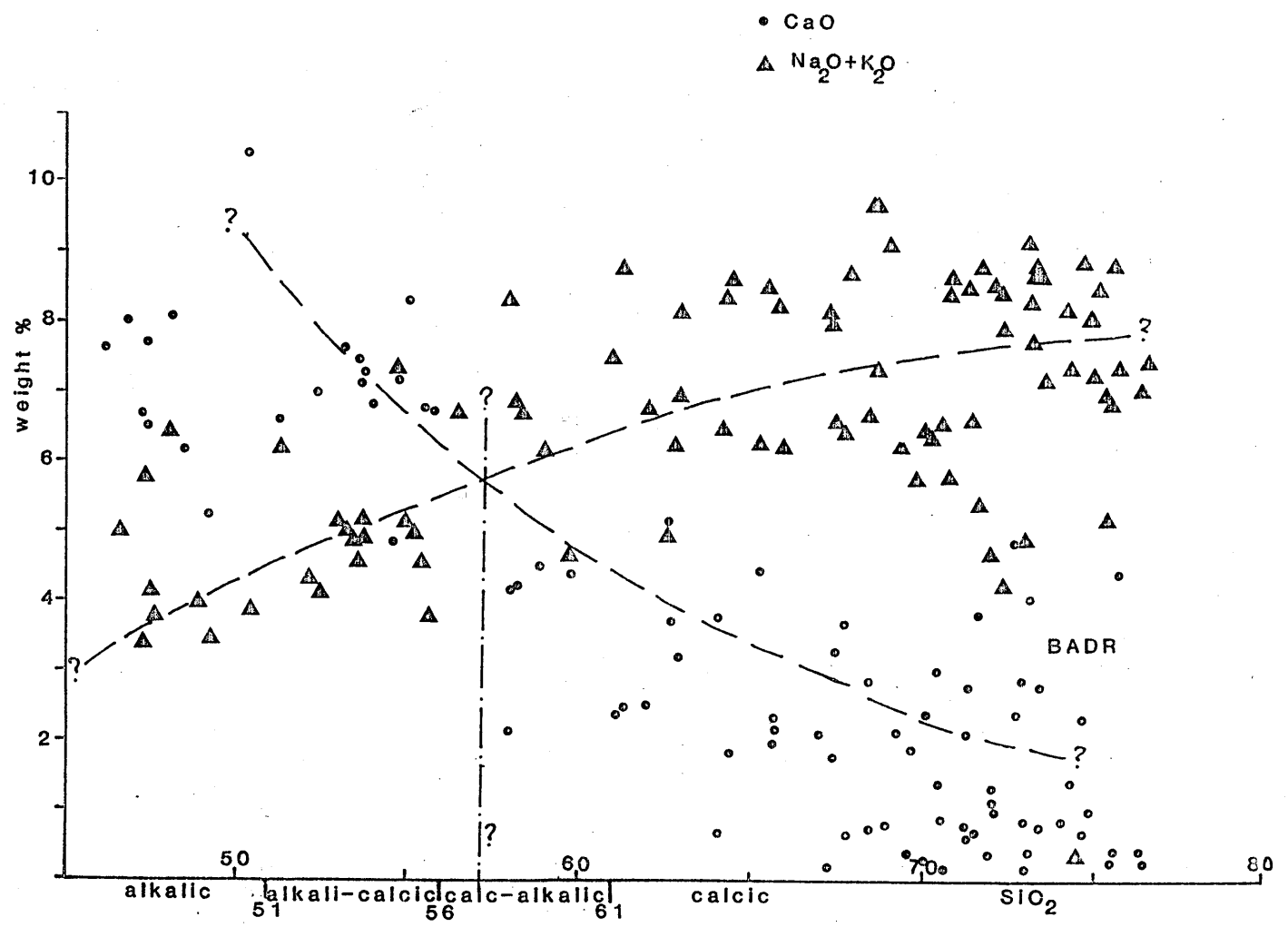
• CaO
▲ Na_2O+K_2O
weight %
10
8
6
4
2
BADR
50
60
70
80
alkalic
alkali-calcic
calc-alkalic
calcic
51
56
61
SiO_2

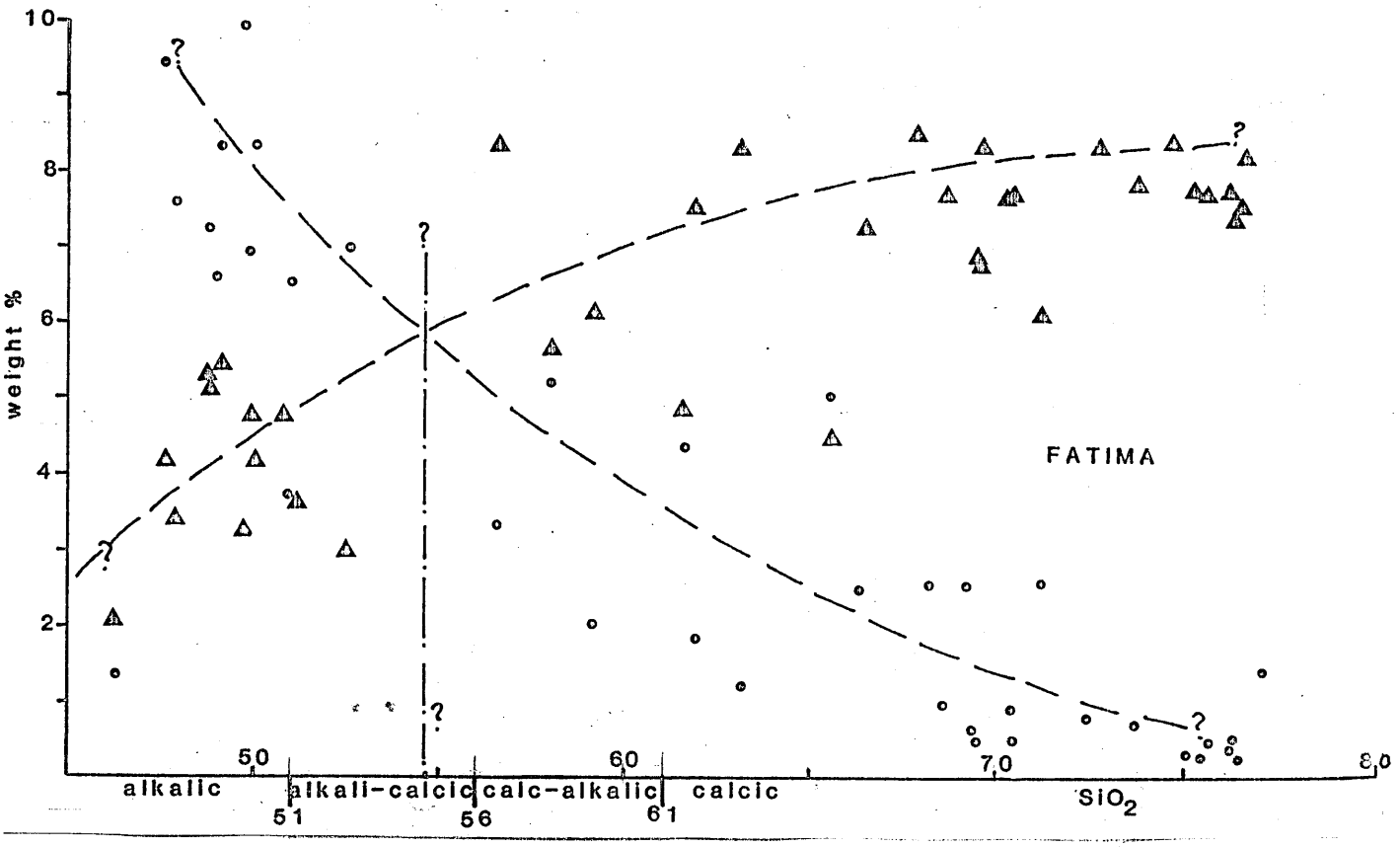
weight %
10
8
6
4
2
FATIMA
50
60
70
80
alkalic
alkali-calcic
calc-alkalic
calcic
51
56
61
SiO_2

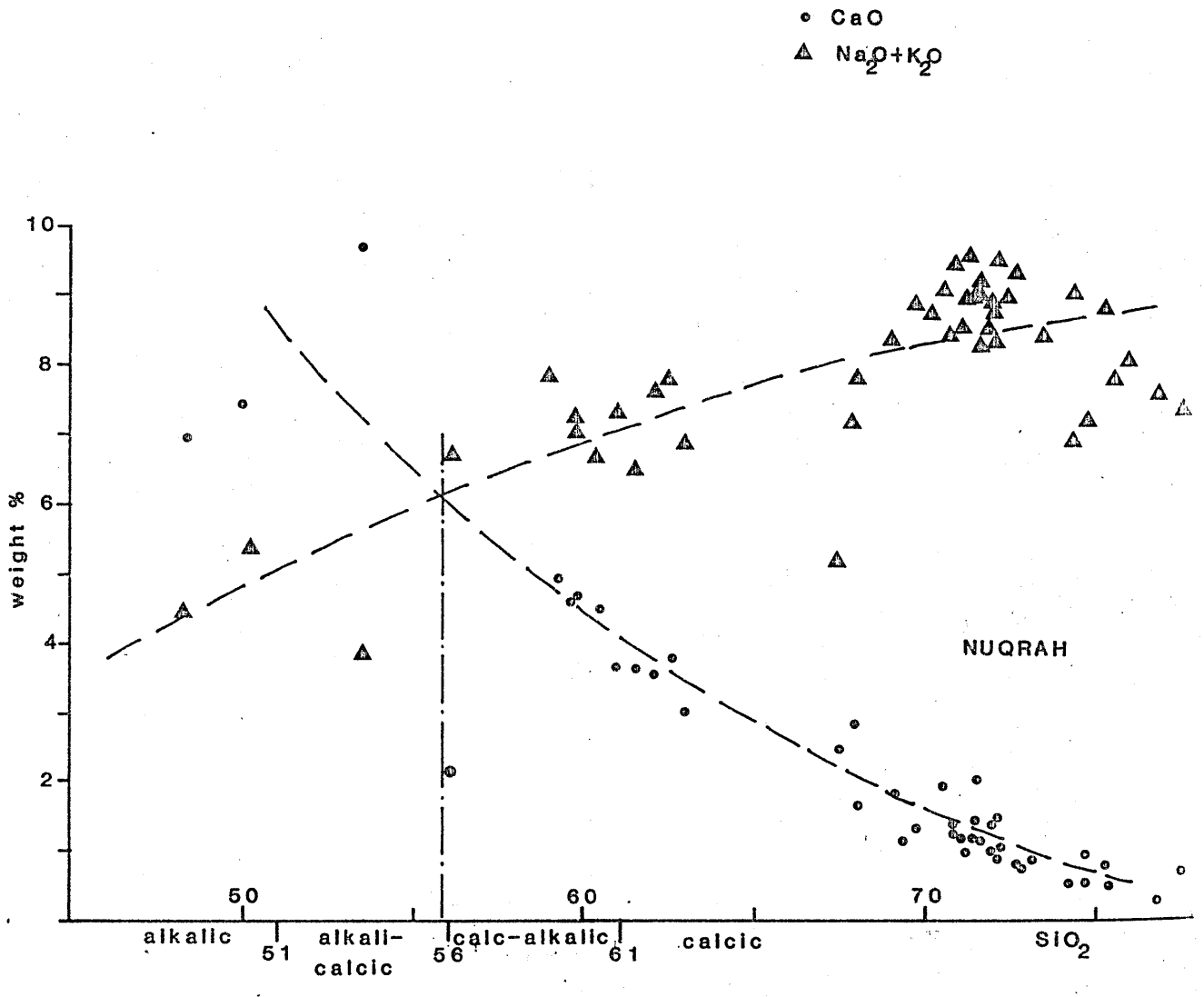

Figure 6.2 Alkali-lime index diagram for the three fieldwork areas; the boundaries of the alkalic, alkali-calcic, calc-alkalic and calcic fields are after Peacock (1931); the alkali-lime indexes for the three areas are indicated.

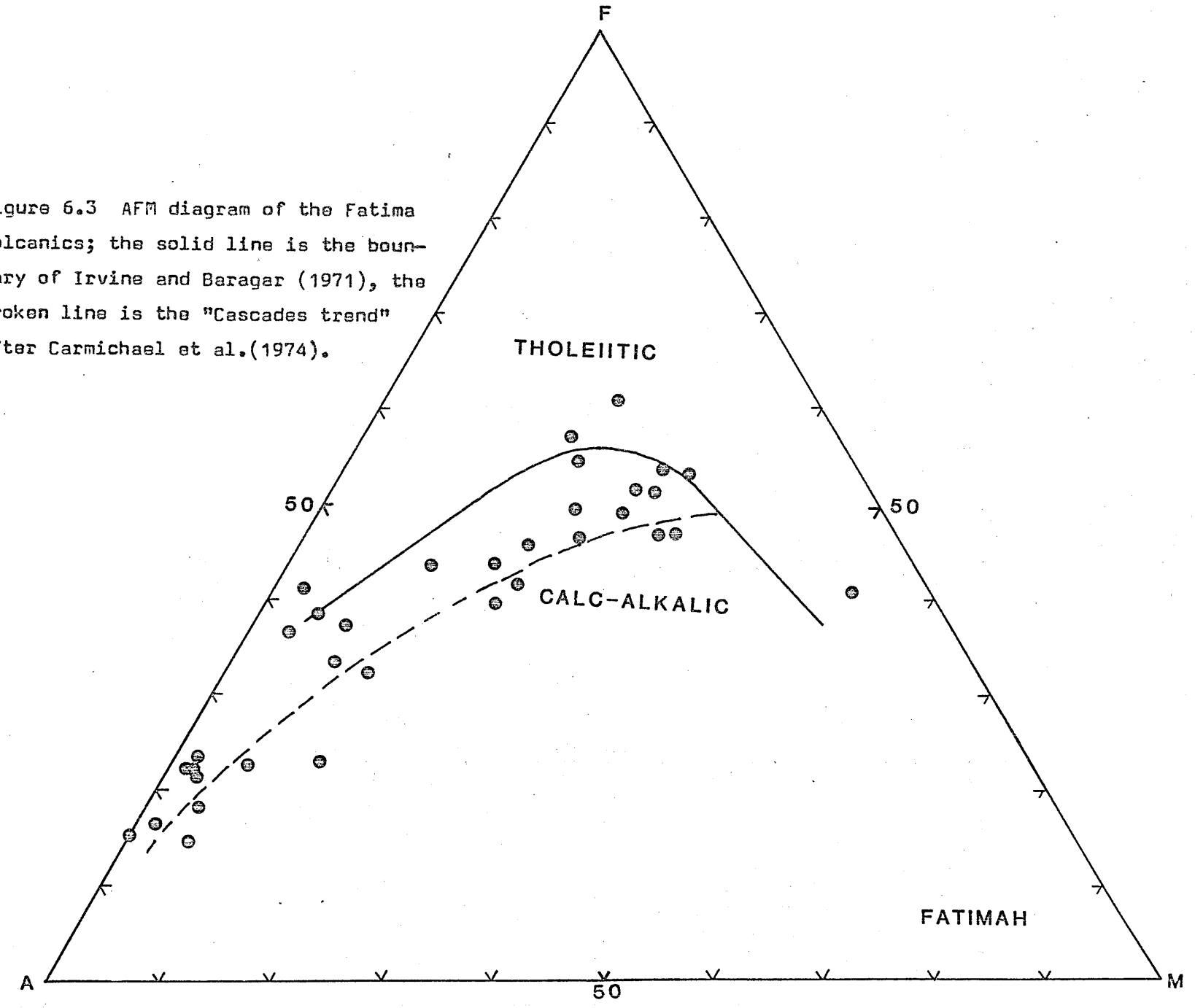

Figure 6.3 AFM diagram of the Fatima volcanics; the solid line is the boundary of Irvine and Baragar (1971), the broken line is the "Cascades trend" after Carmichael et al.(1974).

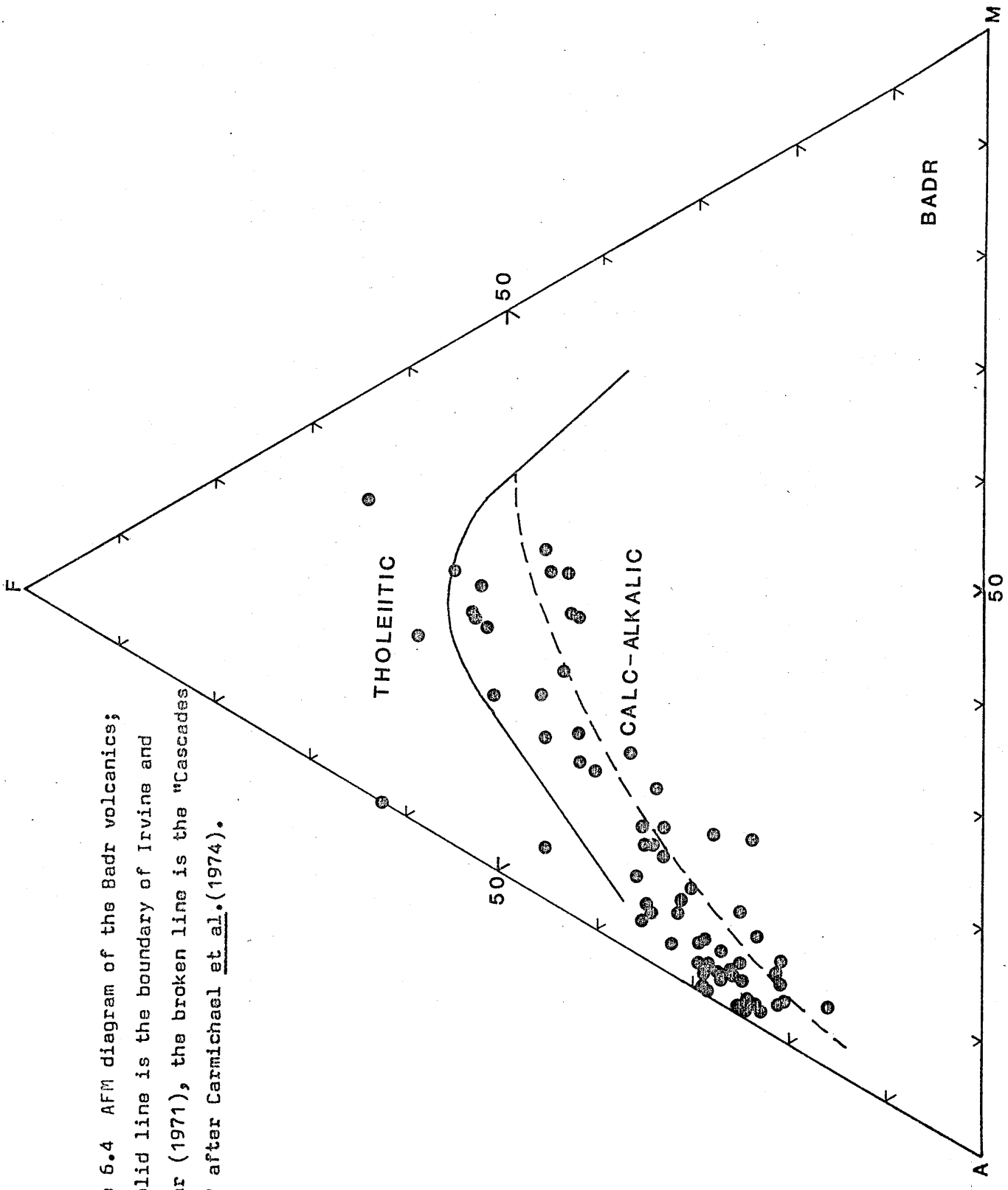

Figure 6.4 AFM diagram of the Badr volcanics; the solid line is the boundary of Irvine and Baragar (1971), the broken line is the "Cascades trend" after Carmichael et al.(1974).

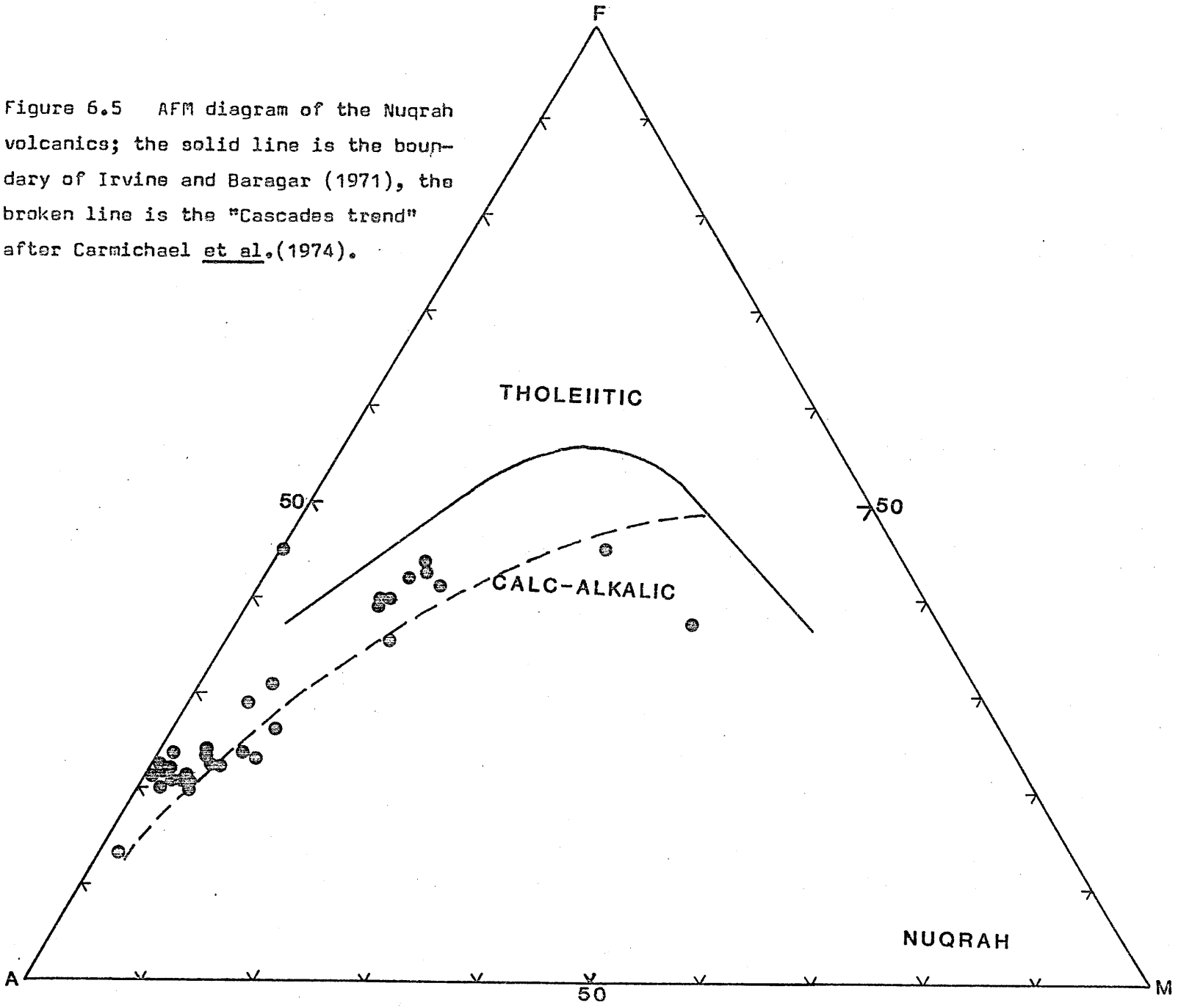

Figure 6.5 AFM diagram of the Nuqrah volcanics; the solid line is the boundary of Irvine and Baragar (1971), the broken line is the "Cascades trend" after Carmichael et al.(1974).

the iron apex), and they should be used in conjunction with alkali-lime index diagrams (Brown, 1981).

Figures 6.3, 6.4 and 6.5 show AFM diagrams for the Fatima, Badr and Nuqrah volcanics, respectively. Using the dividing line between calc-alkalic and tholeiitic suites of Irvine & Baragar (1971) and the calc-alkaline ("Cascades") trend line of Carmichael et al. (1974), it is evident that almost all samples have calc-alkaline affinities and show trends approximately normal to the F-M leg of the triangle. As in Figure 6.1 the Fatima and Badr samples partly fall outside this field, since they are tholeiitic; the Nuqrah samples, however, completely fall within the calc-alkalic field. Since these triangular diagrams are not suitable for quantitative discussions (Miyashiro, 1974), they will not be discussed extensively. Noteworthy, however, is the trend from the older, partly tholeiitic, Fatima (681 Ma) and Badr (634 Ma) sequences towards the younger Nuqrah (626 Ma) volcanic rocks. This trend is common in island-arc environments (Ewart et al., 1973; Ringwood, 1974). AFM diagrams for Hulayfah Group volcanic rocks show clearly tholeiitic trends (Basta et al., 1980).

6.2.5 MgO-FeO-Al_2O_3 diagram

Another, and relatively rare element plot is used by Pearce et al. (1977), namely the MgO-FeO-Al_2O_3 diagram. They argue that despite the general mobility of the major elements, FeO* (total iron as FeO) and Al_2O_3 are relatively immobile during the early stages of alteration. By plotting basaltic andesites of 51 - 56% SiO_2 and using MgO, FeO* and Al_2O_3 (%) Pearce et al. (1977) were able to distinguish five tectonic environments, namely ocean floor/ridge, oceanic island (for example, Hawaii), continental (for example, Indian flood basalts), orogenic (for example, island arcs and active continental margins) and spreading centre islands (for example, Iceland). A tentative plot for the three fieldwork areas (see Figure 6.6) indicates all volcanic rocks to cluster in the orogenic-

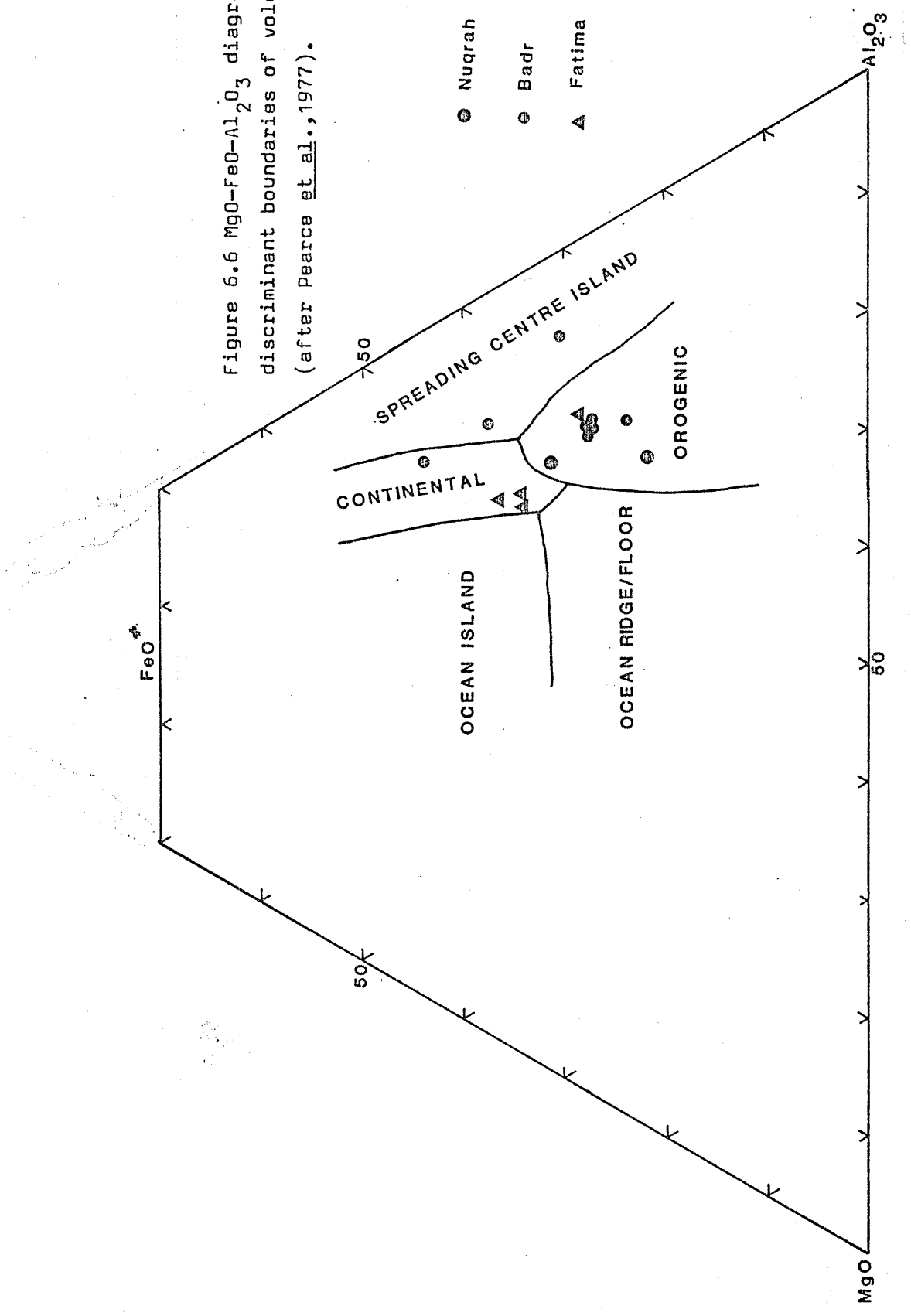

Figure 6.6 MgO-FeO-Al_2O_3 diagram showing discriminant boundaries of volcanic rocks (after Pearce et al.,1977).

continental fields and away from the oceanic environments. No Mg enrichments, reported by Pearce et al. (1977), which could give a broad scatter towards the MgO apex, was seen; any oceanic environment seems to be unlikely for these volcanic rocks.

6.2.6 Relative proportions of rock types

Proportions of basic, intermediate and acidic volcanic rocks have been estimated and plotted by Baker (1968) to establish regional volcanic correlations and indicate apparent evolutionary sequences of island arc volcanism. Relatively immature arcs (S. Sandwich, Tonga, Isu Islands) are dominantly composed of basalts and basaltic andesites; more mature arcs (Japan, Indonesia, Lesser Antilles and Aleutians) are dominantly composed of andesites (Baker, 1968; Ringwood, 1974); dacites, rhyolites and ignimbrites are more common in continental arcs (Ewart, 1981). According to Miyashiro (1974) the proportion of calc-alkalic series rocks increases with advancing development of continental-type crust beneath the volcanic arc.

For the three fieldwork areas, supplemented by Delfour's (1976) data for the older Hulayfah Group of Saudi Arabia, similar plots are produced in Figure 6.7, whereby the boundaries between basalt/andesite and andesite/rhyolite were taken at 52% and 66%, respectively. A clear trend can be seen from the basalt/andesite dominated Hulayfah Group, to the Fatima Group with equal amounts of basalt and rhyolite and the progressively more rhyolite-dominated Badr and Nuqrah volcanics. As will be discussed later, this could reflect a continuous range from maturing arc to continental margin (see also Basta et al., 1980).

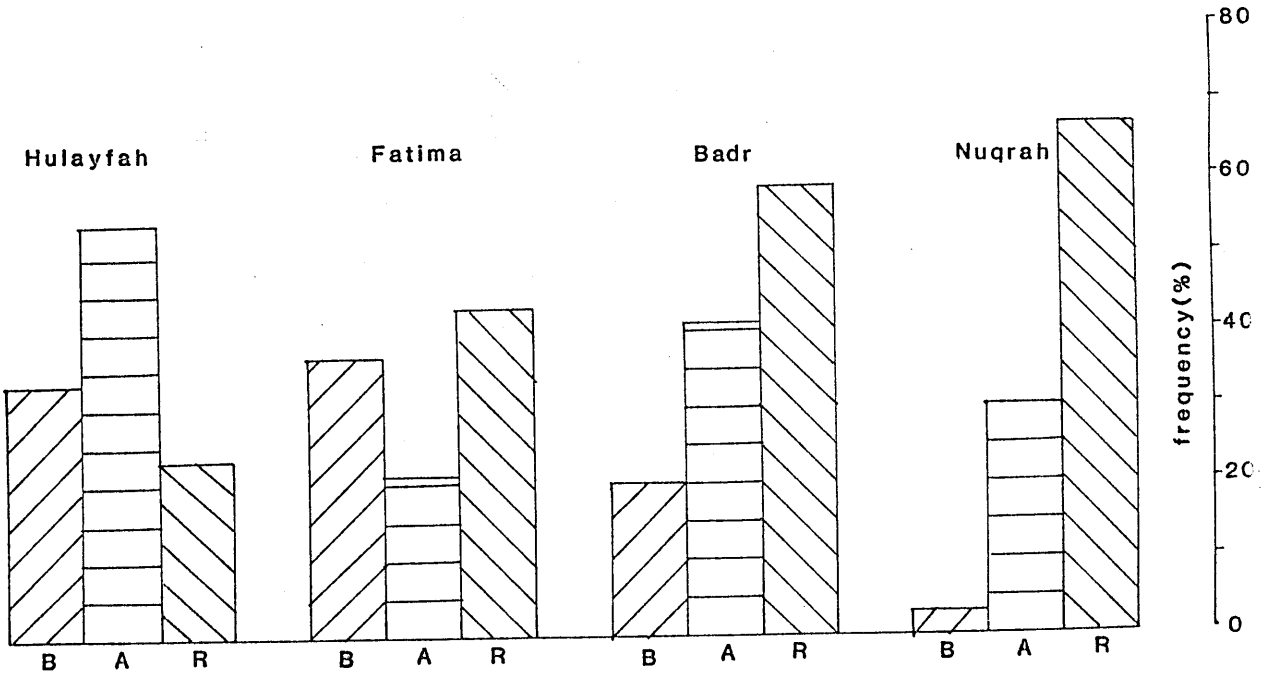

Figure 6.7 Proportions of basalt, andesite and rhyolite of the Hulayfah Group (data after Delfour, 1976) and the three fieldwork areas; B - basalt, A - andesite, R - rhyolite. The boundaries between basalt, andesite and rhyolite are chosen at 52% and 66% respectively.

6.2.7 Comparison with global geochemical data

Table 6.1 gives a comparison of the Fatima, Badr and Nuqrah volcanics (whereby the Hulayfah Group volcanics are included for comparison) with some major element geochemical data of rocks from various tectonic settings, namely immature island arcs (Tonga, Kermadec), mature island arcs (Lesser Antilles, NE Japan arc), active continental margins (Cascades, Central Andes), stable continents (Skaergaard, Palisades) and mid-oceanic ridges (abyssal tholeiites). We have to bear in mind that major elements are subjected to alteration (as outlined in Section 6.2) and that mainly regional trends are of significance.

	mid-oceanic ridges (10)	immature isl. arc (25)	mature isl. arc (89)	cont. margin (31)	continent (8)	Hulayfah Group (24)	Fatima volcanics (33)	Badr volcanics (73)	Nuqrah volcanics (33)
SiO_2	48	53	57	64	51	56	61	68	68
TiO_2	1.5	0.8	0.8	0.5	1.7	0.9	1.0	0.9	0.7
Al_2O_3	16	15	17	16	13	15	15	15	15
FeO*	10	10	8	4	14	8	7	5	4
K_2O	0.4	0.5	0.9	2.7	0.9	1.0	1.7	2.8	3.5
Na_2O/K_2O	8	3.9	2.8	1.7	2.6	8	2.4	2.3	1.5

Table 6.1 Comparison of major element data of world-wide data from Anhaeusser (1973), Miyashiro (1974), Carmichael et al. (1974) and Delfour (1976). Average contents for major elements are given for each group; the amount of analyses, on which the averages are based, are given in brackets.

From Table 6.1 it can be concluded that the Fatima, Badr and Nuqrah area volcanics have island arc to continental margin affinities. Although

the samples of the three areas have higher SiO_2 and K_2O contents (see Table 6.1) and subsequently lower Na_2O/K_2O ratios) than their comparable tectonic settings, their compositions and gradual trends in major elements show that the Hulayfah volcanics, although having relatively high SiO_2 and K_2O contents (see also Appendix D), are comparable with maturing island arcs, the Fatima and Badr volcanics with mature island arcs and the Nuqrah volcanics, although similar to the Badr volcanics, with continental margins. The main rock types of the Hulayfah Group are tholeiitic basalts, andesites and minor dacites (Delfour, 1976); the well-developed Fatima and Badr island arc rocks contain mainly calc-alkalic and some tholeiitic series rocks (rhyolites, andesite, basalts) and the Nuqrah volcanics of presumed continental margin origin are predominant calc-alkalic rhyolites (see Figures 6.3 - 6.5).

6.2.8 Discussion of major element studies

In Table 6.2, the available data of major element studies, supplemented by environmental studies (see Chapters 2, 3 and 4) are combined under the headings of sedimentary environment, major rock type, rock series, alkali-lime index and tectonic environment. All data from the Hulayfah Group are after Delfour (1976) - see Appendix D - ; further studies on traces and REE will be used to check the validity of Table 6.2.

	sedimentary environment	rock type	rock series (AFM)	alkali-lime index	tectonic setting
Hulayfah Group	marine	basalt andesite	tholeiitic	calcic	maturing arc
Fatima Group	shallow marine/ continental	basalt andesite rhyolite	tholeiitic/ calc-alkalic	alkali-calcic to calc-alkalic	mature arc
Badr volcanics	shallow marine/ continental	basalt andesite rhyolite	tholeiitic/ calc-alkalic	calc-alkalic to alkalic-calcic	mature arc
Nuqrah volcanics	continental	rhyolite	calc-alkalic	alkali-calcic	continental margin

Table 6.2 Results of major element studies for the Hulayfah Group, Fatima Group, Badr volcanics and Nuqrah volcanics. Predominant rock types are underlined.

There is a clear evolutionary trend (also indicated by the comparison with global geochemical data of Section 6.2.6) from the tholeiitic Hulayfah Group, comprising maturing arc deposits, towards the predominant calc-alkaline, mature arc deposits of the Fatima and Badr areas and the continental, rhyolitic Nuqrah volcanics.

6.3 Trace element studies

6.3.1 Introduction

Trace elements were analysed routinely in the EDXRF system for Pb, Th, Rb, Sr, Y, Zr, Nb, Ga*, Cu*, Zn*, Cr* and Ni* (Ga* means semi-quantitative data). The last five metals were not analysed for in all samples and Cr and Ni were only determined for basic volcanic rocks. Of the trace elements, Pb, Rb and Sr show increasing scatter with increasing alteration. Co, Cr, Nb, Y, Zn, Zr and the REE are considered to be less mobile (Pearce & Cann, 1973; Garcia, 1978) and Nb, Cr, Y, Zr and Ti have been used extensively as indicators of magma types and tectonic settings (Cann, 1970; Jakeš & Gill, 1970; Pearce & Cann, 1973; Pearce & Gale, 1977; Pearce & Norry, 1979). Harker diagrams are normally used to plot preliminary trace elements, but, as mentioned in Section 6.2.1, they are not useful in quantitative terms. Pb, Th, Rb, Y, Zr and Nb show positive and Sr negative correlations with SiO_2; in general, the Nuqrah samples show better correlations than those of the Fatima and Badr areas. The reason for this is probably, as in similar major element studies, the fact that the Nuqrah volcanics are unmetamorphosed.

6.3.2 Nb-SiO_2 diagram

Small, highly charged elements (also called HFS - high field strength elements) such as Ti, Zr, Y and Nb are very effective in identifying within-plate (high HFS abundances) or volcanic are (lower HFS abundances)

characteristics of igneous rocks, because the concentrations of these elements (notably Nb) are strikingly different in these tectonic environments (Pearce & Gale, 1977). The $Nb-SiO_2$ diagram for the volcanics of the three areas is shown on Figure 6.8; it can be seen clearly that all volcanics fall in the field of volcanic arc magmas and that there is no significant difference between the groups, albeit that the Fatima volcanics have the highest Nb abundances.

6.3.3 TiO_2-Zr diagram

Figure 6.9 shows another common HFS diagram (after Pearce, 1980) in trace element studies, namely the TiO_2-Zr diagram. Compositional fields are indicated for present-day volcanics in different environments: island arcs, oceanic ridge basalts and within-plate. Although developed by Pearce for Recent basalts, this diagram has been used by him and others to compare ancient rocks of different compositions (Gass, 1980; Pearce, 1981). In this diagram, Zr is plotted against a stable major element (Ti). Most volcanics plot within the volcanic island arc field, although there is some overlap with the within-plate field, whereas most basalts plot in the oceanic ridge basalt field. There is no significant difference between the Fatima, Badr and Nuqrah Groups.

6.3.4 Selected geochemical features in trace elements from different tectonic environments

Jakeš and Gill (1970) were the first to evaluate trace elements data for the calc-alkaline, island arc tholeiite and abyssal tholeiite series. They note that the first stage of island arc volcanism often is characterized by IAT series and later stages by calc-alkaline series; magmas of IAT series have a tholeiitic trend on the AFM diagram (see Section 6.2.4) and show low abundances of incompatible elements and unfractionated REE patterns. Later, more evolved, calc-alkaline trends

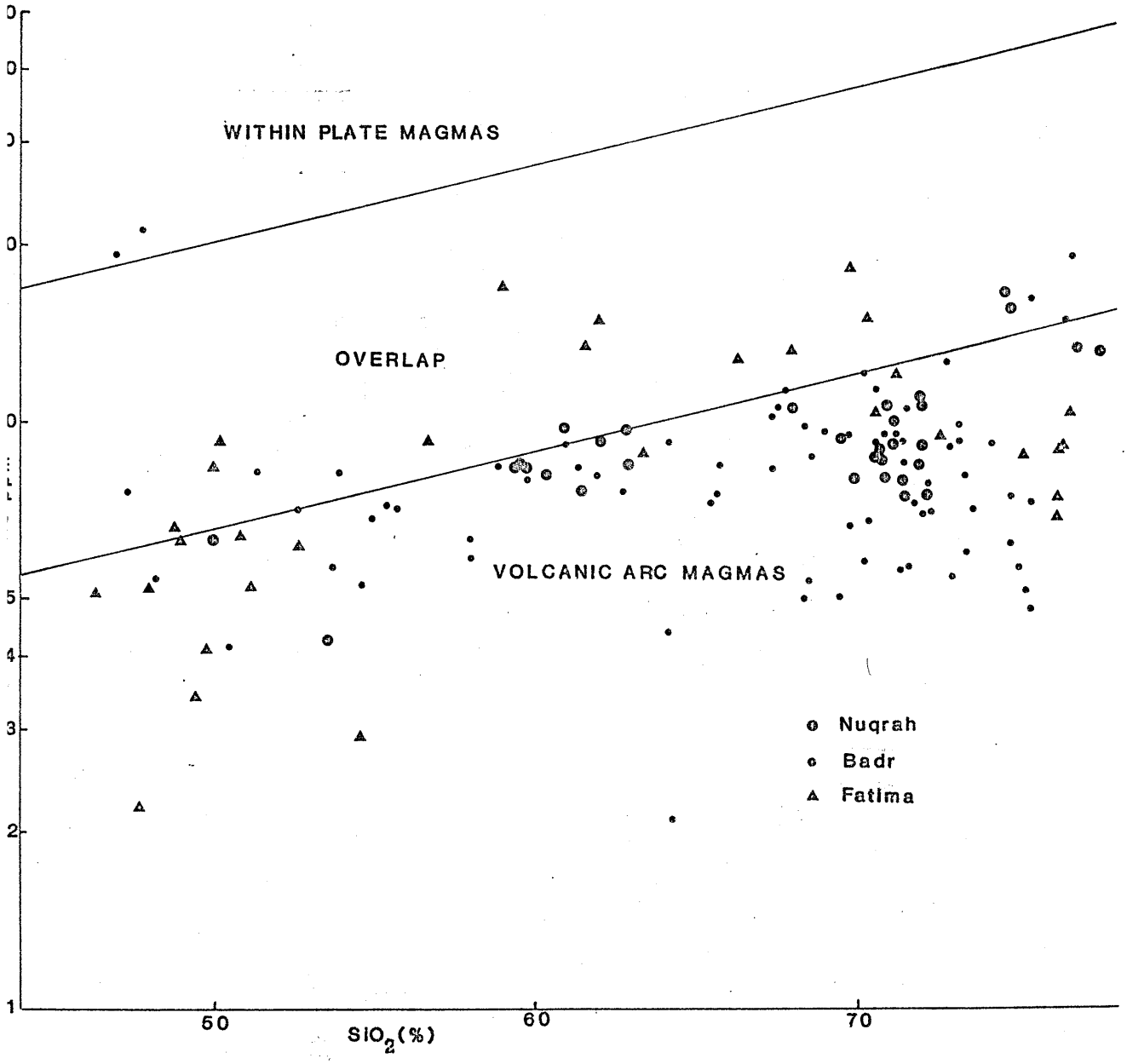

Figure 6.8 $Nb-SiO_2$ diagram, showing data of volcanic rocks from the three fieldwork areas; the boundary lines are after Pearce and Gale (1977) and indicate the overlap between the volcanic arc magmas and the within-plate magmas.

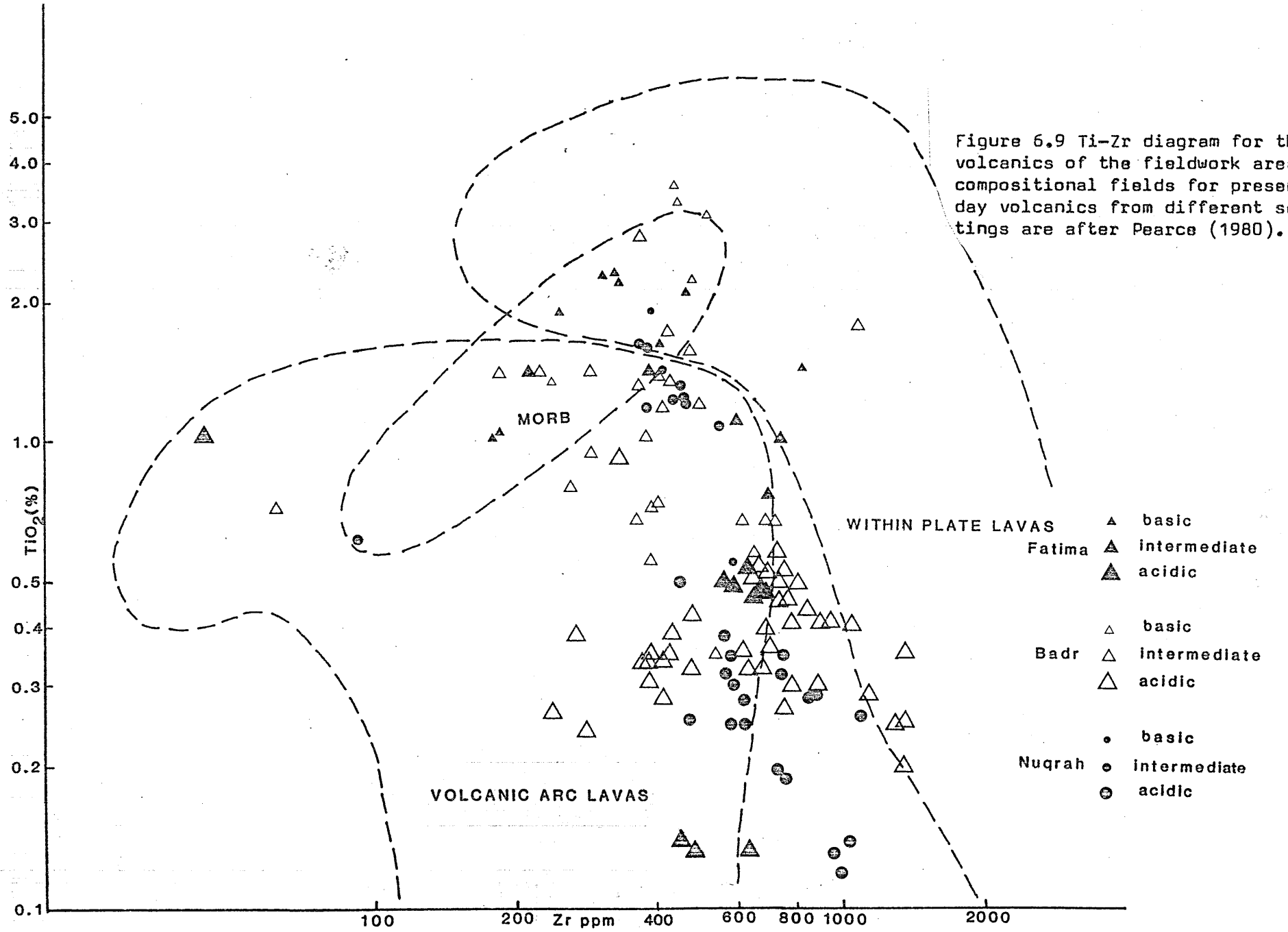

Figure 6.9 Ti-Zr diagram for the volcanics of the fieldwork areas; compositional fields for present-day volcanics from different settings are after Pearce (1980).

show (Jakeš & Gill, op. cit.) higher abundances of incompatible elements for a given SiO_2 content and display fractionated REE patterns.

	Fatima (33)	Badr (73)	Nuqrah (33)	C.A. series (50)	IAT series (50)	Ab. thol. series (50)
Rb	29	55	81	30	3-10	0.2-5.0
Sr	209	250	198	380	100-200	70-150
Ba	313	332	961	270	50-150	6-30
Pb	8	11	12	3-7	2-4	0.5
K/Rb	551	561	444	400-500	1000	1000
Rb/Sr	0.30	0.48	0.67	0.05-0.10	0.01-0.05	0.02
Th	2	2	6	2	0.5	0.15
Ni	27	20	22	18	0-30	30-200
Cr	35	64	84	56	0-50	200-400
La	15	16	26	12	1-6	2-8
La/Yb	4	5	8	6-8	1-2	1-2

Table 6.3 Comparison of the Fatima, Badr and Nuqrah volcanics with data from calc-alkaline, island arc tholeiite and abyssal tholeiite series after Jakeš & Gill (1970). The amount of samples, on which the averages are based, are given in brackets.

Table 6.3 compares the results of Jakeš and Gill (1970) with geochemical data for the Fatima, Badr and Nuqrah areas. It can be seen from this table that all three groups fit in best with the calc-alkaline series which conforms with major element data (see Section 6.2.7) in indicating calc-alkaline trends for these volcanic rocks.

6.3.5 Geochemical patterns in trace elements

A convenient way of comparing magma types in terms of trace element characteristics is to plot the data as geochemical patterns using the amounts of K_2O (%), Rb (ppm), Ba (ppm), TiO_2 (%), Zr (ppm), Hf (ppm), Sm (ppm), P_2O_5 (%), Ce, Ta, Nb, Th, Sr, Ni, Y, Yb, Sc, Cr (all ppm).

All elements are of petrogenetic significance and can be easily analysed by XRF and INAA facilities and their order from Sr-Cr is of increasing compatibility in garnet lherzolite mantle; the REE, which will be discussed in more detail in Section 6.4, are represented by Ce, Sm and Yb (Pearce, 1981). For this analysis only basalts were used, being the least evolved rock types and probably most suitable for distinguishing past tectonic environments. Figure 6.10 shows the Sr-Cr geochemical patterns for basalts in the Fatima, Badr and Nuqrah areas. While comparing these patterns which were normalized to mid-ocean ridge basalts (MORB) with typical MORB, within-plate basalts (WPB) and volcanic arc basalts (VAB) patterns from Pearce (1981, Figure 1), several conclusions can be made. Compared to MORB patterns basalts from the Fatima, Badr and Nuqrah areas are strongly enriched in K, Rb, Ba, Ce, P and Zr and less enriched in Nb and Sm-Sc. The basalts of all areas are strongly depleted in Cr. They differ from the flatter MORB geochemical trace element patterns. Strong K-Th and Ce-Zr enrichment and lower Ta-Nb contents follow volcanic arc trends; the Zr-Ti enrichment, however, is only found in a WPB environment (the strong Cr depletion is common in both environments).

The discussed volcanics clearly show both VAB and WPB variations, their origin, obviously, must be a transitional tectonic environment. Mantle could have had a defined range of compositions, prior to subduction (Pearce, 1981); on the other hand, high Zr and Ti might be caused by processes in later stages of subduction. Many references are made in the literature on these transitional or anomalous settings, for example, 1 - near lateral edges of subduction zones (Sigurdsson et al., 1973), 2 - where fracture zones approximately perpendicular to the trench are being subducted (Stanton & Bell, 1969; Warden, 1970), or 3 - adjacent to continental areas during the initial stages of back-arc spreading or rifting (Bruhn et al., 1978; Saunders et al., 1979; Weaver et al., 1979).

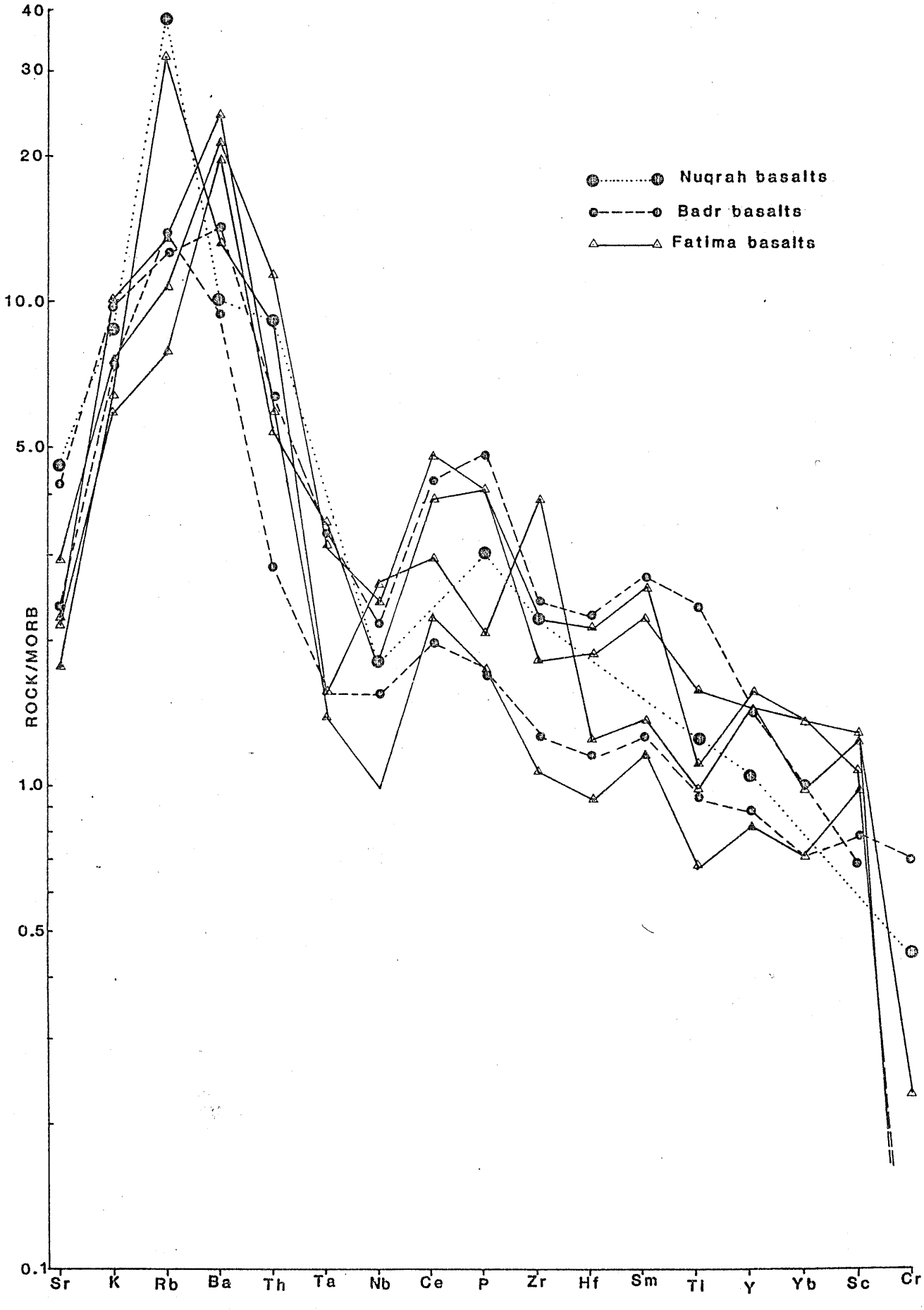

Figure 6.10 Mid oceanic ridge basalt normalized trace element patterns for Arabian Shield basalts. Normalizing values (after Pearce, 1981) : Sr-120ppm, K_2O-0.15%, Rb-2.0ppm, Ba-20ppm, Th-0.2ppm, Ta-0.18ppm, Nb-3.5ppm, Ce-10ppm, P_2O_5-0.12%, Zr-90ppm, Hf-2.4ppm, Sm-3.3ppm, TiO_2-1.5%, Y-30ppm, Yb-3.4ppm, Sc-40ppm,

We have to bear in mind, in dealing with these theories, that we are dealing with 600 - 700 Ma old volcanic rocks with the possibility of various plate geometries.

6.4 Rare earth elements

The abundances of ten rare earth elements (REE), namely La, Ce, Nd, Sm, Eu, Gd, Tb, Tm, Yb and Lu were analysed using standard INAA procedures, for forty samples. In addition to the REE, tne amounts of Th, Ta, Hf, Sc, Co, Fe_2O_3 (%) and Ba (all ppm) were analysed by the same method. The REE patterns for the Fatima, Badr and Nuqrah areas are shown on Figures 6.12, 6.13 and 6.14 respectively. They are all LREE enriched with Ce_N 26-79, 23-92 and 59-72 respectively for the three areas (Ce_N - chrondrite normalized Ce concentrations) and HREE depleted with Yb_N 11-26, 9-24 and 13-16 respectively. The range of Ce_N/Yb_N varies in the Fatima volcanics from 1.80-3.26, in the Badr volcanics from 2.33-6.07 and in the Nuqrah volcanics from 3.81-4.54. The Fatima and Badr show similar REE patterns which are subparallel but show a variety of abundances between different samples; the Nuqrah REE pattern indicates smaller differences in abundances between different samples and the Eu anomalies, both positive and negative, are much larger. Eu anomalies are common for most analyses, nearly all samples show slightly negative Eu anomalies. Some larger negative Eu anomalies with Eu/Eu* down to 0.70, 0.50 and 0.44 respectively in the three areas, do occur (Eu* - calculated contentration of Eu as an average between the Sm and Nd abundances). The samples with the larges negative Eu anomalies are all rhyolites and ignimbrites. REE studies of two successive ignimbrite units in the Badr area (see Chapter 3.4) show identical REE patterns with large negative Eu anomalies within a flow unit. Large positive Eu anomalies with Eu/Eu* up to 1.47 are indicated for the Nuqrah volcanics.

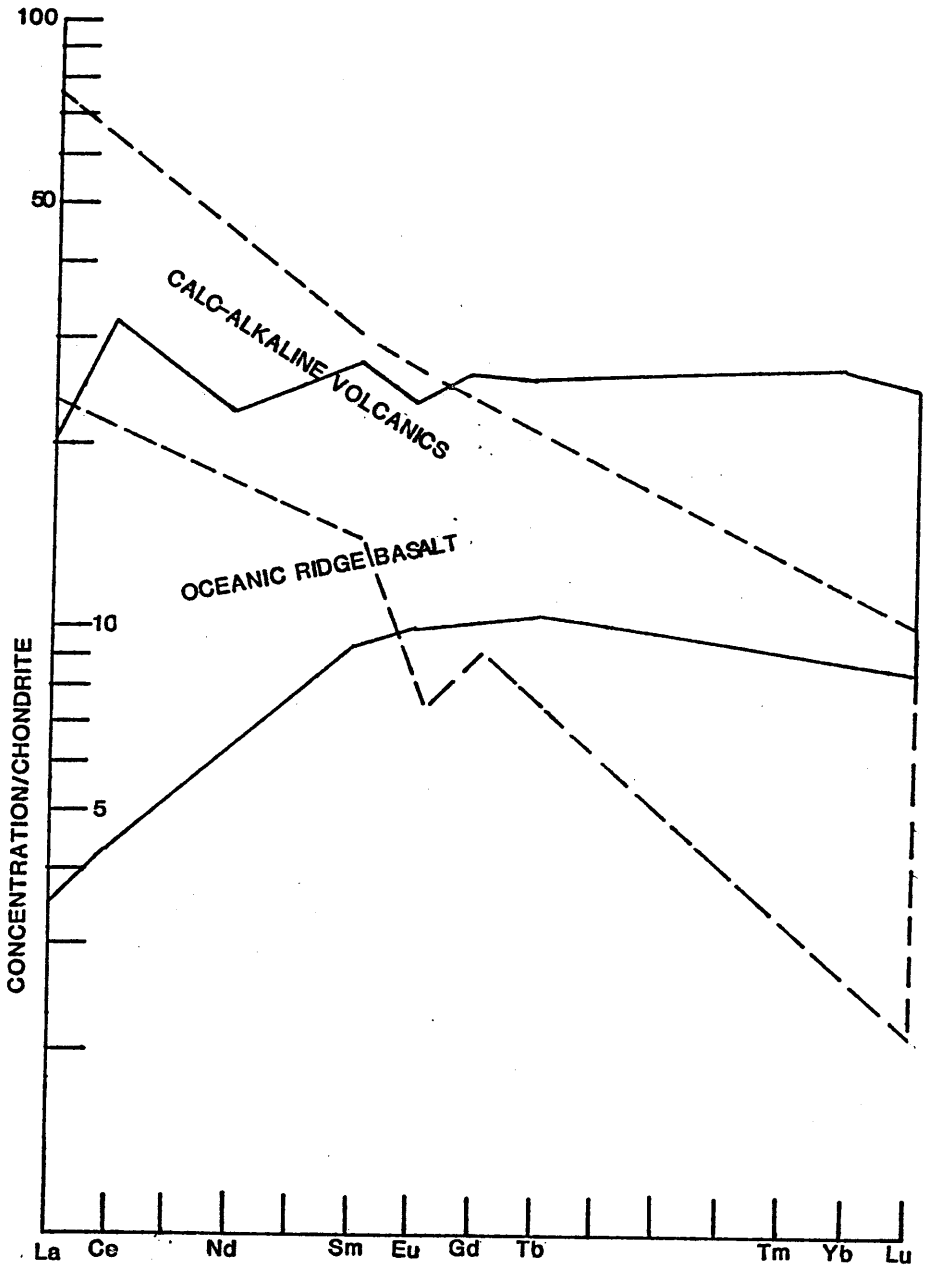

Figure 6.11 Envelopes for calc-alkaline volcanics and oceanic ridge basalts (REE boundaries after Schilling, 1971 and Condie & Swenson, 1973); the envelope for calc-alkaline volcanics does not include data from continental margins.

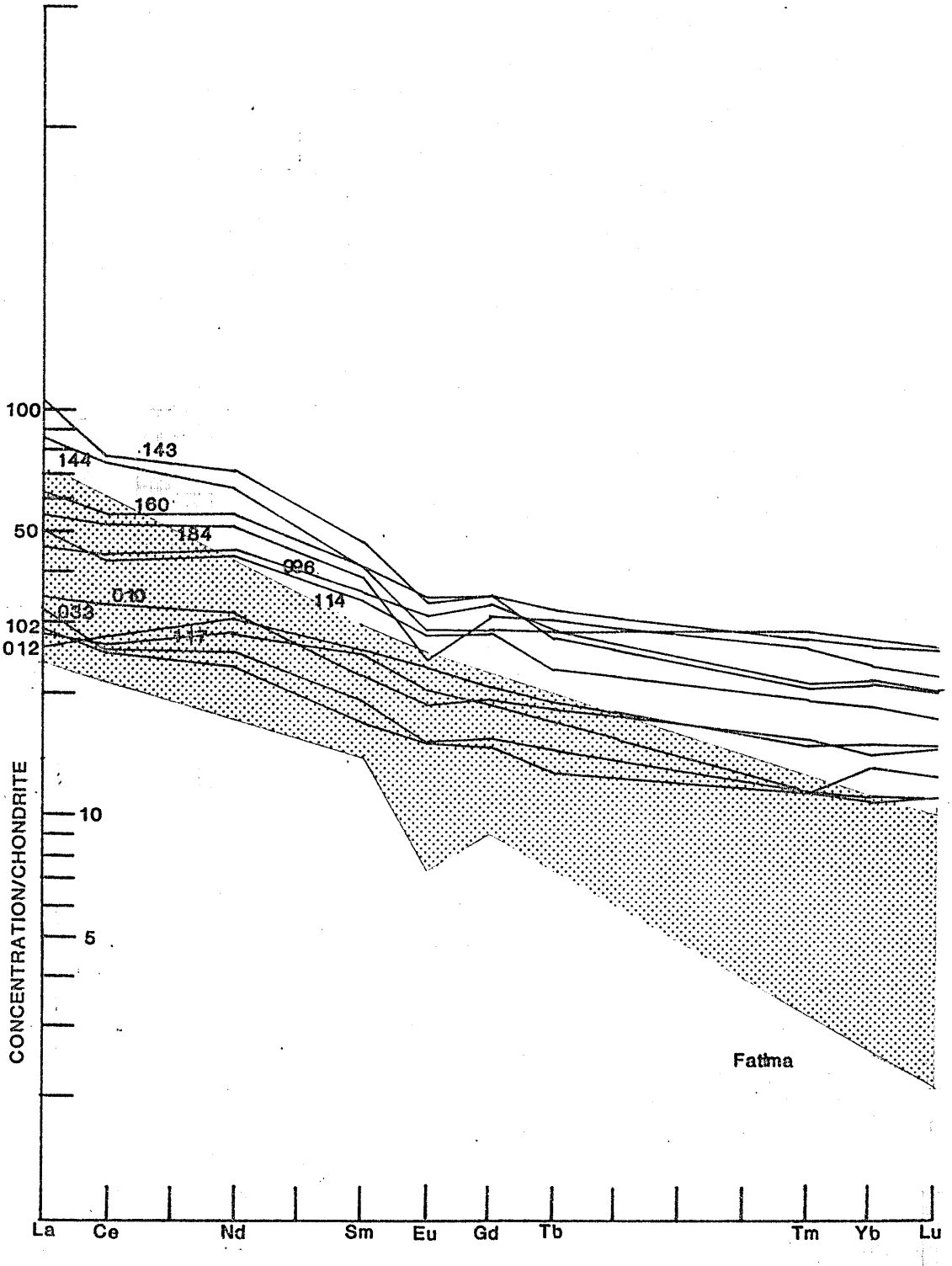

Figure 6.12 Chondrite normalized REE patterns for the Fatima volcanics; the shaded area is the envelope for calc-alkaline rocks after Schilling, 1971; sample numbers are indicated.

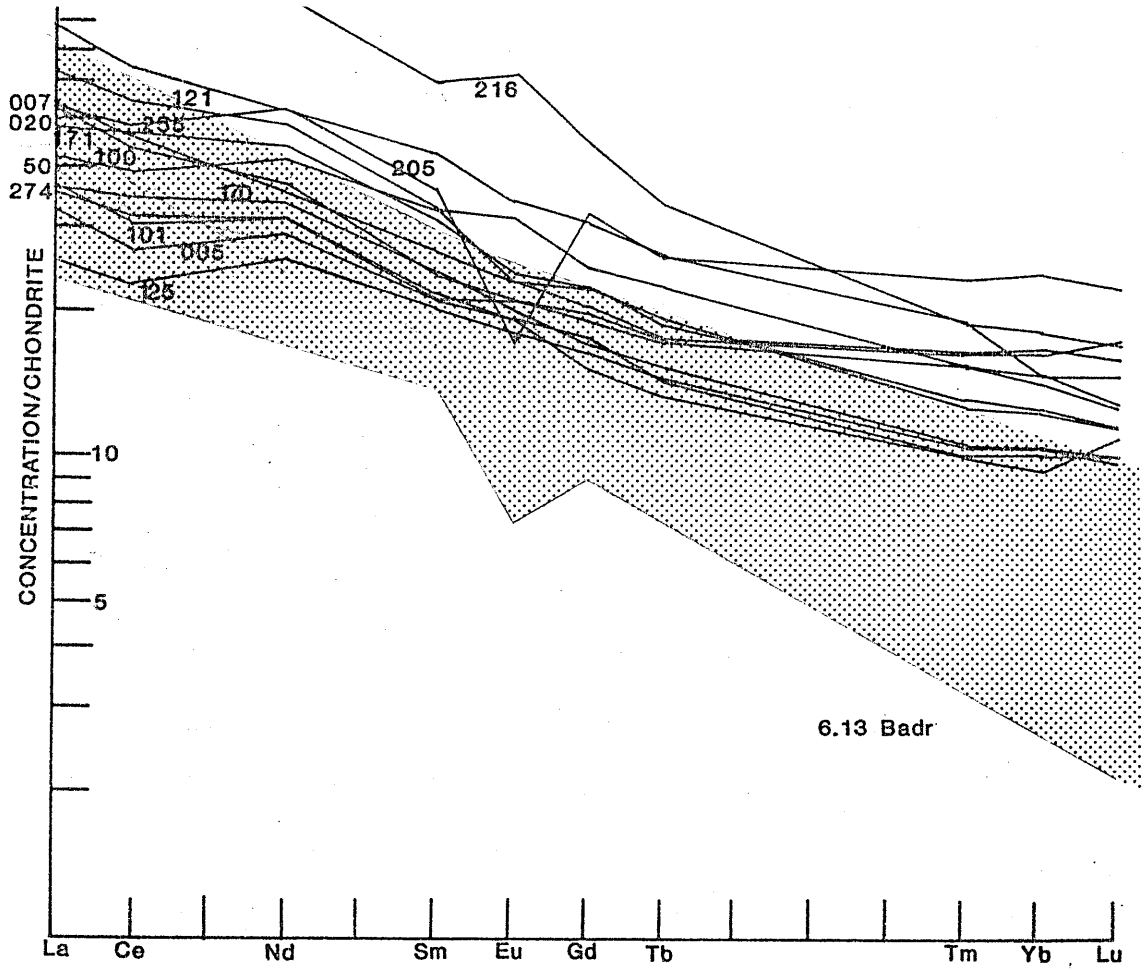

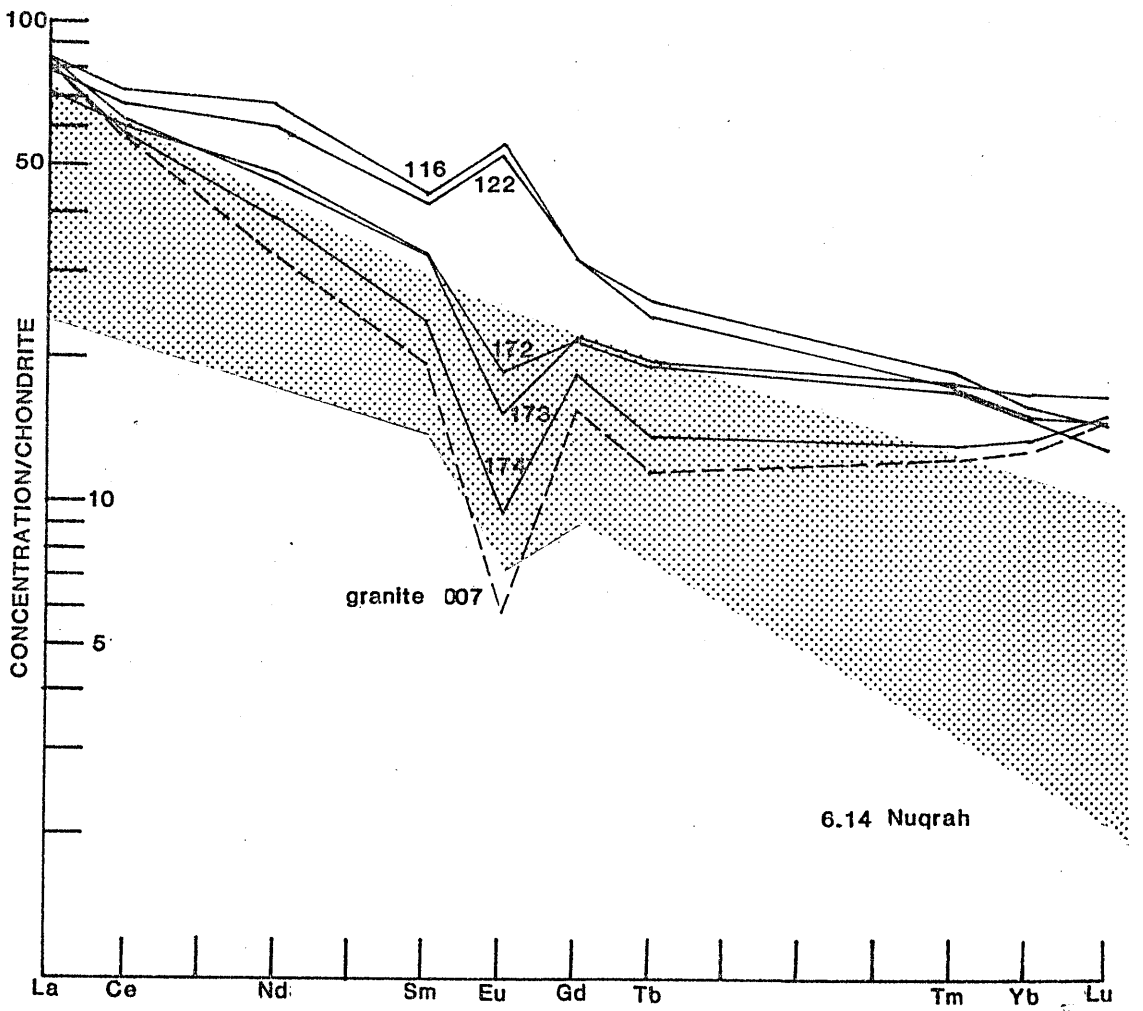

Figures 6.13 and 6.14 Chondrite normalized REE patterns for the Badr and Nuqrah areas; the calc-alkaline envelope is after Schilling (1971) and all sample numbers are indicated.

Many studies have used REE data to interpret the magmatic origin of volcanic rocks (Philpotts et al., 1971; Hermann et al., 1974; Tanaka, 1975; Sun & Hanson, 1976; Taylor, 1977; Fujimaka & Kurasawa, 1980). The stability of the REE which are only slightly affected by alteration and metamorphism in crystalline rocks (Frey et al., 1968; Philpotts et al., 1969) makes them in particular useful for studying ancient volcanics. Because the REE are all geochemically similar (trivalent) they are useful in studying the effects of fractional crystallization; their differences are just large enough to cause that various phenocryst phases in fractional crystallization processes affect the REE in a different but interpretable way (Sun & Hanson, 1976) and gradual changes in distribution coefficients (K_d) mean that REE patterns are valuable to compare (Hanson, 1978).

Most magma types have a distinct REE pattern (Garcia, 1978; Stern, 1979), oceanic ridge basalts and calc-alkaline rocks, for example, can be distinguished by using chondrite normalized REE patterns. Figure 6.11 shows the fields of these groups of rocks (after Schilling, 1971; Condie & Swenson, 1973). Oceanic ridge basalts commonly show LREE depletion have have nearly flat HREE patterns of 10-20 times chondrite abundances. Unfortunately IAT fall in the same field (Kay & Senechal, 1976). Modern calc-alkaline volcanics commonly are LREE enriched and HREE depleted (see Figure 6.11) with Ce_N/Yb_N up to 10.

Comparison of the REE patterns of the Fatima, Badr and Nuqrah areas with those of known origin (see Figure 6.11) indicates that the majority show characteristics of calc-alkaline trends. Strongly enriched LREE are more enriched than is normally the case, but these 10-20 times chondrite abundances do occur (Lopez-Escobar et al., 1977 for S. Chile). Subparallel REE patterns (especially in the Fatima-Badr

areas) and the dominance of plagioclase phenocrysts in more evolved (rhyolites, ignimbrites) rocks, strongly suggests fractional crystallization as the most important process in establishing the basalt- andesite- rhyolite- ignimbrite sequence. The samples with the largest negative Eu anomalies are all ignimbrites and rhyolites and these anomalies probably result from plagioclase or K-feldspar fractionation (Hanson, 1978), since these minerals are characterized by having relatively large mineral-melt distribution coefficients (K_d). Plagioclase and K-feldspar are, indeed, the most common phenocrysts, encountered in petrographic studies of the rhyolites and ignimbrites of the three areas. The positive Eu anomalies of some of the Nuqrah volcanic rocks could result from apatite, hornblende or pyroxene fractionation, or, more likely, from crystal accumulation of plagioclase, the plagioclase not being in equilibrium with the surrounding matrix (Walker, 1974; Peccerillo & Taylor, 1976).

6.5 Conclusions from geochemical data

Geochemical data on major oxides, trace elements and REE, as shown in the preceding sections, indicate the following:

1. Major oxide and REE studies, combined with the trace element data bank, indicate that the majority of the volcanic rocks show calc-alkaline trends, which indicates magmatism above a subduction zone, possibly in an island arc environment (Miyashiro, 1974).
2. AFM studies, the relative abundances of rock types, major and trace element abundances support the island arc environment.
3. It is also possible to establish on geochemical criteria that of the volcanic rocks of the Arabian Shield the Hulayfah Group volcanics have maturing arc affinities, whereas the Fatima and Badr sequences have mature arc characteristics and the Nuqrah

volcanics continental margin patterns.

4. High Zr and Ti contents indicate that a transitional setting between island arc and within-plate is possible. The differences with an island arc setting might be caused by early mantle heterogeneities before subduction or by late-stage reworking of the volcanics. Trace element modelling and petrogenesis, discussed in the next Section, might indicate possible explanations for the environments of the volcanic rocks.

6.6 Petrogenesis

6.6.1 Introduction

The previous Sections have been used to see how major, trace and REE elements can be put to work in looking for a possible tectonic environment. In this Section, the possible petrogenesis of the Fatima, Badr and Nuqrah volcanics will be discussed. Besides already discussed isotopic and geochemical data, element distributions more pertinent to petrogenetic models, especially melting and crystallization models, will be treated separately.

6.6.2 Data relevant to petrogenesis

6.6.2.1 FeO*-MgO ratios

FeO* (FeO* = total Fe as FeO)/MgO ratios have been used frequently (Miyashiro, 1974; Miyashiro & Shido, 1975; Kay, 1977; Basta et al., 1980) as a parameter for fractional crystallization, since the Fe/Mg ratio of residual magma increases in practically all igneous rocks in the early and middle stages of fractional crystallisation (Miyashiro, 1974) and this ratio is considered to be a reliable parameter to represent the degree of fractional crystallization. Figure 6.15 shows SiO_2 vs FeO*/Mg and FeO* vs FeO*/MgO diagrams for the fieldwork areas with dividing lines between the calc-alkaline and tholeiitic fields after Miyashiro and Shido (1975). SiO_2 increases with increasing FeO*/MgO and FeO*

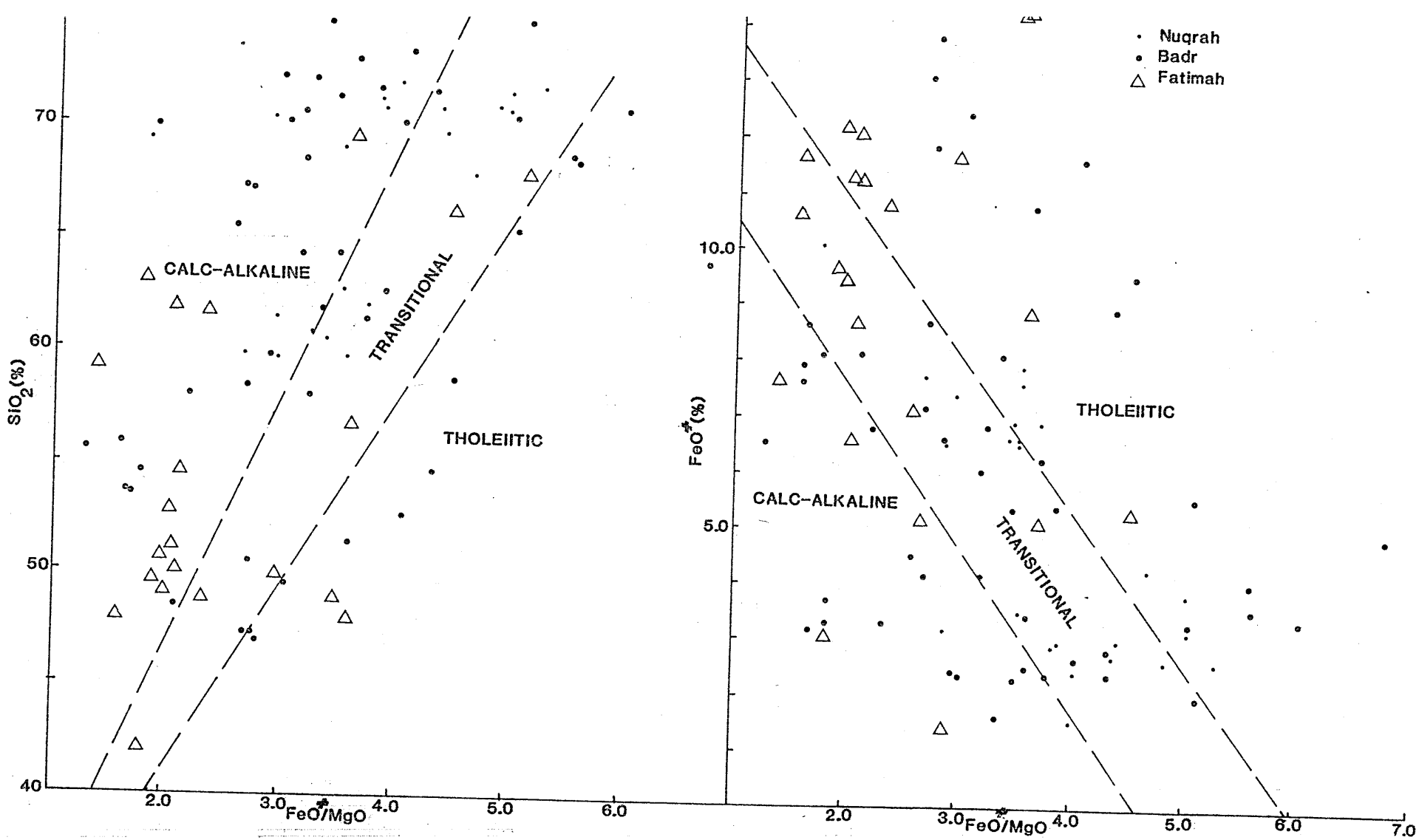

Figure 6.15 FeO*/MgO ratios, plotted against SiO_2 and FeO* for the Fatima, Badr and Nuqrah volcanics; the boundaries are after Miyashiro and Shido, 1975.

shows a negative correlation with FeO*/MgO; this type of correlation is characteristic of calc-alkaline suites and the majority of the volcanics plot in the calc-alkaline to mildly tholeiitic fields. Gradually increasing FeO*/MgO ratios for the basalt-andesite-rhyolite series indicate the sequence of fractional crystallization.

6.6.2.2 Cr/Y diagram

During melting and crystallization processes, incompatible elements may become highly concentrated although major elements show little change. The incompatible elements are thus very useful to analyse petrogenetic models. Y and Cr do not participate in processes that cause mantle heterogeneities and source regions for most basalts probably contained similar Y and Cr abundances to primordeal mantle abundances (Wood, 1979). Variations between basalts can be attributed mainly to differences in their partial melting and fractional crystallization histories (Pearce, 1981). In Figure 6.16 the average compositions of Fatima, Badr and Nuqrah basalts were plotted on a Cr/Y diagram and compared with some typical volcanic arc suites and the petrogenetic pathways that connect them to primordeal mantle (after Pearce, 1981). The partial melting trend for primary melting (see Figure 6.16) is subparallel to the Y-axis, because Cr is strongly partitioned in early mafic crystallizing phases like olivine, spinel and pyroxene, the fractional crystallization trend is initially nearly vertical and changes slope only when plagioclase (without Cr) starts to crystallize (Pearce, op. cit.).

Figure 6.16 indicates that a range of partial melting degrees up to 40% and extensive further fractional crystallization can explain overall variations from the most primitive island arcs (S. Sandwich, Tonga) towards more evolved arcs like the Hebrides and the Lesser Antilles.

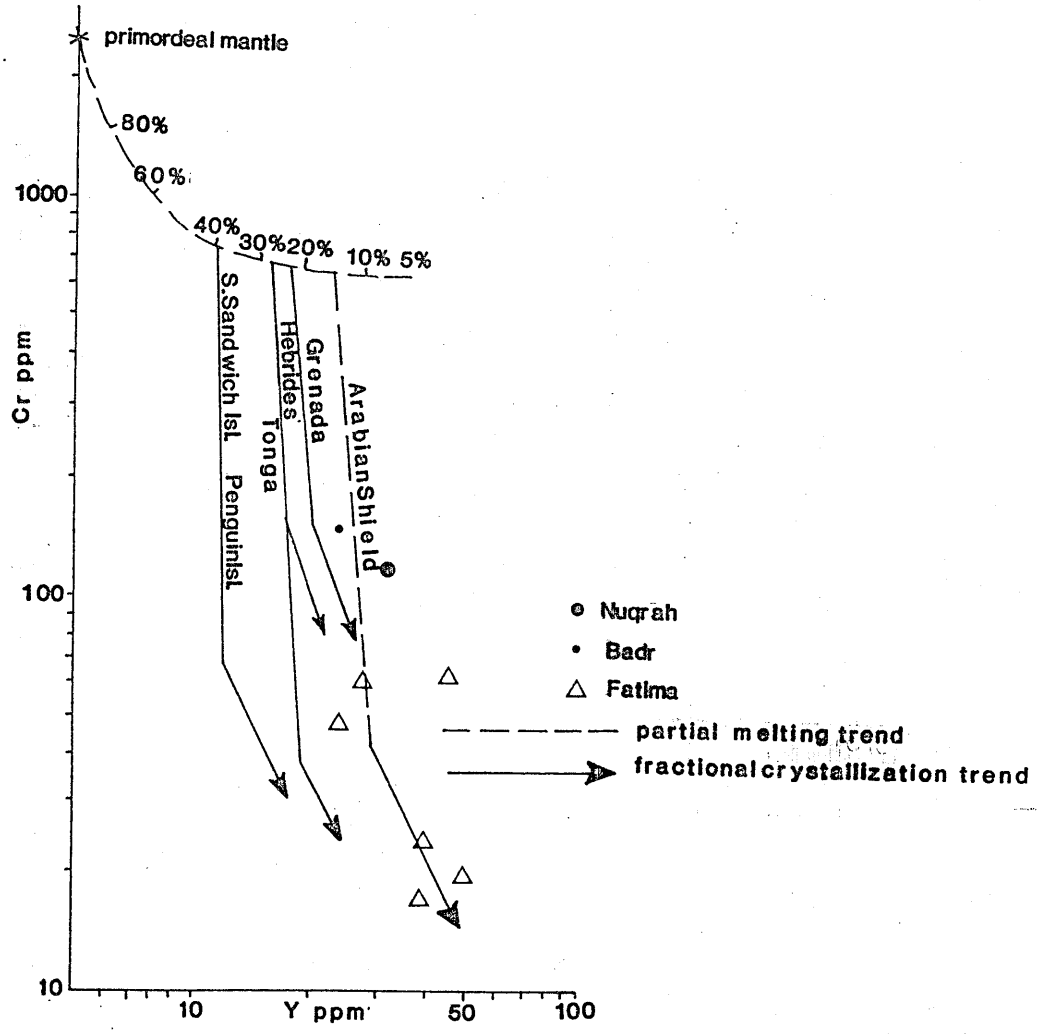

Figure 6.16 Cr/Y diagram for Arabian Shield volcanics, compared with some typical volcanic arc suites and the petrogenetic pathways that connect them to primordeal mantle.(after Pearce, 1981)

The Fatima, Badr and Nuqrah basalts plot towards the right of these known trends, since their Y abundances are generally higher. The tentative petrogenetic pathway for these basalts indicates 10 - 15% partial melting and extensive further fractional crystallization.

6.6.2.3 Sm/Eu against Sm diagram

REE are often used in petrogenetic studies, since they are geochemically very similar (Hanson, 1978, 1980). A plot of Sm/Eu against Sm can be used to interpret the REE data (after Thorpe & Francis, 1979) and especially to investigate further the role of fractional crystallization. The ratio Sm/Eu is a function of Eu anomaly and Sm/Eu ratios of circa 3.2 characterize samples with no Eu anomaly; samples with higher Sm/Eu ratios have greater (negative) Eu anomalies. The samples of the Fatima, Badr and Nuqrah volcanic rocks were plotted, using such a Sm/Eu against Sm diagram, on Figure 6.17. Most of the data cluster around the line Eu/Eu* = 1.0, indicating small Eu anomalies; two Nuqrah samples have positive Eu anomalies and several more evolved volcanic rocks (rhyolites, ignimbrites) have negative Eu anomalies, probably due to late stage plagioclase fractionation. As can be seen from Figure 6.17, most of the variations of the samples can be explained by fractional crystallization of plagioclase, K-feldspar and amphibole/pyroxene. Petrographic studies confirm that plagioclase, K-feldspar and minor amphibole/pyroxene are the main phenocryst phases (biotite was absent in these specimens).

6.6.3 Petrogenetic models

6.6.3.1 Introduction

Major, trace and REE element studies indicate early tholeiitic to later strongly calc-alkalic affinities for the studied volcanics. Modern analogies of these volcanics are situated near destructive plate margins

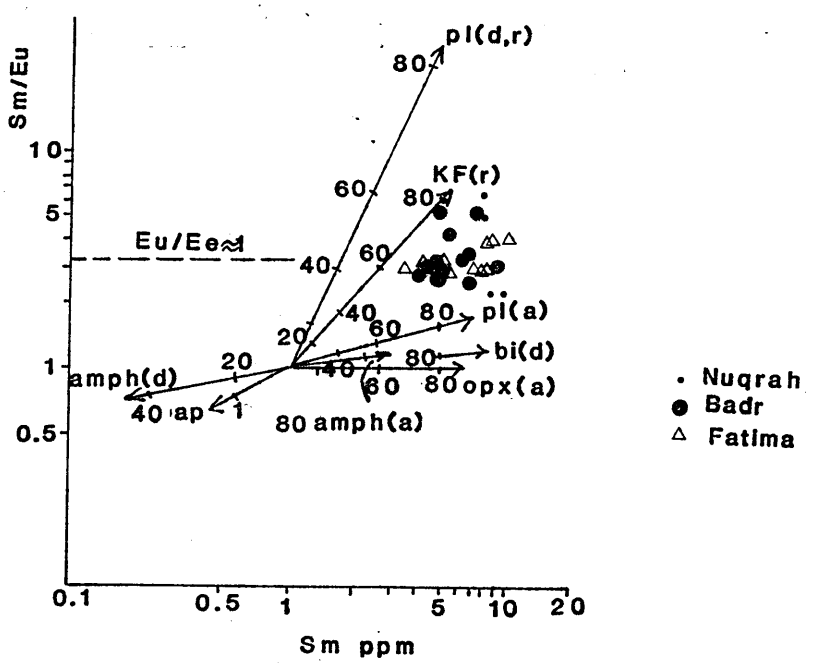

Figure 6.17 Plot of Sm/Eu against Sm for Arabian Shield volcanics; Figures indicate the percentage of crystals removed; pl-plagioclase, KF-alkalifeldspar, bi-biotite, opx-orthopyroxene, amph- amphibole, ap-apatite, a-andesite, d-dacite, r-rhyolite; see text for discussion.

above subduction zones (Pearce, 1981) in an island-arc setting. Characteristic of the Fatima, Badr and Nuqrah volcanics is the basalt-andesite-rhyolite suite. Several petrogenetic models will be discussed within the framework of the island-arc model (after Ringwood, 1974, 1977) to account for the origin of the volcanic suites. These models are: 1. Crustal anatexis, 2. Amphibole-controlled fractional crystallization, and 3. Multistage melting-mixing-fractional crystallization model.

Ringwood's (1974, 1977) scheme is chosen as the basic model for the petrogenesis of island arc systems. In this model (Ringwood, op. cit.) the early tholeiitic stage of arc development is produced by partial melting of the pyrolite wedge above the Benioff zone under the influence of water, released from subducted oceanic crust. The later calc-alkaline stage is produced by deeper partial melting of the pyrolite wedge and quartz-eclogites (derived from subducted oceanic crust) to produce more acidic magmas. The processes of Ringwood's model are illustrated in Figure 6.18.

6.6.3.2 Crustal anatexis

Crustal anatexis of underlying crust could account for some of the geochemical characteristics of the volcanic suites (for example, the anomalous Ti contents). Crustal anatexis of Archaean crust, as suggested by Delfour (1981), however, is unlikely because of field evidence, isotopic data and petrogenetic modelling. There is no field evidence for underlying older crust ("craton") in the Arabian Shield. Investigations by Kröner et al. (1979) failed to identify pre-Pan African (older than 1200 Ma) basement. They report gneisses of an age of 780 Ma, representing pre-Halaban intrusive rocks, emplaced into unidentified crust. Fleck et al. (1980) report as the oldest Arabian

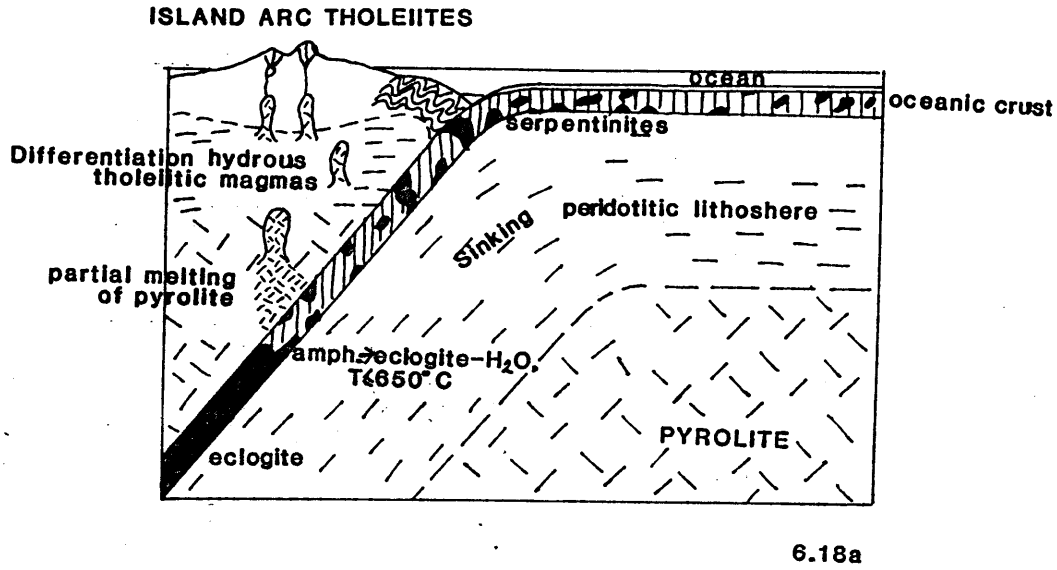

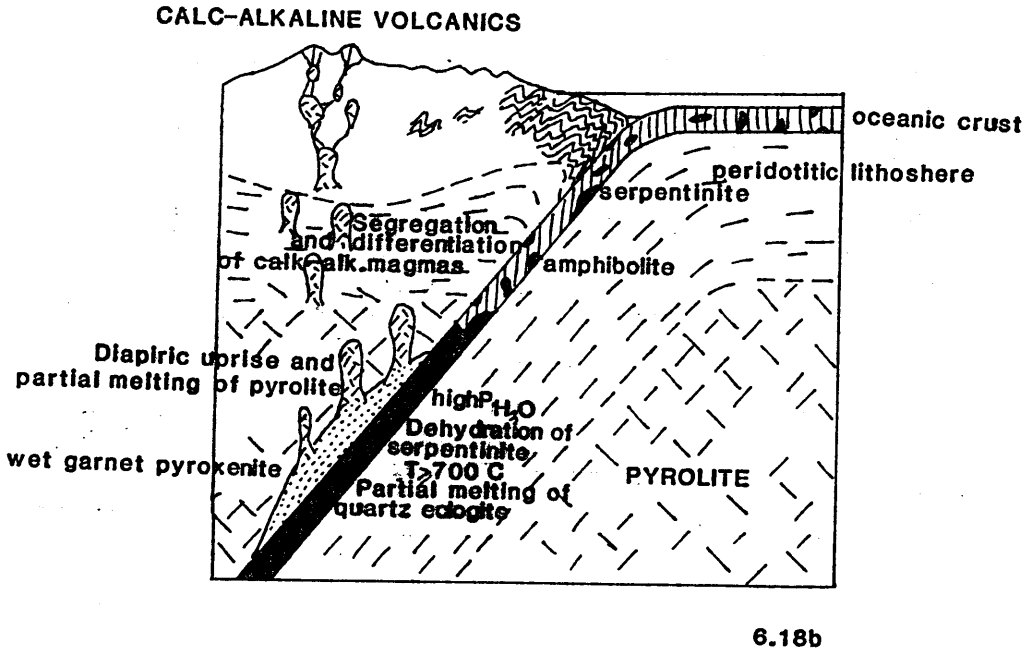

Figure 6.18 Island arc model after Ringwood (1974, 1977); Figure 6.18a illustrates the early stages and Figure 6.18b the later stages of island arc evolution (see text for discussion) .

Shield rocks a basalt of 1165 Ma. Stacey et al. (1980) suggest on the basis of Pb isotopic studies possible Archaean basement in the eastern edge of the Arabian Shield (east of longitude 44° 20' E towards the Al Amar-Idsas belt) with Pb-Pb ages of 2100 ± 300 Ma, underthrusting the Arabian Shield rocks from the east. This is, however, only one interpretation of Pb isotopic data. While the existence of much older basement below the eastern part of the Arabian Shield cannot be ruled out completely, it is unlikely that the bulk of the Shield is underlain by such a basement.

$^{87}Sr/^{86}Sr_i$ ratios for the three studied areas are 0.7021 - 0.7025 for the Fatima area, 0.7027 - 0.7035 for the Badr area and 0.7024 - 0.7030 for the Nuqrah area; all initial ratios are very low. An average initial ratio of 0.7027 could be derived from an initial BABI (basaltic achondrite best initial) of 0.69899 (Papanastassiou & Wasserburg, 1969) with an age of 4.6 Ga with a maintained Rb/Sr ratio of about 0.022 which is realistic for mantle values (Faure & Powell, 1972). Evolution of Rb-rich crust, on the other hand, with Rb/Sr ratios of 0.103 (Leyreloupe, et al., 1977) to 0.265 (Lambert & Heier, 1967) would, after an evolution of about 2 Ga, result in initial ratios of between 0.712 and 0.725. Anatexis of Rb-rich Archaean crust as a possible origin for the volcanics must therefore be precluded.

As suggested in Chapter 5.7.2, it is possible that Late Pan-African crustal anatexis of newly formed and thickened crust has taken place. High initial ratios (mainly Baubron et al., 1976) in the central and northeastern part of the Arabian Shield suggest this. An eastward subduction zone, as proposed by Greenwood et al. (1976), could, in the closing stages of island arc activity and during cratonization, form thickened crust towards the northeastern part of the Arabian Shield and provide suitable conditions for anatexis.

6.6.3.3 Amphibole-controlled fractionation at shallow levels (30 - 100 km depth)

Amphibole-controlled fractionation at shallow levels could cause widespread calc-alkaline trends in the Arabian Shield volcanics. The production of andesites from fractional fusion of amphibolite (derived from subducted MORB) is described by Holloway & Burnham (1972) and Allen et al. (1972). The presented geochemical data, however, make such a process unlikely. Residual liquids with calc-alkaline trends would show little change in K/Na and REE values, compared with MORB data. Strongly increasing K/Na values and LREE enrichment of the analysed samples tell a different story. Amphiboles coexisting with basaltic and andesitic magmas have REE partitioning coefficients, ranging from much less than unity for LREE to near unity for HREE. Since more than 30% melting of basalt is needed to generate andesitic liquids (Green & Ringwood, 1968), the REE of the resultant liquids should be parallel to those of the parents (Stern, 1979; Lopez-Escobar et al., 1977). Andesites generated in such a way should be REE depleted, which is in strong contrast with the observed LREE enrichment. Also, the lower HREE abundances are not explained by this model. The generation of the volcanics by fractionation of amphibole is thus unlikely.

6.6.3.4 A multiple stage melting-mixing-fractional crystallization model

Single stage petrogenetic models are not suitable to explain the characteristics of the Arabian Shield volcanics (see Section 6.6.3.2). A multiple stage model, following the important work of Ringwood (1974, 1977) and supported by Kay (1977) will be discussed and compared with analytical results.

Ringwood (1974, 1977) reviews three main models for the origin of island arc systems. These are: amphibole-controlled fractionation at shallow levels (30 - 100 km), eclogite-controlled fractionation at 100 - 150 km depth and partial melting of mantle at 70 - 100 km. Since the first model is not acceptable (see Ringwood, 1974 and Section 6.6.3.2), a model is proposed for the Arabian volcanics which is a combination of the latter two models of Ringwood. In this model partial melts of subducted oceanic plates mix with the mantle wedge overlying the subduction zone. It is possible to infer the composition of the mantle wedge by looking at the chemistry of the erupted basalts. A mantle composition, as calculated by Kay (1977) will be used for subsequent computations (see Table 6.4 for composition). Chondritic normalized patterns for this peridotite mantle are shown in Figure 6.19 (D). In Ringwood's model (1974) partial melts of subducted basaltic oceanic crust (transformed to eclogite) mix with the overlying mantle wedge at depths of more than 100 km. Kay (1977) calculated, using various garnet-pyroxene ratios for the eclogite and various degrees of melting, numerous partial melts (see Table 6.4, Figure 6.19 - B, C). The upper mantle and partial melts of subducted plates can generate a modified mantle, as shown in Figure 6.20. These bodies of modified mantle could rise because of their relative buouancy and generate partial melts as basalts. Theoretical values for the partial melts of the modified mantle (see Figure 6.20 - E, F) are plotted and compared with an average Arabian Shield basalt (BA 125). The agreement of the chondrite normalized values of BA 125 with the calculated results is striking and it is very likely that this basalt originated as a 5 - 10% partial melt of a modified mantle, as shown in Figures 6.19 and 6.20.

The only element which shows a large deviation is Ti (compare also with Figure 6.10). This cannot be explained by the influence of Ti in minor phases in rutile, ilmenite or zircon, since their presence would strongly

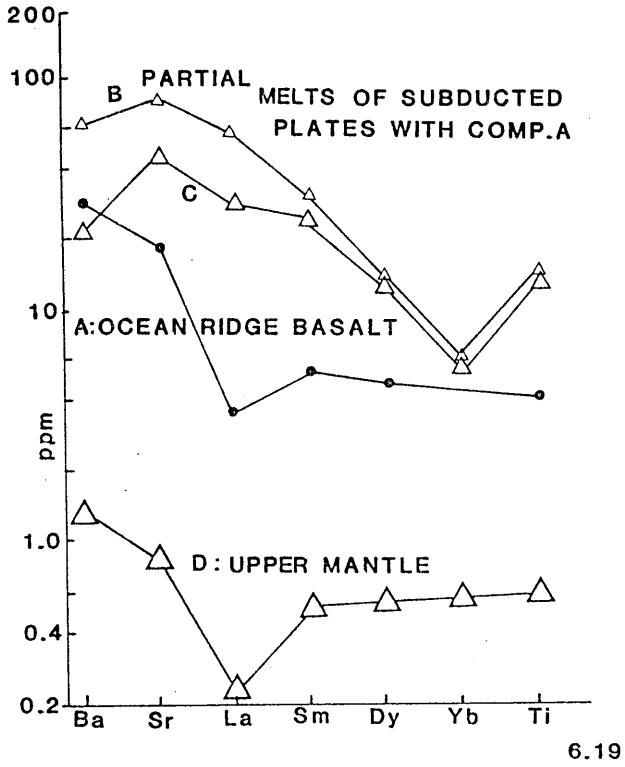

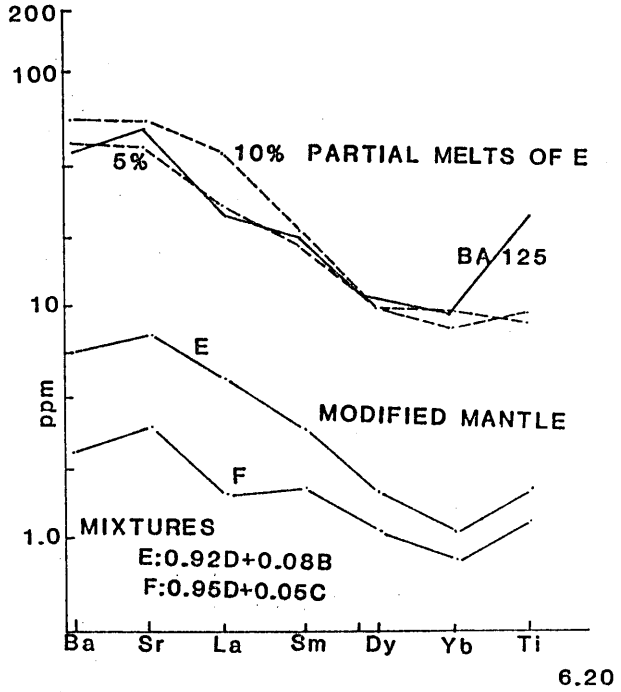

Figure 6.19 Chondrite-normalized mixing members for Arabian Shield volcanics; B and C are partial melts of ocean ridge basalt A, D is a mantle peridotite with a composition as indicated on Table 6.4 (after Kay, 1977).

Figure 6.20 Chondrite-normalized composition of modified mantle, partial melts derived from it and actual composition of an average Arabian Shield basalt (BA 125), compared with these theoretical compositions (after Kay, 1977).

deplete the LREE elements (Hellmann & Green, 1979). Mantle heterogeneities before subduction, as mentioned in Section 6.5, could account for higher Ti and Zr abundances. However, for the Baish/Bahah Group, the oldest volcanic rocks of the Arabian Shield, average Ti abundances for 26 volcanic rocks is 0.26%, i.e. much lower than the average Ti abundances of the younger volcanics which are on average 1.0% (see Table 6.1). Higher Ti (and Zr) concentrations occur only in later stages of the evolution of the Arabian Shield, and it is more likely that these high abundances are caused by processes during late stages of subduction and cratonization. During this stage subduction had ceased and the mantle wedge above the subduction zone would have much lower P_{H_2O} and higher volatile abundances (after Harris & Gass, 1981), which could increase Ti and Zr contents in late crystallizing phases and cause partly within-plate characteristics in an overall island arc setting. Extensive further fractional crystallization, as evidenced by Section 6.6.2 and the REE patterns of Section 6.4 of the basalts causes the generation of the andesite-rhyolite-ignimbrite sequence. This fractional crystallization was dominated at shallow levels by clinopyroxene, amphibole and plagioclase and in the final stage by plagioclase only, producing the negative Eu anomalies.

	D	A	B	C	BA 125
Ba (ppm)	5.4	12.4	240	82	187
Sr	13.3	135	1215	670	639
La	0.082	1.95	22	10.7	8.3
Sm	0.114	1.92	7.1	5.7	4.1
Dy	0.197	2.80	5.3	4.5	- (Tb - 0.76)
Yb	0.139	1.72	1.7	1.4	2.33
Ti (%)	0.041	0.44	1.03 (5% melt)	0.93 (15% melt)	1.43

Table 6.4 Compositions of rock types shown in Figures 6.19 and 6.20; D - mantle peridotite; A - oceanic ridge basalt after Kay et al. (1970); B, C - partial melts of subducted plate with composition A; BA 125 -

7 Evolution of Late Precambrian volcanics in the Arabian Shield

7.1 Introduction

The results of investigations, presented in the previous Chapters show that Late Precambrian volcanics of the Fatima, Badr and Nuqrah areas with an age range of 694 - 608 Ma are of calc-alkaline affinity and have distinct island-arc characteristics. In this Chapter the origin and evolution of the studied volcanics will be discussed in relation to the overall development of the Nubian-Arabian Shield. There are two relevant models for the evolution of the Nubian-Arabian Shield, namely the intracratonic model, whereby the shield has evolved from ensialic belts overlying a basement of sialic material (Engel et al., 1980; Delfour, 1981) and the island arc model, which argues for evolution of several island arcs on oceanic crust, subsequently welded together to form a stable continent (Ringwood, 1974; Gass, 1981). Whichever of these models is accepted, there can be no doubt that the present day crust of the Nubian-Arabian Shield is continental, as evidenced by heat flow, crustal thickness and density (Gass, 1981) and crustal composition (see Chapter 6). If judged by first appearance of within-plate magmatic products this continental character was achieved diachronously between 660 and 570 Ma, being the time-span of the Shammar Volcanics (see Fig. 5.1).

The geology, paleogeography, geochronology, geochemistry and petrology of the Fatima, Badr and Nuqrah volcanics will be discussed and related to these two main models. The analysis focusses first on whether or not the data are consistent with an intracratonic model; the second part assesses the island arc model and a short Nubian-Arabian Shield correlation concludes this Chapter.

7.2 Intracratonic models

Intracratonic models for the evolution of the Nubian-Arabian Shield or of parts thereof have been suggested, amongst others, by El-Shazly and Engel (1978), Church (1979), Kröner (1979), Stern (1979), Engel et al. (1980) and Delfour (1981). The basic assumption for these models, relating to the Nubian-Arabian Shield, is the occurrence of two older sialic cratons on either side of the shield; some authors suggest furthermore that the shield is also underlain by older sialic crust (Stern, 1979; Delfour, 1981). An intracratonic model seems to be valid for large parts of the African continent; the Pan-African Hoggar-Iforas belt is enclosed and underlain by Eburnian (approximately 2000 Ma old) cratons (Bertrand et al., 1978; Black et al., 1979; Bessoles & Trompette, 1980) and the Namibian Damara Belt lies in between the much older Congo and Kalahari cratons and is possibly underlain by sialic material (McWilliams & Kröner, 1981; Hawkesworth et al., in press).

Figure 7.1 illustrates the intracratonic model of Delfour (1981) for the Nubian-Arabian Shield. In his model (Delfour, op. cit.), the Northeast African craton and the Congo craton border the Pan-African fold belt (according to Delfour, 1977, older sialic basement is also inferred at the eastern edge of the Arabian Shield) and a mosaic of small sialic blocks, rejuvenated during the Pan African orogeny lie, surrounded by Pan African mobile belts, in between these blocks. Delfour (op. cit.) assumed that during the Precambrian evolution of the Arabian Shield several tectono-thermal events, accompanied by granitic intrusions (800 - 500 Ma) affected the Upper Proterozoic volcano-sedimentary series and the granitic and metamorphic material considered to represent a pre-existing basement; the younger volcanics are partly of island arc origin. This model envisages that the plutonic rocks of the Arabian Shield (about 55% of the surface area) were

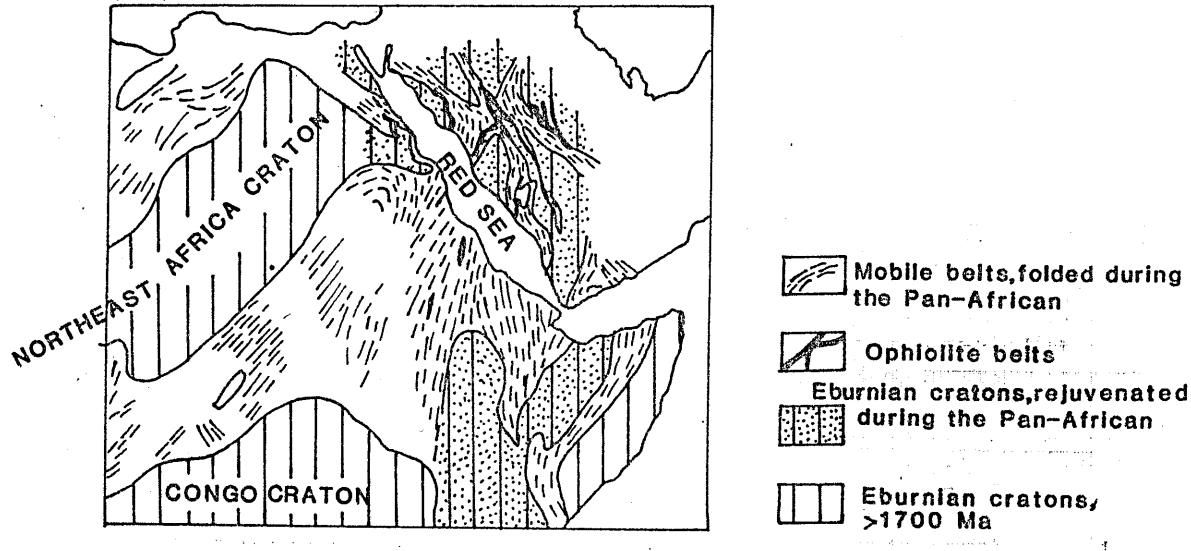

Figure 7.1 The intracratonic model after Delfour (1981) : Eburnean cratons and Pan-African folded belts in NE Africa and Arabia.

produced by reworking or remelting of the older sialic crust. Critical to the intracratonic model is the presence of older (pre-Pan-African) sialic cratons on either side and below the Arabian Shield. There is ample evidence for an older sialic craton to the west of the Nubian-Arabian Shield and east of the Hoggar-Iforas belt. This probably continuous basement complex, called Nile craton (Rocci, 1965) or East Sahara craton (Bertrand et al., 1978), is exposed east of the Hoggar with Rb/Sr ages of at least 2000 Ma (Bertrand et al., 1978), in the Tibesti Mountains (Klitzsch, 1970), in the Uweinat oasis complex with Rb/Sr ages of 2132 ± 200 Ma, 2232 Ma and 2595 Ma (Bessoles & Trompette, 1980) and in isolated outcrops in the western desert of Egypt. Abdel-Monem and Hurley (1979) indicate an age of 1770 ± 40 Ma on detrital zircon grains, separated from a basement gneiss in the eastern desert of Egypt (U/Pb method).

However, there is no convincing evidence of older sialic material below or east of the Arabian Shield. A major thrust belt with ophiolites, the Al Amar-Idsas belt crops out at the eastern edge of the Arabian Shield (Al-Shanti & Mitchell, 1976; Schmidt et al., 1979) and it is to the east of this belt that some authors suggest an older sialic basement (Schmidt et al., 1979; Stacey et al., 1980). Stacey et al. (1980) undertook recently a lead isotope study of the Arabian Shield and it was found that in the easternmost part of the shield, east of longitude 44^{o} 20' towards the the Al Amar-Idsas belt, $^{208}Pb/^{204}Pb$ ratios were distinctly higher than in other parts of the shield. Stacey's data (op. cit.) imply the existence of lower crustal rocks of early Proterozoic age that have underthrust the shield rocks from the east. An age of 2100 ± 300 Ma was calculated for this basement. Unfortunately, the line is poorly defined, one third of the samples being excluded from it. An alternative explanation for the higher $^{208}Pb/^{204}Pb$ ratios

is that reworked late Proterozoic granites, which are highly evolved, act as a Th-enriched source (Duyverman et al., in prep.). Also, conventional Rb/Sr geochronology fails to confirm any pre-Pan-African craton.

Evidence for older sialic rocks below the Arabian Shield is not available. Indeed, Kröner organized a research project specifically to investigate the oldest basement complex of the shield, but specimens collected from the most deformed and structurally lowermost units near Al-Lith (20^{o} 10'; 40^{o} 15') give ages no older than 800 Ma (Kröner et al., 1979). The oldest rocks of the Arabian Shield are in the southern part the Hali Group and the Khamis Mushayt Group (Schmidt et al., 1973; Greenwood et al., 1973) and in the northern part the Rharaba Complex and the Ajal Group (Delfour, 1981). These groups, as conceded by the writers, could well be more highly metamorphic equivalents of overlying rocks. No reliable age older than 900 Ma has been reported for the Arabian Shield (Delfour, 1981; Duyverman & Harris, 1981, in press). Ongoing Sm/Nd isotope studies at the Open University to investigate source regions for Arabian Shield rocks indicate no evidence for sialic basement older than 1000 Ma (Duyverman et al., in prep.).

Rb/Sr geochronological work (see Chapter 5) shows that the increase of initial $^{87}Sr/^{86}Sr$ ratios from the southwestern towards the northeastern part of the shield can be explained by a self-contained evolution of island-arc type rocks without necessarily involving older sialic crust. Rather primitive initial ratios and the lack of K-feldspar and other possibly continentally derived detritus (like the detrital zircons of Abdel-Monem & Hurley, 1979) in the oldest volcanic sedimentary sequences suggest deposition on oceanic crust, geographically isolated from eroding continental areas.

7.3 Island arc models

7.3.1 Introduction

The island arc or island arcs models for the Nubian-Arabian Shield are essentially uniformitarian following the models of Ringwood (1974) for the magmatic processes and that of Mitchell and Reading (1971) for the sedimentary aspects. Jackaman (1972) was the first to mention the calc-alkaline affinities of the Precambrian volcanic rocks of the shield in an island arc environment. Jackaman's analytical data were used to support field data indicating that the southern part of the Arabian Shield consisted of a single arc. In 1976, based primarily on studies of ophiolitic rocks, Bakor et al. proposed a multiple arc model. This model envisaged four N/S trending arcs in Saudi Arabia and several others in NE Africa. Further discussions of the island arc model can be found in Neary et al., 1976; Riofinex, 1977; Gass, 1977; Frisch & Al-Shanti, 1977; Brown & Jackson, 1979; Schmidt et al., 1979; Nasseef & Gass, 1980; Hadley & Schmidt, 1980; Fleck et al., 1980 and Gass, 1981. The basic tenure of these models is that the Nubian-Arabian Shield originated from one or more intraoceanic island arcs above subduction zones which matured with time and accreted to the Nile craton. Various lines of evidence supporting east- and west-dipping subduction zones have been proposed; there is no consensus of opinion at the present time. Evidence for the island arc model will be discussed under different headings, and, where appropriate, compared with results from this study.

7.3.2 Spatial and temporal trends

The occurrence of the oldest rocks in the southwestern part of the Arabian Shield and progressively younger rocks towards the northeast has been repeatedly noted since identified by Brown & Jackson (1960). This spatial trend is caused most likely by uplift and tilting of the

southern Arabian Shield and subsequent differential erosion. This spatial trend coincides with several geochemical trends in alkali abundances, strontium isotope ratio and tholeiitic to calc-alkalic trends, all of which will be discussed later.

Figure 7.2 shows the aerial distribution of the Saudi Arabian volcanics and related sediments (after Hadley & Schmidt, 1980, with inclusion of data from this study). It should be noted that three spatially and temporally separate units, namely the Baish/Bahah Groups (1165 - 837 Ma), the Halaban/Hulayfah Groups (780 - 658 Ma) and the Fatima/Murdama/Shammar Groups (678 - 555 Ma) have all been studied in detail and an island arc origin is indicated for the three units. The Baish/Bahah Groups (studied by Jackaman, 1972) consist of marine volcanics (mainly basalts) with intercalated tuffs and turbidities; no terrigenous detritus is found in these groups. The volcanics have a tholeiitic character and their lime-alkali index indicates calcic affinities. The setting of the Baish/Bahah Groups is considered to be a juvenile island arc. The equivalent Halaban (Dodge et al., 1979) and Hulayfah Groups (Delfour, 1979) consist of predominant andesites, intercalated with tuffs, breccia and sediments. The volcanics have tholeiitic to calc-alkaline trends and their lime-alkali index indicates calcic affinities. The tectonic setting for these groups is an immature island arc. The mainly continental Fatima/Murdama/Shammar Groups, investigated in detail in this study, consist of andesites and rhyolites, intercalated with tuffs, breccia, volcanogenic sediments and limestones. The volcanics have a calc-alkalic trend, a lime-alkali index which indicates calc-alkalic to alkali-calcic affinities and their setting is thought to be varying from mature island arc to continental margin.

Generally, there is a spatial and thus temporal trend in Saudi Arabian

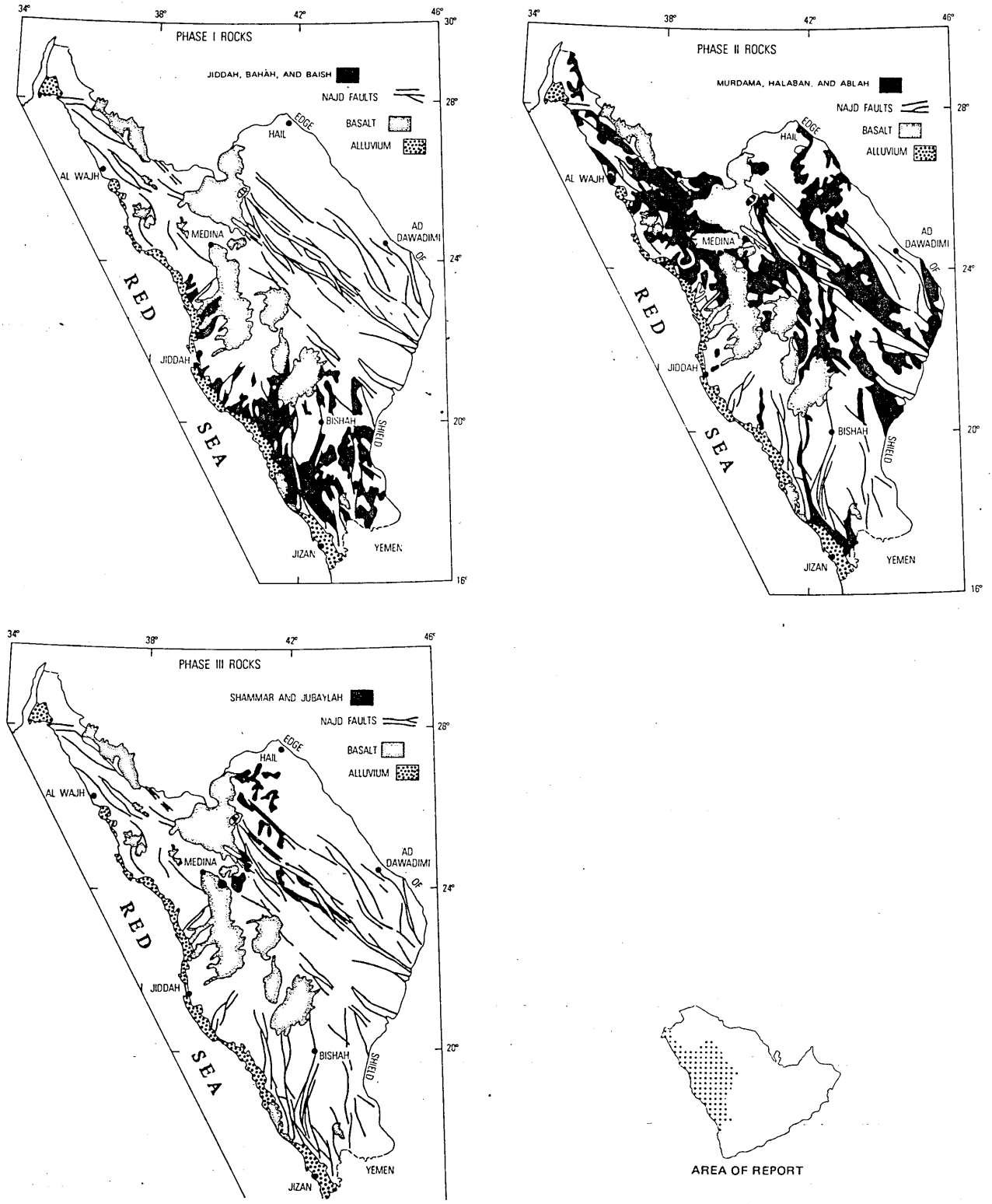

Figure 7.2 Spatial/temporal rock type trends for volcanic-sedimentary rock units of the Arabian Shield (after Hadley & Schmidt, 1980) .

volcanics from tholeiitic to calc-alkaline, accompanied by decreasing alkali-lime indices and a change in setting from juvenile island arcs to continental margin. Although the overall evolution in time in rock type and setting seems to be fairly simple, the distribution of ophiolite belts, indicating possible sutures between island arcs and complex geochemical trends indicate the episodic character of the island arc evolution and the possibility of the existence of several coexisting arc systems.

Present-day arc systems (Gass, 1981) have distances from 100 - 150 kilometres from trench to back-arc basin. If the Arabian Shield ophiolitic belts represent sutures, then several island arc systems of these dimensions could "fit" in the Arabian Shield. Assuming that large parts of the Nubian-Arabian Shield are cratonized island arcs, then an enormous mass of continental crust was produced in the Upper Proterozoic and added to the Nile craton.

7.3.3 Geochemical trends across the Arabian Shield

7.3.3.1 $K_2O/(K_2O + Na_2O)$ ratios of plutonic rocks

Gradual increases in this ratio have been noted and discussed by Greenwood and Brown (1973), Gass (1977) and Nasseef and Gass (1980). Figure 7.3 (after Greenwood & Brown, 1973) indicates this contoured trend for the Arabian Shield. This apparent regional trend from the southwest towards the northeast is probably comparable to $K_2O/(K_2O + Na_2O)$ trends in the western U.S.A. and other volcanic areas (Kuno, 1959, 1966) which are supposed to be produced by anatexis of prebatholitic rocks with a similar gradient (Dodge et al., 1970) or by magma generation at progressively increasing depths along an inclined Benioff zone (Kuno, 1959, 1966; Gilluly, 1971). The second hypothesis seems to be more likely, since anatexis in the Arabian Shield only

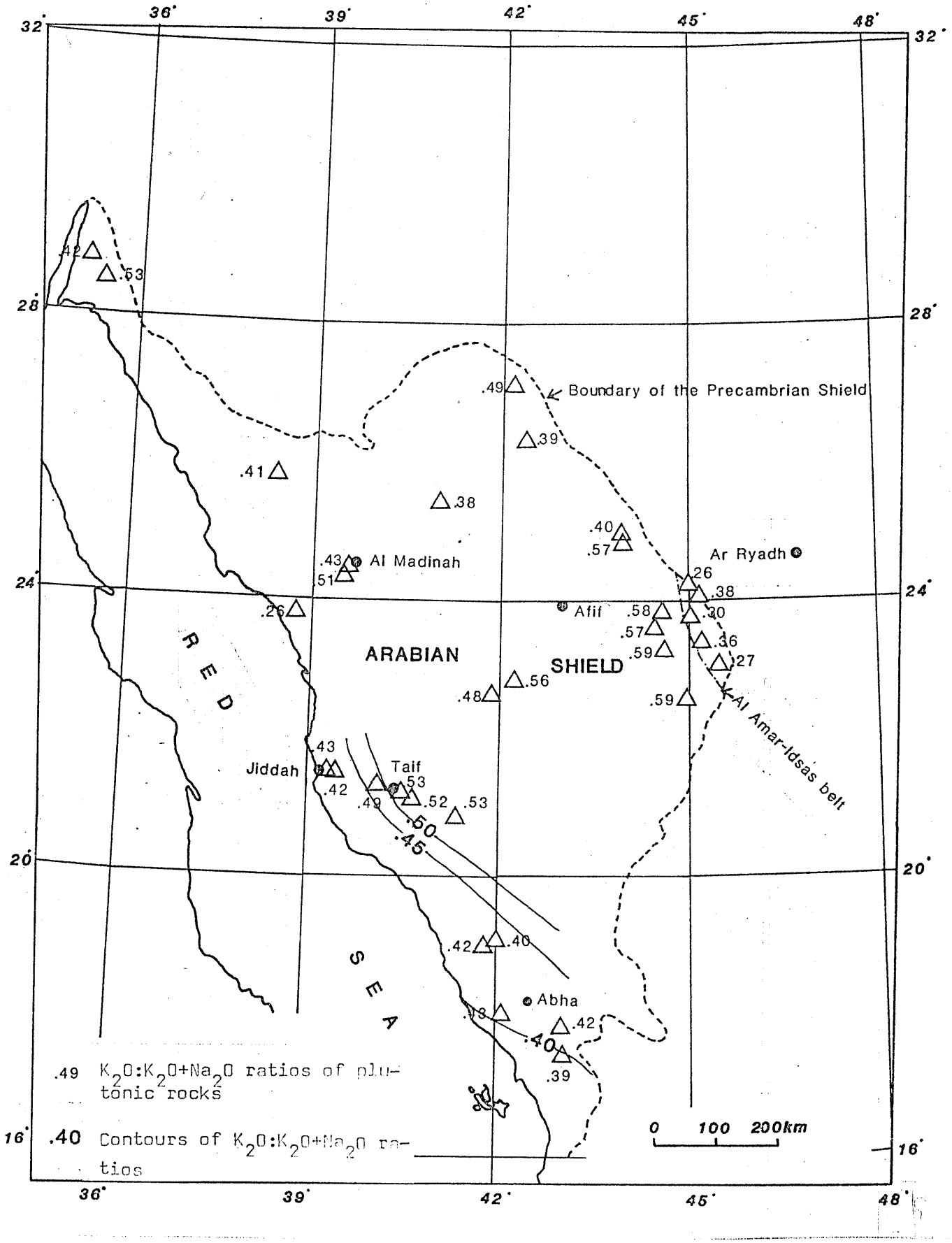

Figure 7.3 Distribution and $K_2O:(K_2O + Na_2O)$ ratios of plutonic rocks of the Arabian Shield; data after Gass (1979), Hadley & Schmidt (1980) and this study.

occurred during the last stages of subduction (see Chapter 5). Gass (1979) and Nasseef and Gass (1980) describe an Arabian Shield traverse in approximately 1000 Ma old granitic rocks. Their $K_2O/(K_2O + Na_2O)$ ratios show a gradual increase from Jeddah (SW) to the eastern edge of the shield (NE) with major breaks near the Al Amar thrust zone, the Najd fault zone and east of Taif that are covered by Late Tertiary alkali basalts.

These geochemical trends and the possible relation of the alkali ratio and the depth of magma generation along a subduction zone (Dickinson, 1968; Gass, 1979) is considered to be suspect in other areas (Hutchison, 1975). It is however, one of many geochemical trends, all pointing towards an island arc origin for the Arabian Shield. There is no consensus for the direction of dip of the assumed subduction zone; most authors favour eastward-dipping zones (Greenwood et al., 1974; Al-Shanti & Mitchell, 1976; Nasseef & Gass, 1980; Fleck et al., 1980), but Schmidt et al. (1979), Hadley and Schmidt (1980) and Kröner (1979) suggest SW dipping zones. An easterly dipping subduction zone seems to be more likely, because there is a gradual change from tholeiitic to calc-alkaline trends across the Arabian Shield, meaning, according to Ringwood (1974) derivation from deeper levels along the subduction zone.

7.3.3.2 Isotopic trends

Isotopic trends and more specifically initial $^{87}Sr/^{86}Sr$ ratios were discussed by Fleck et al. (1980), Brown (1980) and Duyverman and Harris (1981, in press). The evolution of these trends, including new Rb/Sr isotopic data, was discussed in Chapter 5. Pertinent to the island arc evolution theory is, that the oldest rocks of the Arabian Shield have initial ratios of 0.7025 which are inconsistent with derivation from

continental crust (which would produce much higher ratios). There is a gradual increase of initial ratios in time to 0.712 at 555 Ma (see Figure 5.13), because magmas were derived from source regions with progressively higher Rb/Sr ratios as the crust became more evolved. Because of tilting and subsequent erosion of the Arabian Shield these higher ratios do occur in the central and northeastern part of the shield and the lowest values in the southwestern part (see Figure 5.14). Isotopic trends in space and time are consistent with an island arc model whereby an eastward dipping subduction zone with newly formed and thickened crust towards the northeast was active throughout the Pan-African time-span.

7.3.4 Ophiolite belts

Ophiolites or ophiolite belts and incomplete ophiolitic sequences have been described by many workers in the Nubian-Arabian Shield (e.g. Bakor et al., 1976; Brown & Jackson, 1980; Gass, 1981; Delfour, 1981), in the eastern desert of Egypt (Abdel-Gawad, 1970; Shackleton et al., 1980; Nasseef et al., 1980) and in the Sudan (Neary et al., 1976; Fitches et al., in press). The ophiolites of the Arabian Shield are often regarded as marking ancient sutures, but this assumption raises several problems:

1. Do they represent true ophiolites in the Penrose conference sense?
2. Do they form extensive belts that can be traced over long distances?
3. Are they of similar stratigraphic position or do they occur at several stages?

Ad 1. In the Arabian Shield, complete but fragmented ophiolite sequences have been reported from Jabal al Wask (Bakor et al., 1976), Jabal Ess (Shanti & Roobol, 1979) and Bir Umq (Al-Rehaili & Warden, 1980). Figure 7.4 shows the occurrences of these and other ophiolites. Incomplete ophiolite belts are described in the Al Amar-Idsas zone

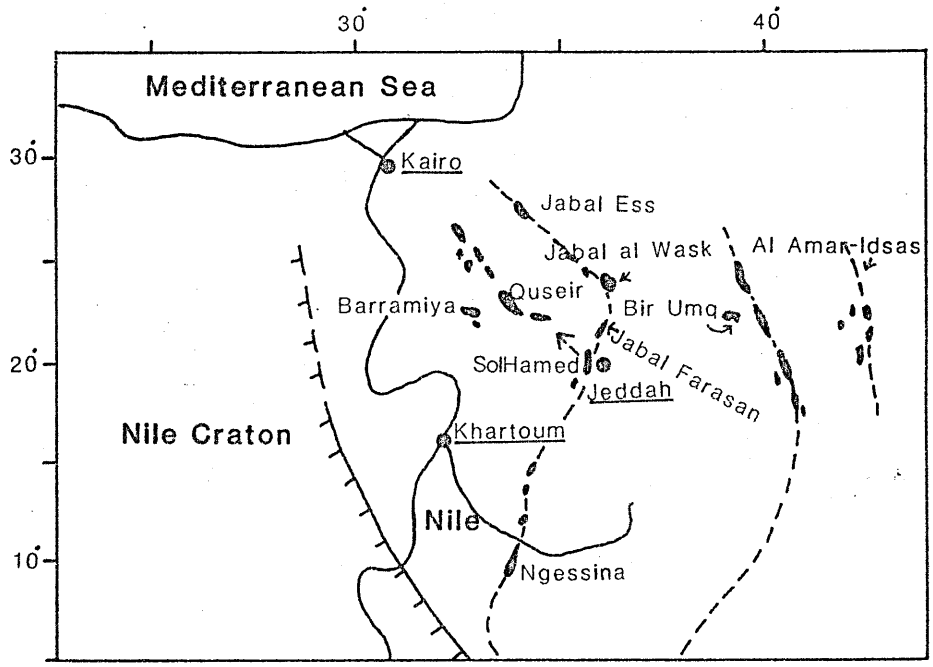

Figure 7.4 Regional distribution of ophiolitic rocks in the Nubian-Arabian Shield. The Shield is shown in its Pre-Red Sea reconstruction, the approximate position of the Nile craton is indicated (after Gass, 1977 and Shackleton, 1979). The broken arrow NW of the Sol Hamed ophiolite indicates the inferred tectonic transport of some of the Egyptian ophiolitic rocks (see text for explanation).

(Al-Shanti & Mitchell, 1976; Frisch & Al-Shanti, 1977) and in the Hulayfah-Hamdah belt (Frisch & Al-Shanti, 1977). The Jabal Farasan ophiolite (Nasseef, pers. comm.) is another incomplete ophiolite mass.

Ad 2. The occurrences of Arabian Shield and other ophiolite belts can be fitted together in several ways (see Figures 7.1 and 7.4). The easternmost Al Amar-Idsas belt and the centrally situated Hulayfah-Hamdah belt are agreed upon by most writers. The continuation of the westerly belt, however, is not at all certain. Tertiary alkali basalts and extensive faulting prohibit accurate correlation. An alternative correlation to the regional reconstruction after Gass (1977) and Shackleton (1979) is given in Figure 7.4. The westerly belt is assumed to consist of Jabal Ess- Jabal al Wask- Jabal Farasan- Sol Hamed and possibly Ngessina. The Sol Hamed-Quseir and Barramiya connection is probably tectonic as the Quseir and Barramiya ophiolitic masses occur in an extensive mêlange (Shackleton et al., 1980).

Ad 3. There is no consensus on the stratigraphic position of the ophiolitic belts. The theories vary between a position equivalent to the Baish Group and several ophiolitic belts at 1000, 800 and 600 Ma respectively (Gass, 1981). It seems to be certain that the ophiolites are emplaced tectonically, with emplacement distances of several hundred kilometres (Shackleton, 1980, for the eastern desert of Egypt). All major ophiolite complexes in the Arabian Shield have tectonic contacts (Bakor et al., 1976; Al-Shanti & Mitchell, 1976; Frisch & Al-Shanti, 1977; Shanti & Roobol, 1979; Al-Rehaili & Warden, 1980; Gass, 1981). Although the ophiolite belts occur in fault contact with, moving towards the northeastern part of the shield, successively younger rock units, the belts

themselves could be of similar age but their emplacement possibly occurred in three or more episodes, stressing the episodic character of the Arabian Shield evolution, as suggested by geochemical and other trends.

7.3.5 Discussion

Most evidence from the Arabian Shield geology (supplemented by data from this study) and from literature studies support the multiple arc origin for all Proterozoic Arabian Shield rocks. Geochemical work by Jackaman (1972), Dodge et al. (1979), Delfour (1979) and in this study (among others) indicate three, partially overlapping periods of island arc evolution. Early, submarine, tholeiitic volcanism for the Baish and Bahah Groups (after Jackaman, 1972) gave way from marine to continental, tholeiitic to calc-alkaline volcanism for the Hulayfah and Halaban Groups (Dodge et al., 1979; Delfour, 1979) and continental, mainly subaerial, calc-alkaline volcanism for the Murdama and Shammar Groups. The overall trend is from juvenile island arc for the oldest rocks (1165 - 837 Ma) to mature arc and continental margin for the Murdama and Shammar Groups (678 - 555 Ma). Geochemical trends in time, isotope studies and field geology support this island arc evolution. The occurrence of several proven ophiolites and the alignment of possible ophiolite belts indicate the possibility of at least three co-existing island arcs in Saudi Arabia. Their emplacement, however, always is tectonically and their distance of transport unknown. The incomplete belts in the western part of the shield enable different interpretations (see Neary et al., 1976 versus Delfour 1981). A new interpretation with realignment of the ophiolite belts, as favoured by the author, is shown in Figure 7.4. The other current intracratonic theories on the evolution of the Arabian Shield are also unlikely because of very low initial strontium ratios of the oldest shield rocks and the absence of evidence for an older craton towards the eastern edge of the

Arabian Shield.

The Fatima, Badr and Nuqrah volcanics belong to the last period of island arc activity of the Arabian Shield. The Fatima and Badr volcanics have been dated at 681 ± 13 Ma and 634 ± 26 Ma, respectively and they were both assigned to the Murdama Group (see Figure 5.1, column 4). Field geology and geochemical studies confirm this assumption. The Nuqrah volcanics were dated at 626 ± 9 Ma and were assigned to the Shammar Group. Their occurrence in the Shammar Group type locality area (Delfour, 1977) and geochemical characteristics confirm this.

The paleogeography for the Fatima Group and Badr volcanics is thought be be shallow marine to continental (see Chapters 2 and 3) and for the Nuqrah volcanics continental (see Chapter 4) with subaerial volcanics and interlayered sediments. Coarse volcanic breccia and the extensive ignimbrites indicate a relatively high topography in this area.

Geochemical studies on major, trace and REE confirm a continuous trend for the Fatima-Badr-Nuqrah volcanics from slightly tholeiitic to calc-alkaline, a decreasing alkali-lime index and a presumed tectonic setting of immature arc to continental margin. Petrogenetic modelling suggests that the basalts of the Fatima/Badr/Nuqrah suites have been formed by melting and mixing of mantle, which is often described in an island arc environment (e.g. Ringwood, 1974). Anomalous Zr and Ti abundances are most likely caused by processes during late stages of subduction and cratonization, when subduction had ceased. Later extensive fractional crystallization, as evidenced by the REE patterns of the studied volcanics, accounts for the extensive and characteristic andesite-rhyolite-ignimbrite sequences in the three areas.

7.4 Proposed model for the evolution of the Nubian-Arabian Shield

Figure 7.5 shows a tentative model for the evolution of the Nubian-Arabian Shield in Late Proterozoic times. The first stage (A) corresponds with the Baish/Bahah Group juvenile arc system with submarine volcanic rocks and sediments (after Jackaman, 1972). Three or more arcs existed during this time. Oceanic crust was originally present in the whole area, representing the Nubian-Arabian Shield; the remnants of this crust are the present-day ophiolite belts. Probably eastward dipping subduction zones caused tholeiitic volcanism and submarine erosion products covered parts of these volcanics. During the deposition of the Hulayfah/Halaban Groups (after Delfour, 1979; Dodge et al., 1979) island arc activity continued (B); further subduction caused extensive tholeiitic to calc-alkaline volcanism and the emerging island arcs were subjected to extensive erosion and redeposition, covering most of the older volcanic and plutonic rocks.

During deposition of the Murdama and Shammar Group rocks (C) the island arcs matured further with the formation of thick continental crust. Subduction ceased and the volcanic products bear the imprint of a change in magma type. The Shammar Group volcanics are fully continental and during their time of deposition a considerable relief existed. The volcanics in this period are slightly tholeiitic to calc-alkaline and extensive erosion took place of the volcanic and plutonic rock units.

A prolonged period of E-W compression (D) further cratonized the Nubian-Arabian Shield, as evidenced by the extensive Najd fault system. An indenter from the east (after Tapponnier & Molnar, 1976) probably caused this compression. In this model, the area east of the Al Amar-Idsas suture actively collided with the rest of the Nubian-Arabian Shield and the craton to the west of this shield. Peralkaline plutonism and volcanism with within-plate characteristics mark the last stage of

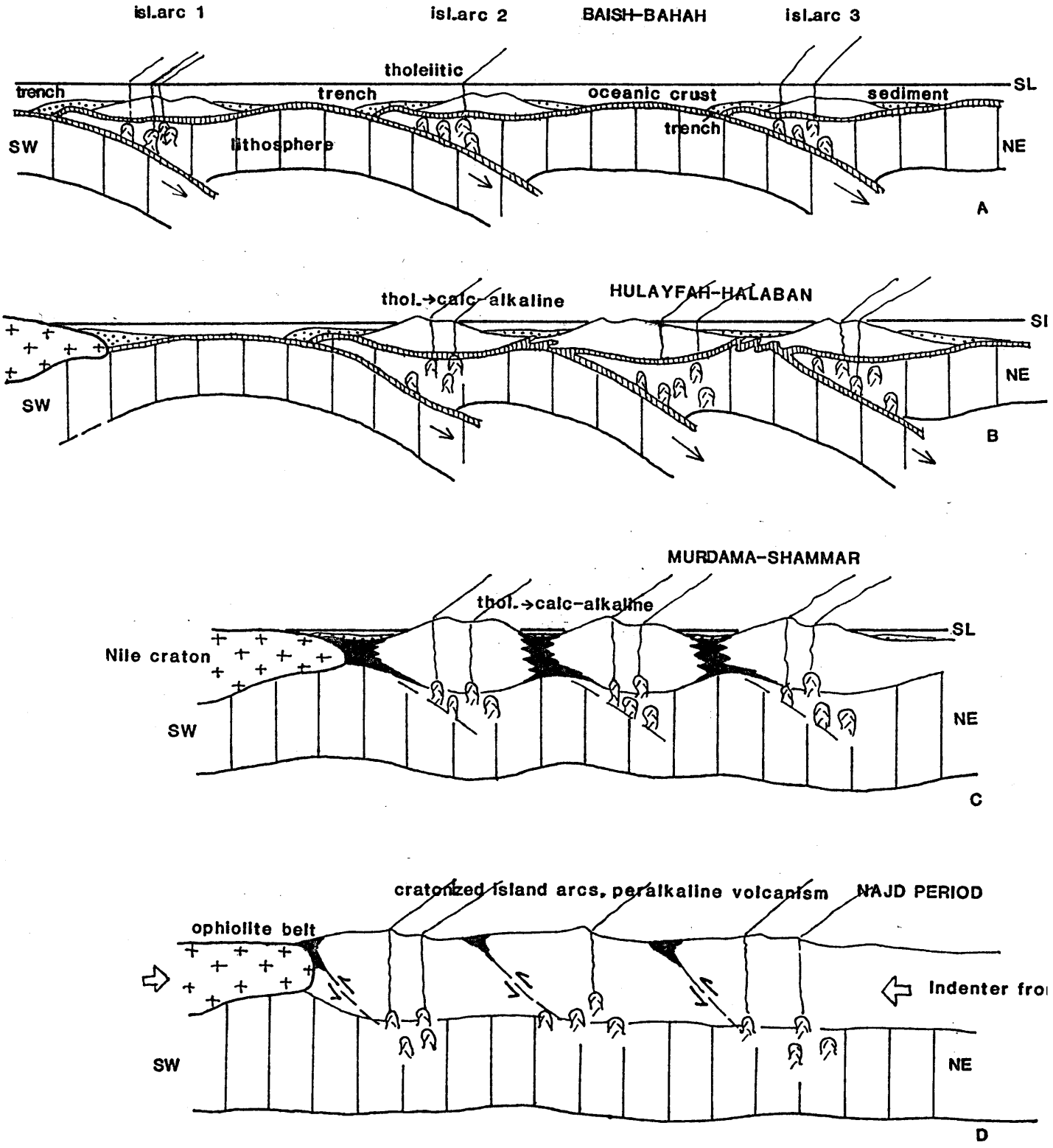

Figure 7.5 Multiple accreting arc model for the Nubian-Arabian Shield. This cartoonlike figure illustrates the major stages of evolution (see text for further explanation) ;SL - sealevel,isl - island, thol - tholeiitic .

cratonization of the Nubian-Arabian Shield and later tilting and differential erosion produced broadly the present-day geological outlook of the shield.

7.5 Correlation with other parts of the Nubian-Arabian Shield

7.5.1 Introduction

Further to the Chapters 1.2 and 1.3 some tentative correlations will be given for Pan-African rocks that also formed part of the Nubian-Arabian Shield. Because of the field of this study, emphasis will be put on the younger volcanic rocks and the possible ophiolite belts. Unknown stratigraphic correlations and poor dating often make correlations difficult.

7.5.2 Oman

Pan-African rocks (1200 - 500 Ma) have been reported from the Sultanate of Oman at several isolated localities. Glennie (1970) describes Pan-African basement rocks at Jebel Jala'an in E. Oman, dated at 860 Ma (Glennie et al., 1974). Hawkins et al. (1981) report on the Pan-African crystalline shield in S. Oman. The Mirbat Plain and the Kuria Muria Islands, consisting of granites and gneisses, invaded by dykes, show a clear NW/SE Najd trend. Continental crust below the Semail (Tethyan) ophiolite in E. Oman has a thickness of about 42 kilometres (Manghani & Coleman, 1981) and probably incorporates cratonized Pan-African crust.

7.5.3 Sudan (northeastern part)

Several ophiolitic and ultramafic bodies have been described in the Sudan. A complete ophiolite sequence, 500 kilometres N of Port Sudan, is described by Fitches et al., 1981 and Fitches et al., in press). This ophiolite is probably the source of the (mélange) olistostrome, described in the eastern desert of Egypt (Shackleton et al., 1980).

This ophiolite continues probably towards the north to Jabal Farasan and Jabal al Wask (see Figure 7.4) with possible ages of emplacement of ca. 800 Ma (Gass, pers. comm.). The Sol Hamed ophiolite is in fault contact with the Nafirdeib volcanic suite (and partly covered by it), a volcanic and volcaniclastic sequence with island arc affinities (Fitches et al., in press). The ophiolite and cover rocks show low-grade metamorphism, are intruded by Pan-African granitic rocks and subsequently covered by flysch-type sediments, comparable with the Egyptian Hammamat series (see Figure 5.3).

The ophiolite belt continues to the south as a discontinuous belt, through possible ophiolite complexes in the S. Red Sea Hills (Alsac, BRGM, pers. comm.) and the Ingessana Hills, described by Kabesh (1961).

A younger volcanic and sedimentary group, unconformably covering the Nafirdeib series is the Awat Group (defined by Ruxton, 1956), which is probably equivalent to the Asoteriba volcanics of Neary et al. (1976) and the Homagar Group (S.M. Ali, pers. comm.). An age of 649 ± 18 Ma has been reported by Cavanagh (1979) for the Asoteriba volcanics. These equivalent rock units have calc-alkaline affinities and probably belong to an island arc sequence. As in the Arabian Shield, granites make up a large part of the terrain (about 60% in NE Sudan - Neary et al., 1976) and after 500 Ma there is widespread within plate volcanism and plutonism, often of peralkaline character. A major difference between NE Sudan (and a large part of Egypt) and the Arabian Shield is the occurrence of widespread plutonism between 500 and 30 Ma in Sudan and Egypt, which has no equivalent in Saudi Arabia. This plutonism comprises syenites and peralkaline granites; the contrasting pattern on both sides of the Red Sea is described by Harris and Gass (1981) as the result of complete depletion in components contributing to peralkaline melts in the sub-Arabian Shield mantle and lower crust at about 500 Ma,

whereas the sub-African mantle continued to produce small quantities of alkaline magma episodically thereafter. Correlations of composition and areal extent indicate a possible correlation of the Asoteriba/Awat/Homagar volcanics with the Murdama Group in Saudi Arabia (see Figure 5.3).

7.5.4 Egypt (mainly Eastern Desert)

Ophiolite occurrences in Egypt have been reported by Garson and Shalaby (1974), Shackleton et al. (1980) and Nasseef et al. (1980). The tectonic and stratigraphic position of these ophiolites, however, is unclear. Ophiolite belts, as postulated by Abdel-Gawad (1970) from satellite imagery, are probably non-existent (Shackleton, pers. comm.) and it is possible, that all ophiolitic rocks are derived from sutures, as postulated by Shackleton et al. (1980) and Fitches et al. (in prep.). Younger volcanic rocks in the Eastern Desert of Egypt include the Dokhan volcanics and the Hammamat series (see Figure 5.3). The Dokhan volcanics have been described by Basta et al. (1980), who claim that the Dokhan volcanics are comparable with the upper part of the Hulayfah Group (as described by Delfour (1975) of mildly tholeiitic to calc-alkaline nature) in the Arabian Shield. The geochemical data of Delfour (1976) support this hypothesis. The Dokhan volcanics (Basta et al., 1980) consist of tholeiitic to calc-alkaline rocks and are comparable with present day mature island arcs. The Hammamat Group consists mainly of immature sediments and is probably equivalent to the Jubailah Group in Saudi Arabia and the flysch-type rocks near Sol Hamed in NE Sudan (see Section 7.5.3).

8 Conclusions

Arguments in favour of a multiple accreting arc model for the evolution of the Late Precambrian Fatima, Badr and Nuqrah volcanic rocks (and associated plutonic rocks) and in a larger framework, for the whole Arabian Shield, can be concluded as follows:

(A - for studied areas; B - for the whole Arabian Shield)

A1 Geochronological studies (Rb/Sr) indicate that the Fatima and Badr rock types belong to the Murdama Group; the Nuqrah volcanics are part of the Shammar Group.

A2 Field and petrological studies indicate that the sedimentary environment of the Murdama Group rocks is shallow marine to continental and that the Shammar Group rocks are continental and show indications of a considerable relief.

A3 Geochemical analyses suggest that the Fatima, Badr and Nuqrah volcanics belong to the calc-alkaline rock series with slightly tholeiitic affinities for the older rock types. The volcanics display a continuous trend of rock types in an evolving island arc setting from mature arc (Fatima and Badr volcanics) to continental margin (Shammar volcanics).

A4 Three or more juvenile island arcs co-existed during the early stages of island arc evolution (Baish/Bahah Groups). These arcs gradually thickened and coalesced in time during further subduction related volcanism and plutonism. Complete cratonization was reached during deposition of the Shammar Group.

A5 Petrogenetic modelling of the basalts shows that these rock types

originated from partial melting of modified mantle; the characteristic andesite-rhyolite-ignimbrite sequence in the three areas is probably caused by extensive further fractional crystallization.

B1 Isotopic studies reveal a gradual increase in initial $^{87}Sr/^{86}Sr$ ratios from the southwestern to the northeastern part of the Arabian Shield, indicating a self-contained Sr evolution without necessarily assuming an older sialic craton in the eastern edge of the shield.

B2 Other geochemical trends (alkalis, major, trace, REE studies) indicate a gradual change in time and space (because of tilting and differential erosion of the Arabian Shield) from early tholeiitic to later calc-alkalic plutonism and volcanism (with concomitant decreasing alkali-lime indices and a shift in rock types from basalt to rhyolite), which indicates island arc activity above an eastward dipping subduction zone.

B3 Three more or less continuous ophiolitic belts can be traced across the Arabian Shield in a NNE/SSW direction. From E to W these belts are: the Al Amar-Idsas belt, the Hulayfah-Hamdah belt and the Jabal al Wask-Jabal Farasan-Sol Hamed (NE Sudan) belt (the latter belt is worst defined). These belts might represent sutures between island arcs.

B4 Tentative correlations with other parts of the Nubian-Arabian Shield show that ophiolitic belts can be traced in NE Sudan, but not in Egypt. Younger volcanics in Sudan and Egypt may be correlated with Arabian Shield rock units.

9 References

Frequently used abbreviations are: IAG - Institute of Applied Geology, Jeddah, Saudi Arabia; USGS - United States Geological Survey, Jeddah, Saudi Arabia; BRGM - Bureau de Recherches Géologiques et Minières, Jeddah, Saudi Arabia; Riofinex - Riotinto Finance and Exploration, Jeddah, Saudi Arabia; DGMR - Directorate General of Mineral Resources, Jeddah, Saudi Arabia. Style and abbreviations are after the guidelines of the Geological Society (London).

Abbey, G. 1980. Studies in "Standard Samples" for use in the general analysis of silicate rocks and minerals. Geostandards Newsletter, Geol. Surv. of Canada, Vol. 4, No. 2, 163-90.

Abdel-Gawad, M. 1970. Interpretation of satellite photographs of the Red Sea and Gulf of Aden. Philos. Trans. R. Soc. London, A.267, 23-40.

Abdel-Monem, A.A. & Hurley, P.M. 1978. U/Pb dating of zircons from psammitic gneisses, Wadi Abu Resheid, Eastern Desert, Egypt. Precambrian Res., 6, A4.

Aguttes, J. 1973. Geology and mineral exploration of the Jabal Sutayhat Sharq quadrangle, 24/38D. BRGM Rep., 73 JED 12.

Alabouvette, B., Chapelain, J.R.le & Pellaton, C. 1975. Geology and mineral exploration of the Yanbu al Bahr quadrangle. BRGM 75 JED 20.

Aldrich, L.T. 1978. Geochronological data from the Arabian Shield, Section 1. DGMR, Project Report SA(IR) 240.

Allen, J.C., Modreski, P.J., Haygood, C. & Boettcher, A.L. 1972. The role of water in the mantle of the earth: The stability of amphiboles and micas. 24th Int. Geol. Cong., Sect. 2, 231-40.

Al-Rehaili, M.H. & Warden, A.J. 1980. Comparison of the Bir Umq and Hamdah ultrabasic complexes, Saudi Arabia. IAG Bull. 3, Vol. 4, 143-56.

Al-Shanti, A.M.S. 1966. Oolitic iron ore deposits in Wadi Fatima between Jeddah and Mecca, Saudi Arabia. DGMR Res. Bull. 2, 51pp.

Al-Shanti, A.M.S. & Mitchell, A.H.G. 1976. Late Precambrian subduction and collision in the Al Amar-Idsas region, Arabian Shield, Kingdom of Saudi Arabia. Tectonophysics, 31, T41-47.

Almond, D.C. 1979. Younger granite complexes of Sudan. IAG Bull. 3, Vol. 1, 151-64.

Anhaeusser, C.R. 1973. The evolution of the early Precambrian crust of southern Africa. Phil. Trans. R. Soc. Lond. A,283, 359-88.

Baker, P.E. 1968. Comparative volcanology and petrology of the Atlantic island arcs. Bull. volcanol., 22-1, 189-206.

Bakor, A.R., Gass, I.G. & Neary, C.R. 1976. Jabal al Wask, Northwest Saudi Arabia: An Eocambrian back-arc ophiolite. Earth planet. Sci. Lett., 30,1-9.

Basta, E.Z., Kotb, H. & Awadallah, M.E. 1980. Petrochemical and geochemical characteristics of the Dokhan Formation at the type locality Jabal Dokhan, Eastern Desert, Egypt. IAG Bull. 3, Vol. 3, 121-40.

Baubron, J.C., Delfour, J. & Vialette, Y. 1976. Geochronological measurements (Rb/Sr;K/Ar) on rocks of the Arabian Shield, Kingdom of Saudi Arabia. BRGM, 76 JED 22.

Bertrand, J.M.L., Caby, R., Ducrot, J., Lancelot, J., Moussine-Pouchkine, A. & Saadallah, A. 1978. The Late Precambrian ensialic linear fold belt of eastern Hoggar (Algeria). Precambrian Res., 7, 349-76.

Bertrand-Sarfati, J. & Raaben, M.E., 1971. Comparaison des ensembles stromatoligues du Précambrien Supérieur du Sahara occidental et de l'oural. Bull. Soc. géol. Fr., Sér. 7, 12, 364-71.

Bessoles, B. & Trompette, R. 1980. Géologie de l'Afrique-la chaine pan-africaine. Mémoire du BRGM, 92, 396pp.

Black, R., Caby, R., Moussine-Pouchkine, A., Bayer, R., Bertrand, J.M., Bouiller, A.M., Fabre, J. & Lesquier, A. 1979. Evidence for Late Precambrian plate tectonics in West Africa. Nature, 278, 223-27.

Bokhari, F.Y. & Kramers, J.D. 1981. Island arc character and Late Precambrian age of volcanics at Wadi Shwas, Hijaz, Saudi Arabia: Geochemical and Sr and Nd evidence. Earth planet. Sci. Lett., 54, 409-22.

Brooks, C., Hart, S.R, & Wendt, I, 1972. Realistic use of two-error regression treatments as applied to Rb-Sr data. Rev. Geophys. Space Phys., 10, 551-77.

Brosset, R. 1977. Geology and mineral exploration of the Bi'r Al Furaysh quadrangle, 24/39C. BRGM Rep., 79 JED 3.

Brosset, R. & Conraux, J. 1978. Geology and mineral exploration of the Jabal Abraq quadrangle, 23/42A. BRGM Rep., 78 JED 1.

Brosset, R. & Delfour, J, 1972. Geology and mineral exploration of the Wadi al Jifn quadrangle, 25/41B. BRGM Rep., 72 JED 14.

Brown, G.C. 1980. Calc-alkaline magma genesis: the Pan-African contributions to crustal growth. IAG Bull. 3, Vol. 3, 19-29.

Brown, G.C. 1981. Calc-alkaline intrusive rocks; Their diversity, evolution and relation to volcanic arcs. In: Orogenic andesites and related rocks, R.S, Thorpe (Ed.), 437-61.

Brown, G.F, 1972. Tectonic map of the Arabian peninsula. DGMR, Map AP-2.

Brown, G.F., Hedge, C. & Marvin, R. 1978. Geochronological data for the Arabian Shield, Section 2. DGMR, Project Rep. SA(IR) 240, 9-20.

Brown, G.F, & Jackson, R.O, 1960. The Arabian Shield. 21st Int. Geol. Cong., Copenhagen, 69-77.

Brown, G.F. & Jackson, R.O, 1979. An overview of the geology of western Arabia, IAG Bull. 3, Vol. 1, 3-11.

Brown, G.F., Jackson, R.O., Bogue, R.G. & Maclean, W.H. 1962. Geology of the southern Hijaz quadrangle, Kingdom of Saudi Arabia. USGS Misc. Geol. Invest., Map I-210A.

Bruhn, R.L., Stern, C.R. & Dewitt, M.J. 1978. Field and geochemical data bearing on the development of a Mesozoic volcano-tectonic rift zone and back-arc basin in southernmost South America. Earth planet. Sci. Lett., 41, 32-46.

Bull, W.B. 1972. Recognition of alluvial fan deposits in the stratigraphic record, In: Recognition of sedimentary environments, E.D. Rigby & W.K. Hamblin (Eds.). Soc. Ec, Pal. Min., Spec. Publ. 16, 63-84.

Cann, J.R. 1970. Rb, Sr, Zr and Nb in some ocean floor basaltic rocks. Earth planet. Sci. Lett., 10, 7-11.

Carmichael, I.S.E., Turner, F.J. & Verhoogen, J. 1974. Igneous petrology. McGraw Hill, 739pp.

Cavanagh, B.J. 1979. Rb/Sr geochronology of some Pre-Nubian igneous complexes of Central and North East Sudan. Ph.D. thesis, Univ. of Leeds.

Chapelain, J.R.le. 1971. Geology and mineral exploration of the Al Qusayrah quadrangle, 25/41C. BRGM Rep., 71 JED 26.

Chappell, B.W. & White, A.J.R. 1974. Two contrasting granite types. Pacific Geology, 8, 173-74.

Chave, K.E. 1952. A solid solution between calcite and dolomite. J. Geol. Chicago, 60, 190-2.

Chayes, F. 1964. A petrographic distinction between Cenozoic volcanics in and around the open oceans. J. geophys. Res., 69(8), 1573-88.

Church, W.R. 1979. Granitic and metamorphic rocks of the Taif area, western Saudi Arabia: Discussion and reply-Discussion. Geol. Soc. Am. Bull.I, 90, 893-94.

Condie, K.C. & Swenson, D.H. 1973. Compositional variations in three Cascade stratovolcanoes: Jefferson, Rainier and Shasta. Bull. Volcanol., Ser. 2, 37, 205-30.

Cooper, J.A., Stacey, J.S., Stoeser, D.B. & Fleck, R.J. 1979. An evaluation of the zircon method for isotopic dating in the southern Arabian craton, Kingdom of Saudi Arabia. DGMR, Proj. Rep. SA(IR) 257.

Delfour, J. 1970. Sulphide mineralization at Nuqrah (25/41A) and Jabal Sayid (23/40A, B). BRGM Rep. 70 JED 22.

Delfour, J. 1975a. Volcanism and mineral deposits of the Arabian-Nubian Shield. BRGM Rep. 75 JED 24.

Delfour, J. 1975b. Geology and mineral exploration of the Nuqrah quadrangle, 25/41A. BRGM Rep. 75 JED 28.

Delfour, J. 1976. Geology of the Nuqrah quadrangle. BRGM Rep. 76 JED 3.

Delfour, J. 1977. Geology of the Nuqrah quadrangle, 25E, Kingdom of Saudi Arabia. DGMR, Geol. Map GM-28.

Delfour, J. 1979. Upper Proterozoic volcanic activity in the northern Arabian Shield, Kingdom of Saudi Arabia. IAG Bull. 3, Vol. 2, 59-77.

Delfour, J. 1981. Geologic, tectonic and metallogenetic evolution of the northern part of the Precambrian Arabian Shield (Kingdom of Saudi Arabia). Bull. du BRGM, II, 1-2, 1-19.

Delhemmes, R. 1976. Jabal al Bayda quadrangle, 24/39A. In: BRGM Ann. Rep. 76 JED 2.

Dickinson, W.R. 1968. Circum-Pacific andesite types. Journ. Geophys. Res., Vol. 73, 2261-69.

Dixon, T.H. 1979. The evolution of continental crust in the Late Precambrian Egyptian Desert. Ph.D. thesis, Univ. of California.

DGMR. 1979. Summary of geochronology of the Arabian Shield. Mapping Section, DGMR, OF-01-09.

Dodge, F.C.W., Bateman, P.C. & Wollenberg, H.A. 1970. Compositional variations within intrusive sequences of granitic rocks of the central Sierra Nevada (Abs.). Geol. Soc. Am. Abs., Vol. 2, 87.

Dodge, F.C.W., Fleck, R.J., Hadley, D.G. & Millard, H.T. 1979. Geochemistry and $^{87}Sr/^{86}Sr$ ratios of the Halaban rocks of the Central Arabian Shield. USGS, Proj. Rep. 253, 1-23.

Duyverman, H.J. & Harris, N.B.W. 1981 (in press). Late Precambrian evolution of Afro-Arabian crust from ocean to craton: Discussion. Geol. Soc. Am. Bull.

Duyverman, H.J., Harris, N.B.W, & Hawkesworth, C.J. In prep. Crustal accretion versus reworking: Nd and Sr isotope evidence from the Arabian Shield.

Duyverman, H.J. & Roobol, M.J. 1981. Gas pipes in Eocambrian volcanic breccias. Geol. Mag. 118, 265-70.

El-Shazly, E.M. & Engel, A.E.J. 1978. Proterozoic rifting and refractionation of northern Africa. Precambrian Res., 6, A20.

Engel, A.E.J., Dixon, T.H. & Stern, R.J. 1980. Late Precambrian evolution of Afro-Arabian crust from ocean to craton. Geol. Soc. Am. Bull., 91, 699-706.

Ewart, A. 1981. The mineralogy and petrology of Tertiary-Recent orogenic volcanic rocks with special reference to the andesite-basalt compositional range. In: Andesites, R.S. Thorpe (Ed.), J. Wiley & Sons, 25-95.

Ewart, A., Brian, W.B. & Gill, J. 1973. Mineralogy and geochemistry of the younger volcanic islands of Tonga, SW Pacific. J. Petrol., 14, 429-65.

Eyjkelboom, G. 1970. BRGM general mineral exploration and geologic mapping program. BRGM Rep. 70 JED 1.

Faure, G. & Powell, J.L. 1972. Strontium isotope geology. Springer Verlag, New York, 188pp.

Fisher, R.V. 1961. Proposed classification of volcaniclastic sediments and rocks. Bull. Geol. Soc. Am., 72, 1409-14.

Fisher, R.V. 1966. Rocks composed of volcanic fragments and their classification. Earth Sci. Rev. 1, 287-98.

Fitch, F.H. 1978a. Informal lithostratigraphic lexicon for the Arabian Shield. DGMR TR 1978 1, 163pp.

Fitch, F.H. 1978b. Informal lithostratigraphic lexicon for the Arabian Shield, First Supplement. DGMR TR 1978 12, 45pp.

Fitch, F.H. 1979. Informal lithostratigraphic lexicon for the Arabian Shield, Second Supplement. DGMR TR 1979 11, 22pp.

Fitches, W.R., Graham, R.H., Hussein, I.M., Ries, A.C. & Shackleton, R.M. In Press. The Late Precambrian ophiolite of Sol Hamed, NE Sudan. Journ. Geol. Soc.

Fitches, W.R., Graham, R.H., Ries, A.C. & Shackleton, R.M. 1981. The Sol Hamed ophiolite, NE Sudan, 11th Coll. of Afr. Geol. (Abs.), 5.

Fleck, R.J., Coleman, R.G., Cornwall, H.R., Greenwood, H.R., Hadley, D.G. Schmidt, D.L., Prinz, W.C. & Ratte, J.C. 1976. Geochronology of the Arabian Shield, Western Saudi Arabia: K/Ar results. Geol. Soc. Am. Bull., 87, 9-21.

Fleck, R.J., Greenwood, W.R., Hadley, D.G., Anderson, R.E. & Schmidt, D.L. 1980. Age and evolution of the southern part of the Arabian Shield. IAG Bull. 3, Vol. 3, 1-19.

Frey, F.A., Haskin, M.A., Peotz, J.A. & Haskin, L.A. 1968. Rare earth abundances in some basic rocks. J. Geophys. Res., 73, 6085-98.

Friedman, G.M. 1965. Terminology of crystallization textures and fabrics in sedimentary rocks. J. Sediment. Petrol., 36, 747-54.

Frisch, W. & Al-Shanti, A.M.S. 1977. Ophiolitic belts and the collision of island arcs in the Arabian Shield. Tectonophysics, 43, 293-306.

Fujimaki, H. & Kurasawa, H. 1980. Lateral variations of REE pattern of basaltic magma across the Japan arc. Jap. Assoc. Min. Pet. Econ. Geol., 75, 9, 313-22.

Garcia, M.O. 1978. Criteria for the identification of ancient volcanic arcs. Earth Sci. Rev., 14, 147-65.

Garrett, P. 1970. Phanerozoic stromatolites: Noncompetitive ecologic restriction by grazing and burrowing animals. Science, 169, 171-73.

Garson, M.S. & Shalaby, I.M. 1976. Precambrian-Lower Paleozoic plate tectonics and metallogenesis in the Red Sea region. Geol. Ass. Can. Spec. Paper 14, 573-96.

Gass, I.G. 1977. The evolution of the Pan African crystalline basement in NE Africa and Arabia. J. Geol. Soc. London, 134, 129-38.

Gass, I.G. 1979. Evolutionary model for the Pan-African crystalline basement. IAG Bull. 3, Vol. 1, 11-21.

Gass, I.G. 1980. Pan African (Upper Proterozoic) plate tectonics of the Arabian-Nubian Shield. In: Precambrian plate tectonics, A. Kröner (Ed.), Elsevier, Amsterdam, 387-405.

Gass, I.G. 1981. Upper Proterozoic (Pan-African) calc-alkaline magmatism in northeastern Africa and Arabia. In: Andesites and related rocks, R.S. Thorpe (Ed.), J. Wiley & Sons, London, 591-609.

Gebelein, C.D. 1972. Open marine subtidal and intertidal stromatolites (Florida, the Bahamas and Bermuda). In: Dev. in Sedimentology-Stromatolites, M.R. Walker (Ed.), Elsevier, Amsterdam, 381-88.

Gilluly, J. 1971. Plate tectonics and magmatic evolution. Geol. Soc. Am. Bull., 82, 2382-97.

Gilboy, C.F. & Skiba, W. 1978a. Geology of the As Salaym quadrangle, 22/39B. DGMR, Map GM-33.

Gilboy, C.F. & Skiba, W. 1978b. Geology of the Al Kahmil quadrangle, 22/39D. DGMR, Map GM-35.

Glennie, K.W 1977. Outline of the geology of Oman. Mem. Soc. Géol. France, 8, 25-31.

Glennie, K.W., Boeuf, M.G.A., Hughes Clarke, M.W., Moody-Stuart, M., Pilaar, W.F.H. & Reinhardt, B.M. 1974. The geology of the Oman Mountains. Verhand. Kon. Nederlandse Geol. Mijnb. Gen. 31, 423pp.

Goldsmith, R. & Kouther, J. 1965. Report on fieldwork in the Mahd al Dahab area, 23/40B, D.USGS Techn. Lett.6.

Goldsmith, R. & Kouther, J. 1966. Geology of the Mahd al Dahab-Umm ad Damar area, 23/40-41. USGS Techn. Lett. 56.

Green, T.H. & Ringwood, A.E. 1968. Genesis of the calc-alkaline igneous rock suite. Contrib. Mineral. Petrol., 18, 105-62.

Greenwood, W.R., Anderson, R.E., Fleck, E.J. & Roberts, R.J. 1977. Precambrian geologic history and plate tectonic evolution of the Arabian Shield. USGS Proj. Rep. 222.

Greenwood, W.R. & Brown, G.F. 1973. Petrology and chemical analysis of selected plutonic rocks from the Arabian Shield, Kingdom of Saudi Arabia. DGMR, Bull. 9, 1-9.

Greenwood, W.R., Hadley, D.G., Anderson, R.E., Fleck, R.J. & Schmidt, D.L. 1976. Late Proterozoic cratonization in southwestern Saudi Arabia. Philos. Trans. R. Soc. Lond. A, 280, 517-27.

Greenwood, W.R., Roberts, R.J. & Baghdady, A. 1974. Mineral belts in western Saudi Arabia. USGS Proj. Rep. 177.

Hadley, D.G. 1973. Geology of the Sahl al Matran quadrangle, 26/38C. USGS, Map GM-6.

Hadley, D.G. & Schmidt, D.L. 1980. Sedimentary rocks and basins of the Arabian Shield and their evolution. IAG Bull. 3, Vol. 4, 26-50.

Hanson, G.N. 1978. The application of trace elements to the petrogenesis of igneous rocks of granitic composition. Earth planet. Sci. Lett., 38, 26-43.

Hanson, G.N. 1980. Rare earth elements in petrogenetic studies of igneous systems. Ann. Rev. Earth planet Sci. Lett., 371-406.

Harris, N.B.W. & Gass, I.G. 1981. Significance of contrasting magmatism in North East Africa and Saudi Arabia. Nature, 289, 395-96.

Hashad, A.H. 1980. Present status of geochronological data on the Egyptian basement complex. IAG Bull. 3, Vol. 3, 31-46.

Hawkesworth, C.J., Gledhill, A.R., Roddick, J.C., Miller, R.McG. & Kröner, A. 1981 (in press). Rb/Sr and $^{40}Ar/^{39}Ar$ studies bearing on models for the thermal evolution of the Damara belt, Namibia.

Hawkins, T.R.W., Hindle, D. & Strugnell, R. 1981. Outline of the stratigraphy and structural framework of Southern Dhofar (Sultanate of Oman). Geologie en Mijnbouw, 60, 247-56.

Hellman, P.L. & Green, T.H. 1979. The role of sphene as an accessory phase in the high-pressure partial melting of hydrous mafic compositions. Earth planet. Sci. Lett., 42, 191-201.

Hermann, A.G, Potts, M.J. & Knake, D. 1974. Geochemistry of the rare earth elements in spilites from the oceanic and continental crust. Contrib. Mineral. Petrol., 44, 1-16.

Hirayama, J. 1977. Stratigraphy of the Fatima Formation. DGMR Techn. Rec. TR 1977 8, 8pp.

Hofmann, H.J. 1973. Stromatolites: Characteristics and utility. Earth Sci. Rev., 9, 339-73.

Holloway, J.R. & Burnham, C.W. 1972. Melting relations of basalt with equilibrium water pressure less than total pressure. J. Petrol., 13, 1-29.

Hutchinson, C.S. 1975. Correlation of Indonesian active volcanic geochemistry with Benioff zone depth. Geol. Mijnbouw, 54, 157-68.

Irvine, T.N. & Baragar, W.R.A. 1971. A guide to the chemical classification of the common volcanic rocks. Can. J. Earth Sci., 8, 523-48.

Jackaman, B. 1972. Genetic and environmental factors controlling the formation of massive sulphide deposits of Wadi Bidah and Wadi Wassat, Saudi Arabia. DGMR Techn. Rec. TR 1972 1.

Jackson, N.J. 1980. Correlation of Late Proterozoic stratigraphies, NE Africa and Arabia: Summary of an IGCP Project 164 Report. J. geol. Soc. London, 137, 629-34.

Jackson, N.J. & Ramsay, C.R. 1980. Time-space relationships of Upper Precambrian volcanic and sedimentary units in the Central Arabian Shield. J. geol. Soc. London, 137, 617-28.

Jakeš, P. & Gill, J. 1970. Rare earth elements and the island arc tholeiitic series. Earth planet. Sci. Lett., 9, 17-28.

Johnson, R.F. & Trent, V.A. 1966. Mineral reconnaisance of the Wadi Al Ays quadrangle, 25/38C. USGS Techn. Lett., 45.

Johnson, R.F. & Trent, V.A. 1967. Mineral reconnaisance of the Al Jizl quadrangle, 26/37A. USGS Map MI-10.

Kabesh, M.L. 1961. The geology and economic minerals and rocks of the Ingessana Hills. Min. of Min. Res., Geol. Surv. Dep., Khartoum, Bull. 11, 61pp.

Kahr, V.P. & Agocs, W.B. 1962. Geologic and magnetic reconnaisance survey of an iron bearing area of Wadi Sawawin, 27-28/35. DGMR Rep. 161.

Karpoff, R. 1955. Observations préliminaires sur le socle ancien de l'Arabie. C.R. Somm. Soc. géol. Fr., 105-106.

Karpoff, R. 1957. Esquisse géologique de l'Arabie Séoudite. Bull. Soc. géol. Fr., 6, Sér. 7, 653-97.

Karpoff, R. 1960. L'antecambrian de la peninsula Arabique. 21st Int. geol. Cong. Copenhagen, 78-94.

Kay, R.W. 1977. Geochemical constraints on the origin of Aleutian magmas. In: Island arcs, deep sea trenches and back arc basins, M. Talwani & W.C. Ritman (Eds.). Am. Geophys. Union, 229-42.

Kay, R.W., Hubbard, N. & Gast, P. 1970. Chemical characteristics and origin of oceanic ridge volcanic rocks. J. Geophys. Res., 75, 1585-1613.

Kay, R.W. & Senechal, R.G. 1976. The rare earth geochemistry of the Troodos ophiolite complex. J. Geophys. Res., 81, 964-70.

Kemp, J. 1976. The Al Ays quadrangle, 25C and the Mahd al Dahab quadrangle, 23E. BRGM Ann. Rep. 76 JED 2.

Kemp, J., Pellaton, C. & Galvez, J.Y. 1980. Geochronological investigations and geological history in the Precambrian of north-western Saudi Arabia. BRGM, OF-01-1.

Klitzsch, E. 1970. Die Strukturgeschichte der Zentralsahara. Geol. Rndsch. 59, 2.

Korolyuk, I.K. 1960. Subdivision of the Cambrian and Precambrian of eastern Siberia according to stromatolites. 21st Int. Geol. Cong. Copenhagen, 8, 113-118.

Kröner, A. 1979. Pan African plate tectonics and its repercussions on the crust of northeast Africa. Geol. Rndsch. 68, 565-83.

Kröner, A., Roobol, M.J., Ransay, C.R. & Jackson, N.J. 1979. Pan African ages of some gneissic rocks in the Saudi Arabian Shield. J. Geol. Soc. London, 136, 455-61.

Kuno, H. 1959. Origin of Cenozoic petrographic provinces of Japan and surrounding areas. Bull. Volcanol., 2, 20, 37-76.

Kuno, H. 1966. Lateral variations of basalt magma type across continental margins and island arcs. Bull. Volcanol., 29, 195-222.

Kuno, H. 1968. Differentiation of basalt magmas. In: Basalts, Vol. 2, H.H. Hess & A. Poldervaart (Eds.). Interscience, J. Wiley & Sons, 623-88.

Lambert, I.B. & Heier, K.S. 1967. The vertical distribution of uranium, potassium and thorium in the continental crust. Geochim. Cosmochim. Acta, 31, 377-90.

Leca, X. 1970. Mineral resources and geology of the Jabal Sahah quadrangle 22/44D. BRGM Rep. 70 JED 7.

Leggo, P. 1968. Some recent isotopic investigations. 12th Ann. Rep. Inst. African Geol. Leeds, 45-46.

Leyreloupe, A., Dupuy, C. & Andriambolona, R. 1977. Catazonal xenoliths in French Neogene volcanic rocks: Constitution of the lower crust. Contrib. Mineral. Petrol., 63, 283-300.

Lopez-Escobar, L., Frey, F.A. & Vergara, M. 1977. Andesites and high-alumina basalts from the Central-South Chile High Andes: Geochemical evidence bearing on their petrogenesis. Contrib. Mineral. Petrol., 63, 199-228.

Macdonald, G.A. & Katsura, T. 1964. Chemical composition of Hawaiian lavas. J. Petrol., 5, 82-133.

Manghani, M.J. & Coleman, R.G. 1981. Gravity profiles across the Semail ophiolite, Oman. J. Geophys. Res., 86, 84, 2509-25.

Mason, R. 1978. Petrology of the metamorphic rocks. Allen & Unwin, London, 254pp.

McWilliams, M.O. & Kröner, A. 1981 (in press). Paleomagnetism and tectonic evolution of the Pan African Damara belt, southern Africa. J. Geophys. Res.

Mitchell, A.H. & Reading, H.G. 1971. Evolution of island arcs. J. Geol. Chicago, 79, 253-84.

Miyashiro, A. 1974. Volcanic rock series in island arcs and active continental margins. Am. J. Sci., 274, 321-55.

Miyashiro, A. & Shido, F. 1975. Tholeiitic and calc-alkalic series in relation to the behaviour of titanium, vanadium, cromium and nickel. Am. J. Sci., 275, 265-77.

Moore, J.G. & Peck, D.L. 1962. Accretionary lapilli in volcanic rocks of the western continental United States. U.S. J. Geol., 70, 182-93.

Nakamura, N. 1974. Determination of REE, Ba, Fe, Mg, Na and K in carbonaceous and ordinary meteorites. Geochim. Cosmochim. Acta, 38, 757-75.

Nasseef, A.O., Bakor, A.R. & Hashad, A.H. 1980. Petrography of possible ophiolitic rocks along the Qift-Quseir road, Eastern Desert, Egypt. IAG Bull. 3, Vol. 4, 144-57.

Nasseef, A.O. & Gass, I.G. 1977. Granitic and metamorphic rocks of the Taif area, western Saudi Arabia. Bull. geol. Soc. Am., 88, 1721-30.

Nasseef, A.O. & Gass, I.G. 1980. Arabian Shield granite traverse. IAG Bull. 3, Vol. 4, 77-82.

Neary, C.R., Gass, I.G. & Cavanagh, B.J. 1976. Granitic association of northeastern Sudan. Bull. geol. Soc. Am., 87, 1501-12.

Nebert, K., Alshaibi, A.A., Awlia, M., Bounny, I., Nawab, Z.A., Sharief, O.H., Sherbini, O.A. & Yeslam, A.H. 1974. Geology of the area north of Wadi Fatima, Kingdom of Saudi Arabia. IAG Bull. 1, 31pp.

Papanastassiou, D.A. & Wasserburg, G.J. 1969. Initial strontium isotopic abundances and the resolution of small time differences in the formation of planetary objects. Earth planet. Sci. Lett., 5, 361-76.

Paul, D.K., Potts, P.J., Gibson, I.L. & Harris, P.G. 1975. Rare earth abundances in Indian kimberlite. Earth planet. Sci. Lett., 25, 151-58.

Peacock, M.A. 1931. Classification of igneous rock series. J. Geol. Chicago, 39, 54-67.

Pearce, J.A. 1980. Geochemical evidence for the genesis and eruptive setting of lavas from Tethyan ophiolites. Proc. Int. Ophiolite Symp., Cyprus, 261-72.

Pearce, J.A. 1981. Trace element characteristics of lavas from destructive plate boundaries. In: Andesites and related rocks, R.S. Thorpe (Ed.), J. Wiley & Sons, 525-48.

Pearce, J.A. & Cann, J.R. 1973. Tectonic setting of basic volcanic rocks using trace element analyses. Earth planet. Sci. Lett., 19, 290-300.

Pearce, J.A. & Gale, G.H. 1977. Identification of ore-deposition environment from trace-element geochemistry of associated igneous host rocks. In: Volcanic processes in ore genesis. Geol. Soc. London Publ. 7, 14-24.

Pearce, J.A. & Norry, M.J. 1979. Petrogenetic implications of Ti, Zr, Y and Nb variations in volcanic rocks. Contrib. Mineral. Petrol., 67, 33-47.

Pearce, T.H., Gorman, B.E. & Birkett, T.C. 1977. The relationship between major element chemistry and tectonic environment of basic and intermediate volcanic rocks. Earth planet. Sci. Lett., 36, 121-32.

Peccerillo, A. & Taylor, S.R. 1976. Geochemistry of Eocene calc-alkaline volcanic rocks from the Katasmonu area, northern Turkey. Contrib. Mineral. Petrol., 58, 63-81.

Pellaton, C. 1979. Geological map of the Yanbu al Bahr quadrangle, 24C, Kingdom of Saudi Arabia. DGMR, Map GM-48C.

Perret, F.A. 1937. The eruption of Mt. Pelée 1929-1932. Carnegie Inst. Washington.

Pettijohn, E.J. 1975. Sedimentary rocks. Harper, New York, 628pp.

Philpotts, J.A., Martin, W. & Schnetzler, C.C. 1971. Geochemical aspects of some Japanese lavas. Earth planet. Sci. Lett., 12, 89-96.

Philpotts, J.A., Schnetzler, C.C. & Hart, S.R. 1969. Submarine basalts: Some K, Rb, Sr, Ba, rare earths, H_2O and CO_2 data bearing on the alteration and modification by plagioclase and possible source materials. Earth planet. Sci. Lett., 7, 293-99.

Potts, P.J., Thorpe, O.W. & Watson, J.S. 1982 (in press). Determination of the rare-earth element abundances in 29 international rock standards by instrumental neutron activation analysis: a critical appraisal of calibration errors. Chem. Geol.

Potts, P.J., Webb, P.W. & Watson, J.S. 1982 (in prep.). Energy dispersive XRF analysis of silicate rocks of major and trace elements. Chem. Geol.

Preiss, W.V. 1972. Intercontinental correlation. In: Stromatolites, M.R. Walker (Ed.), Elsevier, Amsterdam, 359-69.

Reineck, H.E. & Singh, I.B. 1973. Depositional sedimentary environments. Springer Verlag, Berlin, 439pp.

Ringwood, A.E. 1974. The petrological evolution of island arc systems. J. geol. Soc. London, 130, 183-204.

Ringwood, A.E. 1977. Petrogenesis in island arc systems. In: Island arcs, deep sea trenches and back-arc basins, M. Talwani & W.C. Pitman (Eds.). Am. Geophys. Union, 311-24.

Riofinex, 1977. A preliminary review of mineral opportunities in Saudi Arabia. Riofinex Rep. RF 1977 1.

Rocci, G. 1965. Essai d'interprétation de mesure géochronologiques: La structure de l'ouest africain. Sci. Terre Fr., 10, 3-4, 461-79.

Rogers, J.J.W., Ghuma, M.A., Nagg, R.M., Greenberg, J.K. & Fallager, P.D. 1978. Plutonism in Pan-African belts and the geologic evolution of northeastern Africa. Earth planet. Sci. Lett., 39, 109-17.

Roobol, M.J. & Smith, A.L. 1976. Mt. Pelée, Martinique: A pattern of alternating eruptive styles. Geology, 4, 521-24.

Routti, J.T. 1969. Sampo, a Fortran IV program for computer analysis of famma spectra from GE(LI) detectors, and other spectra with peaks. Am. Gov. Rep., VCRL-19452, 31pp.

Ruxton, B.P. 1956. Major rock groups of the northern Red Sea Hills, Sudan. Geol. Mag., 93, 314-30.

Saunders, A.D., Tarney, J., Stern, C.R. & Dalziel, I.W.D. 1979. Geochemistry of Mesozoic marginal basin floor igneous rocks from Southern Chile. Geol. Soc. Am. Bull., 90, 237-58.

Schilling, J.G. 1971. Sea-floor evolution - rare earth evidence. Phil. Trans.R. Soc. Lond., A, 268, 663-706.

Schmid, R. 1981. Descriptive nomenclature and classification of pyroclastic rocks and fragments: Recommendations of the IUGS Subcommission on the systematics of igneous rocks. Geology, 9, 41-43.

Schmidt, D.L., Hadley, D.L., Greenwood, W.R., Gonzalez, L., Coleman, R.G. & Brown, G.F. 1973. Stratigraphy and tectonism of the southern part of the Precambrian Shield of Saudi Arabia. DGMR Bull. 8.

Schmidt, D.L., Hadley, D.G. & Stoesser, D.B. 1979. Late Proterozoic crustal history of the Arabian Shield, Southern Najd province, Kingdom of Saudi Arabia. IAG Bull. 3, Vol. 2, 41-58.

Schopf, J.W., Dehler, D.Z., Horodyski, R.J. & Kuenvolden, K.A. 1971. Biogenecity and significance of the oldest known stromatolites. Jour. Paleontol., 45, 477-85.

Schürmann, H.M. 1974. The Precambrian of North Africa. Brill, Leiden, 351pp.

Shackleton, R.M. 1979. Precambrian tectonics of North-East Africa. IAG Bull. 3, Vol. 2, 1-6.

Shackleton, R.M., Ries, A.C., Graham, R.H. & Fitches, W.R. 1980. Late Precambrian ophiolitic mélange in the eastern desert of Egypt. Nature, 285, 472-74.

Shanti, M. & Roobol, M.J. 1979. A Late Proterozoic ophiolite complex at Jabal Ess in northern Saudi Arabia. Nature, 279, 488-91.

Sigurdsson, H., Tomblin, J.F., Brown, G.M., Holland, J.G. & Arculus, P.J. 1973. Strongly undersaturated magmas in the Lesser Antilles island arc. Earth planet. Sci. Lett., 18, 285-95.

Skiba, W.J. 1980. The form and evolution of Late Precambrian plutonic masses in the Jiddah-Rabiq-Wadi Al Quaha area, Saudi Arabia. IAG Bull. 3, Vol. 3, 105-21.

Sparks, R.S.J. 1977. Stratigraphy and geology of the ignimbrites of Vulsini volcano, Central Italy. Geol. Rndsch., 64, 497-523.

Sparks, R.S.J., Self, S. & Walker, G.P.L. 1973. Products of ignimbrite eruptions. Geology, 1, 115-18.

Sparks, R.S.J. & Walker, G.P.L. 1973. The ground surge deposit: a third type of pyroclastic rock. Nature, 241, 62-64.

Sparks, R.S.J. & Wright, J.V. 1979. Welded air-fall tuffs. Geol. Soc. Am. Spec. Paper 180, 155-66.

Stacey, J.S., Doe, B.R., Roberts, R.R., Delevaux, M.H & Gramlich, J.W. 1980. A lead isotope study of mineralization in the Saudi Arabian Shield. Contrib. Mineral. Petrol.,74, 175-88.

Stanton, R.L. & Bell, J.D. 1969. Volcanic and associated rocks of the New Georgia groups, British Solomon Islands Protectorate. Overseas Geol. Mineral Resources, 10, 113-45.

Steiger, R.J. & Jäger, E. 1977. Subcommission on geochronology: Convention on the use of decay constants in geo- and cosmochronology. Earth planet. Sci. Lett., 36, 359-62.

Stern, R.J. 1979. Late Precambrian ensimatic volcanism in the Central Eastern Desert of Egypt. Ph. D. thesis, Univ. of California.

Streckeisen, A. 1976. To each plutonic rock its proper name. Earth Sci. Rev. 12, 1-33.

Streckeisen, A. 1979. Classification and nomenclature of volcanic rocks, lamprophyres, carbonatites and melilitic rocks: Recommendations and suggestions of the IUGS Subcommission on the systematics of igneous rocks. Geology, 7, 331-5.

Sun, S.S. & Hanson, G.N. 1976. Rare earth element evidence for differentiation of Mc Murdo volcanics, Ross Island, Antarctica. Contrib. Mineral. Petrol., 54, 139-55.

Tanaka, T. 1975. Geological significance of rare earth elements in Japanese geosynclinal basalts. Contrib. Mineral. Petrol., 52, 233-46.

Tapponnier, P. & Molnar, P. 1976. Slip-line field theory and large-scale continental tectonics. Nature, 264, 319-24.

Taylor, S.R. 1977. Island arc models and the composition of the continental crust. In: Island arcs, deep sea trenches and back-arc basins, M. Talwani & W.C. Pitman (Eds.). Am Geophys. Union, 325-36.

Thorpe, R.S. & Francis, P.W. 1979. Variations in Andean andesite compositions and their petrogenetic significance. Tectonophysics, 57, 53-70.

USGS, Aramco.1963. Geological map of the Arabian Peninsula. USGS Misc. Invest. Map I-270A.

Vail, J.R. 1976. Outline of the geochronology and tectonic units of the basement complex of northeast Africa. Proc. R. Soc. Lond., A, 250, 127-41.

Vail, J.R. 1979. Outline of the geology and mineralization of the Nubian Shield east of the Nile valley, Sudan. IAG Bull. 3, Vol. 1, 97-106.

Wager, L.R. & Deer, W.A. 1939. The petrology of the Skaergaard intrusion, Kangerdlugsskag, East Greenland. Meddl.om Gronland, 105, 4, 1-352.

Walker, G.P.L. 1972. Crystal concentrations in ignimbrites. Contrib. Mineral. Petrol., 36, 135-46.

Warden, A.J. 1970. Evolution of Aoba caldera, New Hebrides. Bull. Volcanol., 34, 107-40.

Weaver, S.D., Saunders, A.D., Pankhurst, R.J. & Tarney, J. 1979. A geochemical study of magmatism associated with the initial stages of back-arc spreading. Contrib. Mineral. Petrol., 68, 151-69.

Weaver, B.L. & Tarney, J. 1980. Continental crust composition and nature of the lower crust: Constraints from mantle Nd-Sr isotope correlation. Nature, 286, 342-46.

Williamson, J.H. 1968. Least squares fitting of a straight line. Can. J. Phys., 46, 1845-47.

Winkler, H.G.F. 1974. Petrogenesis of metamorphic rocks. Springer Verlag, New York, 320 pp.

Wood, D.A. 1979. Dynamic partial melting: Its application to the petrogenesis of basalts erupted in Iceland, the Faroe Islands, the Isle of Skye (Scotland) and the Troodos Massif (Cyprus). Geochim. Cosmochim. Acta, 43, 1031-46.

York, D. 1967. The best isochron. Earth planet. Sci. Lett., 2, 479-82.

York, D. 1969. Least squares fitting of a straight line with correlated errors. Earth planet. Sci. Lett., 5, 320-24.

Appendix A1 - Sample preparation

In each of the three areas (Wadi Fatima, Badr and Nuqrah) representative rock samples were selected. The slight amount of weathering and excellent outcrops of the, mainly volcanic, successions enabled sampling of fresh material. Normally samples of at least one kilogram were taken, but rock samples for isotopic dating were at least five kilograms. Samples for dating were collected in suites, each representing a single rock type. These rock types of a suite should be of variable chemical composition to give a good spread in Rb/Sr ratio. Also, it was of great importance to ascertain that the samples belonged to one geological body, representing a single "event". This was done by carefully studying the local geology and by limiting the sample area to a few hundreds of metres in surface area.

All samples were washed and dried, weathered patches were removed. About half was retained for thin sectioning and further reference. The rest was crushed in stages using rock splitters, jaw crushers and finally a Tema tungsten-carbide disc mill to produce about 200 grams of fine powder. A part of this powder was retained for future reference and the remainder used for analysis by INAA, EDXRF and mass spectrometer.

Appendix A2 - The EDXRF System

The Link System Meca 10-44 energy dispersive XRF spectrometer on which whole rock geochemical data were obtained is a departure from the conventional use of wavelength dispersive XRF systems for rock analysis. In this method, samples are excited using a low power (50 watt) X-ray tube and their fluorescent X-rays detected by a Si(Li) detector. The resulting electronic pulses are processed with a Harwell Processor/ Multi-Channel Analyser System which outputs their energy spectra. Sophisticated peak-stripping of these spectra gives elemental X-ray intensities which are transformed by mass absorption correction programs to oxide concentrations. An extensive review of the EDXRF system is given by Potts et al. (in prep.).

Thirteen major elements can be determined simultaneously as oxides (Na, K, Mg, Al, Si, P, S*, Ca, Ti, V*, Mn, Fe, Ba*; the data for S, V and Ba are semi-quantitative) and the loss on ignition was determined separately prior to fusion. Detection levels range from 0.40% (Na_2O) and 0.12% (MgO) down to 0.005% (MnO) at the 50% relative error level. Accuracy is normally better than 2% relative; the precision limits are as follows: standard deviation for oxides is better than 1% relative or 0.1% absolute whichever is greater (for Na_2O respectively 2% or 0.2%).

Trace elements may be analysed for twelve elements simultaneously (Pb, Th, Rb, Sr, Y, Zr, Nb, Ga*, Cu*, Zn*, Cr*, Ni*; the data for the latter five elements are semi-quantitative) and detection limits vary between 2 and 5 ppm at the 50% relative error level. Accuracy is normally better than 2% relative; the precision limits for traces are: standard deviation is better than 1% relative or 1 ppm absolute whichever is greater.

In addition to the normal analysis, the following tests were performed for dating purposes. Duplicate analyses were done, using the two sides of the pellet and the counting time for analysing the energy spectrum was enlarged three times, i.e. 3 x 800 sec. instead of 800 sec. to produce better counting statistics. In this way, reproducibility was generally better than 1.5% (2 sigma error) and this value was used in isochron calculations.

Standards used in the EDXRF systems are AGV-1, BCR-1, G-2 and GSP-1 (see Appendix C3 for geochemical data of these standards).

Abbreviations for rock types, as used in the next Chapters, are: bas - basalt, dol - dolomite, ign - ignimbrite, f.tuff - fine tuff, volc.br. - volcanic breccia, cgl - conglomerate, gr - granite, ss - sandstone, si.st. - siltstone, mud - mudstone, dol.ss - dolomitic sandstone, rhy - rhyolite, and - andesite, amph - amphibolite, qu-dior. - quartzdiorite, gb - gabbro, ton - tonalite.

Appendix A3 - Instrumental neutron activation analysis

This technique is used routinely at the Open University for 17 elements including ten REE (La, Ce, Nd, Sm, Eu, Gd, Tb, Tm, Yb, Lu, Th, Ta, Hf, Sc, Co, Fe_2O_3, Ba). INAA provides extremely sensitive and accurate determinations at concentrations down to 0.01 ppm. Powdered rock samples (300 mg) are irradiated at the Ascot Reactor Centre for one week, each batch of samples including a multi-element standard (normally this standard was one of the international standards GSP-1 or RGM-1) and the Open University standard AC(OURS), a micro granitic rock from Ailsa Craig, NW Scotland. Counting of gamma spectra is undertaken at the OU using two germanium detectors, one LEPS for the low energy spectrum 60-200 KeV and a coaxial detector for higher energy gamma radiation 500-2,000 KeV. Spectra are analysed using the peak fitting programme SAMPO (after Routti, 1969) and data corrected using an exponential correction programme developed in this department. The technique is particularly valuable for REE determinations and is therefore a powerful tool for petrogenetic processes. The INAA method is described extensively by Paul et al. (1975) and, more recently, by Potts et al. (1982, in press). Potts et al. (op. cit.) mention an accuracy of < 5% and a precision of < 4% for routine INAA work (1 sigma error on the mean).

In using INAA data for REE, the element abundances were normalised to mantle values for easier comparison of REE for different rocks. The occurrence of higher concentrations for the elements with even atomic numbers as compared to the concentrations for the elements with odd atomic numbers (the Oddo-Harkins effect) can be eliminated in this way and the concentration variations from element to element smoothed out (Hanson, 1980). The normalizing values are (after Nakamura, 1974): La - 0.329, Ce - 0.865, Nd - 0.63, Sm - 0.203, Eu - 0.077, Gd - 0.276, Tb - 0.052, Tm - 0.034, Yb - 0.22, Lu - 0.0339.

Appendix A4 - Mass-spectrometer and isochron fitting

The Mass-spectrometer, used at the Open University is a VG-Isomass 54E thermal ionization mass-spectrometer, controlled by a Hewlett Packard minicomputer 9845A. Strontium was extracted using standard ion exchange techniques. All $^{87}Sr/^{86}Sr$ ratios are measured to 0.01% or better (2 sigma errors). NBS-987 ($SrCO_3$) was used as standard and ran regularly with the samples. The results were normalized to the current value of the standard NBS-987, using a best value of 0.71014 ± 4. Precision of the isotope data was normally better than 0.01% and this value was used in isochron computations. In some cases, however, slightly larger errors in the $^{87}Sr/^{86}Sr$ ratios imposed an error of 0.02%.

Isochron fitting from the Rb/Sr ratios and the $^{87}Sr/^{86}Sr$ ratios of a suite of samples was done by the least squares regression method, minimizing the deviation of data points from the best fit line; the preferred method takes into account the analytical errors in both co-ordinates (York, 1967, 1969; Williamson, 1968). For the isochron computing and graphic display use was made of the IGS Isotope Geology facilities (Desk Top Hewlett-Packard 9845B). This computer indicated the age, initial ratio (intercept) and MSWD (mean square weighted deviates). Results with MSWD $\geq$ 2.5 were considered to be errorchrons (Brooks et al., 1972) and the resulting errors in age and initial ratios were multiplied by the square root of the MSWD. Errors quoted in age and initial ratio are 2 sigma errors. A Rb decay constant $\lambda^{87}Rb = 1.42 \times 10^{-11} a^{-1}$ was used following Steiger & Jäger (1977).

Appendix B - Classification

Plutonic rocks are classified on their mineral content, following the recommendations of Streckeisen (1976) the following mineral are considered: Q - quartz, A - alkalifeldspar, P - plagioclase, F - feldspathoids, M - mafic and related minerals. Rocks with M less than 90% are named according to their position in the QAPF diagram.

Volcanic flow rocks are classified according to Streckeisen (1979). The often fine-grained nature of the volcanics and their oxidation often prohibit modal analyses. As a basis of volcanic classification the SiO_2-content was used (SiO_2 less than 52% basalt; from 52% to 66% andesite; SiO_2 more than 66% rhyolite), also taking into account the colour index. This classification, whereby dacites were not separately distinguished, is common usage in Saudi Arabia. Geochemical data (see for example Figure 6.8) indicate that dacites are relatively rare, compared to andesites and rhyolites.

Volcaniclastic rocks are subdivided according to Fisher (1961, 1966), see Figure A.1. (His definition of volcaniclastics is: "... the entire field of clastic products composed in part of, or entirely of volcanic fragments."). Lapilli tuffs were included in the tuff field and the boundary between tuffs and volcanic breccia/agglomerate chosen at 10 mm, being a useful subdivision for the encountered volcaniclastics. Volcanic breccia can be separated from agglomerates because they contain coherent fragments of pre-existing rocks, while agglomerates are solidified in flight (Schmid, 1980; Fisher, 1966). A special type of volcanic rock, the ignimbrites (products of nuées ardentes) can be included in both flow rocks and volcaniclastics; they will be discussed separately.

Sedimentary rocks clearly show characteristics of transport and re-deposition, or of chemical deposition. They are subdivided according to the grainsize scale of Pettijohn (1975), see Figure A1. Gravel-sized sediments are included in the sandstones.

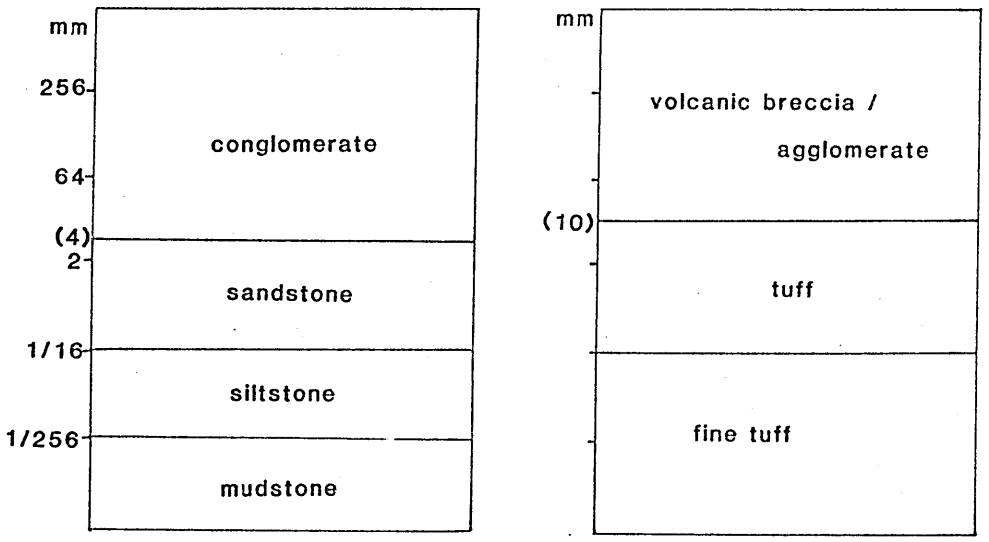

Figure A.1 Terminology and grainsize of sedimentary rocks and of volcaniclastics (after Pettijohn, 1975; Fisher, 1961, 1966); tuffs were subdivided into pumice, crystal, lithic or mixed tuffs.

Appendix C1 Whole rock compositions (Fatima area)

Rock type	bas	dol	bas	ign	ign	tuff	bas	volc.br.	f.tuff	bas	cgl	bas	gr
Sample	FA010	FA011	FA012	FA030	FA031	FA032	FA033	FA040	FA041	FA050	FA051	FA052	FA053
Si(% oxide)	50.10	15.21	***	69.63			49.19			46.22	57.42	41.76	76.64
Ti	1.45	0.03		0.49			1.02			1.92	0.88	2.21	0.14
Al	16.69	0.44		14.82			16.78			15.99	15.19	14.93	12.96
Fe	12.51	0.00		5.71			10.48			12.63	9.33	12.89	1.02
Mn	0.14	0.08		0.14			0.19			0.03	0.13	0.17	0.01
Mg	5.11	7.58		1.39			4.70			13.48	2.05	7.21	0.23
Ca	8.37	34.27		0.52			8.44			1.30	4.70	7.50	0.32
Na	3.22	0.34		7.78			3.93			2.09	5.96	2.29	3.50
K	0.96	0.00		0.06			1.52			0.00	0.10	2.50	4.73
P	0.25	0.08		0.11			0.21			0.00	0.16	0.33	0.04
Ba	0.02	0.00		0.00			0.06			0.00	0.01	0.02	0.05
V	0.06	0.00		0.00			0.04			0.07	0.03	0.10	0.00
S	0.00	0.00		0.01			0.00			0.00	0.05	0.00	0.00
LOI	2.61	42.20		0.84			4.57			7.36	2.49	8.18	0.66
Total	101.49	100.23		101.50			101.13			101.40	98.50	100.09	100.30
Pb(ppm)	11.0	9.0	6.1	7.5	9.3	11.0	5.5	5.9	9.5	3.3	6.8	6.4	9.9
Th	4.9	<2 *	<2	4.4	2.7	3.1	<2	<2	2.1	<2	<2	<2	7.8
Rb	64.2	3.7	5.1	4.7	22.7	24.6	26.7	24.4	31.0	<3	6.2	51.9	94.5
Sr	211	130	469	53.7	119.2	75.8	270	120	152	44.7	302	62.5	67.2
Y	44.2	<2	30.4	60.0	49.7	51.8	24.5	40.6	48.2	27.9	22.8	38.7	27.1
Zr	358	15.4	131	336	308	308	89.3	181	277	124	99.0	168	114
Nb	9.3	<2	4.5	13.7	13.7	8.6	3.4	5.8	8.5	5.1	3.8	4.6	4.6
Ga	26.1	<5	21.3	14.9	18.3	17.7	19.7	14.4	21.1	22.9	20.3	21.5	11.3
Cu	5.0	14.5	62.0	52.6	5.4	5.2	39.8	<5	25.8	151	5.0	717	16.6
Zn	108.4	7.3	105.5	148	90.1	94.8	100.6	145	74.4	97.3	68.0	129	20.0
Cr	64.0	n.d **	n.d	n.d	n.d	n.d	n.d	n.d	n.d	61.2	n.d	68.6	n.d
Ni	28.4	n.d	n.d	n.d	n.d	n.d	n.d	n.d	n.d	38.9	n.d	110	n.d

*- <2 means below detection limit
**- n.d means not determined
***- totals less than 98.50 or more than 101.50 were deleted

Whole rock compositions (Fatima area, continued)

Rock type	ss	ign	tuff	tuff	gr	dike	si.st	ss	volc.br	ign	ign	bas
Sample	FA060	FA061	FA070	FA071	FA073	FA080	FA090	FA091	FA093	FA094	FA095	FA096
Si(% oxide)	59.84		70.34	66.23	73.67	54.49	69.00	72.49	56.61		76.24	48.90
Ti	1.00		0.48	0.55	0.19	1.41	0.92	0.14	1.46		0.17	2.38
Al	14.14		13.50	15.33	12.78	16.18	12.68	13.15	16.25		12.30	14.78
Fe	7.04		5.41	5.98	1.74	9.62	7.57	2.29	9.97		2.42	15.80
Mn	0.07		0.14	0.12	0.05	0.16	0.16	0.06	0.16		0.09	0.25
Mg	2.17		0.38	1.19	0.38	4.16	2.98	0.00	2.48		0.23	4.07
Ca	5.19		0.98	2.55	0.78	3.42	2.12	0.85	3.36		0.47	6.60
Na	1.10		5.97	5.27	3.64	5.45	0.17	5.97	8.35		5.05	4.22
K	2.84		1.77	2.01	4.19	2.44	2.93	3.53	0.00		2.41	0.89
P	0.22		0.12	0.13	0.02	0.59	0.18	0.05	0.44		0.03	0.49
Ba	0.07		0.08	0.07	0.08	0.05	0.08	0.07	0.00		0.07	0.05
V	0.03		0.01	0.01	0.01	0.04	0.01	0.00	0.16		0.01	0.06
S	0.00		0.00	0.00	0.00	0.00	0.05	0.10	0.00		0.00	0.00
LOI	6.67		0.77	1.56	0.97	2.42	2.65	0.57	2.40		0.79	1.99
Total	100.02		99.95	101.00	98.50	100.43	101.50	99.09	101.50		100.28	100.48
pb(ppm)	11.2	9.0	7.5	12.5	10.6	4.3	12.2	7.8	8.1	7.5	10.7	4.2
Th	4.3	2.1	2.9	2.1	8.2	<2	5.5	3.6	<2	<2	4.4	<2
Rb	67.4	17.5	17.7	29.3	107.5	76.2	44.6	39.4	<3	<3	35.3	15.6
Sr	95.6	273	75.1	431	97.1	187	199	279	59.7	210	68.0	262
Y	29.1	51.3	47.7	56.8	27.6	30.0	56.1	48.1	41.1	7.8	55.2	44.3
Zr	181	324	293	319	126	108.4	300	227	193	39.6	318	163
Nb	9.3	10.9	11.0	12.8	5.0	2.9	8.6	9.5	9.3	2.5	9.1	6.3
Ga	16.7	17.9	13.2	22.2	14.5	19.9	17.7	20.8	19.1	<5	20.2	19.2
Cu	15.7	<5	10.1	5.5	<5	66.6	37.0	5.3	39.4	13.3	7.1	32.0
Zn	73.6	105.2	94.1	132	29.3	104.5	123	109.3	124	39.0	113	153
Cr	n.d	n.d	n.d	<30	n.d	n.d	n.d	n.d	<30	n.d	n.d	<30
Ni	n.d	n.d	n.d	<20	n.d	n.d	n.d	n.d	<20	n.d	n.d	<20

Whole rock compositions (Fatima area, continued)

Rock type	ss	ss	bas	dol.ss	dike	gr	dike	ss	bas	tuff	mud	cgl
Sample	FA100	FA101	FA102	FA103	FA105	FA111	FA112	FA113	FA114	FA116	FA117	FA120
Si(% oxide)	59.26	58.58	49.70	31.07	76.13	75.69	61.81	39.82	47.97	63.10		
Ti	0.98	0.68	1.05	0.11	0.16	0.22	1.11	0.60	2.30	1.07		
Al	16.75	16.89	16.66	2.33	13.37	12.73	15.45	10.66	15.87	15.07		
Fe	6.51	4.82	10.66	0.65	1.59	1.01	8.12	6.66	15.86	3.35		
Mn	0.01	0.05	0.15	0.15	0.04	0.04	0.14	0.20	0.24	0.01		
Mg	8.82	7.13	4.98	14.54	0.50	0.72	2.67	7.28	4.00	1.67		
Ca	0.51	1.05	9.96	21.01	0.29	0.52	1.33	14.16	7.68	1.26		
Na	0.29	5.57	2.85	0.00	5.76	4.22	5.73	1.61	2.71	4.20		
K	2.86	1.57	0.37	0.00	1.83	3.50	1.86	1.85	0.68	4.11		
P	0.18	0.17	0.16	0.05	0.02	0.07	0.33	0.23	0.44	0.20		
Ba	0.01	0.01	0.02	0.00	0.11	0.06	0.03	0.01	0.00	0.06		
V	0.01	0.01	0.05	0.00	0.01	0.00	0.02	0.01	0.05	0.02		
S	0.00	0.01	0.00	0.06	0.02	0.00	0.00	0.04	0.02	0.00		
LOI	5.31	3.71	3.56	30.59	1.18	1.04	2.02	17.31	3.63	4.99		
Total	101.50	100.25	100.17	100.56	101.01	100.52	100.62	100.44	101.45	99.11		
Pb(ppm)	<2	5.7	3.9	6.5	11.4	10.7	7.9	9.6	4.9	4.9	2.9	3.9
Th	3.9	<2	<2	<2	4.5	5.5	<2	4.3	<2	2.6	<2	<2
Rb	47.1	19.7	6.4	<3	47.6	45.9	39.9	28.8	8.7	115	3.4	25.3
Sr	14.5	78.2	496	232	50.1	124	172	187	569	223	65.6	254
Y	23.4	22.1	23.7	8.1	42.3	13.8	38.2	41.4	39.6	21.4	31.5	37.4
Zr	163	119	90.2	41.6	242	99.4	165	121	154	21.9	104.9	155
Nb	4.6	3.6	4.1	3.6	7.5	3.6	3.7	4.5	5.2	8.9	4.6	5.8
Ga	13.8	<5	20.2	<5	13.1	13.0	18.9	14.5	23.2	25.0	19.9	20.4
Cu	5.9	16.3	141	15.0	<5	16.3	<5	30.8	68.8	97.1	5.0	11.2
Zn	58.7	36.5	102.7	37.0	29.9	29.8	125	106.8	166	65.6	119	125
Cr	n.d	n.d	49.4	n.d	n.d	n.d	n.d	n.d	30	42.2	n.d	n.d
Ni	n.d	n.d	31.4	n.d	n.d	n.d	n.d	n.d	24.3	<20	n.d	n.d

Whole rock compositions (Fatima area, continued)

Rock type	ss	volc.br	mud	cgl	ss	volc.br	volc.br	tuff	ign	ign	cgl	mud
Sample	FA120	FA122	FA131	FA132	FA133	FA140	FA141	FA142	FA143	FA144	FA145	FA146
Si(% oxide)				52.10	61.53	70.52	61.57	59.11	61.94	71.13	57.82	62.19
Ti				2.02	0.66	1.30	1.11	1.05	0.79	0.47	1.28	0.79
Al				15.99	16.85	12.95	14.96	16.94	17.17	13.66	15.38	15.29
Fe				12.99	7.03	5.32	7.88	8.53	7.26	5.28	9.06	6.41
Mn				0.32	0.10	0.11	0.19	0.14	0.34	0.12	0.22	0.05
Mg				5.95	2.47	0.65	3.01	5.31	3.14	0.39	3.54	5.59
Ca				2.74	3.34	1.30	4.40	2.02	1.89	2.69	5.23	1.85
Na				5.54	6.25	5.61	1.49	0.91	0.84	6.14	4.76	3.42
K				0.09	0.31	1.19	3.35	5.28	4.47	0.05	0.46	1.01
P				0.42	0.15	0.14	0.37	0.34	0.20	0.07	0.40	0.12
Ba				0.00	0.01	0.05	0.06	0.10	0.10	0.00	0.06	0.02
V				0.05	0.02	0.00	0.01	0.01	0.01	0.01	0.01	0.02
S				0.00	0.00	0.00	0.03	0.00	0.00	0.00	0.01	0.10
LOI				3.29	2.63	1.46	3.04	3.55	3.35	0.93	2.62	3.74
Total				101.50	101.35	99.80	101.49	101.09	101.50	100.94	100.79	101.50
Pb(ppm)	4.7	4.5	12.6	10.1	6.5	8.6	8.9	7.6	12.0	10.3	6.7	6.8
Th	4.6	2.5	2.9	<2	2.8	2.4	3.6	3.1	3.4	3.9	2.1	<2
Rb	37.0	16.7	47.4	6.6	9.7	20.5	51.3	81.3	65.9	4.5	11.9	33.9
Sr	33.5	227	25.7	92.8	313	93.2	503	201	214	100.9	385	112
Y	29.4	38.4	33.7	57.2	18.1	46.9	52.9	63.8	65.2	57.1	38.8	20.1
Zr	222	138	175	238	114	280	293	372	348	323	170	134
Nb	7.8	5.0	7.4	7.2	3.7	10.7	13.6	17.0	15.0	12.3	7.0	4.2
Ga	21.8	16.1	15.8	19.7	17.6	14.1	22.0	30.5	30.8	17.2	17.9	23.1
Cu	<5	17.4	9.2	113	38.5	19.5	12.4	12.1	27.0	21.8	20.4	<5
Zn	76.6	123	95.5	164	67.1	101.6	154	125	123	125	121	62.2
Cr	n.d	n.d	n.d	n.d	n.d	n.d	n.d	<30	<30	n.d	46.6	n.d
Ni	n.d	n.d	n.d	n.d	n.d	n.d	n.d	<20	<20	n.d	25.4	n.d

Whole rock compositions (Fatima area, continued and Badr area)

Rock type	bas	ss	ign	ign	ign	bas	bas	dol	gr	gr	ign	mud
Sample	FA160	FA180	FA181	FA182	FA183	FA184	FA185	FA190	BA001	BA002	BA003	BA004
Si(% oxide)	49.90			69.37	67.96	50.80	51.17	7.36	65.28	62.67	71.33	
Ti	1.65			0.52	0.49	2.14	1.80	0.02	0.60	0.69	0.35	
Al	16.19			14.37	15.08	15.91	14.34	0.36	16.33	16.98	13.68	
Fe	12.91			5.82	5.74	13.45	13.34	0.00	4.43	5.27	2.60	
Mn	0.28			0.15	0.15	0.08	0.15	0.11	0.07	0.08	0.07	
Mg	3.92			0.63	1.95	6.29	5.75	19.76	2.01	2.52	0.67	
Ca	6.97			2.64	0.57	3.60	6.53	36.07	4.50	3.73	2.14	
Na	3.57			6.81	8.56	5.43	3.65	0.00	4.12	4.48	4.33	
K	1.14			0.08	0.00	0.06	0.00	0.00	2.14	1.80	2.36	
P	0.49			0.12	0.09	0.43	0.35	0.06	0.19	0.18	0.08	
Ba	0.06			0.02	0.01	0.01	0.01	0.00	0.07	0.08	0.06	
V	0.03			0.02	0.00	0.07	0.06	0.00	0.01	0.01	0.01	
S	0.00			0.00	0.00	0.00	0.00	0.00	0.00	0.06	0.08	
LOI	2.60			0.90	0.42	3.32	3.56	36.57	1.46	2.66	1.47	
Total	99.71			101.43	101.02	101.50	100.71	100.31	101.22	101.21	99.15	
Pb(ppm)	7.6	7.6	7.9		9.0	4.9	4.6	7.6	8.4	13.4	11.4	10.4
Th	2.6	<2	2.1		3.9	<2	<2	<2	2.9	4.1	5.0	3.2
Rb	21.2	9.7	12.4		<3	6.8	3.5	<3	47.0	43.3	65.7	38.1
Sr	359	383	125		50.6	166	367	220	388	376	323	204
Y	47.0	47.0	38.4		61.3	56.1	49.8	2.4	22.7	20.0	24.9	26.7
Zr	201	201	160		343	234	207	12.7	160	141	194	190
Nb	8.4	8.4	<2		13.3	6.4	5.3	<2	6.2	5.7	5.6	6.0
Ga	25.6	25.6	17.3		17.6	17.9	20.6	14.0	n.d	n.d	14.4	14.7
Cu	11.3	11.3	23.4		69.2	76.1	54.5	127	n.d	n.d	2.2	<5
Zn	156	156	177		162	120	131	11.0	n.d	n.d	53.9	61.1
Cr	<30	<30	n.d		n.d	n.d	<30	n.d	n.d	n.d	n.d	n.d
Ni	<20	<20	n.d		n.d	n.d	24.2	n.d	n.d	n.d	n.d	n.d

Whole rock compositions (Badr area, continued)

Rock type	rhy	ss	ign	tuff	f.tuff	tuff	ign	ign	ign	ign	f.tuff
Sample	BA005	BA006	BA007	BA008	BA009	BA010	BA011	BA011B	BA012	BA012B	BA020
Si(% oxide)		72.46	75.50	58.00		72.07	73.55	74.71	70.30	73.26	72.86
Ti		0.25	0.43	0.94		0.35	0.33	0.31	0.34	0.36	0.28
Al		13.46	13.17	16.93		13.24	13.71	13.25	13.29	14.13	13.47
Fe		2.44	3.44	7.63		2.56	2.60	2.22	2.64	2.75	2.78
Mn		0.07	0.01	0.12		0.10	0.06	0.05	0.11	0.06	0.08
Mg		0.00	0.00	2.12		0.61	0.31	0.39	0.79	0.54	0.69
Ca		4.86	0.36	4.18		1.31	0.81	0.23	3.03	0.28	2.94
Na		2.09	7.42	4.04		3.39	4.73	3.98	2.46	3.38	2.43
K		2.26	0.01	2.82		4.66	3.50	3.30	3.48	3.54	2.56
P		0.00	0.18	0.22		0.11	0.06	0.08	0.10	0.09	0.00
Ba		0.08	0.04	0.07		0.10	0.07	0.10	0.08	0.06	0.06
V		0.00	0.01	0.02		0.01	0.00	0.01	0.01	0.01	0.00
S		0.04	0.08	0.04		0.03	0.00	0.00	0.03	0.00	0.02
LOI		1.97	0.52	2.81		1.20	0.57	1.03	4.30	1.56	1.95
Total		100.02	101.16	99.94		99.74	100.30	99.66	100.96	100.02	100.12
Pb(ppm)	13.0	18	10.6	17.0	9.6	51.0	9.0	13.7	18.0	12.7	9.8
Th	<2	8.3	2.4	4.1	2.8	7.7	<2	6.7	6.8	5.1	2.8
Rb	34.0	65.1	4.1	62.9	3.1	99.7	99.1	74.7	90.2	87.5	67.2
Sr	295	425	80.3	336	84.9	181	347	129	148	107.5	296
Y	31.0	29.6	37.0	27.1	38.6	27.9	42.4	23.6	29.9	26.4	35.5
Zr	135	180	239	157	253	198	239	195	209	211	208
Nb	4.4	6.6	7.3	5.9	6.8	7.0	7.1	6.3	6.9	6.1	5.5
Ga	18.8	n.d	n.d	n.d	13.3	n.d	15.8	123	n.d	17.2	14.8
Cu	12.7	n.d	n.d	n.d	<5	n.d	<5	<5	n.d	8.6	6.2
Zn	299	n.d	n.d	n.d	23.5	n.d	74.5	39.1	n.d	60.6	62.8
Cr	n.d	n.d	n.d	n.d	n.d	n.d	n.d	n.d	n.d	n.d	n.d
Ni	n.d	n.d	n.d	n.d	n.d	n.d	n.d	n.d	n.d	n.d	n.d

Whole rock compositions (Badr area, continued)

Rock type	ign	tuff	ign	and	and	f.tuff	f.tuff	dike	tuff	volc.br	f.tuff	ign
Sample	BA021	BA022	BA099	BA100	BA101=BD1	BA102	BA103=BD2	BA104	BA105	BA106	BA107	BA108
Si(% oxide)	72.02	65.64	72.76	52.45	53.62	64.16	60.92	47.34	59.70	61.12	75.29	68.51
Ti	0.33	0.77	0.29	2.83	1.33	0.69	0.68	3.02	1.21	1.19	0.26	0.36
Al	14.08	15.36	13.20	11.03	16.05	13.07	15.62	14.68	13.73	15.28	10.29	15.94
Fe	3.34	4.94	3.35	12.98	8.80	6.65	5.78	14.55	7.32	7.34	3.76	3.51
Mn	0.09	0.12	0.03	0.14	0.10	0.09	0.13	0.20	0.18	0.25	0.11	0.08
Mg	0.27	1.75	0.29	2.84	4.68	1.88	1.63	4.87	2.30	4.65	0.00	1.87
Ca	1.12	2.25	0.29	8.96	7.33	3.82	2.56	7.70	4.41	2.43	6.70	0.79
Na	6.00	1.90	2.97	4.15	5.27	5.29	4.34	2.55	2.74	5.10	1.78	1.86
K	2.68	4.34	6.31	0.00	0.00	1.27	3.13	1.67	2.00	1.03	0.00	5.39
P	0.06	0.26	0.04	0.46	0.20	0.13	0.28	0.76	0.49	0.44	0.08	0.06
Ba	0.08	0.07	0.12	0.00	0.00	0.03	0.04	0.06	0.05	0.01	0.01	0.07
V	0.00	0.01	0.00	0.05	0.03	0.01	0.01	0.06	0.01	0.01	0.01	0.01
S	0.02	0.00	0.00	0.02	0.00	0.01	0.00	0.18	0.00	0.00	0.00	0.00
LOI	0.91	3.47	0.89	5.07	3.51	3.96	3.78	3.16	5.35	2.50	0.89	2.88
Total	101.00	100.88	100.49	100.90	100.92	101.09	98.90	100.80	99.49	101.35	99.81	101.33
Pb(ppm)	10.1	8.7	9.5	18.0	8.4	10.1	11.8	22.0	8.1	10.1	13.0	13.1
Th	2.8	2.7	10.3	3.0	3.5	2.7	2.5	<2	3.5	3.2	3.0	6.2
Rb	45.1	123	128	3.9	4.5	27.5	98.8	45.4	33.5	28.2	3.3	153
Sr	70.0	279	81.5	221	251	107.2	180	464	151	378	747	135
Y	51.7	35.9	67.4	37.2	30.6	26.7	56.2	39.8	52.7	48.5	20.5	46.4
Zr	315	201	557	185	187	166	346	253	243	213	120	303
Nb	7.9	7.6	12.8	7.1	5.6	4.8	9.2	21.4	8.0	6.7	4.8	8.8
Ga	19.2	19.1	19.1	n.d	22.8	14.0	24.2	n.d	18.3	20.7	n.d	19.7
Cu	8.6	11.4	<5	n.d	34.1	5.5	<5	n.d	6.4	6.1	n.d	<5
Zn	60.6	91.0	42.0	n.d	69.7	61.6	171	n.d	108.6	105.4	n.d	60.3
Cr	n.d	n.d	n.d	n.d	106.4	58.2	n.d	n.d	<30	n.d	n.d	n.d
Ni	n.d	n.d	n.d	n.d	36.5	<20	n.d	n.d	<20	n.d	n.d	n.d

Whole rock compositions (Badr area, continued)

Rock type	Tuff	ign	and	tuff	ss	bas	ign	tuff	volc.br	tuff	volc.br	ss
Sample	BA109	BA210	BA121	BA122	BA123	BA125	BA130	BA131	BA132	BA150	BA151	BA152
Si(% oxide)	68.42	68.93	53.57	67.33	69.71	48.02	68.26	75.09	54.55	69.40	71.44	
Ti	0.51	0.57	1.39	0.53	0.57	1.43	0.50	0.38	1.41	0.79	0.39	
Al	14.66	15.20	16.50	14.36	14.09	18.24	15.68	11.98	17.79	13.13	14.06	
Fe	3.91	4.50	9.55	4.36	4.04	8.93	4.10	2.65	9.79	6.80	3.14	
Mn	0.11	0.10	0.16	0.20	0.09	0.17	0.08	0.11	0.19	0.05	0.08	
Mg	0.63	0.73	5.20	1.54	2.00	3.76	0.53	0.31	2.03	0.53	0.66	
Ca	2.88	0.87	7.21	1.80	1.92	8.29	0.50	4.33	4.78	2.21	2.78	
Na	5.84	5.58	3.12	1.74	2.28	5.45	5.64	3.42	5.87	6.22	2.72	
K	0.92	3.66	1.49	4.84	1.92	0.99	4.07	1.86	1.48	0.08	2.75	
P	0.09	0.14	0.56	0.08	0.13	0.21	0.13	0.09	0.35	0.27	0.08	
Ba	0.03	0.10	0.05	0.12	0.07	0.01	0.11	0.08	0.03	0.00	0.06	
V	0.00	0.00	0.03	0.00	0.00	0.04	0.00	0.01	0.03	0.01	0.01	
S	0.00	0.00	0.01	0.00	0.00	0.00	0.00	0.01	0.00	0.04	0.03	
LOI	0.91	1.11	2.43	3.22	2.14	5.51	0.71	1.17	1.97	0.91	2.02	
Total	98.91	101.49	101.27	100.33	100.56	101.05	100.31	101.49	100.27	100.44	100.22	
Pb(ppm)	13.5	13.7	7.1	14.6	11.1	4.0	11.8	16.8	10.4	6.3	13.5	8.4
Th	5.3	4.9	2.8	4.5	5.8	2.0	3.7	3.7	<2	2.1	5.0	4.7
Rb	12.1	50.2	27.1	131	65.8	27.0	73.5	28.1	39.1	7.4	75.6	3.3
Sr	1246	175	470	265	144	639	157	477	649	149	290	70.2
Y	143	44.8	31.8	57.5	24.5	26.7	46.7	20.3	24.8	27.7	40.2	21.3
Zr	327	330	211	349	199	114	361	135	91.8	132	216	178
Nb	5.4	9.7	8.2	10.2	6.7	5.4	10.0	5.2	5.3	5.0	5.7	4.5
Ga	18.8	20.9	19.1	22.4	14.7	13.5	21.1	12.7	19.6	13.2	18.4	12.6
Cu	9.7	<5	22.0	6.5	<5	73.2	<5	5.7	7.6	16.9	<5	<5
Zn	104.7	120	136	112	46.4	74.2	72.2	27.6	91.7	56.9	71.1	36.5
Cr	n.d	n.d	135	n.d	n.d	175	n.d	n.d	<30	n.d	n.d	n.d
Ni	n.d	n.d	66.7	n.d	n.d	29	n.d	n.d	<20	n.d	n.d	n.d

Whole rock compositions (Badr area, continued)

Rock type	gr	tuff	tuff	bas	bas	dol	ign	ign	sill	f.tuff	ign	ign
Sample	BA160	BA161	BA162	BA170	BA171	BA172	BA174	BA175	BA200	BA201	BA202	BA203
Si(% oxide)	55.32	71.20	74.76	50.39	55.34		78.09	78.12	57.92	67.33	70.06	67.67
Ti	1.04	0.33	0.27	1.37	1.20		0.30	0.30	1.06	0.41	0.41	0.41
Al	17.12	14.08	12.63	18.15	16.58		13.52	12.84	18.28	16.88	14.91	15.24
Fe	8.18	3.31	3.14	9.69	7.21		3.60	3.67	7.49	3.60	3.61	3.74
Mn	0.13	0.13	0.04	0.15	0.11		0.06	0.05	0.23	0.11	0.05	0.09
Mg	4.50	0.36	0.00	3.20	8.02		0.05	0.00	3.03	1.38	1.73	0.33
Ca	6.89	0.86	0.63	10.30	8.34		0.40	0.43	2.15	0.22	0.26	0.71
Na	3.88	6.67	5.32	3.96	3.59		5.03	5.66	8.02	1.77	0.86	5.99
K	1.12	1.92	2.82	0.00	0.84		3.93	3.09	0.33	6.25	5.59	2.89
P	0.34	0.07	0.02	0.00	0.52		0.03	0.03	0.25	0.04	0.08	0.10
Ba	0.05	0.05	0.06	0.01	0.02		0.08	0.06	0.01	0.09	0.05	0.11
V	0.13	0.13	0.04	0.04	0.03		0.00	0.00	0.02	0.01	0.00	0.00
S	0.05	0.05	0.00	0.00	0.02		0.06	0.00	0.00	0.02	0.00	0.00
LOI	2.09	1.51	0.59	3.92	1.20		0.94	0.44	2.23	2.29	2.83	1.27
Total	100.69	100.49	100.28	101.48	100.00		101.09	99.69	100.97	100.40	100.44	98.50
Pb(ppm)	7.1	11.5	10.9	4.8	6.7	10.7	16.3	8.7	8.9	18.2	16.1	14.1
Th	<2	2.7	5.4	<2	<2	6.5	6.1	6.2	3.0	6.4	6.1	5.4
Rb	20.6	32.4	47.2	<3	11.9	41.0	61.5	50.6	8.8	132	143	43.0
Sr	467	90.9	64.8	315	444	168	75.0	54.5	365	137	41.0	197
Y	24.7	52.7	47.6	23.5	81.7	23.6	65.0	48.3	31.2	58.3	68.5	69.4
Zr	180	336	370	120	201	155	442	392	191	515	463	454
Nb	5.9	8.6	7.6	4.2	7.4	7.5	8.2	9.4	6.4	10.6	12.1	11.5
Ga	19.4	17.6	16.5	25.6	19.4	16.0	16.2	16.1	26.0	21.3	28.0	19.5
Cu	15.6	<5	<5	38.1	31.4	6.8	<5	7.0	26.8	<5	<5	<5
Zn	119	76.5	64.8	104.0	110	67.8	71.4	54.4	94.4	82.4	101.4	58.0
Cr	n.d	n.d	n.d	<30	n.d	n.d	n.d	n.d	n.d	n.d	n.d	n.d
Ni	n.d	n.d	n.d	<20	n.d	n.d	n.d	n.d	n.d	n.d	n.d	n.d

Whole rock compositions (Badr area, continued)

Rock type	ign	ign	ign	ign	ign	ign	ign	tuff	and	bas	volc.br	and
Sample	BA204	BA205	BA206	BA207	BA208	BA209	BA210	BA211	BA215	BA216	BA217	BA218
Si(% oxide)	74.06	71.00	71.25	73.03	70.75	72.82	74.16		58.24	46.78		54.95
Ti	0.44	0.46	0.50	0.47	0.59	0.37	0.40		0.96	3.30		1.42
Al	14.07	13.58	14.27	12.53	14.61	12.94	11.95		17.28	15.42		16.68
Fe	3.68	3.73	4.03	3.72	4.29	3.20	3.23		7.89	13.10		9.04
Mn	0.10	0.10	0.09	0.08	0.05	0.09	0.10		0.16	0.20		0.14
Mg	0.66	0.56	0.47	0.23	0.33	0.26	0.86		2.63	4.28		4.54
Ca	0.98	0.44	0.63	0.23	0.19	0.84	1.45		4.30	8.07		7.27
Na	4.78	5.30	5.76	4.64	5.97	5.28	3.72		5.94	3.62		3.75
K	3.76	3.53	2.98	3.17	2.80	3.07	3.76		0.83	1.45		1.42
P	0.08	0.09	0.12	0.10	0.11	0.11	0.14		0.21	1.36		0.39
Ba	0.07	0.06	0.05	0.06	0.05	0.07	0.06		0.06	0.11		0.04
V	0.00	0.00	0.00	0.01	0.00	0.01	0.01		0.02	0.04		0.14
S	0.00	0.01	0.00	0.06	0.00	0.00	0.00		0.01	0.02		0.00
LOI	1.60	1.23	1.21	0.86	0.54	1.02	1.87		2.75	2.55		1.76
Total	100.68	100.09	101.36	99.19	100.23	100.15	101.21		101.28	100.30		101.43
Pb(ppm)	13.5	12.6	12.4	8.6	8.8	10.5	10.7	16.7	7.9	5.3	9.9	7.2
Th	6.0	6.6	3.8	3.3	4.8	2.7	4.1	6.8	3.3	<2	2.3	2.2
Rb	57.7	39.6	46.6	45.8	40.3	39.9	56.4	193	14.6	25.3	<3	30.0
Sr	108.5	58.1	103.0	72.8	56.4	66.2	71.4	20.5	458	504	98.1	652
Y	59.5	54.3	58.5	52.8	55.3	57.2	52.8	82.8	32.6	45.2	26.7	30.2
Zr	422	381	400	372	376	350	341	521	148	225	178	202
Nb	11.3	9.5	9.5	10.0	9.6	9.1	9.3	14.1	5.0	19.5	5.5	6.9
Ga	17.3	18.5	16.8	14.8	20.6	18.9	13.9	58.1	20.8	22.9	16.2	16.1
Cu	<5	<5	<5	<5	<5	<5	<5	71.5	29.4	20.8	9.1	12.9
Zn	86.8	66.6	85.9	77.3	56.4	73.2	84.7	148	98.3	101.1	96.7	87.2
Cr	n.d	n.d	n.d	n.d	n.d	n.d	n.d	n.d	<30	n.d	n.d	94.2
Ni	n.d	n.d	n.d	n.d	n.d	n.d	n.d	n.d	<20	n.d	n.d	36.4

Whole rock compositions (Badr area, continued)

Rock type	tuff	volc.br	volc.br	volc.br	tuff	ign	ign	ign	ign	ign	ign	gr
Sample	BA219	BA220	BA224	BA225	BA226	BA227	BA228	BA229	BA251	BA252	BA253	BA254
Si(% oxide)	70.44	51.31		64.03		65.61	69.69	68.28	49.61	72.15	70.11	49.20
Ti	0.59	2.29		0.68		0.57	0.50	0.50	2.42	0.34	0.34	2.77
Al	14.46	13.67		18.19		14.93	15.49	15.49	17.75	14.34	15.34	16.30
Fe	4.59	11.94		5.46		4.65	4.09	4.17	13.76	2.71	2.95	13.26
Mn	0.05	0.18		0.16		0.12	0.10	0.07	0.18	0.09	0.05	0.23
Mg	1.30	2.96		0.73		0.42	0.49	0.53	4.07	0.82	0.66	5.11
Ca	1.39	6.63		0.71		2.05	0.49	0.69	4.50	1.05	2.46	5.39
Na	2.67	6.17		5.77		5.37	6.01	5.83	1.46	4.10	4.19	2.79
K	4.07	0.12		2.59		2.98	3.93	3.94	0.21	4.41	2.64	0.67
P	0.15	0.87		0.14		0.12	0.13	0.12	0.26	0.11	0.08	0.38
Ba	0.08	0.01		0.05		0.10	0.11	0.11	0.00	0.10	0.07	0.03
V	0.01	0.03		0.01		0.01	0.01	0.01	0.04	0.07	0.01	0.04
S	0.00	0.01		0.04		0.07	0.03	0.01	0.00	0.00	0.00	0.00
LOI	1.70	4.31		1.73		2.27	0.29	0.40	6.82	0.93	1.38	4.70
Total	101.50	100.50		100.29		99.27	101.36	100.15	100.94	101.22	100.28	100.87
Pb(ppm)	11.7	6.4	7.9	11.0	13.4	14.0	12.8			12.1	8.8	
Th	3.5	<2	5.9	4.9	2.7	4.3	5.1			5.5	6.2	
Rb	115	4.9	47.5	64.2	87.3	46.1	56.1			86.9	75.4	
Sr	111	175	160	211	127	180	70.0			358	427	
Y	61.0	44.8	43.8	44.2	43.5	46.4	41.5			24.4	22.5	
Zr	362	237	342	358	319	322	334			190	197	
Nb	9.2	8.2	10.2	9.3	9.6	8.5	9.8			7.0	5.8	
Ga	20.0	15.4	20.4	26.1	21.0	21.4	19.6			14.8	15.9	
Cu	<5	<5	7.8	5.0	<5	<5	<5			8.4	<5	
Zn	115	102.9	57.2	108.4	86.3	98.8	85.5			44.6	28.5	
Cr	n.d	n.d	n.d	<30	n.d	n.d	n.d			n.d	n.d	
Ni	n.d	n.d	n.d	<20	n.d	n.d	n.d			n.d	n.d	

Whole rock compositions (Badr area, continued)

Rock type	bas	rhy	rhy	ign	ss	tuff	ign	and	rhy	rhy	and	and
Sample	BA255	BA256	BA257	BA260	BA270	BA271	BA272	BA274	BA275	BA275B	BA300	BA301
Si(% oxide)	47.27	75.32	76.38	76.44	49.64	64.21	61.89	55.67	74.82		61.32	65.48
Ti	3.52	0.25	0.25	0.20	2.42	0.73	1.59	1.49	0.24		0.35	1.16
Al	13.13	12.74	11.76	10.59	18.69	16.36	15.36	14.19	13.63		15.28	15.17
Fe	15.37	3.41	3.36	3.00	11.42	5.95	8.97	8.45	1.84		6.95	6.26
Mn	0.28	0.05	0.04	0.03	0.14	0.13	0.13	0.14	0.04		0.13	0.12
Mg	5.03	0.25	0.20	0.00	3.96	1.54	2.40	4.75	0.50		1.69	1.11
Ca	6.71	0.51	0.40	0.10	6.45	1.93	1.31	6.83	1.02		2.58	2.44
Na	4.73	2.86	2.27	3.08	3.08	5.45	5.75	2.85	4.49		4.81	4.96
K	1.11	4.18	4.88	4.45	0.76	3.24	0.99	0.97	3.58		4.06	3.58
P	0.58	0.01	0.03	0.00	0.40	0.20	0.56	0.43	0.05		0.45	0.39
Ba	0.02	0.01	0.03	0.01	0.04	0.06	0.02	0.08	0.07		0.06	0.07
V	0.07	0.00	0.01	0.00	0.04	0.01	0.02	0.04	0.00		0.01	0.01
S	0.00	0.01	0.00	0.00	0.00	0.00	0.00	0.00	0.00		0.00	0.00
LOI	1.69	0.92	0.55	0.60	1.52	1.54	2.41	3.78	0.90		1.09	0.71
Total	99.51	100.52	100.16	98.50	98.56	101.35	101.40	99.67	101.17		99.78	101.41
Pb(ppm)	4.3	11.2	10.5	14.6	8.1	<2	6.4	4.5	8.6	2.0	10.3	12.1
Th	<2	13.1	8.8	11.9	4.8	<2	<2	<2	5.4	2.0	4.8	6.8
Rb	23.1	126	116	116	25.1	10.3	16.8	17.5	68.4	<3	69.0	69.2
Sr	276	90.6	97.6	46.6	166	38.9	173	536	174	76.3	401	528
Y	42.5	80.7	76.9	74.4	54.0	4.0	52.7	27.1	23.2	8.3	37.2	38.8
Zr	220	688	646	663	415	31.7	239	146	142	76.0	273	293
Nb	7.6	16.5	15.0	19.2	9.9	2.1	8.1	7.1	5.7	4.0	8.4	7.5
Ga	19.6	24.5	22.8	20.0	16.1	<5	22.2	18.8	15.0	9.7	17.3	15.0
Cu	31.0	<5	<5	<5	<5	<5	<5	27.2	7.6	12.7	15.6	5.5
Zn	126	102.6	55.7	68.5	64.4	13.6	132	106.1	37.6	20.5	91.6	88.9
Cr	<30	n.d	n.d	n.d	n.d	<30	n.d	215	n.d	n.d	n.d	n.d
Ni	<20	n.d	n.d	n.d	n.d	<20	n.d	89.2	n.d	n.d	n.d	n.d

Whole rock compositions (Badr area, continued and Nuqrah area)

Rock type	volc.br	qudior	qudior	qudior	qudior	rhy	dol	volc.br	amph	gr	gr	gb
Sample	BA303	BA304	BA305	BA306	BA307	BA308	BA309	BA310	NU003	NU004	NU005	NU006
Si(% oxide)	71.67	53.52	53.85		53.68	67.12		58.80	59.36	73.13	74.09	48.34
Ti	0.36	1.35	1.28		1.47	0.68		1.15	1.64	0.18	0.24	0.24
Al	13.99	16.98	16.55		15.81	15.09		15.27	15.25	13.63	13.21	17.74
Fe	2.76	9.28	8.84		9.58	5.40		8.63	8.75	2.60	3.04	4.67
Mn	0.06	0.14	0.14		0.14	0.12		0.08	0.19	0.04	0.07	0.09
Mg	0.68	5.20	4.51		4.76	0.56		2.11	2.44	0.17	0.58	9.32
Ca	3.89	7.51	6.88		7.20	2.18		4.61	4.93	0.86	1.88	16.38
Na	2.10	4.02	3.67		3.94	5.75		4.59	4.69	5.29	4.19	1.06
K	2.61	1.07	1.38		1.07	2.46		1.61	2.19	3.19	2.29	0.00
P	0.10	0.54	0.49		0.53	0.24		0.57	0.80	0.02	0.06	0.03
Ba	0.05	0.03	0.05		0.02	0.07		0.03	0.17	0.07	0.12	0.00
V	0.01	0.03	0.04		0.03	0.01		0.02	0.02	0.01	0.01	0.03
S	0.00	0.00	0.00		0.00	0.02		0.00	0.01	0.00	0.00	0.06
LOI	1.63	1.77	2.26		2.27	0.80		2.37	0.70	0.89	1.72	0.71
Total	99.91	101.44	99.94		100.50	101.50		100.29	101.14	100.08	101.50	98.67
Pb(ppm)	14.9	7.0	7.1	10.4	9.1	14.2	9.4	10.3	6.7	20.9	11.9	4.4
Th	7.2	<2	<2	<2	<2	3.2	5.2	2.1	<2	7.6	3.9	<2
Rb	85.5	12.7	21.3	3	14.9	39.9	38.5	27.1	<3	74.6	30.7	3.8
Sr	674	581	561	2112	522	163	160	397	64.4	78.5	190	265
Y	28.1	27.9	29.2	34.3	31.7	52.3	22.4	31.7	8.8	51.3	24.8	6.7
Zr	215	201	213	217	225	307	98.0	212	28.8	342	123	18.2
Nb	7.3	8.3	8.2	10.1	8.6	8.4	7.3	8.5	2.1	8.9	5.7	<2
Ga	15.9	21.7	16.6	30.7	20.5	22.3	17.3	11.8	13.3	5.9	13.0	11.6
Cu	8.1	37.4	35.4	<5	37.1	7.8	<5	38.5	89.6	17.9	5.1	42.5
Zn	63.0	105	112	109.5	114	86.3	40.6	91.0	81.1	107.8	47.5	37.2
Cr	n.d	n.d	n.d	n.d	n.d	n.d	n.d	n.d	n.d	n.d	n.d	n.d
Ni	n.d	n.d	n.d	n.d	n.d	n.d	n.d	n.d	n.d	n.d	n.d	n.d

Whole rock compositions (Nugrah area, continued)

Rock type	gr	gr	gr	volc.br	ign	ign	tuff	sill	tuff	tuff	tuff	ign
Sample	NU007	NU110	NU111	NU112	NU113	NU114	NU115	NU116	NU117	NU118	NU119	NU120
Si(% oxide)	75.20	75.00	66.79	61.42	62.90	71.97	65.78	59.74	77.47	71.88	70.94	76.79
Ti	0.13	0.13	0.70	1.20	1.09	0.27	0.64	1.60	0.13	0.19	0.20	0.13
Al	13.52	13.45	15.42	14.68	14.91	13.96	14.50	15.08	11.63	13.99	13.84	11.71
Fe	1.54	1.55	4.26	7.28	6.90	3.31	4.36	8.60	1.27	2.66	2.79	2.21
Mn	0.04	0.04	0.07	0.16	0.13	0.07	0.09	0.18	0.01	0.08	0.07	0.03
Mg	0.14	0.18	1.34	2.26	0.00	0.25	1.91	2.33	0.17	0.09	0.52	0.21
Ca	0.80	0.49	2.49	3.65	3.00	0.93	3.66	4.64	0.78	0.98	0.99	0.26
Na	4.16	4.70	4.65	4.66	4.75	4.81	3.95	4.93	3.06	4.90	5.05	3.43
K	3.80	4.14	2.50	1.80	2.09	4.69	2.65	2.34	4.31	3.87	3.84	4.23
P	0.02	0.01	0.11	0.49	0.42	0.03	0.11	0.73	0.03	0.03	0.01	0.04
Ba	0.09	0.11	0.07	0.09	0.13	0.16	0,09	0.16	0.01	0.11	0.10	0.02
V	0.00	0.00	0.02	0.02	0.02	0.00	0.02	0.02	0.00	0.00	0.00	0.00
S	0.00	0.00	0.00	0.01	0.03	0.00	0.00	0.00	0.14	0.00	0.00	0.00
LOI	0.45	1.04	1.51	2.72	2.24	0.69	3.21	1.15	1.28	1.15	0.96	0.67
Total	99.87	100.84	99.93	100.44	98.50	101.14	100.97	101.50	100.29	99.93	99.31	99.74
Pb(ppm)	13.3	15.9	9.6	12.2	11.0	7.7	13.0	10.2	11.3	15.5	14.2	15.6
Th	8.9	12.5	4.6	2.9	5.6	9.4	3.9	3.7	11.4	8.3	9.0	11.9
Rb	100.5	103.9	58.6	51.5	41.0	55.5	41.4	53.6	76.8	92.0	89.9	83.0
Sr	89.8	118	311	381	376	157	388	391	51.4	86.8	85.6	54.1
Y	26.1	20.8	19.3	37.3	34.0	41.0	22.1	40.2	64.6	53.6	52.8	63.8
Zr	140	136	188	197	189	276	187	190	476	375	369	422
Nb	6.1	5.4	6.5	7.7	8.5	8.5	6.2	8.3	13.1	11.1	10.9	13.4
Ga	16.4	15.4	17.8	19.8	19.4	19.6	16.4	21.0	20.4	19.3	23.1	19.9
Cu	<5	<5	12.6	14.5	16.1	6.4	33.1	8.2	8.4	<5	5.1	<5
Zn	31.6	37.2	52.0	96.8	85.6	56.8	64.0	94.0	103.8	88.9	92.9	118
Cr	n.d	n.d	n.d	n.d	n.d	n.d	n.d	<30	n.d	n.d	n.d	n.d
Ni	n.d	n.d	n.d	n.d	n.d	n.d	n.d	<20	n.d	n.d	n.d	n.d

Whole rock compositions (Nuqrah area, continued)

Rock type	volc.br	tuff	tuff	ign	volc.br	ign	ign	gr	tuff	volc.br	volc.br	volc.br
Sample	NU121	NU122	NU123	NU124	NU125	NU126	NU127	NU130	NU131	NU133	NU134	NU135
Si(% oxide)	74.57	59.44	59.47	62.00	60.33	60.91	62.63	67.29	67.93	71.93		72.00
Ti	0.14	1.66	1.46	1.31	1.24	1.22	1.23	0.32	0.56	0.25		0.25
Al	11.71	15.19	14.73	14.83	13.90	14.37	14.65	14.59	13.54	13.90		13.88
Fe	2.71	8.77	8.13	7.57	7.35	7.22	7.33	4.13	4.69	2.93		2.68
Mn	0.05	0.18	0.17	0.18	0.18	0.20	0.18	0.09	0.12	0.07		0.07
Mg	0.13	2.21	2.47	1.83	1.94	1.84	1.87	2.86	0.90	0.50		0.60
Ca	0.96	4.94	4.57	3.61	4.45	3.62	1.23	2.83	1.63	1.39		1.49
Na	3.20	4.76	4.48	4.67	4.19	4.63	4.97	3.50	5.00	4.80		4.07
K	3.99	2.24	2.39	3.01	2.45	2.66	3.75	1.61	3.38	4.51		4.65
P	0.00	0.80	0.64	0.57	0.56	0.55	0.55	0.10	0.15	0.04		0.07
Ba	0.05	0.14	0.12	0.13	0.09	0.11	0.12	0.08	0.07	0.11		0.12
V	0.01	0.02	0.02	0.01	0.02	0.02	0.02	0.01	0.01	0.07		0.01
S	0.04	0.04	0.00	0.00	0.04	0.03	0.03	0.00	0.00	0.00		0.04
LOI	1.50	1.11	1.55	1.78	3.10	2.81	1.36	2.50	0.52	0.34		1.10
Total	99.06	101.50	100.20	101.50	99.84	100.19	101.50	99.91	98.50	100.78		101.03
Pb(ppm)	20.7	10.0	12.0	9.1	11.5	11.2	11.2	11.2	12.5	15.6	15.9	13.4
Th	12.8	4.1	5.4	4.0	8.6	8.9	6.9	8.0	9.6	12.4	10.5	10.0
Rb	67.3	47.8	38.2	78.3	65.2	68.0	62.5	82.6	96.8	97.8	94.0	96.2
Sr	103.9	407	401	340	342	333	325	42.8	143	98.4	87.9	113
Y	69.3	38.7	41.1	44.2	45.0	46.8	44.2	67.6	53.6	47.2	44.9	45.8
Zr	511	185	204	225	219	231	232	303	296	292	446	305
Nb	15.8	8.5	8.5	9.2	8.2	9.8	9.7	9.3	10.6	10.9	8.9	9.1
Ga	19.8	22.2	20.1	19.0	23.2	22.0	22.1	22.6	20.6	19.4	17.4	19.6
Cu	5.4	8.2	6.6	8.2	8.0	8.4	7.8	<5	10.2	7.2	6.3	7.7
Zn	114	97.0	88.1	96.6	104.5	103.8	98.3	89.3	118	87.3	83.2	82.6
Cr	n.d	n.d	<30	n.d	n.d	n.d	<30	n.d	n.d	n.d	n.d	n.d
Ni	n.d	n.d	<20	n.d	n.d	n.d	<20	n.d	n.d	n.d	n.d	n.d

Whole rock compositions (nuqrah area, continued)

Rock type	tuff	volc.br	volc.br	volc.br	volc.br	volc.br	volc.br	volc.br	bas	volc.br	rhy	cgl
Sample	NU136	NU137	NU138	NU139	NU140	NU141	NU154	NU155	NU156	NU157	NU158	NU159
Si(% oxide)	71.28	70.75	70.66	71.13	71.42		70.88	68.94	50.05	70.41	74.53	72.39
Ti	0.28	0.32	0.32	0.28	0.28		0.31	0.38	1.91	0.35	0.26	0.32
Al	14.17	13.87	14.48	14.36	14.19		13.89	14.13	16.60	13.94	12.79	13.28
Fe	3.27	3.22	3.46	2.98	3.02		3.07	3.86	11.16	3.58	2.86	3.94
Mn	0.08	0.14	0.09	0.09	0.08		0.06	0.01	0.18	0.07	0.03	0.05
Mg	0.77	0.77	0.62	0.27	0.17		0.63	0.98	5.66	1.10	0.00	0.51
Ca	1.45	1.27	1.40	1.17	1.12		1.21	1.84	7.42	1.96	0.51	0.81
Na	4.42	4.28	4.96	4.94	4.67		4.51	4.91	4.03	5.18	4.28	4.40
K	4.54	4.12	4.46	4.59	4.46		4.01	3.41	1.31	3.89	4.78	4.89
P	0.09	0.04	0.03	0.03	0.05		0.07	0.13	0.36	0.10	0.02	0.04
Ba	0.12	0.12	0.15	0.16	0.17		0.08	0.07	0.02	0.09	0.09	0.08
V	0.01	0.01	0.01	0.00	0.00		0.00	0.01	0.03	0.01	0.00	0.00
S	0.00	0.00	0.00	0.01	0.00		0.00	0.00	0.00	0.00	0.00	0.00
LOI	0.92	1.21	0.32	0.26	0.50		1.02	0.96	2.23	0.75	0.63	0.54
Total	101.40	100.12	100.96	100.26	100.13		99.97	99.70	100.96	101.43	100.78	101.25
Pb(ppm)	10.9	9.8	15.1	16.3	14.5	12.9	13.5	8.1	7.1	11.8	11.4	17.1
Th	9.2	7.2	9.9	12.3	9.9	18.9	11.4	7.6	<2	9.9	13.1	8.5
Rb	103.9	100.9	94.3	100.5	97.2	158	94.0	125	75.7	122	119.3	140..
Sr	106.2	109.4	128	115	108.1	164	94.6	129	543	134	52.7	154
Y	43.7	44.2	42.2	44.6	46.4	35.1	46.1	44.1	31.9	41.7	91.6	43.1
Zr	303	280	376	424	432	201	295	274	199	266	544	223
Nb	9.3	8.7	9.1	10.0	8.9	9.1	8.9	8.2	6.3	8.8	16.6	7.2
Ga	18.5	18.2	20.2	18.8	20.5	16.0	19.6	22.9	19.1	21.1	19.9	21.0
Cu	8.3	7.7	10.7	12.8	7.2	<5	6.7	14.1	18.2	22.8	<5	23.2
Zn	86.2	80.2	95.8	88.4	82.9	31.9	69.8	82.9	117	75.0	78.4	78.5
Cr	n.d	n.d	n.d	n.d	n.d	n.d	n.d	n.d	110	n.d	n.d	n.d
Ni	n.d	n.d	n.d	n.d	n.d	n.d	n.d	n.d	44.9	n.d	n.d	n.d

Whole rock compositions (Nuqrah area, continued and dating samples)

Rock type	volc.br	gr	gr	gr	rhy	rhy	rhy	and	bas	tuff	tuff	ign
Sample	NU160	NU161	NU170	NU171	NU172	NU173	NU174	NU175	FD01	FD02	FD03	FD04
Si(% oxide)	69.60	56.23	70.23	48.39	71.48	72.12		53.45	48.78	76.49	75.11	75.28
Ti	0.35	2.10	0.49	1.58	0.50	0.26		0.61	1.40	0.59	0.46	1.17
Al	13.75	15.18	14.21	16.42	13.19	13.89		17.20	17.22	12.19	12.20	12.66
Fe	3.33	9.92	4.09	13.00	4.25	3.13		7.27	11.75	2.68	2.46	2.49
Mn	0.08	0.18	0.10	0.19	0.10	0.10		0.13	0.20	0.11	0.12	0.11
Mg	0.68	3.15	0.74	5.41	0.76	0.25		6.65	4.57	0.20	0.24	0.25
Ca	1.26	5.07	1.58	6.99	2.03	1.00		9.61	7.25	0.59	0.46	0.48
Na	4.60	4.36	5.61	3.77	7.60	5.63		3.10	3.84	5.18	4.96	5.09
K	4.26	2.30	3.00	0.66	0.67	3.33		0.76	1.51	2.33	2.78	2.78
P	0.06	0.61	0.12	0.18	0.19	0.05		0.05	0.38	0.05	0.05	0.01
Ba	0.10	0.09	0.09	0.04	0.08	0.10		0.01	0.03	0.07	0.08	0.09
V	0.01	0.03	0.01	0.05	0.00	0.00		0.03	0.03	0.01	0.01	0.01
S	0.02	0.00	0.00	0.20	0.02	0.00		0.00	0.00	0.00	0.00	0.00
LOI	0.54	1.02	0.40	3.36	0.63	0.14		2.07	4.10	0.64	0.39	0.72
Total	98.64	100.24	100.67	100.24	101.50	100.00		100.95	101.06	100.73	99.03	99.84
Pb(ppm)	12.8	8.3	11.0	7.6	13.3	8.3	11.2	5.1	4.5	9.8	12.0	11.9
Th	11.4	4.3	7.3	<2	7.9	8.9	7.7	<2	<2	2.7	4.3	3.0
Rb	105.9	63.5	65.4	27.8	15.6	71.0	86.3	17.6	27.2	33.8	34.4	39.8
Sr	115	520	194	570	181	118	87.7	472	360	74.9	54.5	66.2
Y	49.6	37.2	36.2	24.6	34.5	36.3	28.1	13.1	37.9	51.0	54.6	54.9
Zr	372	213	238	97.7	227	238	195	45.6	159	304	311	312
Nb	9.5	7.9	6.6	3.1	7.5	7.7	6.6	4.3	6.7	10.4	8.9	9.2
Ga	18.7	20.3	20.5	21.2	16.3	14.2	17.0	15.4	25.1	14.8	19.5	18.6
Cu	12.5	12.3	9.5	23.0	<5	<5	5.6	28.4	8.4	<5	<5	<5
Zn	87.6	90.2	80.6	122	98.0	63.6	46.3	56.7	139	103.4	129	99.0
Cr	n.d	n.d	n.d	n.d	n.d	n.d	n.d	263	<30	n.d	n.d	n.d
Ni	n.d	n.d	n.d	n.d	n.d	n.d	n.d	47.9	30.8	n.d	n.d	n.d

Whole rock compositions (Dating samples, continued)

Rock type	and	dike	dike	gr	rh.dike	tuff	bas	gr	amph	and	f.tuff	ign
Sample	FD05	FD06	FD07	FD08	FD09	FD10	FD11	FD12	FD13	BD1=BA101	BD2=BA103	BD3
Si(% oxide)	52.55	72.61			68.45	76.05	47.63	65.39	48.71	53.62	60.92	71.56
Ti	1.79	0.18			0.63	0.15	0.73	0.52	0.34	1.33	0.68	0.42
Al	14.33	13.23			15.25	12.40	16.10	15.09	16.57	16.05	15.62	13.56
Fe	12.52	2.27			4.37	1.77	11.75	5.91	10.38	8.80	5.78	3.54
Mn	0.14	0.09			0.07	0.03	0.22	0.14	0.18	0.10	0.13	0.08
Mg	5.59	0.38			1.22	0.19	6.79	1.58	16.57	4.68	1.63	0.00
Ca	7.08	1.33			1.04	0.29	9.41	5.73	10.65	7.33	2.56	0.72
Na	2.95	5.64			4.97	4.34	2.54	3.59	1.16	5.27	4.34	5.77
K	0.00	1.76			2.80	3.41	1.56	0.91	0.30	0.60	3.23	3.16
P	0.36	0.03			0.16	0.02	0.30	0.15	0.07	0.20	0.18	0.10
Ba	0.02	0.25			0.06	0.09	0.02	0.03	0.02	0.00	0.04	0.09
V	0.06	0.00			0.01	0.00	0.04	0.02	0.03	0.03	0.01	0.01
S	0.01	0.08			0.00	0.00	0.00	0.00	0.00	0.00	0.00	0.00
LOI	3.68	2.34			2.10	0.97	2.83	1.50	2.63	3.51	3.78	0.84
Total	101.08	100.19			101.13	99.71	99.92	99.96	101.26	100.92	98.90	99.85
Pb(ppm)	6.0	8.6	6.2	8.2	11.7	6.8	4.5		3.4	8.4	11.8	11.0
Th	2.8	4.2	6.3	13.5	2.8	3.8	<2		<2	3.5	2.5	3.9
Rb	<3	43.3	69.7	69.2	62.2	51.6	27.3		9.5	4.5	98.8	39.7
Sr	469	102.9	86.6	64.2	177	73.1	623		26.2	251	180	82.2
Y	49.8	53.4	18.1	38.5	45.6	42.7	14.5		11.9	30.6	56.2	54.1
Zr	202	291	109.0	115	235	216	44.5		31.9	187	346	387
Nb	6.1	5.5	3.7	4.9	5.3	6.9	2.2		2.3	5.6	9.2	10.7
Ga	20.9	15.3	14.9	13.8	18.4	13,4	13.4		6.9	22.8	24.2	14.7
Cu	37.3	5.5	6.8	7.3	6.7	<5	24.0		39.0	34.1	<5	<5
Zn	107.3	49.9	29.4	24.9	95.4	41.1	73.0		65.7	69.7	171	58.9
Cr	<30	n.d	n.d	n.d	n.d	n.d	138		n.d	106.4	n.d	n.d
Ni	27.6	n.d	n.d	n.d	n.d	n.d	49.9		n.d	36.5	n.d	n.d

Whole rock compositions (Dating samples, continued)

Rock type	tuff	qudior	ton	ton	ton	ton	ton	gr	gr	gr	gr	gr	gr
Sample	BD4	BD5	HT1	HT2	HT3	HT4	HT5	HA1	HA2	HA3	HA4	HA5	HA6
Si(% oxide)	62.66	53.11	67.62	67.53		62.42				75.58			
Ti	0.73	1.42	0.43	0.41		0.71				0.12			
Al	16.29	16.40	16.58	16.13		14.96				12.32			
Fe	6.03	9.60	3.19	2.89		6.66				1.11			
Mn	0.13	0.15	0.06	0.05		0.10				0.02			
Mg	1.40	4.84	1.14	1.11		2.49				0.04			
Ca	3.24	7.63	3.71	3.34		8.11				0.40			
Na	5.52	4.06	5.11	8.11		3.83				4.24			
K	2.65	1.08	1.32	1.48		1.11				4.56			
P	0.21	0.53	0.15	0.15		0.15				0.03			
Ba	0.07	0.04	0.05	0.03		0.03				0.01			
V	0.01	0.03	0.01	0.01		0.02				0.00			
S	0.00	0.00	0.04	0.02		0.00				0.00			
LOI	1.56	1.89	1.18	0.68		0.91				0.49			
Total	100.50	100.78	100.59	98.94		98.50				98.92			
Pb(ppm)	7.3	12.1	10.9	11.9	8.6	9.1	10.3	7.7	10.4	11.6	11.2	9.6	13.6
Th	<2	4.6	<2	2.7	<2	<2	2.3	3.5	3.1	5.7	6.7	5.0	8.2
Rb	15.4	64.5	29.3	32.8	26.7	26.5	31.3	116	94.0	94.3	71.7	73.4	89.3
Sr	597	317	498	469	350	246	525	10.6	35.1	35.8	40.7	33.1	133
Y	29.3	33.4	8.6	7.9	5.9	29.4	12.4	23.3	24.6	37.3	33.7	26.3	45.7
Zr	200	177	97.3	85.5	117	200	104.6	127	126	159	217	185	371
Nb	7.7	4.5	3.2	2.3	3.3	4.0	3.1	8.0	2.6	10.5	10.2	6.8	10.6
Ga	23.1	19.1	20.1	20.4	18.8	16.8	19.4	263	22.1	21.8	19.5	19.3	19.3
Cu	31.9	5.7	6.8	<5	36.9	19.2	19.7	<5	8.2	<5	<5	<5	<5
Zn	109.7	91.6	66.9	63.6	56.2	81.5	60.0	43.8	26.3	52.4	37.0	29.3	87.2
Cr	n.d	n.d	n.d	n.d	n.d	n.d	n.d	n.d	n.d	n.d	n.d	n.d	n.d
Ni	n.d	n.d	n.d	n.d	n.d	n.d	n.d	n.d	n.d	n.d	n.d	n.d	n.d

Appendix C2 Neutron activation analyses

Irradiation No. Sample No.	LUX HD BA001	LVX HD NU122	LWX HD NU174	LXX HD BA020	LZX HD BA007	L1X HD BA100	L3X HD NU007	L4X HD FA102	L2X USGS GSP-1	
La	13.1	25.8	25.9	16.9	17.3	13.5	25.8	9.4	176.2	
Ce	27.6	58.9	51.1	37.6	38.95	34.3	49.6	21.8	425.6	
Nd	17.6	37.8	25.0	23.1	22.4	26.3	20.6	14.8	210.4	
Sm	3.5	8.5	4.9	4.9	5.5	6.6	3.9	3.4	24.3	
Eu	0.98	4.03	0.72	0.93	1.31	2.36	0.46	1.15	2.29	
Gd	3.5	8.7	(5.0)	5.3	5.7	6.9	(4.3)	3.97	n.d	
Tb	0.60	1.27	0.72	0.89	0.92	1.17	0.60	0.66	1.55	
Tm	0.35	0.60	0.44	0.57	0.57	0.54	0.41	0.39	(0.34)	
Yb	2.10	3.34	2.92	3.67	3.62	3.25	2.73	2.39	1.80	
Lu	0.31	0.51	0.52	0.55	0.57	0.49	0.40	0.37	((0.1))	
Th	2.14	4.31	7.60	3.31	2.82	0.99	10.15	1.24	106.4	
Ta	1.33	0.63	0.99	1.01	1.44	0.73	1.63	0.24	0.87	
Hf	4.23	4.44	5.34	5.27	5.61	4.26	4.32	2.20	15.18	
Sc	14.0	33.4	8.26	10.3	11.92	45.9	3.4	50.1	{8.0}	STD
Co	89.8	22.1	44.2	54.5	83.1	53.3	61.6	42.1	6.6	
Fe_2O_3 %T	4.33	8.50	2.06	2.62	3.34	12.84	1.69	10.87	4.22	
Ba	481	1304	924	431	((40))	n.d	713	112	{1300}	STD

Analysed relative to rock standards AC(OURS) and USGS GSP-1; Sc and Ba analysed relative to USGS GSP-1 with 8 and 1300 ppm respectively; data in single brackets have errors > 10% and in double brackets > 20%; n.d - not determined

Neutron activation analysis, continued

Irradiation No. Sample No.	MFX HD BA201	MBX HD BA202	MDX HD BA203	MIX ND BA204	MAX HD BA205	MJX HD BA206	MGX HD BA207	MCX HD BA208	MHX USGS GSP-1	
La	24.1	28.0	32.0	24.6	26.1	25.2	25.0	25.8	182.0	
Ce	55.0	67.7	70.3	55.5	54.7	55.3	54.7	54.3	404.5	
Nd	35.6	39.1	42.0	34.6	33.0	34.8	32.6	33.4	203.6	
Sm	8.7	8.4	9.6	7.5	7.4	8.2	7.6	7.7	24.8	
Eu	1.31	1.28	1.37	1.13	1.3	1.34	1.31	1.37	2.13	
Gd	8.3	8.1	(10.4)	7.5	(8.9)	8.1	7.8	8.9	n.d	
Tb	1.46	1.60	1.67	1.37	1.37	1.41	1.30	1.46	1.60	
Tm	0.90	1.02	1.04	0.88	0.82	0.90	0.81	0.87	(0.24)	
Yb	5.45	6.86	6.62	5.65	5.38	5.50	5.37	5.56	1.65	
Lu	0.82	1.03	1.01	0.86	((0.8))	0.84	0.83	0.83	0.16	
U	(2)	(3)	(3)	(2)	(2)	(1)	(2)	(2)	(2)	
Th	3.71	4.81	4.73	4.02	3.64	3.89	3.70	3.71	101.3	
Ta	0.81	0.79	0.89	0.80	0.75	0.84	1.04	0.89	0.83	
Hf	8.40	11.3	10.94	9.53	9.09	9.37	8.98	8.88	13.42	
Sc	9.6	11.0	11.5	11.4	11.1	11.8	11.7	11.1	{8.0}	STD
Co	24.2	7.0	19.1	19.8	17.1	24.7	39.0	26.7	6.6	
Fe_2O_3 %T	2.97	3.41	3.48	3.40	3.93	3.80	3.56	3.98	4.24	
Ba	617	434	902	565	274	424	496	270	{1300}	STD

Analysed relative to rock standards AC(OURS) and USGS GSP-1; Sc and Ba analysed relative to USGS GSP-1 with 8 and 1300 ppm respectively; data in single brackets have errors > 10% and in double brackets > 20%; n.d - not determined

Neutron activation analysis, continued

Irradiation No.	SIX	SXX	SWX	SZX	SVX	S3X	S4X	SUX	S2X	
Sample No.	HD BA171	HD BA255	HD BA274	HD BA216T2	HD BA275T2	HD NU116	HD NU172	HD NU173	USGS RGM-1	
La	16.1	16.9	12.2	30.3	17.4	27.3	23.9	26.6	25.6	
Ce	40.0	42.6	30.9	80.0	32.2	62.5	52.0	54.7	49.3	
Nd	28.2	33.0	22.3	56.7	15.4	42.1	30.8	30.6	22.0	
Sm	6.4	8.9	5.0	12.2	2.9	8.9	6.7	6.7	4.2	
Eu	1.91	2.77	1.55	4.75	0.55	4.25	1.40	1.17	0.64	
Gd	6.4	8.6	4.7	12.3	(3.1)	8.6	5.8	5.9	n.d	
Tb	1.00	1.40	0.81	1.76	0.48	1.35	0.98	1.02	0.69	
Tm	0.47	0.66	0.37	0.64	0.35	0.63	0.56	0.61	0.42	
Yb	2.79	4.00	2.32	3.35	2.27	3.50	3.29	3.65	2.68	
Lu	0.40	0.58	0.32	0.44	0.34	0.48	0.44	0.55	0.38	
Th	1.01	1.26	0.65	2.00	5.00	4.70	6.20	6.90	14.90	
Ta	0.52	0.61	0.42	1.53	0.72	0.62	0.66	1.12	0.92	
Hf	4.54	5.37	3.19	5.57	3.80	4.76	5.74	6.27	5.96	
Sc	26.3	47.3	24.6	27.1	4.1	27.8	5.8	10.0	{5.0}	STD
Co	36.2	46.4	32.8	35.6	27.1	16.1	20.4	43.0	2.1	
Fe_2O_3 %T	9.13	15.70	8.24	12.97	1.82	8.24	4.10	2.96	1.88	
Ba	240	282	243	880	600	1213	623	740	{760}	STD

Analysed relative to rock standards AC(OURS) and USGS RGM-1; Sc and Ba analysed relative to USGS RGM-1 with 5 and 760 ppm respectively; data in single brackets have errors > 10%; n.d - not determined

Neutron activation analysis, continued

Irradiation No. Sample No.	T3X HD FA010	TWX HD FA012	TZX HD FA033	TXX HD FA096	TUX HD FA114	TVX HD FA117	T1X HD FA160	T4X HD FA184	T2X USGS RGM-1	
La	11.2	8.4	10.5	15.4	16.4	9.2	19.8	18.0	24.7	
Ce	29.3	23.6	22.2	39.5	38.3	22.5	48.7	45.0	46.4	
Nd	20.5	19.4	15.8	29.1	28.8	18.1	36.1	32.3	21.2	
Sm	4.6	5.3	3.9	7.5	7.0	5.1	8.4	8.0	3.9	
Eu	1.44	1.82	1.17	2.41	2.21	1.55	2.71	1.91	0.59	
Gd	5.3	5.7	4.3	8.2	7.8	5.2	9.7	8.6	n.d	
Tb	0.91	1.00	0.70	1.40	1.24	0.89	1.49	1.61	0.63	
Tm	0.54	0.51	0.39	0.72	0.67	0.37	0.69	0.88	0.36	
Yb	3.10	3.33	2.43	4.70	4.12	2.96	4.60	5.29	2.46	
Lu	0.48	0.49	0.37	0.69	0.60	0.42	0.68	0.77	0.37	
Th	1.77	0.48	1.18	1.08	1.25	0.63	2.28	2.88	13.80	
Ta	0.28	0.36	0.25	0.63	0.41	0.24	0.57	0.47	0.85	
Hf	2.97	3.32	2.25	4.52	4.02	2.42	5.22	6.66	5.58	
Sc	49.3	40.3	39.9	51.4	35.9	44.5	42.6	45.3	{5.0}	STD
Co	40.4	59.2	42.0	73.2	43.9	23.5	30.2	40.2	2.1	
Fe_2O_3 %T	12.46	13.47	10.60	16.05	15.86	13.19	12.75	13.23	1.81	
Ba	268	69	494	393	147	219	437	386	{760}	STD

Analysed relative to rock standards AC(OURS) and USGS RGM-1; Sc and Ba analysed relative to USGS RGM-1 with 5 and 760 ppm respectively; n.d - not determined

Neutron activation analysis, continued

Irradiation No. Sample No.	TLX HD BA005	TNX HD BA101	TKX HD BA121	TPX HD BA125	TSX HD BA170	TQX HD FA094	TTX HD FA143	TMX HD FA144	TRX USGS RGM-1	
La	10.7	12.0	20.5	8.3	11.8	3.0	33.7	28.3	24.0	
Ce	23.5	28.5	48.4	19.8	26.6	6.3	68.0	64.9	44.0	
Nd	18.2	19.9	31.4	16.0	19.5	4.1	44.6	39.8	20.3	
Sm	4.4	4.9	6.6	4.1	4.6	0.9	9.7	8.4	4.3	
Eu	1.49	1.70	1.86	1.41	1.49	0.27	2.57	2.20	0.58	
Gd	4.9	5.5	6.5	4.7	4.2	(0.8)	9.7	9.3	n.d	
Tb	0.74	0.90	1.02	0.76	0.70	0.14	1.67	1.54	0.63	
Tm	0.34	0.50	0.43	0.36	0.35	(0.09)	0.95	0.99	0.38	
Yb	2.32	3.11	2.76	2.33	2.01	0.49	5.76	6.12	2.36	
Lu	0.34	0.45	0.40	0.34	0.30	0.08	0.88	0.92	0.39	
Th	1.00	2.45	0.82	0.57	0.97	0.44	3.17	3.18	13.4	
Ta	0.33	0.48	0.44	0.28	0.30	0.14	0.80	1.17	0.83	
Hf	2.84	4.62	4.53	2.71	2.72	0.55	7.71	7.69	5.51	
Sc	25.0	27.6	24.9	31.4	26.1	2.2	22.3	17.7	{5.0}	STD
Co	22.3	42.7	33.9	33.9	32.0	10.5	8.1	31.6	2.0	
Fe_2O_3 %T	7.46	8.70	9.47	9.00	9.82	1.35	6.88	4.94	1.92	
Ba	455	n.d	321	187	((34))	((13))	938	(61)	{760}	STD

Analysed relative to rock standards AC(OURS) and USGS RGM-1; Sc and Ba analysed relative to USGS RGM-1 with 5 and 760 ppm respectively; data in single brackets have errors > 10% and in double brackets > 20%; n.d - not determined

Appendix C3 - Analytical results for standards (major and trace elements)

Sample	BCR-1 (mean,12 anal.)	BCR-1 (Abbey,1980)	G-2 (mean,12 anal.)	G-2 (Abbey,1980)	GSP-1 (mean,20 anal.)	GSP-1 (Abbey,1980)	AGV-1 (mean,13 anal.)	AGV-1 (Abbey,1980)
Si(% oxide)	54.84	54.53	68.73	69.22				
Ti	2.24	2.26	0.50	0.48				
Al	13.59	13.72	15.22	15.40				
Fe	13.31	13.42	2.70	2.68				
Mn	0.19	0.18	0.03	0.03				
Mg	3.56	3.48	0.73	0.75				
Ca	7.05	6.97	1.92	1.96				
Na	3.36	3.30	4.09	4.06				
K	1.66	1.70	4.50	4.46				
P	0.36	0.36	0.13	0.13				
Ba	0.07	0.08	0.22	0.21				
V	0.07	0.07	0.01	0.01				
S	0.05	0.04	0.01	0.01				
LOI	-0.31	-0.31	0.42	0.42				
Total	100.04	99.80	99.21	99.82				
Pb(ppm)	54.1	54			35.8	33		
Th	103.7	105			6.9	6.4		
Rb	249.5	250			67.8	67		
Sr	236.5	240			675	660		
Y	29.7	29			21.3	19		
Zr	495.4	500			233	230		
Nb	25.3	23			14.8	16		
Ga	21.0	23			20.4	21		
Cu	31.1	33			58.1	59		
Zn	105.1	105			88.9	86		

Appendix D - Whole rock compositions of the Hulayfah Group (after Delfour, 1976)

ROCK TYPE	Quartz keratophyre	Diabase (diorite)	Quartz keratophyre	Amygdaloidal basalt	Amygdaloidal basalt	Amygdaloidal basalt	Amygdaloidal basalt
LOCATION	South Nuqrah	Drill hole - North Nuqrah	Drill hole - South Nuqrah	Drill hole - South Nuqrah	Drill hole - North Nuqrah	Drill hole - South Nuqrah	Drill hole - South Nuqrah
Latitude	25°36'05"	25°38'30"	25°35'45"	25°35'45"	25°38'30"	25°35'45"	25°35'45"
Longitude	41°26'35"	41°26'20"	41°26'35"	41°26'35"	41°26'20"	41°26'35"	41°26'35"
SAMPLE	79F-JD1129	NU10-JD1410	NU8-JD1420	NU8-JD1421	NU7-JD1422	NU5-JD1423	NU21-JD1884
SiO_2	74.65	53.00	77.15	50.90	48.30	52.10	51.00
TiO_2	0.30	2.18	0.23	0.43	0.93	0.40	0.38
Al_2O_3	12 20	13.70	12.10	14.20	14.25	13.80	14.20
Fe_2O_3	1.60	3.25	1.25	2.15	3.20	2.35	2.02
FeO	1.90	8.15	0.85	6.30	6.00	5.90	5.75
MnO	0.12	0.20	0.05	0.13	0.15	0.11	0.13
MgO	0.60	3.90	1.40	10.60	10.80	9.90	10.33
CaO	2.80	5.90	0.80	8.10	6.85	8.40	8.76
Na_2O	3.95	3.70	5.60	1.30	2.75	2.05	2.25
K_2O	0.70	2.75	0.10	0.25	1.10	0.75	0.43
P_2O_5	0.07	0.53	0.00	0.10	0.16	0.08	0.08
H_2O^+	1.20	2.00	0.05	5.70	5.10	3.75	3.96
H_2O^-	0.02	0.16	0.10	0.15	0.15	0.25	0.10
CO_2	0.00	0.58	0.29	0.00	0.11	0.00	0.04
S	0.00	0.00	0.62	0.05	0.10	0.12	-
SO_3	-	-	-	-	-	-	0.80
TOTAL	100.11	100.00	100.59	100.36	99.84	99.96	100.23

ROCK TYPE	Aphanitic basalt	Pillow of aphanitic basalt	Porphyritic andesite	Porphyritic andesite	Aphanitic andesite	Welded rhyodacite tuff	Porphyritic andesite	Porphyritic andesite	Tuffaceous andesite	Dacite
LOCATION	4.5 km NW. of Nuqrah	13 km SE. of Bi'r al Quṣayrah	Jabal at Tīn	Jabal 'Afinah	Jabal at Tīn	Jabal at Tīn	Jabal at Tuwayn	Jabal Muṣayna'ah	Jabal Muṣayna'ah	Jabal 'Afinah
Latitude	25°37'30"	25°16'45"	25°46'20"	25°51'20"	25°44'35"	25°44'30"	25°48'25"	25°44'55"	25°45'40"	25°52'30"
Longitude	41°25'50"	41°29'50"	40°47'55"	40°49'00"	40°47'15"	40°48'35"	40°48'35"	40°42'10"	40°41'50"	40°47'40"
SAMPLE	79F-JD1120	86B-JD1813	78D-JD3892	78D-JD3893	78H-JD3931	78H-JD3936	78D-JD3952	78G-JD3988	78C-JD3989	78D-JD4054
SiO_2	50.00	49.20	56.60	58.80	54.30	63.80	51.80	49.20	53.20	56.40
TiO_2	1.65	0.48	1.38	1.55	1.07	0.57	0.90	1.06	1.06	0.64
Al_2O_3	14.60	12.55	15.70	15.60	15.70	17.20	17.10	16.00	17.50	15.05
Fe_2O_3	3.80	3.70	4.40	4.35	3.20	1.95	6.90	4.65	4.30	3.10
FeO	7.10	3.45	3.40	3.30	5.25	1.65	2.05	3.70	3.10	4.50
MnO	0.20	-	0.15	0.10	0.16	0.06	0.17	0.17	0.13	0.16
MgO	6.10	4.75	4.15	2.80	6.20	2.20	7.10	7.85	5.10	5.60
CaO	11.35	13.05	7.00	4.35	8.50	5.05	7.60	8.35	8.30	7.10
Na_2O	2.75	2.95	3.50	4.35	3.10	6.00	4.55	2.50	3.05	2.65
K_2O	0.35	1.80	1.15	2.45	0.55	0.45	0.35	2.50	0.75	0.50
P_2O_5	0.20	0.33	0.36	0.55	0.20	0.17	0.12	0.19	0.20	0.12
H_2O^+	1.20	2.10	1.85	1.95	2.00	1.10	1.65	3.10	2.75	2.65
H_2O^-	0.10	0.05	0.10	0.00	0.04	0.00	0.00	0.05	0.10	0.15
CO_2	0.22	4.95	-	-	-	-	-	-	-	-
S	0.00	-	-	-	-	-	-	-	-	-
SO_3	-	0.01	0.05	0.035	0.03	0.05	0.02	0.055	0.025	0.025
TOTAL	99.62	99.37	99.79	100.20	100.30	100.26	100.32	99.38	99.57	98.65

ROCK TYPE	Amygdaloidal basalt	Altered dacite	Basalt	Quartz keratophyre	Quartz keratophyre	Diabase (gabbro)	Porphyritic andesite
LOCATION	Drill hole - South Nuqrah	Jabal Abū Nubtah, 11 km SE. of Jabal Māwān	Bulghah, 15 km SE. of Jabal Māwān	Muṣayna'ah ancient mine	Muṣayna'ah ancient mine	Muṣayna'ah ancient mine	Muṣayna'ah ancient mine
Latitude	25°35'45"	25°04'35"	25°02'30"	25°43'00"	25°44'45"	25°44'30"	25°44'45"
Longitude	41°26'35"	41°34'50"	41°35'50"	40°43'30"	40°43'45"	40°43'30"	40°43'45"
SAMPLE	NU18-JD1930	86B-JD2011	86G-JD2014	78G-JD286	78G-JD296	78G-JD316	78G-JD334
SiO_2	53.10	48.80	48.50	67.65	65.80	52.30	53.20
TiO_2	0.40	1.15	1.23	0.35	0.40	1.00	1.10
Al_2O_3	14.35	15.00	17.90	10.00	11.20	14.10	14.00
Fe_2O_3	1.50	1.95	1.70	4.70	5.10	4.10	5.50
FeO	6.35	8.95	7.70	7.50	6.95	9.20	7.30
MnO	0.12	0.22	0.16	0.07	0.07	0.15	0.10
MgO	11.40	5.30	6.20	1.40	0.85	6.20	5.70
CaO	7.25	7.20	10.55	1.25	1.45	8.70	6.30
Na_2O	1.60	2.10	2.80	5.15	4.45	2.25	2.90
K_2O	0.10	0.16	0.23	0.95	2.90	1.00	2.15
P_2O_5	0.09	0.25	0.14	0.10	0.15	0.15	0.25
H_2O^+	3.85	4.65	2.70	0.70	0.55	1.00	1.25
H_2O^-	0.15	0.20	0.15	0.15	0.20	0.10	0.10
CO_2	0.03	3.90	0.25	-	-	-	-
S	-	-	-	-	-	-	-
SO_3	0.10	0.13	0.05	-	-	-	-
TOTAL	100.39	99.96	100.26	99.97	100.07	100.25	99.85